ISSN 1007-9327 (print)
ISSN 2219-2840 (online)

World Journal of *Gastroenterology*

World J Gastroenterol 2018 March 14; 24(10): 1063-1180

Published by Baishideng Publishing Group Inc

World Journal of Gastroenterology

Contents

Weekly Volume 24 Number 10 March 14, 2018

MINIREVIEWS

ORIGINAL ARTICLE

Basic Study

Retrospective Cohort Study

Retrospective Study

ABOUT COVER

Editorial board member of *World Journal of Gastroenterology*, Georgios Tsoulfas, MD, PhD, Associate Professor, Department of Surgery, Aristotle University of Thessaloniki, 66 Tsimiski St, Thessaloniki 54622, Greece

AIMS AND SCOPE

World Journal of Gastroenterology (*World J Gastroenterol*, *WJG*, print ISSN 1007-9327, online ISSN 2219-2840, DOI: 10.3748) is a peer-reviewed open access journal. *WJG* was established on October 1, 1995. It is published weekly on the 7th, 14th, 21st, and 28th each month. The *WJG* Editorial Board consists of 642 experts in gastroenterology and hepatology from 59 countries.

The primary task of *WJG* is to rapidly publish high-quality original articles, reviews, and commentaries in the fields of gastroenterology, hepatology, gastrointestinal endoscopy, gastrointestinal surgery, hepatobiliary surgery, gastrointestinal oncology, gastrointestinal radiation oncology, gastrointestinal imaging, gastrointestinal interventional therapy, gastrointestinal infectious diseases, gastrointestinal pharmacology, gastrointestinal pathophysiology, gastrointestinal pathology, evidence-based medicine in gastroenterology, pancreatology, gastrointestinal laboratory medicine, gastrointestinal molecular biology, gastrointestinal immunology, gastrointestinal microbiology, gastrointestinal genetics, gastrointestinal translational medicine, gastrointestinal diagnostics, and gastrointestinal therapeutics. *WJG* is dedicated to become an influential and prestigious journal in gastroenterology and hepatology, to promote the development of above disciplines, and to improve the diagnostic and therapeutic skill and expertise of clinicians.

INDEXING/ABSTRACTING

World Journal of Gastroenterology (*WJG*) is now indexed in Current Contents®/Clinical Medicine, Science Citation Index Expanded (also known as SciSearch®), Journal Citation Reports®, Index Medicus, MEDLINE, PubMed, PubMed Central and Directory of Open Access Journals. The 2018 edition of Journal Citation Reports® cites the 2016 impact factor for *WJG* as 3.365 (5-year impact factor: 3.176), ranking *WJG* as 29th among 79 journals in gastroenterology and hepatology (quartile in category Q2).

NAME OF JOURNAL
World Journal of Gastroenterology

ISSN
ISSN 1007-9327 (print)
ISSN 2219-2840 (online)

LAUNCH DATE
October 1, 1995

FREQUENCY
Weekly

EDITORIAL OFFICE
Ze-Mao Gong, Director
World Journal of Gastroenterology
Baishideng Publishing Group Inc
7901 Stoneridge Drive, Suite 501,
Pleasanton, CA 94588, USA
Telephone: +1-925-2238242
Fax: +1-925-2238243
E-mail: editorialoffice@wjgnet.com
Help Desk: http://www.f6publishing.com/helpdesk
http://www.wjgnet.com

PUBLISHER
Baishideng Publishing Group Inc
7901 Stoneridge Drive, Suite 501,
Pleasanton, CA 94588, USA
Telephone: +1-925-2238242
Fax: +1-925-2238243
E-mail: bpgoffice@wjgnet.com
Help Desk: http://www.f6publishing.com/helpdesk
http://www.wjgnet.com

PUBLICATION DATE
March 14, 2018

INSTRUCTIONS TO AUTHORS
Full instructions are available online at http://www.wjgnet.com/bpg/gerinfo/204

ONLINE SUBMISSION
http://www.f6publishing.com

World Journal of Gastroenterology

Submit a Manuscript: http://www.f6publishing.com

World J Gastroenterol 2018 March 14; 24(10): 1063-1071

DOI: 10.3748/wjg.v24.i10.1063

ISSN 1007-9327 (print) ISSN 2219-2840 (online)

MINIREVIEWS

Inflammatory bowel disease registries for collection of patient iron parameters in Europe

Jonas Halfvarson, Fraser Cummings, Olof Grip, Guillaume Savoye

Jonas Halfvarson, Department of Gastroenterology, Faculty of Medicine and Health, Örebro University, Örebro SE 70182, Sweden

Fraser Cummings, Department of Gastroenterology, Southampton University Hospital NHS Foundation Trust, Southampton, Hampshire SO16 6YD, United Kingdom

Olof Grip, Department of Gastroenterology, Skåne University Hospital, Malmö S-20502, Sweden

Guillaume Savoye, Service d'hépato-gastroentérologie, CHU de Rouen-Hôpital Charles Nicolle, Rouen 76031, France

ORCID number: Jonas Halfvarson (0000-0003-0122-7234); Fraser Cummings (0000-0002-9659-3247); Olof Grip (0000-0001-5033-7451); Guillaume Savoye (0000-0002-9200-2067).

Author contributions: All authors contributed equally to the conception and topics for this review and to revising the article critically for intellectual content; all authors approved the final version of the manuscript for submission.

Conflict-of-interest statement: Halfvarson J has received honoraria/grants from Abbvie, Celgene, Hospira, Janssen, Medivir, MSD, Pfizer, Sandoz, Takeda, Tillotts Pharma, and Vifor Pharma; Cummings F has received honoraria/grants from Biogen, Abbvie, Ferring, Hospira, Janssen, Pfizer, MSD, Napp, Pharmacosmos, Shield Therapeutics, Takeda, and Vifor Pharma; Grip O has received honoraria from Abbvie, Ferring, Janssen, Takeda, and Vifor Pharma; and Savoye G has received honoraria from HAC Pharma France, Pharmacosmos, and Vifor Pharma.

Manuscript source: Unsolicited manuscript

Correspondence to: Jonas Halfvarson, MD, PhD, Associate Professor, Department of Gastroenterology, Faculty of Medicine and Health, Örebro University, Örebro SE 70182, Sweden. jonas.halfvarson@regionorebrolan.se
Telephone: +46-19-303000
Fax: +46-19-6021774

Received: December 14, 2017
Peer-review started: December 15, 2017
First decision: December 27, 2017
Revised: February 2, 2018
Accepted: February 9, 2018
Article in press: February 9, 2018
Published online: March 14, 2018

Abstract

Iron deficiency without anemia and iron deficiency anemia are common and frequently overlooked complications of inflammatory bowel disease. Despite the frequency and impact of iron deficiency in inflammatory bowel disease, there are gaps in our understanding about its incidence, prevalence and natural history and, consequently, patients may be undertreated. Medical registries have a key role in collecting data on the disease's natural history, the safety and effectiveness of drugs in routine clinical practice, and the quality of care delivered by healthcare services. Even though iron deficiency impacts inflammatory bowel disease patients and healthcare systems substantially, none of the established European inflammatory bowel disease registries systematically collects information on iron parameters and related outcomes. Collection of robust iron parameter data from patient registries is one way to heighten awareness about the importance of iron deficiency in this disease and to generate data to improve the quality of patient care, patient outcomes, and thus quality of life. This objective could be achieved through collection of specific laboratory, clinical, and patient-

reported measurements that could be incorporated into existing registries. This review describes the status of current European inflammatory bowel disease registries and the data they generate, in order to highlight their potential role in collecting iron data, to discuss how such information gathering could contribute to our understanding of iron deficiency anemia, and to provide practical information in regard to the incorporation of accumulated iron parameter data into registries.

Key words: Anemia; Iron deficiency; Registries; Inflammatory bowel disease; Patient care

Core tip: Despite its prevalence, iron deficiency is often overlooked in inflammatory bowel disease (IBD). More data are required to fully understand the epidemiology, treatment, and quality of care around iron deficiency in IBD. We suggest that IBD registries are ideally positioned to collect these data from routine clinical practice. We discuss the laboratory, clinical, and patient-reported data that could be collected, and review how best to incorporate collection of these data into existing registries.

Halfvarson J, Cummings F, Grip O, Savoye G. Inflammatory bowel disease registries for collection of patient iron parameters in Europe. *World J Gastroenterol* 2018; 24(10): 1063-1071 Available from: URL: http://www.wjgnet.com/1007-9327/full/v24/i10/1063.htm DOI: http://dx.doi.org/10.3748/wjg.v24.i10.1063

INTRODUCTION

The current healthcare landscape relies heavily on controlled trials to generate evidence to support regulatory approval of new drugs and inform treatment of patients[1-4]. While scientifically rigorous, the applicability to everyday clinical situations might be questionable, since it does not necessarily include a cohort that is representative of the real-world patient population[5]. In contrast, registries have a key role in acquiring, maintaining, analyzing and, ultimately, publishing data that reveal how drugs are used in routine clinical practice. Medical registries can survey the demographics of patients with a particular medical condition, collect data on the use of a particular pharmaceutical product, class of products or use of a particular medical device, or be used to evaluate the quality of care delivered. Consequently, the use of national registries to generate real-world data is of great value, particularly in complex diseases such as inflammatory bowel disease (IBD), namely Crohn's disease and ulcerative colitis.

Iron deficiency anemia (IDA) is ranked as one of the world's ten leading causes of years lived with disability[6] and can manifest in a broad range of symptoms, including chronic fatigue, increased susceptibility to infection, tachycardia, sleep disturbance, impaired cognitive function, hair loss, and changes to skin and nails[7]. Iron deficiency without anemia (ID) and IDA are two of the most common systemic complications of IBD; estimates of prevalence indicate that ID occurs in 60%-80% of people with IBD, with the prevalence of anemia ranging from 16% to 74%[8].

For patients with IBD, IDA can be caused by a variety of factors[8] and affect a range of physical, personal, and social parameters, impairing work productivity and ultimately compounding the diminished quality of life (QoL) associated with IBD alone[9]. The economic burden of IBD is elevated by the presence of IDA; a retrospective review of healthcare claims data in the US estimated the direct treatment costs for each IBD patient to be substantially higher for those with anemia versus those without[10].

The natural history of IDA in IBD is not fully understood and its occurrence remains underestimated[11], so patients are potentially undertreated. The gaps in our understanding require comprehensive longitudinal data collection-an important source of which may be the collection of iron parameter data from patient registries. The objectives of this review article are to describe the status of current European IBD registries and the data they generate, to highlight the potential role of IBD registries in collecting IDA data and contributing to our understanding of IDA, and to provide practical information in regard to the incorporation of collated iron parameter data into IBD registries.

EXISTING REGISTRIES

Registry searches

A literature search was conducted to identify IBD registries that are currently collecting data in Europe, using the PubMed online database and internet searches. The search term "inflammatory bowel disease registry" was used and results were reviewed to identify articles meeting the inclusion criteria. The reference lists of any article meeting the inclusion criteria were reviewed manually to identify additional relevant publications. Where articles were identified, the name of the registry was used as a search term in the Google internet search engine in an attempt to find further relevant information. Where a web page did not provide information in English, translation software was used to determine if the information was relevant. For inclusion in this review, studies were required to have met the following criteria, in regard to the registry: (1) Being disease-specific with information on IBD; (2) being located in a European country; and (3) currently collecting data. Registries that were specific to treatment, and not disease, were excluded. Details of the registries identified are shown in Table 1. Note

Table 1 Examples of active inflammatory bowel disease registries in Europe

Name	Country	Year established	Description and aim	IBD Study population	Data collected
Competence Network IBD Registry[27]	Germany	2015	Scientists, physicians, clinics, research institutes, and industry with an interest in research to improve the care of patients with IBD	Approximately 50000 (anticipated)	IBD frequency and course; comorbidity incidence; efficacy of treatment; predictive parameters; subgroup characterization; outpatient vs inpatient costing; guideline implementation; service delivery
ENEIDA[28,29]	Spain	2006	Promotion of clinical and genetic studies in IBD, epidemiology of IBD, clinical outcomes, and drug safety in IBD treatment	> 11000	Patient demographics, disease classification, treatment outcomes and safety, phenotype, and family history of IBD
EPIMAD[18,30-34]	Northern France	1988	To provide reliable data on the epidemiology of IBD to healthcare authorities, provide data to search for a cause of disease, and describe in a population-based setting the natural history and real-life management of IBD	All IBD patients in region (approximately 20000 patients)	Patient demographics and disease data
SWIBREG[35]	Sweden	2005	To serve as a decision support tool in everyday life, assessing disease activity and quality of life	> 40000 (adult and pediatric)	Patient demographics and disease data, drug history, treatment and disease outcomes, surgical interventions, patient-reported outcomes. Capacity to enter information about comorbidities
SIBDC[12]	Switzerland	2005	To build understanding of the consequences of IBD on the physical, mental, and social conditions of IBD patients	Voluntary national database of > 2500 patients	Patient demographics, disease and treatment information. Patient blood samples are kept in a biobank providing a databank of genetic and disease information
UK IBD Registry[13]	United Kingdom	2013	To drive improvement in patient care and access to care across the United Kingdom, inform commissioning and service design, improve understanding of long, term outcomes in IBD, provide local, regional, and national data in order to better define the pattern of ulcerative colitis and Crohn's disease, and support IBD research	Approximately 20000 (adult and pediatric)	Patient demographics, disease data, any surgical interventions, drug history, treatment and disease outcomes, disease activity scores and patient-reported outcomes
Pediatric registries					
CEDATA[36]	Austria and Germany	2004	Developed and operated by the working group of chronic inflammatory bowel diseases of the Society for Pediatric Gastroenterology and Nutrition; aims to improve the care of children and adolescents with IBD.	Approximately 1000	Patient demographics, disease and treatment data
SPIRIT-IBD[37]	Spain	1996	To understand the incidence and prevalence of IBD in pediatric patients	Approximately 2000	Patient demographics, disease and treatment data
EUROKIDS[38,39]	Europe and Israel	2004	To audit the diagnostic workup of pediatric IBD patients and to accurately describe disease in newly diagnosed pediatric IBD patients	Approximately 4000	Patient demographics, disease and treatment data

IBD: Inflammatory bowel disease; IDA: Iron deficiency anemia.

that the list of identified registries presented here may not be exhaustive, as small local or regional registries may not be visible to such a search, and this work is not intended to be a complete systematic review.

Data collected by European registries on IBD

Items common to the IBD registries include: number of patients with IBD in the region covered, information on clinical characteristics, medication, treatment effectiveness,

Table 2 Suggested iron deficiency anemia-related parameters to collect in an inflammatory bowel disease registry

Laboratory measurements
Hemoglobin level
Serum ferritin level
Transferrin saturation level
Soluble transferrin receptor level
Hepcidin
Mean corpuscular volume
Mean corpuscular hemoglobin
C-reactive protein level
Clinical observations
Identification of ID/IDA-related symptoms
Duration of possible ID/IDA-related symptoms
Number of, duration of, and reasons for healthcare visits
Medication usage
Patient-reported outcomes
Quality-of-life questionnaires
Fatigue questionnaires
Work productivity and activity questionnaires
Treatment decisions
Iron supplement (oral or IV)
IBD medication
Surgical procedures

IBD: Inflammatory bowel disease; IDA: Iron deficiency anemia.

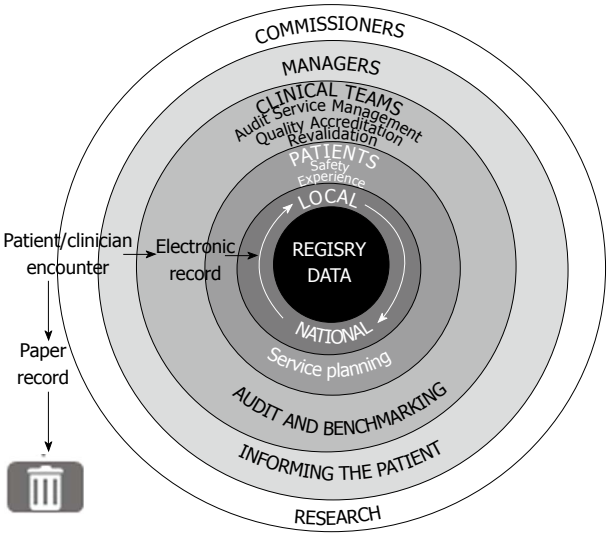

Figure 1 Data recorded at the point of care on an electronic system can be used to achieve a wide range of local and national objectives.

and service delivery. Some information is registry specific, such as biobanking of blood samples for genotyping, as within the Swiss cohort[12]. It is notable that, despite the prevalence of ID/IDA among IBD patients, none of the registries identified explicitly were collecting information on iron parameters and related outcomes in a systematic manner at the time of this review.

The approach to data collection and verification varies among registries. For example, in EPIMAD (Registre des Maladies Inflammatoires Chroniques de l'Intestin du Nord Ouest de la France), data are collected by interviewer practitioners when possible cases of IBD are identified, and a diagnosis of IBD is verified by two expert practitioners. Each patient can be followed, if necessary, for 2 years until a final diagnosis is confirmed. In contrast, the UK IBD Registry utilizes electronic data-entry systems, such that data are collected in real time at the point of care (Figure 1). Some of the data-entry tools allow for the upload of laboratory data directly into the system, such that, after negotiations with the relevant providers, iron parameters could be added to the data collected with relative ease[13]. Similarly, the Swedish Quality Registry for Inflammatory Bowel Disease (SWIBREG) - which is notable in being well established and in covering half of the Swedish IBD population-can be linked to other national registers to evaluate etiology, prognosis, and outcomes of different treatment modalities[14].

Despite the coverage of these registries, the initial research questions used, the configuration of data-collection systems, and available resources (both financial and personnel) all impose limits on the data they can gather. Information about medications to treat conditions concomitant to IBD, such as ID and IDA, may not be captured. Similarly, the collection and inclusion of patient-reported outcome (PRO) data in existing IBD registries is not a trivial undertaking. Given the importance of ID-related symptoms, the collection and analysis of PRO questionnaires is important and should be considered.

HOW SHOULD IDA-RELATED DATA BE COLLECTED IN IBD REGISTRIES?

Although national healthcare databases collect and store data from blood tests on anemias, ID, and the drugs used in their treatment, they do not seem to be an appropriate way to collect data on IDA in IBD. In general, such databases are optimized to collect high-level administrative data, and do not describe IBD patients adequately to offer the level of medical detail needed to research the natural history of disease. This is also the case for databases owned by agencies involved in reimbursement of medical treatment. From this, a clear need for prospective and specific collection of iron parameter data can be established, which may be achieved through the adaptation of existing IBD registries.

Even though IDA and ID are common in IBD, and exert a substantial burden on patients and healthcare systems[8-10], none of the established European IBD registries systematically collects information on iron parameters and related outcomes. Addressing this shortfall in data collection requires examination of the primary objectives of the registries in question, and consideration of parameters that could answer further research questions around this objective. The parameters collected would be determined by the type of registry (condition-, product-, or service-based) and should serve its primary research objective; suggestions

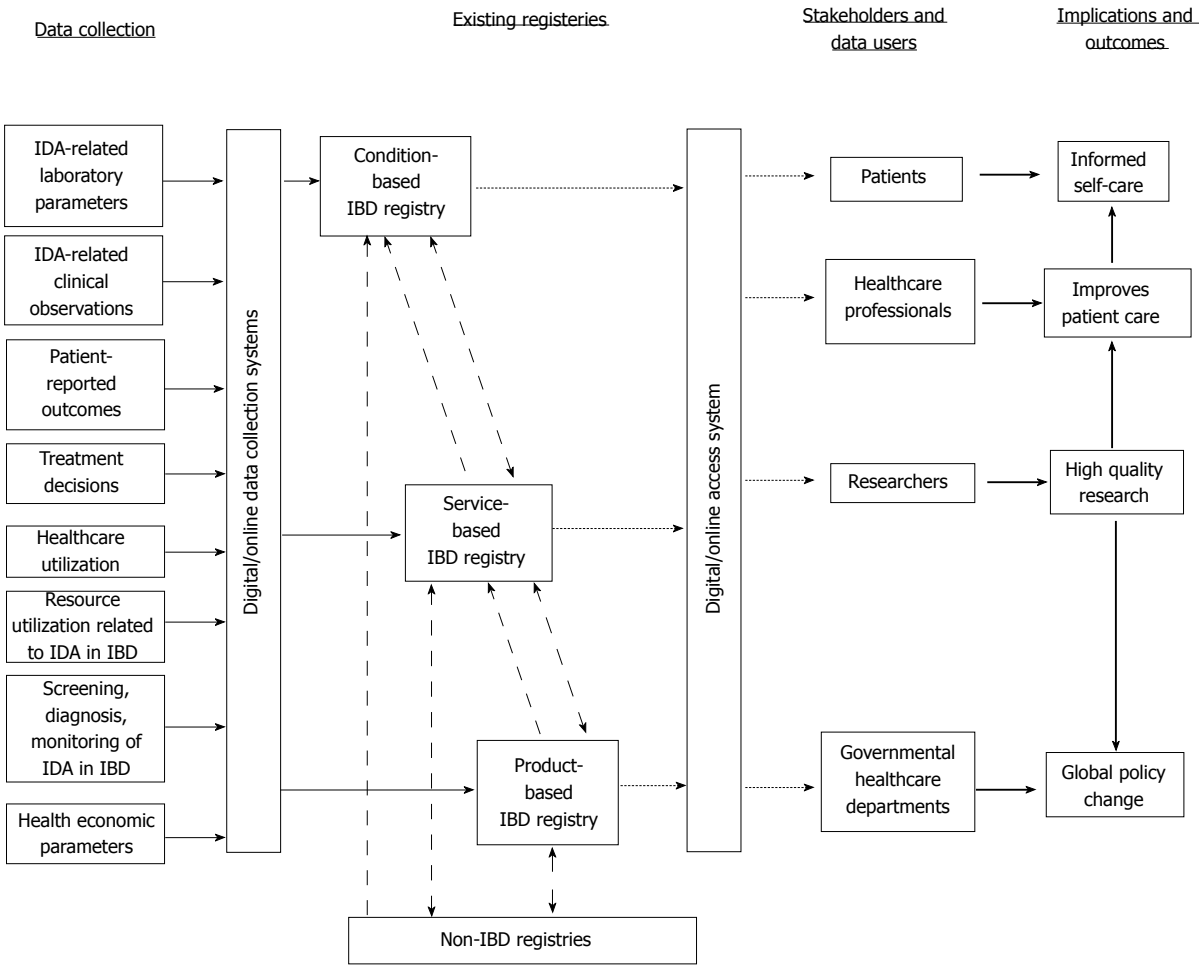

Figure 2 Collection and flow of data between existing healthcare registries to support various outcomes for multiple stakeholders. Solid line: flow of patient-level data; dashed line: flow of pseudo-anonymized data; dash-dot line: flow of aggregated anonymized data; block arrows, overall and relationships between implications. IBD: Inflammatory bowel disease; IDA: Iron deficiency anemia.

are listed in Table 2.

A condition-based registry designed to monitor epidemiology of IBD could also collect data to provide snapshots of the prevalence and severity of IDA. Longitudinal analyses of IDA duration and disease course, with the potential to identify commonly associated factors-including ID-related burden occurring during pregnancy-could also be included. To chronicle the natural history of IDA, it is necessary to collect longitudinal information on clinical, biochemical and endoscopic disease activity; data from imaging techniques such as magnetic resonance imaging should ideally be included. In line with the current European Crohn's and Colitis Organisation (ECCO) consensus on the diagnosis and management of ID with and without anemias in IBD[15], a basic dataset may comprise hemoglobin levels, transferrin saturation and serum ferritin levels, and perhaps mean corpuscular volume and mean corpuscular hemoglobin. Measuring C-reactive protein would inform the interpretation of serum ferritin levels, which may be elevated by inflammation. Recording the levels of individual iron parameters (rather than a diagnosis of anemia) would offer a more detailed view of ID and the capacity to investigate concepts such as absolute and functional ID[15]. To further understand the impact that ID and IDA have on disease course and its influence on the response to treatment the registry would need to collect medication history and validated disease activity scores/PROs that evaluate fatigue, QoL, and impaired productivity. Fatigue is a key symptom of ID (and of IBD) and can be quantified using a validated scoring system such as the functional assessment of chronic illness therapy-fatigue (FACIT-F)-Fatigue questionnaire[16]. There are several tools available to measure QoL in patients with IBD or, more recently, disability[17,18], although these do not necessarily distinguish between the burden of ID/IDA and IBD.

A product-based registry (focused on IBD treatment) could be used to monitor use of iron supplements. Information on prescribed iron replacement therapy, including doses, may be recorded as either oral or intravenous, to illustrate any impact of a different choice of iron administration route.

A service-based registry would typically have a different dataset, including information on the use of healthcare (including hospitalizations and surgery),

and the resource utilization attributable to ID and IDA in IBD. Collection of data on screening, diagnosis, and monitoring of ID and IDA in IBD could offer a perspective on aspects of quality of care, with reference to the recommendations of the European Consensus on the Diagnosis and Management of Iron Deficiency and Anaemia in Inflammatory Bowel Diseases[15]. If an economic perspective is deemed valuable, observations on impaired work productivity and activity can be collected, as well as information on absences from work or full-time education, healthcare attendance, need for surgery, and medication adherence and persistence.

A registry would ideally use appropriate digital and online technologies to make it easier for sites to contribute data, including enabling data entry at point of care and a facility for patients to submit disease-related information. Incentives for teams to use these technologies might include the opportunity to deliver data-driven care to patients. Patients may also be given access to presentations of these data to facilitate supported self-management, and improve patient participation and empowerment. An example of success in this area is Improve Care Now-a network of people from 95 care centers in the United States, Qatar, and United Kingdom that has the objective of improving the health, care, and costs for children and adolescents with IBD[19]. The centers involved in this initiative collect data about treatment and performance in a standardized format; the tools for best practice in the treatment of these patients, with the related evidence, is shared within the network, leading to substantial improvements in patient outcomes and better patient safety[20].

Cross-registry interoperability and integration, to facilitate sharing of data with existing healthcare systems and resources, would be highly beneficial; Figure 2 illustrates a potential model for how data could move between registries and shows the potential outcomes for stakeholders. Collection and incorporation of unique pseudoanonymized national personal identifiers of patients enables connections to be made between registries. IDA is prevalent in patients with renal disease, heart disease, and cancer, and can affect cognitive development/function and resistance to infection[21,22]. Correlation between disease registries in IBD, oncology, heart failure, and mental health could offer completely new perspectives on improving the multidisciplinary care of patients with ID. Further connections could be made with drug prescription databases with the intention of correlating disease outcomes with specific treatment information. Linkage of an IBD registry with national service-based registries could show the frequency of outpatient visits, inpatient care, surgery, and co-existing disease, based on the international classification of disease codes. Linkage with mortality databases would provide an additional view of disease outcomes. A potential barrier to sharing of data is the governance issues around information. Any such sharing should comply with the registry's ethical requirements and national laws covering data protection. If there are restrictions on exporting personal data from the country, steps must be taken to anonymize and aggregate the information. It is also important to understand exactly what is of interest to a collaborating registry, and to identify and characterize all variables collected, as these may vary between registries[14].

HOW CAN EXISTING IBD REGISTRIES BE ADAPTED TO COLLECT IDA-RELATED PARAMETERS?

The current IBD registries are positioned well to collect iron parameter data and link these with IBD-specific data. Although it is beyond the scope of this article to provide detailed guidance on adapting a registry to collect a new set of variables, there are several factors that should be considered, in regard to the prospective collection of iron parameters in an IBD registry. Initially, it is important to consider the change in scope of a registry, in terms of its expected redefined purpose, objectives, and overall outputs. While it may be tempting to maximize the opportunities for data collection, this must be balanced against the importance of collecting high-quality, reliable data with no significant increased burden associated with their entry to the database. Limiting the scope of a registry ensures that specific objectives and well-defined research questions can be established in order to specify what outputs should be sought. Defining and confirming the scope of any changes with all stakeholders will optimize the work needed as the changes to the registry are implemented. When the objectives have been clearly established, the data to be collected can then be determined. The data collection method should suit the data type. The practicalities of incorporating collection of iron parameters into an existing IBD registry could present a challenge, as it would depend on the healthcare system in which the registry operates. Ideally, the addition of new parameters to a registry should not generate substantially more work for sites contributing to the registry. With the introduction of electronic medical records and network integration it is theoretically possible for iron parameter data from medical laboratories to be automatically added to a medical record and uploaded to a registry database. This would greatly minimize the resources needed for data entry, avoiding the review and entry of information from unstructured case notes, and circumventing double entry of data. However, there are currently barriers to this approach. Firstly, retrieval of data from laboratory service providers requires negotiation, financial commitment, and often improvement of IT facilities. This problem is magnified if a country has multiple service providers, each of which is presenting data in a proprietary format, thus requiring a large amount of interface development work. Secondly, the use of electronic medical records is still not widely used, and standards of interoperability are yet to be

established. The functioning of a registry could be complicated if data source inputs present information in a range of formats that have to be interpreted before they can be used. Many commercial providers offer digital and online interfaces to facilitate data capture in a registry; however, there can be great variation between them in terms of financial cost, ease-of-use, and features (not all of which may be necessary or relevant to an individual registry)[23]. Indeed, the quality and capabilities of different software used to manage data in clinical studies and registries can vary greatly, raising barriers in interoperability and evaluation of data across studies[24]. Open-source software offers an alternative that is both low-cost and can be modified by researchers to suit specific requirements[24]. A key role for national and international registries would be to define data submission frameworks that enable the entry of data from a range of different sources.

The rise in health technologies that are accessible from personal mobile devices is likely to have an important role in collection of PROs. Electronic PRO data collection has many advantages relating to easy, accurate, and complete collection of data that is potentially of great value to investigators and healthcare systems[25]. In the context of a registry, as opposed to a clinical trial, it may make sense for a patient to be able to complete PRO information using their own mobile device, rather than attending an appointment. Although this adds a level of convenience for both patient and healthcare team, a number of barriers still remain including data security, patient compliance with data collection, and what to do if a patient does not possess a suitable device[25]. Nevertheless, ePROs show promise; indeed, pilot studies of an electronic data submission method implemented by the SWIBREG registry have proved successful and its launch is imminent in some regions in Sweden. A UK study to collect ePROs in an elective orthopedic setting showed great promise, gathering reliable data but also highlighting that the ePRO system may not be adequate for some patients[26].

The incorporation of iron parameter data into European IBD registries offers great opportunities to improve the care of IBD patients. Firstly, highlighting the prevalence of IDA in the IBD population would show the unmet need in this patient group in countries across Europe. It is notable that the ECCO guidelines for diagnosis and management of ID and IDA in IBD recommend that all patients with IBD should be assessed for the presence of anemia[15]. Robust data are necessary to heighten awareness of the importance of IDA in IBD and to lobby healthcare systems to improve access to the full range of iron supplementation therapies. Secondly, longitudinal analysis of iron parameters and treatment could offer a perspective to assess some aspects of the quality of care that patients receive, including the management of IDA and ID, as well as the numbers of patients who receive optimal treatment. Thirdly, the inclusion of QoL information and PROs would offer perspectives on how optimal treatment could change the burden of IDA on the patient, as well as potentially providing economic arguments for the use of iron supplementation. Finally, the information collected could inform service planning at the local and national level, including on how resources should be managed to provide improved access to nursing support or access to infusion suites. Periodic assessment of the data collected in national registries would also provide information needed for clinical audits and quality improvement programs.

Beyond the local and national level, the collection and comparison of iron parameters by multiple registries would allow the relationship between IBD and IDA to be examined from different perspectives, stemming from each registry's specific remit, leading to the generation of new research questions and ultimately improving patient care. A further possibility would be the pooling of data between national registries to identify and study any differences in patterns of disease, and to compare practices in healthcare service delivery. A very large dataset should also able to highlight any rare effects that might not be evident from a single national registry. This initiative would, of course, require agreement on the collection of a basic dataset and standardization of methodologies, as well as addressing how data should be anonymized and aggregated to comply with the legal aspects of sharing data across national borders.

CONCLUSION

Iron deficiency and IDA are common and often overlooked complications of IBD. Historically, ID and IDA have been accepted as part of IBD, and not as an issue to be addressed and treated independently. The prevailing attitude was that treatment of IBD would lead to the resolution of anemia, so organized research efforts to understand ID in patients with IBD were minimal. In recent years, however, opinion has shifted, with a growing acknowledgement that ID/IDA is an issue to be managed concomitantly with IBD. A recent consensus statement provides up-to-date guidance on the diagnosis, treatment and prevention of ID/IDA in IBD[15]. Despite the frequency and impact of ID and IDA in IBD, there are gaps in our understanding about its incidence, prevalence, natural history, and particularly its impact on patients. Due to similarities between symptoms of IBD and ID/IDA, the identification of ID/IDA-specific symptoms in the IBD population is necessary. There is, therefore, a clear need to collect robust, structured data around ID/IDA in IBD, its treatment, and on related service delivery. Despite potential limitations (possible selection bias and potential variability in data quality), it has been suggested that 'real-world' data have a greater applicability to the routine clinical setting than the findings of controlled trials[5]. Current digital technologies and networking capabilities raise the prospect of an acquisition and analysis of real-world

data that is (and should be) easier than ever before. With appropriate planning, information governance structures, adaptation, and negotiation, registries are ideally placed to collect this information in a routine clinical practice setting. The direct input by patients of self-reported data can capture and quantify symptoms such as fatigue and cognitive impairment, which can otherwise be difficult to evaluate. If multiple registries were to commence collection of ID/IDA data in IBD as a standard, there would be an opportunity to compare and pool data collected from multiple sources. Although this endeavor would be challenging, the ultimate benefit to the care of patients with IBD would be substantial.

ACKNOWLEDGEMENTS

Vifor Pharma provided funding for an initial meeting of authors at which the content of this article was discussed. Under the direction of the authors, AXON Communications provided writing and editorial, assistance in formatting, proofreading, copy editing and fact checking, funded by Vifor Pharma.

REFERENCES

1 **Gionchetti P**, Dignass A, Danese S, Magro Dias FJ, Rogler G, Lakatos PL, Adamina M, Ardizzone S, Buskens CJ, Sebastian S, Laureti S, Sampietro GM, Vucelic B, van der Woude CJ, Barreiro-de Acosta M, Maaser C, Portela F, Vavricka SR, Gomollón F; ECCO. 3rd European Evidence-based Consensus on the Diagnosis and Management of Crohn's Disease 2016: Part 2: Surgical Management and Special Situations. *J Crohns Colitis* 2017; **11**: 135-149 [PMID: 27660342 DOI: 10.1093/ecco-jcc/jjw169]

2 **Gomollón F**, Dignass A, Annese V, Tilg H, Van Assche G, Lindsay JO, Peyrin-Biroulet L, Cullen GJ, Daperno M, Kucharzik T, Rieder F, Almer S, Armuzzi A, Harbord M, Langhorst J, Sans M, Chowers Y, Fiorino G, Juillerat P, Mantzaris GJ, Rizzello F, Vavricka S, Gionchetti P; ECCO. 3rd European Evidence-based Consensus on the Diagnosis and Management of Crohn's Disease 2016: Part 1: Diagnosis and Medical Management. *J Crohns Colitis* 2017; **11**: 3-25 [PMID: 27660341 DOI: 10.1093/ecco-jcc/jjw168]

3 **Harbord M**, Eliakim R, Bettenworth D, Karmiris K, Katsanos K, Kopylov U, Kucharzik T, Molnár T, Raine T, Sebastian S, de Sousa HT, Dignass A, Carbonnel F; European Crohn's and Colitis Organisation [ECCO]. Third European Evidence-based Consensus on Diagnosis and Management of Ulcerative Colitis. Part 2: Current Management. *J Crohns Colitis* 2017; **11**: 769-784 [PMID: 28513805 DOI: 10.1093/ecco-jcc/jjx009]

4 **Magro F**, Gionchetti P, Eliakim R, Ardizzone S, Armuzzi A, Barreiro-de Acosta M, Burisch J, Gecse KB, Hart AL, Hindryckx P, Langner C, Limdi JK, Pellino G, Zagórowicz E, Raine T, Harbord M, Rieder F; European Crohn's and Colitis Organisation [ECCO]. Third European Evidence-based Consensus on Diagnosis and Management of Ulcerative Colitis. Part 1: Definitions, Diagnosis, Extra-intestinal Manifestations, Pregnancy, Cancer Surveillance, Surgery, and Ileo-anal Pouch Disorders. *J Crohns Colitis* 2017; **11**: 649-670 [PMID: 28158501 DOI: 10.1093/ecco-jcc/jjx008]

5 **Silverman SL**. From randomized controlled trials to observational studies. *Am J Med* 2009; **122**: 114-120 [PMID: 19185083 DOI: 10.1016/j.amjmed.2008.09.030]

6 **GBD 2015 Disease and Injury Incidence and Prevalence Collaborators**. Global, regional, and national incidence, prevalence, and years lived with disability for 310 diseases and injuries, 1990-2015: a systematic analysis for the Global Burden of Disease Study 2015. *Lancet* 2016; **388**: 1545-1602 [PMID: 27733282 DOI: 10.1016/S0140-6736(16)31678-6]

7 **Ghosh K**. Non haematological effects of iron deficiency - a perspective. *Indian J Med Sci* 2006; **60**: 30-37 [PMID: 16444088 DOI: 10.4103/0019-5359.19676]

8 **Stein J**, Dignass AU. Management of iron deficiency anemia in inflammatory bowel disease - a practical approach. *Ann Gastroenterol* 2013; **26**: 104-113 [PMID: 24714874]

9 **Danese S**, Hoffman C, Vel S, Greco M, Szabo H, Wilson B, Avedano L. Anaemia from a patient perspective in inflammatory bowel disease: results from the European Federation of Crohn's and Ulcerative Colitis Association's online survey. *Eur J Gastroenterol Hepatol* 2014; **26**: 1385-1391 [PMID: 25264983 DOI: 10.1097/MEG.0000000000000200]

10 **Ershler WB**, Chen K, Reyes EB, Dubois R. Economic burden of patients with anemia in selected diseases. *Value Health* 2005; **8**: 629-638 [PMID: 16283863 DOI: 10.1111/j.1524-4733.2005.00058.x]

11 **Stein J**, Bager P, Befrits R, Gasche C, Gudehus M, Lerebours E, Magro F, Mearin F, Mitchell D, Oldenburg B, Danese S. Anaemia management in patients with inflammatory bowel disease: routine practice across nine European countries. *Eur J Gastroenterol Hepatol* 2013; **25**: 1456-1463 [PMID: 24100539 DOI: 10.1097/MEG.0b013e328365ca7f]

12 **Swiss IBD Cohort (SIBDC)**. Zurich: Department of Gastroenterology and Hepatology, Department of Internal Medicine, University Hospital of Zurich. [cited July 31, 2017]. 2017 Available from: URL: http://www.ibdcohort.ch/

13 **The UK IBD Registry**. London: British Society of Gastroenterology; 2017 [cited July 31, 2017]. Available from: URL: http://ibdregistry.org.uk/

14 **Brooke H**, Holzmann M, Olén O, Talbäck M, Feychting M, Berglund A, Ludvigsson J, Ljung R. Enhancing evidence based medicine: Twelve tips for conducting register-based research. *MedEdPublish* 2016; **5**: 43 [DOI: 10.15694/mep.2016.000071]

15 **Dignass AU**, Gasche C, Bettenworth D, Birgegård G, Danese S, Gisbert JP, Gomollon F, Iqbal T, Katsanos K, Koutroubakis I, Magro F, Savoye G, Stein J, Vavricka S; European Crohn's and Colitis Organisation [ECCO]. European consensus on the diagnosis and management of iron deficiency and anaemia in inflammatory bowel diseases. *J Crohns Colitis* 2015; **9**: 211-222 [PMID: 25518052 DOI: 10.1093/ecco-jcc/jju009]

16 **Tinsley A**, Macklin EA, Korzenik JR, Sands BE. Validation of the functional assessment of chronic illness therapy-fatigue (FACIT-F) in patients with inflammatory bowel disease. *Aliment Pharmacol Ther* 2011; **34**: 1328-1336 [PMID: 21999576 DOI: 10.1111/j.1365-2036.2011.04871.x]

17 **Alrubaiy L**, Rikaby I, Dodds P, Hutchings HA, Williams JG. Systematic review of health-related quality of life measures for inflammatory bowel disease. *J Crohns Colitis* 2015; **9**: 284-292 [PMID: 25576752 DOI: 10.1093/ecco-jcc/jjv002]

18 **Gower-Rousseau C**, Sarter H, Savoye G, Tavernier N, Fumery M, Sandborn WJ, Feagan BG, Duhamel A, Guillon-Dellac N, Colombel JF, Peyrin-Biroulet L; and the International Programme to Develop New Indexes for Crohn's Disease (IPNIC) group; International Programme to Develop New Indexes for Crohn's Disease (IPNIC) group. Validation of the Inflammatory Bowel Disease Disability Index in a population-based cohort. *Gut* 2017; **66**: 588-596 [PMID: 26646934 DOI: 10.1136/gutjnl-2015-310151]

19 **Improve Care Now [internet]**; 2017 [cited July 31, 2017]. Available from: URL: http://www.improvecarenow.org/

20 **Crandall WV**, Margolis PA, Kappelman MD, King EC, Pratt JM, Boyle BM, Duffy LF, Grunow JE, Kim SC, Leibowitz I, Schoen BT, Colletti RB; ImproveCareNow Collaborative. Improved outcomes in a quality improvement collaborative for pediatric inflammatory bowel disease. *Pediatrics* 2012; **129**: e1030-e1041 [PMID: 22412030 DOI: 10.1542/peds.2011-1700]

21 **Abbaspour N**, Hurrell R, Kelishadi R. Review on iron and its importance for human health. *J Res Med Sci* 2014; **19**: 164-174 [PMID: 24778671]

22 **Peyrin-Biroulet L**, Williet N, Cacoub P. Guidelines on the diagnosis and treatment of iron deficiency across indications: a

systematic review. *Am J Clin Nutr* 2015; **102**: 1585-1594 [PMID: 26561626 DOI: 10.3945/ajcn.114.103366]
23 **Shah J**, Rajgor D, Pradhan S, McCready M, Zaveri A, Pietrobon R. Electronic Data Capture for Registries and Clinical Trials in Orthopaedic Surgery: Open Source versus Commercial Systems. *Clin Orthop Relat Res* 2010; **468**: 2664-2671 [PMID: 20635174 DOI: 10.1007/s11999-010-1469-3]
24 **Müller J**, Heiss KI, Oberhoffer R. Implementation of an open adoption research data management system for clinical studies. *BMC Res Notes* 2017; **10**: 252 [PMID: 28683771 DOI: 10.1186/s13104-017-2566-0]
25 **Coons SJ**, Eremenco S, Lundy JJ, O'Donohoe P, O'Gorman H, Malizia W. Capturing Patient-Reported Outcome (PRO) Data Electronically: The Past, Present, and Promise of ePRO Measurement in Clinical Trials. *Patient* 2015; **8**: 301-309 [PMID: 25300613 DOI: 10.1007/s40271-014-0090-z]
26 **Malhotra K**, Buraimoh O, Thornton J, Cullen N, Singh D, Goldberg AJ. Electronic capture of patient-reported and clinician-reported outcome measures in an elective orthopaedic setting: a retrospective cohort analysis. *BMJ Open* 2016; **6**: e011975 [PMID: 27324718 DOI: 10.1136/bmjopen-2016-011975]
27 **Competence Network Inflammatory Bowel Disease**. Call for tenders for the Project: Long-term Observation of Patients with Chronic Inflammatory Bowel Disease: Establishment of a Registry [information document]. [cited July 31, 2017]. Kiel: Competence Network Inflammatory Bowel Disease, 2013 Available from: URL: http://www.kompetenznetz-ced.de/Aktuelle_Meldung/items/ausschreibung-zur-einrichtung-eines-nationalen-ced-registers-91.html?file=tl_files/Downloads/PDF/Presse/2014/Ausschreibung_Langzeitregister_KN%20CED.pdf
28 Grupo Espanol de Trabajo en Enfermdad de Crohn y Colitis Ulcerosa [Internet]. Bilbao: Grupo Espanol de Trabajo en Enfermdad de Crohn y Colitis Ulcerosa [internet]; 2016 Características y objetivos de ENEIDA [Features and objectives of ENEIDA]. [cited July 31, 2017]. Available from: URL: http://geteccu.org/eneida/caracteristicas-y-objetivos-de-eneida
29 **Andreu M**, Márquez L, Domènech E, Gisbert JP, García V, Marín-Jiménez I, Peñalva M, Gomollón F, Calvet X, Merino O, Garcia-Planella E, Vázquez-Romero N, Esteve M, Nos P, Gutiérrez A, Vera I, Cabriada JL, Martín MD, Cañas-Ventura A, Panés J; Spanish GETECCU group (ENEIDA project). Disease severity in familial cases of IBD. *J Crohns Colitis* 2014; **8**: 234-239 [PMID: 24016462 DOI: 10.1016/j.crohns.2013.08.010]
30 **Charpentier C**, Salleron J, Savoye G, Fumery M, Merle V, Laberenne JE, Vasseur F, Dupas JL, Cortot A, Dauchet L, Peyrin-Biroulet L, Lerebours E, Colombel JF, Gower-Rousseau C. Natural history of elderly-onset inflammatory bowel disease: a population-based cohort study. *Gut* 2014; **63**: 423-432 [PMID: 23408350 DOI: 10.1136/gutjnl-2012-303864]
31 **Chouraki V**, Savoye G, Dauchet L, Vernier-Massouille G, Dupas JL, Merle V, Laberenne JE, Salomez JL, Lerebours E, Turck D, Cortot A, Gower-Rousseau C, Colombel JF. The changing pattern of Crohn's disease incidence in northern France: a continuing increase in the 10- to 19-year-old age bracket (1988-2007). *Aliment Pharmacol Ther* 2011; **33**: 1133-1142 [PMID: 21488915 DOI: 10.1111/j.1365-2036.2011.04628.x]
32 **Gower-Rousseau C**, Savoye G, Colombel JF, Peyrin-Biroulet L. Are we improving disease outcomes in IBD? A view from the epidemiology side. *Gut* 2014; **63**: 1529-1530 [PMID: 24287275 DOI: 10.1136/gutjnl-2013-306045]
33 **Gower-Rousseau C**, Vasseur F, Fumery M, Savoye G, Salleron J, Dauchet L, Turck D, Cortot A, Peyrin-Biroulet L, Colombel JF. Epidemiology of inflammatory bowel diseases: new insights from a French population-based registry (EPIMAD). *Dig Liver Dis* 2013; **45**: 89-94 [PMID: 23107487 DOI: 10.1016/j.dld.2012.09.005]
34 **Penninck E**, Fumery M, Armengol-Debeir L, Sarter H, Savoye G, Turck D, Pineton de Chambrun G, Vasseur F, Dupas JL, Lerebours E, Colombel JF, Peyrin-Biroulet L, Gower-Rousseau C; EPIMAD Group. Postoperative Complications in Pediatric Inflammatory Bowel Disease: A Population-based Study. *Inflamm Bowel Dis* 2016; **22**: 127-133 [PMID: 26355466 DOI: 10.1097/mib.0000000000000576]
35 **Jakobsson GL**, Sternegård E, Olén O, Myrelid P, Ljung R, Strid H, Halfvarson J, Ludvigsson JF. Validating inflammatory bowel disease (IBD) in the Swedish National Patient Register and the Swedish Quality Register for IBD (SWIBREG). *Scand J Gastroenterol* 2016; **52**: 216-221 [PMID: 27797278 DOI: 10.1080/00365521.2016.1246605]
36 Gesellschaft für Pädiatrische Gastroenterologie und Ernährung[internet]. Berlin: Gesellschaft für Pädiatrische Gastroenterologie und Ernährung; 2017 CEDATA-GPGE. [cited July 31, 2017]. Available from: URL: http://www.gpge.de/cedata-gpge/
37 **Martín-de-Carpi J**, Rodríguez A, Ramos E, Jiménez S, Martínez-Gómez MJ, Medina E; SPIRIT-IBD Working Group of Sociedad Española de Gastroenterología, Hepatología y Nutricion Pediátrica. Increasing incidence of pediatric inflammatory bowel disease in Spain (1996-2009): the SPIRIT Registry. *Inflamm Bowel Dis* 2013; **19**: 73-80 [PMID: 22535573 DOI: 10.1002/ibd.22980]
38 European Society for Paediatric Gastroenterology, Hepatology and Nutrition[internet]. 2017 Paediatric and adolescent inflammatory bowel diseases [cited July 31, 2017] Available from: URL: http://www.espghan.org/about-espghan/committees/gastroenterology/working-groups/paediatric-and-adolescent-ibd/
39 **de Bie C**. Pediatric Inflammatory Bowel Disease: from diagnosis to transition. PhD thesis, Erasmus Universiteit Rotterdam [internet];. 2012 [cited July 31, 2017] Available from: URL: https://repub.eur.nl/pub/37166/120907_Bie,%20Charlotte%20Irene%20de.pdf

P- Reviewer: Gassler N, Gazouli M, Sergi CM **S- Editor**: Gong ZM
L- Editor:A **E- Editor**: Ma YJ

World Journal of Gastroenterology

Submit a Manuscript: http://www.f6publishing.com

World J Gastroenterol 2018 March 14; 24(10): 1072-1083

DOI: 10.3748/wjg.v24.i10.1072

ISSN 1007-9327 (print) ISSN 2219-2840 (online)

ORIGINAL ARTICLE

Basic Study

Narrow line between benefit and harm: Additivity of hyperthermia to cisplatin cytotoxicity in different gastrointestinal cancer cells

Vaidotas Cesna, Arturas Sukovas, Aldona Jasukaitiene, Rima Naginiene, Giedrius Barauskas, Zilvinas Dambrauskas, Saulius Paskauskas, Antanas Gulbinas

Vaidotas Cesna, Giedrius Barauskas, Department of Surgery, Lithuanian University of Health Sciences, Kaunas LT-50161, Lithuania

Arturas Sukovas, Saulius Paskauskas, Department of Obstetrics and Gynecology, Lithuanian University of Health Sciences, Kaunas LT-50161, Lithuania

Aldona Jasukaitiene, Zilvinas Dambrauskas, Antanas Gulbinas, Institute for Digestive Research, Lithuanian University of Health Sciences, Kaunas LT-50161, Lithuania

Rima Naginiene, Neuroscience Institute, Lithuanian University of Health Sciences, Kaunas LT-50161, Lithuania

ORCID number: Vaidotas Cesna (0000-0003-4719-8483); Arturas Sukovas (0000-0001-7007-3959); Aldona Jasukaitiene (0000-0002-4606-1963); Rima Naginiene (0000-0001-5770-2618); Giedrius Barauskas (0000-0002-4321-7280); Zilvinas Dambrauskas (0000-0003-2173-1294); Saulius Paskauskas (0000-0001-9930-4124); Antanas Gulbinas (0000-0002-6683-1339).

Author contributions: Cesna V, Sukovas A analyzed the data and drafted the manuscript; Jasukaitiene A performed most of experiments; intracellular cisplatin concentration analysis was performed by Naginiene R; Barauskas G, Paskauskas S and Gulbinas A designed and coordinated the research; Gulbinas A and Dambrauskas Z revised the manuscript for important intellectual content; all authors have read and approved the final version to be published.

Supported by the Research Council of Lithuania, No. SEN-01/2015.

Institutional review board statement: The study was reviewed and approved by the Kaunas Regional Biomedical Research Ethics Committee.

Conflict-of-interest statement: All authors have nothing to disclose.

Data sharing statement: No additional data are available.

Manuscript source: Unsolicited manuscript

Correspondence to: Zilvinas Dambrauskas, MD, PhD, Lecturer, Professor, Surgeon, Lithuanian University of Health Sciences, Institute for Digestive Research, Eiveniu str., 4, Kaunas LT-50161, Lithuania. zilvinas.dambrauskas@lsmuni.lt
Telephone: +370-68-669255
Fax: +370-37-326179

Received: December 2, 2017
Peer-review started: December 2, 2017
First decision: December 27, 2017
Revised: January 2, 2018
Accepted: January 16, 2018
Article in press: January 16, 2018
Published online: March 14, 2018

Abstract

AIM

To investigate the response to hyperthermia and chemotherapy, analyzing apoptosis, cytotoxicity, and cisplatin concentration in different digestive system cancer cells.

METHODS

AGS (gastric cancer cell line), Caco-2 (colon cancer cell line) and T3M4 (pancreatic cancer cell line) were

treated by cisplatin and different temperature setting (37 ℃ to 45 ℃) either in isolation, or in combination. Treatment lasted for one hour. 48 h after the treatment viability was evaluated by MTT, cell apoptosis by Annexin V-PE and 7ADD flow cytometry. Intracellular cisplatin concentration was measured immediately after the treatment, using mass spectrometry. Isobologram analysis was performed to evaluate the mathematical combined effect of temperature and cisplatin.

RESULTS

AGS cells were the most sensitive to isolated application of hyperthermia. Hyperthermia, in addition to cisplatin treatment, did not provoke a synergistic effect at intervals from 37 ℃ to 41 ℃ in neither cancer cell line. However, a temperature of 43 ℃ enhanced cisplatin cytotoxicity for Caco-2 cells. Moreover, isobologram analysis revealed mathematical antagonistic effects of cisplatin and temperature combined treatment in AGS cells; variations between synergistic, additive, and antagonistic effects in Caco-2 cells; and additive and antagonistic effects in T3M4 cells. Combined treatment enhanced initiation of cell apoptosis in AGS, Caco-2, and T3M4 cells by 61%, 20%, and 19% respectively. The increase of intracellular cisplatin concentration was observed at 43 ℃ by 30%, 20%, and 18% in AGS, Caco-2, and T3M4 cells, respectively.

CONCLUSION

In addition to cisplatin, hyperthermia up to 43 ℃ does not affect the viability of cancer cells in a synergistic manner.

Key words: Hyperthermal intraperitoneal chemotherapy; Cisplatin; Hyperthermia; Isobolograms; Gastric cancer; Pancreatic cancer; Colon cancer

Core tip: Hyperthermal intraperitoneal chemotherapy is widely used as a standard treatment option for peritoneum invading gastrointestinal cancer. Our *in vitro* results suggest that optimal temperature has to be taken into consideration for achieving optimal therapeutic effect. In addition to cisplatin, hyperthermia up to 43 ℃ does not affect the viability of AGS, Caco-2, and T3M4 cells in a synergistic manner. However, some regimens of hyperthermia and cisplatin treatment are beneficial regarding an increase in intracellular cisplatin concentration and enhancement apoptosis of gastrointestinal cancer cells.

Cesna V, Sukovas A, Jasukaitiene A, Naginiene R, Barauskas G, Dambrauskas Z, Paskauskas S, Gulbinas A. Narrow line between benefit and harm: Additivity of hyperthermia to cisplatin cytotoxicity in different gastrointestinal cancer cells. *World J Gastroenterol* 2018; 24(10): 1072-1083 Available from: URL: http://www.wjgnet.com/1007-9327/full/v24/i10/1072.htm DOI: http://dx.doi.org/10.3748/wjg.v24.i10.1072

INTRODUCTION

For the past two decades, hyperthermal intraperitoneal chemotherapy (HIPEC) has been considered as a treatment option for peritoneum invading gastrointestinal cancers[1]. Various studies have demonstrated improved survival rates for gastric[2] and colorectal cancers[3-5]. The clinical application of hyperthermia is based on the assumption that it may enhance the effect of the chemotherapy, especially cisplatin-based treatments[6-8]. There are some experimental studies providing evidence that hyperthermia can affect cell membranes, cytoskeletons, synthesis of macromolecules, increase drug-induced DNA damage, and inhibit the repair of drug-induced DNA damage[9]. Hyperthermia may provide higher local cisplatin concentrations in tissues, indicating the pharmacokinetic advantage of its use and reduction of systemic toxicity[10]. Hyperthermia-induced PARP blockade can increase chemotherapy-induced damage in BRCA-competent cells of ovarian and colon cancer[11].

However, the results of available studies on the synergy of hyperthermia and cisplatin chemotoxicity, initiation of apoptosis, and intracellular accumulation of cisplatin in different gastrointestinal cancer cells are controversial. The opposite effect of hyperthermia on cisplatin sensitivity was observed in mismatch repair deficiency and mismatch repair proficiency in colon cancer cell lines[12]. Isolated hyperthermia only temporarily inhibited cell proliferation without cytotoxic effects on gastric cancer cell lines. However, a synergistic effect of hyperthermia and chemotherapy on inhibiting proliferation and induction of cell death via the apoptotic pathway was reported[13]. Interestingly, the hyperthermia-mediated increase of cellular accumulation of cisplatin and persistent DNA damage in gastric cancer cells was observed only with the addition of tumor necrosis factor[14]. The expression of heat shock genes and proteins provides an adaptive mechanism for stress tolerance, allowing cells to survive non-physiologic conditions. However, the same adaptive mechanism can ultimately favor malignant transformation by interfering with pathways that regulate cell growth and apoptosis. Cytoprotection and thermotolerance raised the concern that heat-treated tumor cells might also be resistant to attack by immune effector mechanisms[15]. Data on the additive effect of hyperthermia in terms of enhanced chemo-cytotoxicity in cancer cells of pancreatic origin are scarce.

Therefore, the aim of this study was to analyze the additivity of hyperthermia to cisplatin effects in gastric, pancreatic, and colorectal cancer cell lines evaluating cell cytotoxicity, apoptosis, and intracellular cisplatin concentration.

MATERIALS AND METHODS

Human cancer cell lines

The AGS and Caco-2 cell lines were purchased from

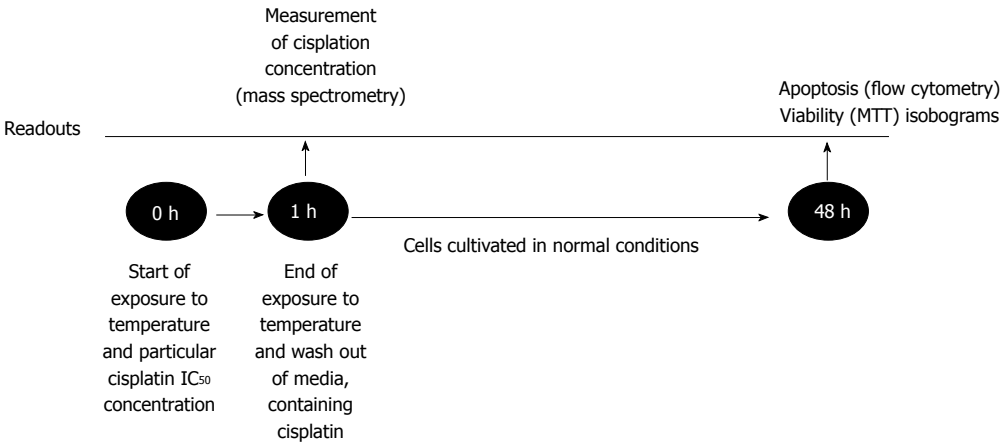

Figure 1 Design of experiment.

American Type Cell Culture (ATCC Manassas, VA, United States). AGS cell line is derived from a gastric adenocarcinoma of the stomach of a 54 year-old Caucasian female with no prior anti-cancer treatment. Caco-2 cells were isolated from a primary colonic tumor in a 72-year-old Caucasian male using the explant culture technique. Forms moderately well differentiated adenocarcinomas consistent with colonic primary grade Ⅱ, in nude mice. T3M4 cell line was obtained as a gift from the European Pancreas Center (Heidelberg, Germany). This cell line was derived from a lymph node metastasis of the Japanese male patient, diagnosed with pancreatic ductal adenocarcinoma. It is characterized as pancreatic adenocarcinoma producing CEA, K-ras activated, and with slow cell growth. Cells were grown in RPMI medium (Gibco/Invitrogen, Carlsbad, CA, United States) with the addition of 10% fetal bovine serum (Gibco/Invitrogen) and 1% penicillin/streptomycin solution (Gibco/Invitrogen). Flasks with cells were cultured in a humid incubator with a CO_2 level of 5% and temperature of 37 ℃.

Design of experiment

Cancer cells were cultivated for 24 h in the conditions described above. Afterwards, cells were treated by one of two separate factors: temperature (37 ℃, 38 ℃, 39 ℃, 40 ℃, 41 ℃, 42 ℃, 43 ℃, 44 ℃, 45 ℃) or IC_{50} dose of cisplatin, which was specifically determined for each cell line. Moreover, the combination of hyperthermia and cisplatin treatment was applied (Figure 1). The duration of treatment was 1 h as it reflected the treatment time under the clinical conditions of HIPEC. Cells were heated in humid incubators at particular temperature regimens. When temperature of the media reached desired level, we started the countdown of one hour exposure. Medium temperature was controlled by the electronic thermometer. Following the treatment, the medium was changed, and cells were cultivated for 48 h under the conditions as previously described. Afterwards, MTT and flow cytometry were performed (see "MTT assay" and "Cell apoptosis"). All experiments were repeated at least three times.

MTT assay

Cytotoxicity of cisplatin or/and hyperthermia was determined by MTT [3-(4, 5-dimethylthiazol-2-Yl)-2, 5-diphenyltetrazolium bromide] (Gibco/Invitrogen) assay. The plate was incubated for 4 h at 37 ℃ after 5 mg/mL of the MTT reagent was added to the wells. Then the supernatant was removed, and DMSO (dimethyl sulfoxide) (Carl Roth GmbH, Karlsruhe, Germany) was added to solubilize the resulting formazan crystals. Absorbance measurements were made at 570 nm on the Sunrise spectrophotometer (Tecan GmbH, Grodig, Austria).

Cell apoptosis

The changes in apoptosis were evaluated after treatment of the cells by hyperthermia (43 ℃) and the previously determined IC_{50} of cisplatin (specific for particular cell line). Untreated cisplatin cells and normothermia (37 ℃) cultivated cells were defined as controls. Forty-eight hours after the experiment (Figure 1), the rate of apoptosis was determined by flow cytometer Guava Nexin Annexin V Assay (Merck, Millipore United States and Canada). All the procedures were performed according to the manufacturer's instructions. Samples were measured using a Guava Personal Cell Analysis (PCA) Flow Cytometer (Merck, Millipore) and CytoSoft software.

Intracellular concentration of cisplatin

Immediately after the experiment, the cell lysate samples were diluted ten times with high purity deionized water. Concentration of total intracellular cisplatin was analyzed by inductively coupled plasma mass spectrometer (ICP-MS) NexION™ 300D (PerkinElmer, United States) equipped with nickel cones and a quartz cyclonic spray chamber as a sample introduction system and using collision mode kinetic energy discrimination (KED) with helium gas (purity ⩾ 99.999%) to remove polyatomic interferences.

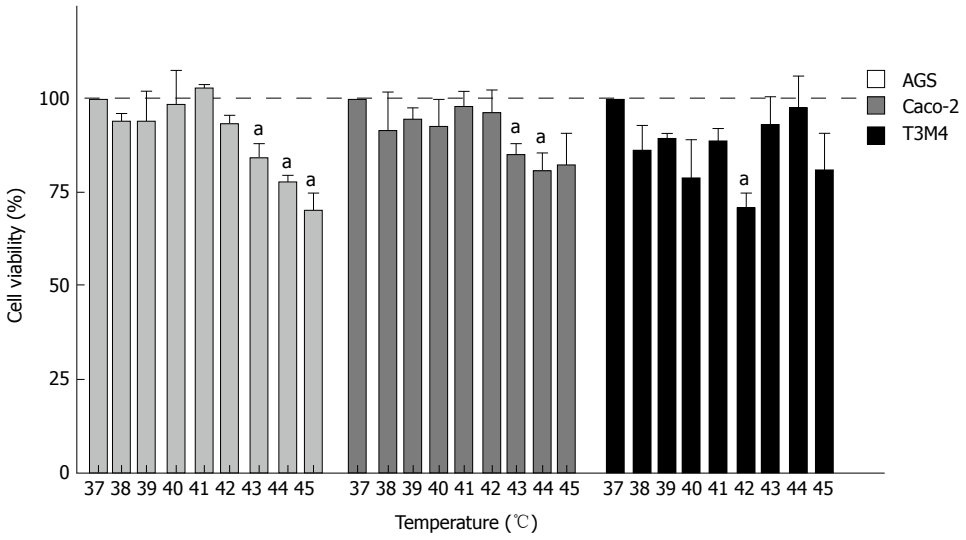

Figure 2 The different effect of the temperature on cancer cell viability. Following a one-hour exposure of AGS, Caco-2, and T3M4 cells to temperatures ranging from 37 ℃ to 42 ℃, there were no significant viability changes. Starting at 43 ℃, viability gradually decreased in AGS and Caco-2 cells. Activation of viability was evident in T3M4 cells at temperatures of 43 ℃ and 44 ℃. All data were compared with a control group (viability of cells at temperature of 37 ℃ set as 100%). Statistical analysis was performed using the Mann-Whitney *U* test comparing selected groups to the control. $^{a}P < 0.05$ *vs* control.

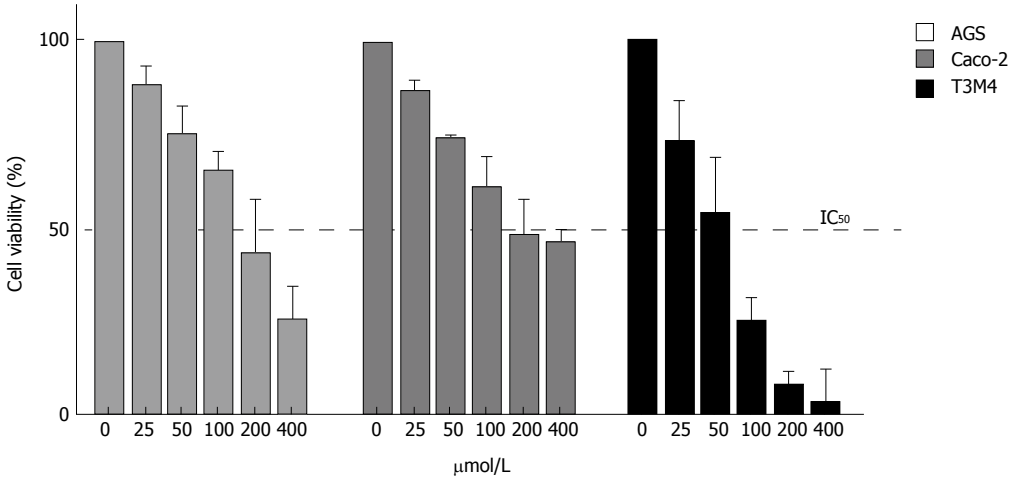

Figure 3 The influence of different cisplatin doses on cancer cell viability. Exposure to gradually increasing doses of cisplatin resulted in a linear decrease of viability in all cancer cell lines. T3M4 cells were the most sensitive to cisplatin, followed by Caco-2 and AGS cells. All data were compared with the control group (viability of cells at 37 ℃ set as 100%). Data are presented as the mean ± SE from ≥ 3 replicates.

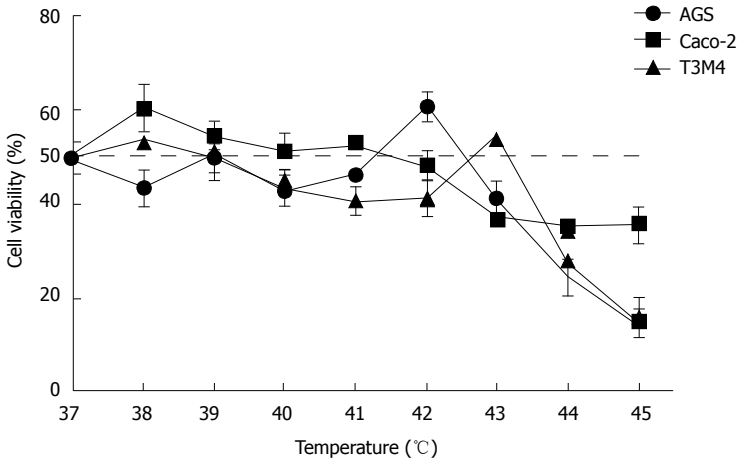

Figure 4 Effect of temperature and cisplatin (IC_{50}) combinations on cancer cell viability. The increase of temperature had no significant additional effect on cancer cell viability with the exception of extreme hyperthermia (44 ℃-45 ℃). Peaks of enhanced viability were observed in AGS and T3M4 cells at temperatures of 42 ℃ and 43 ℃. Data are equalized to control (untreated cells) as 100% and shown in percentages. Dashed line shows IC_{50}.

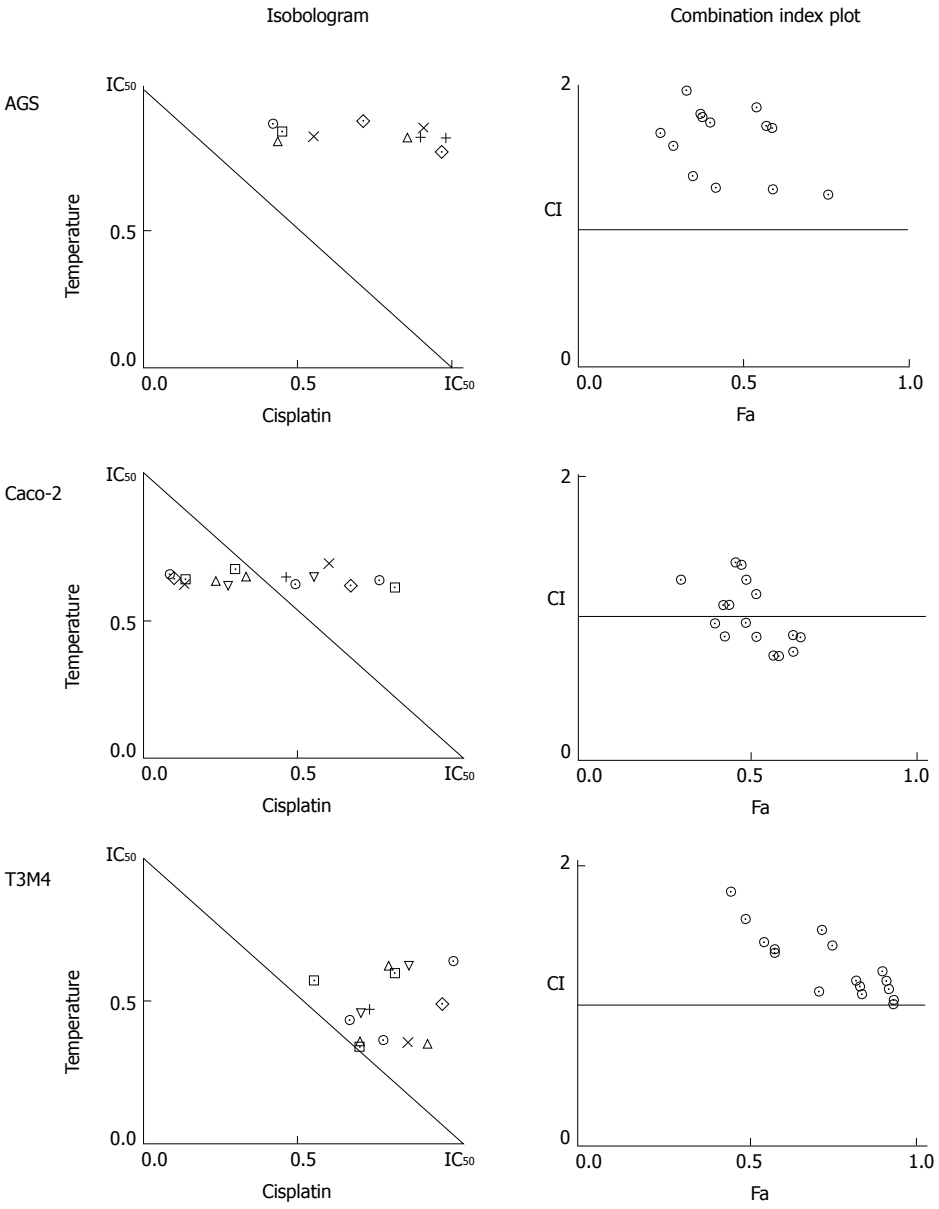

Figure 5 Interaction of temperature and cisplatin using the isobologram method for cancer cell viability. Mathematically revealed combined effects of hyperthermia and cisplatin differ in AGS, Caco-2, and T3M4 cell lines. The isobologram represents the interaction between cisplatin and temperature resulting in inhibition of cancer cell growth. The solid line in the diagram (Combination Index = 1) indicates the alignment of theoretical values of an additive interaction between two effectors and represents calculated conditions required to inhibit cell growth by 50%. Mathematically calculated IC_{50} for AGS cells: temperature 51 ℃, cisplatin 159 μmol/L; Caco-2 cells: temperature 66 ℃, cisplatin 328 μmol/L; T3M4 cells: temperature 61 ℃, cisplatin 0 μmol/L. Treatment combination points falling above the line indicate mathematical antagonism (below synergism, on the line additivity). Combination points that are distant from the line are not shown. Tables on the right represent the CI of selected combinations.

The calibration graphs for determination of Platinum by ICP-MS were prepared in the range of 0-50 ng/mL using Pure Plus 10 mg/L Multi-Element calibration standard 4 (PerkinElmer, United States). The working conditions of the spectrometer were optimized daily in order to obtain the maximal sensitivity and stability.

Isobologram analysis

To identify the confidence limits for the additive action of hyperthermia and cisplatin, isobologram analysis was applied. Data for analysis was obtained from the MTT test (Figure 4). Temperature data points of 38 ℃, 39 ℃, 40 ℃, 41 ℃, 42 ℃, 43 ℃, 44 ℃, and 45 ℃, and cisplatin concentration data points of 25 μmol/L, 50 μmol/L, 100 μmol/L, 200 μmol/L, and 400 μmol/L were used to define the dose effect curve for temperature and cisplatin, respectively. For combined treatment analysis, the following combinations of factors were used: 39 ℃ + 50 μmol/L; 39 ℃ + 100 μmol/L; 39 ℃ + 200 μmol/L; 40 ℃ + 50 μmol/L; 40 ℃ + 100 μmol/L; 40 ℃ + 200 μmol/L; 41 ℃ + 50 μmol/L; 41 ℃ + 100 μmol/L; 41 ℃ + 200 μmol/L; 42 ℃ + 50 μmol/L; 42 ℃ + 100 μmol/L; 42 ℃ + 200 μmol/L; 43 ℃ + 50 μmol/L; 43 ℃ + 100 μmol/L; 43 ℃ + 200 μmol/L; 44 ℃ + 50 μmol/L; 44 ℃ + 100 μmol/L; 44 ℃ + 200 μmol/L. The Chou median effect equation was used[16]. It provides

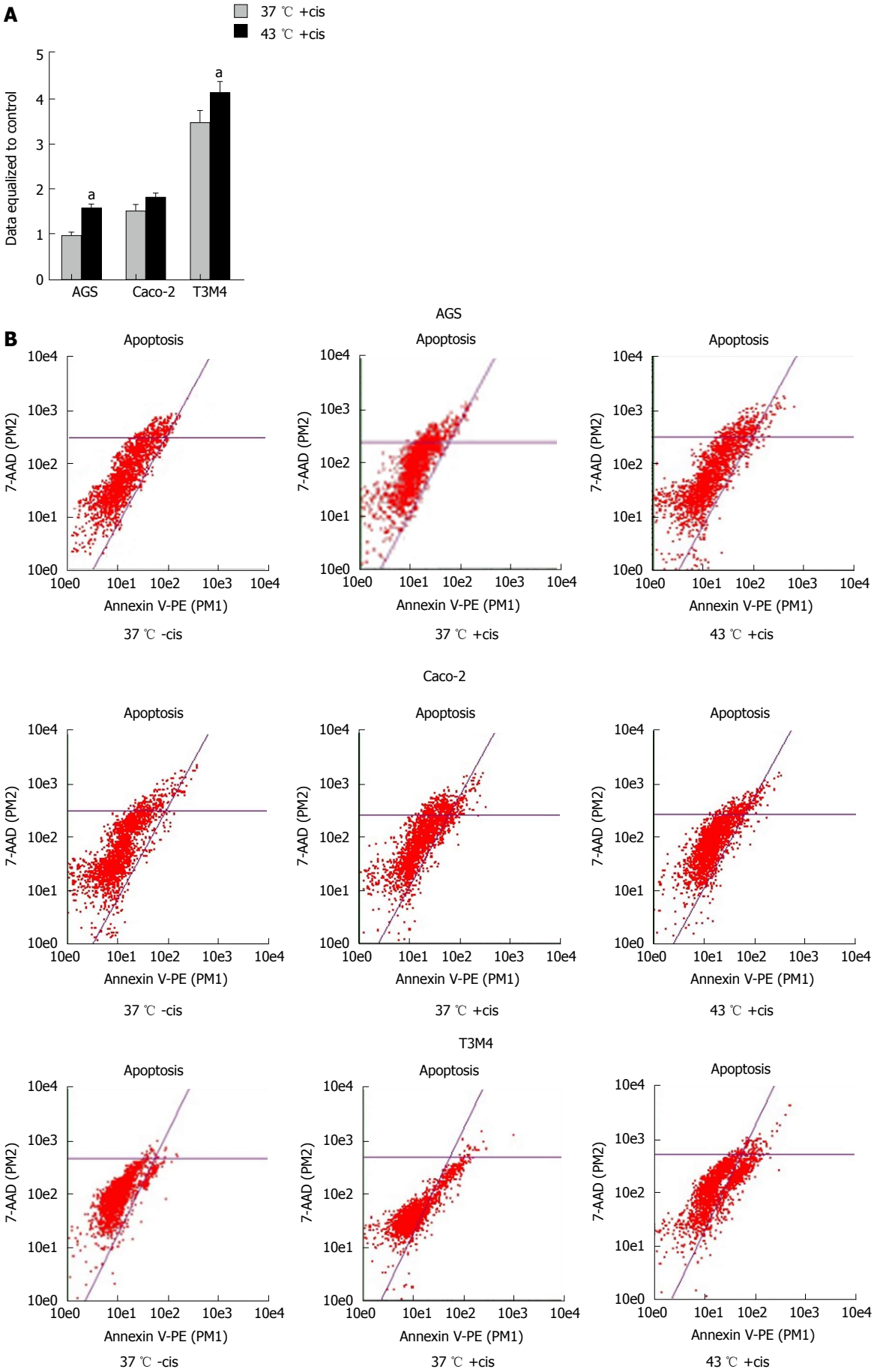

Figure 6 Apoptotic effect of temperature and cisplatin in cancer cells. A: Early apoptosis was significantly induced by hyperthermia in cisplatin-treated cells, with the exception of Caco-2 cells, where temperature had no significant role. The dashed line represents control rates of apoptosis in untreated cells. Statistical analysis was performed using the Mann-Whitney *U* test. $^{a}P < 0.05$. B: Dot plots presenting change of apoptosis in cisplatin untreated/treated cells and cultivated in hyperthermia. "-cis": Cisplatin untreated cells; "+cis": Cisplatin treated cells.

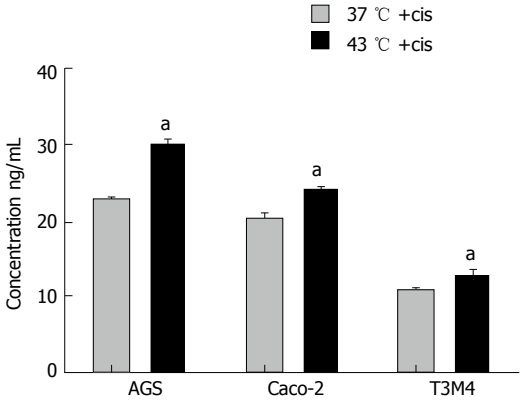

Figure 7 The change of the intracellular cisplatin concentration. Temperature of 43 ℃ significantly increased the intracellular concentration of cisplatin in all analyzed cell lines. Data are shown as concentrations of ng/mL. Statistical analysis was performed using the Mann-Whitney *U* test. $^{a}P < 0.05$. "+cis": Cisplatin treated cells.

the theoretical basis for the combination index (CI), which enabled quantification of drug interaction affects defining synergism (CI < 1), additivity (CI = 1), or antagonism (CI > 1). The CompuSyn software (CompuSyn, Inc., Paramus, NJ, United States) was used for calculations.

RESULTS

Different cell lines have specific responses to hyperthermia

To evaluate the effect of hyperthermia *per se* on different cancer cells *in vitro*, we examined the response of the AGS, Caco-2, and T3M4 cell lines to temperature using a stepwise increase of one degree ranging from 37 ℃ to 45 ℃. Cell viability was determined by MTT assay. Every cell line demonstrated a different pattern of response to hyperthermia (Figure 2). AGS cells were the most sensitive one to hyperthermia, where a temperature rise from 41 ℃ to 45 ℃ gradually decreased its viability by 30%. In the 37 ℃ to 41 ℃ interval, the viability stayed constant. Cells affected by 43 ℃, 44 ℃, and 45 ℃ dropped their viability rate by 16%, 22 ℃, and 30%, respectively, as compared to the control (37 ℃). A temperature increase from 37 ℃ to 42 ℃ had no significant effect on Caco-2 cells, but at 43 ℃ and 44 ℃, its viability dropped by 14% and 20%, respectively, but stayed constant at higher temperatures. The response of T3M4 cells to the changes of temperature was different. Temperatures from 37 ℃ to 42 ℃ decreased its viability by 30%. At 43 ℃, the viability of T3M4 cells sharply increased by 20% and stayed at this level in higher temperatures. Overall, only the AGS cell line responded to hyperthermia as implied, with gradual inhibition of cell viability.

Different cell lines respond to cisplatin in a comparable linear pattern but with specific sensitivity

Cisplatin induced a dose-dependent suppressor effect on cancer cell viability, with a similar linear response in the AGS, Caco-2, and T3M4 cell lines. Pancreatic cancer cells (T3M4) were the most sensitive, revealing cisplatin IC_{50} at 48 μmol/L. The IC_{50} for Caco-2 was 194 μmol/L, and for AGS, it was 182 μmol/L (Figure 3).

Insufficient temperature regimens can be detrimental in combined hyperthermic chemotherapy

Previously determined IC_{50} doses of cisplatin were used for particular cell lines during this experiment. Simultaneous exposure of cells to hyperthermic conditions and cisplatin triggered different response in AGS, Caco-2, and T3M4 cells (Figure 4). Overall, temperatures ranging from 37 ℃ to 41 ℃ had no detectable additive effect to cisplatin cytotoxicity. Interestingly, we observed peaks of viability in AGS (42 ℃, increase by 33%) and T3M4 (43 ℃, increase by 32%) cells. Higher temperatures, in addition to cisplatin exposure, inhibited cell growth dramatically; AGS viability dropped by 70% and T3M4 dropped by 76% at 45 ℃. Application of hyperthermia in addition to cisplatin in the Caco-2 cell line gradually improved the cytotoxic effect and decreased the viability of cells by one-fourth from 43 ℃ to 45 ℃. In summary, application of hyperthermia (43 ℃ and higher) in addition to cisplatin might enhance its cytotoxic effect in the Caco-2 cell line. However, lower (*e.g.*, < 43 ℃) temperature regimens may even promote cell proliferation and worsen expected hyperthermal chemotherapy effects in AGS and T3M4 cell lines.

Isobologram analysis: Unpredictable response of the cells to hyperthermia and cisplatin

We constructed isobolograms to reveal if the combined application of hyperthermia and cisplatin had synergistic, antagonistic, or additive effects. Combination of temperature and cisplatin was strongly antagonistic for AGS cells in all studied data points. Combined application of hyperthermia and cisplatin was tripled in Caco-2 cells: synergistic (at 40 ℃ with 50 μmol/L and 100 μmol/L of cisplatin, at 43 ℃ with 50 μmol/L, 100 μmol/L, and 200 μmol/L cisplatin, at 44 ℃ with 50 μmol/L , 100 μmol/L, and 200 μmol/L of cisplatin), additive (at 39 ℃ with 100 μmol/L of cisplatin, at 41 ℃ with 100 μmol/L cisplatin, and at 42 ℃ with 50 μmol/L and 100 μmol/L of cisplatin), and antagonistic (at 39 ℃ with 200 μmol/L of cisplatin, at 40 ℃ with 200 μmol/L cisplatin, at 41 ℃ with 50 μmol/L and 200 μmol/L cisplatin, and at 42 ℃ with 200 μmol/L of cisplatin). Combined treatment of T3M4 at 41 ℃ with 200 μmol/L cisplatin, at 42 ℃ with 50 μmol/L cisplatin, and at 44 ℃ with 100 μmol/L and 200 μmol/L of cisplatin had an additive effect. The remaining combinations were antagonistic (Figure 5).

Hyperthermia addition to cisplatin enhances rates of early apoptosis

Annexin V-PE flow cytometry analysis was performed to evaluate rates of early apoptosis. Cisplatin induced early

Table 1 Overview of results

Cell line	Effect of temperature at 43 ℃ on cancer cells viability	IC_{50} dose of cisplatin	Combined effect of temperature, at 43 ℃ and IC_{50} dose of cisplatin on cancer cells viability	Effect of temperature in addition to IC_{50} dose of cisplatin on cancer cell apoptosis	Effect of temperature on intracellular cisplatin concentration
AGS	↓↓	182	↓	↑	↑↑↑
Caco-2	↓	194	↓↓	-	↑↑
T3M4	-	48	-	↑	↑

The number of the arrows represents strength of effect.

apoptosis in Caco-2 and T3M4 cells 1.5-fold and 3.4-fold, respectively. The number of dead/late apoptotic cells was insignificant in the following groups: 0.5% of Caco-2 cells and 2.9% of T3M4 cells. Hyperthermia of 43 ℃ in addition to cisplatin induced early apoptosis as compared to cells treated in normothermia by 20% in Caco-2 (1% of dead cells) and 19% (3.9% dead cells) in T3M4, respectively. Interestingly, early apoptosis was not significantly induced by isolated cisplatin treatment in AGS cells. Rates of AGS early apoptosis were not significantly induced by an isolated cisplatin treatment. However, application of combined treatment with hyperthermia and cisplatin increased early apoptosis by 61% (0.4% dead cells) (Figure 6).

Hyperthermia increases intracellular cisplatin concentration

Hypothesizing that hyperthermia promotes delivery of cisplatin to cancer cells, we aimed to measure intracellular cisplatin concentrations. Analysis was performed immediately following a one-hour exposure to the IC_{50} of cisplatin at 37 ℃ and 43 ℃. Overall, 43 ℃ promoted an increase of intracellular cisplatin concentration. The concentration was significantly increased in AGS, Caco-2, and T3M4 cells by 30%, 20%, and 18%, respectively (Figure 7).

DISCUSSION

Hyperthermal intraperitoneal chemotherapy has been applied to treat peritoneal carcinomatosis for gastric[17-19], colorectal[20], ovarian[21], and peritoneal mesothelioma[22] and has aided in prolonged long-term survival in selected patients[23-26]. In HIPEC, intraperitoneal free cancer cells and the serous surface of the bowel and peritoneum are exposed to high concentrations of chemotherapy agents. Hyperthermia itself may affect cell cytoskeletons, cell membranes, synthesis of macromolecules, and DNA repair mechanisms[9].

As the origin, genotypes, and phenotypes of free cancer cells may be quite different, it seems unreasonable to treat all peritoneal metastases the same way. Until now, basic information regarding the contribution of hyperthermia to intraperitoneal chemotherapeutic agents in different gastrointestinal cancers is poor and controversial. In this *in vitro* study, we have applied hyperthermia and chemotherapy for 1 h in order to mimic clinical conditions. We have performed our aimed readouts at 48 h following the experiment as the earlier readouts have not proven any changes.

We have chosen three most common peritoneum invading GI cancers in our study, selecting one cancer cell line per cancer type. It is known that various cancer cells of same cancer type are different in the manner of apoptosis, biomarker expression etc [27]. This study is an overview, which leads to a better knowledge of gastric, pancreatic and colorectal cancer cell response to simultaneous hyperthermia and cisplatin treatment.

Until now, our analyzed cells are well examined in various aspects. AGS cells in 516 analyzed genes, have 40 mutations, like KRAS, WNK1 and WNK2[28]. Overexpression of HER-2, EGFR, VEGF, Bcl-2 biomarkers was investigated in gastric cancer cells[29]. Mutations of *SMAD4* and *TP53* genes and overexpression of *ILF3*, *TIMP3* genes are present in Caco-2 cells[30-32] . T3M4 are the least examined cells. No known gene mutations were found[33] and they are known to overexpress growth factors as FGFR4[34].

Our experiments revealed the differences of cell viability in response to isolated hyperthermia. We even observed positive effects of isolated hyperthermia on the viability of pancreatic cancer cells. We hypothesize that this effect could be related to the activation of the cytoprotective heat shock proteins (HSP), an effect described in other studies[35]. It is known that higher temperatures can enhance thermotolerance by activating HSPs[36]. However, gastric cancer cells (AGS) and colon cancer cells (Caco-2) responded to hyperthermia with a significant drop of viability at 43 ℃. One study demonstrated that hyperthermia alone can significantly reduce viability of the Colon 26 cancer cells[37]. The investigation of the effect of local heat used for ablation of tumor nodules showed that exposing cultured Caco-2 cells to 48 ℃ for 2 h resulted in an approximately 80% reduction of cell viability[38]. However, in our study, the viability of Caco-2 cells decreased only by 14% after exposure to 43 ℃ for 1 h.

Hyperthermia may enhance the effect of chemotherapy, especially cisplatin-based treatments[6-8]. Ferraro *et al*[39] studied the effects of hyperthermia and cisplatin on model protein hen eggs and revealed that increased temperature enhanced cisplatin cytotoxicity.

Tang *et al*[13] have shown a synergistic effect of hyperthermia and chemotherapy inhibiting

proliferation in six gastric cancer cell lines, including AGS, in a certain range of chemoagent (cisplatin) concentration. Moreover, hyperthermia, in addition to chemotherapy, induced cell apoptosis as the major type of death. MicroRNA-218 upregulation and increased chemosensitivity were observed in gastric cancer cells after exposing them to hyperthermal conditions[40]. However, in our study, only temperatures higher than 43 ℃ in addition to cisplatin exposure inhibited cell growth. In the isobologram analysis, the combination of temperature and cisplatin was antagonistic for AGS cells. On the contrary, AGS cells showed an increased viability of 33% at 42 ℃. This is an important observation as it may highlight the possibility that technically incorrect temperature regimens may activate metabolism of cancer cells and increase their resistance to chemotherapy. Interestingly, we observed that application of cisplatin to gastric cancer (AGS) cells for one h had no significant impact on cell apoptosis. However, the combination of cisplatin and hyperthermia (43 ℃) increased the affect by 61%. Our results suggest that temperature and cisplatin are not always acting in synergy as was shown by isobolograms.

Previous *in vitro* investigations have revealed that the response of the colon cancer cells to hyperthermia and chemotherapeutic drug differ by cell type. Some authors have shown that hyperthermia alone significantly decreased the viability of the Colon 26 cancer cells[37], and the cytotoxic effect of cisplatin[41] was enhanced at hyperthermal conditions. After exposure to 43 ℃, the activity of oxaliplatin markedly and rapidly increased, indicating its inhibiting potential in Colon 26 cells[42]. Significant synergy of hyperthermia and chemotherapy was detected in CX-1 cells[43] in similar experimental conditions (42 ℃ for 1 h). Some authors described similar results in HCT116+ch2 (MMR-) cells that were resistant to heat treatment at temperatures of 41 ℃ and 42 ℃[12]. The exposition of the colon carcinoma cell lines CX-1 and HTC 116 to 42 ℃ for 1 h revealed no change in cell viability[13,43]. Moreover, HCT116+ch2 (MMR-) cells exposed to a mild heat were 1.42-fold more resistant to cisplatin[12]. We observed that the addition of hyperthermia to cisplatin treatment had a slight positive influence on Caco-2 cell viability. At 43 ℃, cisplatin had an insignificant effect regarding apoptosis, whereas intracellular cisplatin concentration was elevated by 26% as compared to the control. Isobologram analysis showed approximately 50% of selected cisplatin and temperature treatment combinations acted in a synergistic manner, indicating that some of hyperthermic chemotherapy regimens might be useful.

Recent studies reported that hyperthermia increased sensitivity to gemcitabine[44] and enhanced gemcitabine-related apoptotic cell death in pancreatic cancer cells[45]. Moreover, the improved drug delivery and antitumor effects in combination with mild hyperthermia were reported [46].

The combined cytotoxic effect of cisplatin and hyperthermia in T3M4 cells was evident only when the temperature was higher than 43 ℃. These cells were the most sensitive to cisplatin with the lowest IC_{50}. Cisplatin amplified apoptosis by 3.4-fold and hyperthermia increased the effect by 19%; however, it was 3-fold less in the gastric cancer cell line. Similar to AGS cells, T3M4 isobologram analysis revealed that the combination of treatments acted in an antagonistic manner in most of the selected combinations; however, in few of them, the additive effect of the two agents was revealed. An extremely limited increase of intracellular cisplatin concentration in hyperthermia could be observed in pancreatic cancer cells. Our experiments elucidated that the response of T3M4 cells differs from other studied gastrointestinal cancer cells (AGS and Caco-2). A review by Loggie *et al*[47] postulated that hyperthermia combined with chemotherapy is probably beneficial for less aggressive tumors and should be the standard of care for appendiceal and colorectal cancers.

Caco-2 cell results varied from the other cells in our study. In some cases, they acted in unpredictable manner. One of the possible explanations for this discrepancy, would be that Caco-2 cells can differentiate their phenotype prior to post-confluence stage, and lead to the change of morphology, degree of differentiation etc[48].

In summary, we have proven that the role of hyperthermia in addition to cisplatin is different in gastric, colonic, and pancreatic cancer cells. The overview of the basic results is shown in Table 1. Different cancer cells respond to combined treatments in different manners, and temperature-induced apoptosis is initiated by various pathways[49].

In conclusion, hyperthermia up to 43 ℃ in addition to cisplatin does not influence AGS, Caco-2, and T3M4 cell viability in a synergistic manner. However, some regimens of hyperthermia and cisplatin treatment are beneficial regarding the apoptotic response and an increase of intracellular cisplatin concentration.

ARTICLE HIGHLIGHTS

Research background

Hyperthermal intraperitoneal chemotherapy is an option to treat peritoneum invading gastrointestinal cancer. Until now the results of hyperthermal intraperitoneal chemotherapy (HIPEC) treatment are controversy, needing unification in selected parameters of the treatment. In different cancer centers, the procedure varies in time setting, hyperthermia level and different chemotherapy drugs are used.

Research motivation

As HIPEC is widely used in clinical practice, still there is a lack of studies, analyzing the impact of hyperthermia and cisplatin to cancer cells. The cellular response to the treatment is still not clear. There is no clear data defining optimal timing and temperature of the procedure.

Research objectives

Our objective was to analyze gastric, pancreatic and colorectal cancer cells response to hyperthermia and cisplatin treatment regarding viability, change of intracellular cisplatin concentration and apoptosis rate.

Research methods

We used AGS (gastric cancer), T3M4 (pancreatic cancer) and Caco-2 (colorectal cancer) cells. Mimicking HIPEC procedure, cells were treated with specific to each cell line IC_{50} dose of cisplatin at the temperature regimens ranging from 37 ℃ to 45 ℃. Treatment lasted for one hour. Later cells were harvested in normothermia, changing cisplatin containing media to fresh one. Immediately after experiment, intracellular cisplatin concentration was measured, using mass spectrometer analysis. For other readouts cells were harvested for 48 hours in normal conditions. MTT test was performed for cellular viability evaluation and isobologram analysis. We used flow cytometry to determine apoptosis change of hyperthermia and cisplatin treatment.

Research results

Cells responded to hyperthermia (ranging from 38 ℃ to 45 ℃) in a different manner. Viability of AGS cells was the most hyperthermia-dependent, decreasing by 30% (from 41 ℃ to 45 ℃). Caco-2 cell viability had no change in the interval from 38 ℃ to 42 ℃. Higher temperature regimens dropped its viability rate by 14%-20%. T3M4 cells reacted differently. Viability dropped until 42 ℃, but at higher temperature regimens, we observed increase of viability. While in simultaneous hyperthermia and cisplatin treatment, we observed no change of viability until 41 ℃ in all cancer cells. Higher temperatures inhibited cell growth. Interestingly, we observed peaks of viability in AGS (42 ℃, increase by 33%) and T3M4 (43 ℃, increase by 32%) cells. Putting all MTT data to isobologram analysis, we observed synergistic, antagonistic, or additive effects of combined treatment. Hyperthermia and cisplatin treatment was strongly antagonistic in AGS cells. In Caco-2 cells we observed synergistic, additive and antagonistic effects of simultaneous treatment. Few combined treatment regimens were additive for T3M4 cells, and remaining antagonistic. Cisplatin induced early apoptosis in Caco-2 and T3M4 cells 1.5-fold and 3.4-fold, respectively. Hyperthermia of 43 ℃ in addition to cisplatin induced early apoptosis as compared to cells treated in normothermia by 20% in Caco-2 and 19% in T3M4, respectively. Hyperthermia strongly decreased intracellular cisplatin concentration in AGS, Caco-2, and T3M4 cells by 30%, 20%, and 18%, respectively.

Research conclusions

Our data suggest that HIPEC conditions have to be cancer type dependent and well revised. Particular temperature regimens can do more harm, than benefit, by activating cell division and growth.

Research perspectives

To get better knowledge of hyperthermia and cisplatin treatment effects, future studies should include more cancer cell lines per cancer type. Also, *in vivo* vehicle should be established.

REFERENCES

1 **Glehen O**, Mohamed F, Gilly FN. Peritoneal carcinomatosis from digestive tract cancer: new management by cytoreductive surgery and intraperitoneal chemohyperthermia. *Lancet Oncol* 2004; **5**: 219-228 [PMID: 15050953 DOI: 10.1016/S1470-2045(04)01425-1]

2 **Coccolini F**, Cotte E, Glehen O, Lotti M, Poiasina E, Catena F, Yonemura Y, Ansaloni L. Intraperitoneal chemotherapy in advanced gastric cancer. Meta-analysis of randomized trials. *Eur J Surg Oncol* 2014; **40**: 12-26 [PMID: 24290371 DOI: 10.1016/j.ejso.2013.10.019]

3 **Bloemendaal AL**, Verwaal VJ, van Ruth S, Boot H, Zoetmulder FA. Conventional surgery and systemic chemotherapy for peritoneal carcinomatosis of colorectal origin: a prospective study. *Eur J Surg Oncol* 2005; **31**: 1145-1151 [PMID: 16084051 DOI: 10.1016/j.ejso.2005.06.002]

4 **Glehen O**, Cotte E, Schreiber V, Sayag-Beaujard AC, Vignal J, Gilly FN. Intraperitoneal chemohyperthermia and attempted cytoreductive surgery in patients with peritoneal carcinomatosis of colorectal origin. *Br J Surg* 2004; **91**: 747-754 [PMID: 15164446 DOI: 10.1002/bjs.4473]

5 **Chua TC**, Esquivel J, Pelz JO, Morris DL. Summary of current therapeutic options for peritoneal metastases from colorectal cancer. *J Surg Oncol* 2013; **107**: 566-573 [PMID: 22688776 DOI: 10.1002/jso.23189]

6 **Bergs JW**, Franken NA, Haveman J, Geijsen ED, Crezee J, van Bree C. Hyperthermia, cisplatin and radiation trimodality treatment: a promising cancer treatment? A review from preclinical studies to clinical application. *Int J Hyperthermia* 2007; **23**: 329-341 [PMID: 17558732 DOI: 10.1080/02656730701378684]

7 **Alvarez-Berríos MP**, Castillo A, Mendéz J, Soto O, Rinaldi C, Torres-Lugo M. Hyperthermic potentiation of cisplatin by magnetic nanoparticle heaters is correlated with an increase in cell membrane fluidity. *Int J Nanomedicine* 2013; **8**: 1003-1013 [PMID: 23493492 DOI: 10.2147/IJN.S38842]

8 **Gabano E**, Colangelo D, Ghezzi AR, Osella D. The influence of temperature on antiproliferative effects, cellular uptake and DNA platination of the clinically employed Pt(II)-drugs. *J Inorg Biochem* 2008; **102**: 629-635 [PMID: 18037490 DOI: 10.1016/j.jinorgbio.2007.10.006]

9 **van de Vaart PJ**, van der Vange N, Zoetmulder FA, van Goethem AR, van Tellingen O, ten Bokkel Huinink WW, Beijnen JH, Bartelink H, Begg AC. Intraperitoneal cisplatin with regional hyperthermia in advanced ovarian cancer: pharmacokinetics and cisplatin-DNA adduct formation in patients and ovarian cancer cell lines. *Eur J Cancer* 1998; **34**: 148-154 [PMID: 9624250 DOI: 10.1016/S0959-8049(97)00370-5]

10 **Ried M**, Potzger T, Braune N, Diez C, Neu R, Sziklavari Z, Schalke B, Hofmann HS. Local and systemic exposure of cisplatin during hyperthermic intrathoracic chemotherapy perfusion after pleurectomy and decortication for treatment of pleural malignancies. *J Surg Oncol* 2013; **107**: 735-740 [PMID: 23386426 DOI: 10.1002/jso.23321]

11 **Schaaf L**, Schwab M, Ulmer C, Heine S, Mürdter TE, Schmid JO, Sauer G, Aulitzky WE, van der Kuip H. Hyperthermia Synergizes with Chemotherapy by Inhibiting PARP1-Dependent DNA Replication Arrest. *Cancer Res* 2016; **76**: 2868-2875 [PMID: 27013194 DOI: 10.1158/0008-5472.CAN-15-2908]

12 **Sottile ML**, Losinno AD, Fanelli MA, Cuello-Carrión FD, Montt-Guevara MM, Vargas-Roig LM, Nadin SB. Hyperthermia effects on Hsp27 and Hsp72 associations with mismatch repair (MMR) proteins and cisplatin toxicity in MMR-deficient/proficient colon cancer cell lines. *Int J Hyperthermia* 2015; **31**: 464-475 [PMID: 26043026 DOI: 10.3109/02656736.2015.1026848]

13 **Tang R**, Zhu ZG, Qu Y, Li JF, Ji YB, Cai Q, Liu BY, Yan M, Yin HR, Lin YZ. The impact of hyperthermic chemotherapy on human gastric cancer cell lines: preliminary results. *Oncol Rep* 2006; **16**: 631-641 [PMID: 16865266 DOI: 10.3892/or.16.3.631]

14 **Buell JF**, Reed E, Lee KB, Parker RJ, Venzon DJ, Amikura K, Arnold S, Fraker DL, Alexander HR. Synergistic effect and possible mechanisms of tumor necrosis factor and cisplatin cytotoxicity under moderate hyperthermia against gastric cancer cells. *Ann Surg Oncol* 1997; **4**: 141-148 [PMID: 9084851 DOI: 10.1007/BF02303797]

15 **Milani V**, Noessner E. Effects of thermal stress on tumor antigenicity and recognition by immune effector cells. *Cancer Immunol Immunother* 2006; **55**: 312-319 [PMID: 16151807 DOI: 10.1007/s00262-005-0052-3]

16 **Chou TC**. Theoretical basis, experimental design, and computerized simulation of synergism and antagonism in drug combination studies. *Pharmacol Rev* 2006; **58**: 621-681 [PMID: 16968952 DOI: 10.1124/pr.58.3.10]

17 **Seshadri RA**, Glehen O. Cytoreductive surgery and hyperthermic intraperitoneal chemotherapy in gastric cancer. *World J Gastroenterol* 2016; **22**: 1114-1130 [PMID: 26811651 DOI: 10.3748/wjg.v22.i3.1114]

18 **Yonemura Y**, Canbay E, Li Y, Coccolini F, Glehen O, Sugarbaker PH, Morris D, Moran B, Gonzaletz-Moreno S, Deraco M, Piso P, Elias D, Batlett D, Ishibashi H, Mizumoto A, Verwaal V, Mahtem H. A comprehensive treatment for peritoneal metastases from gastric cancer with curative intent. *Eur J Surg Oncol* 2016; **42**: 1123-1131 [PMID: 27160355 DOI: 10.1016/j.ejso.2016.03.016]

19 **Yuan M**, Wang Z, Hu G, Yang Y, Lv W, Lu F, Zhong H. A retrospective analysis of hyperthermic intraperitoneal chemotherapy for gastric cancer with peritoneal metastasis. *Mol Clin Oncol* 2016; **5**: 395-399 [PMID: 27446587 DOI: 10.3892/mco.2016.918]

20 **Simkens GA**, van Oudheusden TR, Braam HJ, Wiezer MJ, Nienhuijs SW, Rutten HJ, van Ramshorst B, de Hingh IH. Cytoreductive surgery and HIPEC offers similar outcomes in patients with rectal peritoneal metastases compared to colon cancer patients: a matched case control study. *J Surg Oncol* 2016; **113**: 548-553 [PMID: 27110701 DOI: 10.1002/jso.24169]

21 **Spiliotis J**, Halkia E, Lianos E, Kalantzi N, Grivas A, Efstathiou E, Giassas S. Cytoreductive surgery and HIPEC in recurrent epithelial ovarian cancer: a prospective randomized phase III study. *Ann Surg Oncol* 2015; **22**: 1570-1575 [PMID: 25391263 DOI: 10.1245/s10434-014-4157-9]

22 **Kepenekian V**, Elias D, Passot G, Mery E, Goere D, Delroeux D, Quenet F, Ferron G, Pezet D, Guilloit JM, Meeus P, Pocard M, Bereder JM, Abboud K, Arvieux C, Brigand C, Marchal F, Classe JM, Lorimier G, De Chaisemartin C, Guyon F, Mariani P, Ortega-Deballon P, Isaac S, Maurice C, Gilly FN, Glehen O; French Network for Rare Peritoneal Malignancies (RENAPE). Diffuse malignant peritoneal mesothelioma: Evaluation of systemic chemotherapy with comprehensive treatment through the RENAPE Database: Multi-Institutional Retrospective Study. *Eur J Cancer* 2016; **65**: 69-79 [PMID: 27472649 DOI: 10.1016/j.ejca.2016.06.002]

23 **Michalakis J**, Georgatos SD, de Bree E, Polioudaki H, Romanos J, Georgoulias V, Tsiftsis DD, Theodoropoulos PA. Short-term exposure of cancer cells to micromolar doses of paclitaxel, with or without hyperthermia, induces long-term inhibition of cell proliferation and cell death in vitro. *Ann Surg Oncol* 2007; **14**: 1220-1228 [PMID: 17206477 DOI: 10.1245/s10434-006-9305-4]

24 **Zhang XL**, Hu AB, Cui SZ, Wei HB. Thermotherapy enhances oxaliplatin-induced cytotoxicity in human colon carcinoma cells. *World J Gastroenterol* 2012; **18**: 646-653 [PMID: 22363135 DOI: 10.3748/wjg.v18.i7.646]

25 **Steel GG**, Peckham MJ. Exploitable mechanisms in combined radiotherapy-chemotherapy: the concept of additivity. *Int J Radiat Oncol Biol Phys* 1979; **5**: 85-91 [PMID: 422420 DOI: 10.1016/0360-3016(79)90044-0]

26 **Verwaal VJ**, van Ruth S, de Bree E, van Sloothen GW, van Tinteren H, Boot H, Zoetmulder FA. Randomized trial of cytoreduction and hyperthermic intraperitoneal chemotherapy versus systemic chemotherapy and palliative surgery in patients with peritoneal carcinomatosis of colorectal cancer. *J Clin Oncol* 2003; **21**: 3737-3743 [PMID: 14551293 DOI: 10.1200/JCO.2003.04.187]

27 **Li Q**, Wennborg A, Aurell E, Dekel E, Zou JZ, Xu Y, Huang S, Ernberg I. Dynamics inside the cancer cell attractor reveal cell heterogeneity, limits of stability, and escape. *Proc Natl Acad Sci USA* 2016; **113**: 2672-2677 [PMID: 26929366 DOI: 10.1073/pnas.1519210113]

28 **Zang ZJ**, Ong CK, Cutcutache I, Yu W, Zhang SL, Huang D, Ler LD, Dykema K, Gan A, Tao J, Lim S, Liu Y, Futreal PA, Grabsch H, Furge KA, Goh LK, Rozen S, Teh BT, Tan P. Genetic and structural variation in the gastric cancer kinome revealed through targeted deep sequencing. *Cancer Res* 2011; **71**: 29-39 [PMID: 21097718 DOI: 10.1158/0008-5472.CAN-10-1749]

29 **Jin Z**, Jiang W, Wang L. Biomarkers for gastric cancer: Progression in early diagnosis and prognosis (Review). *Oncol Lett* 2015; **9**: 1502-1508 [PMID: 25788990 DOI: 10.3892/ol.2015.2959]

30 **Fleming NI**, Jorissen RN, Mouradov D, Christie M, Sakthianandeswaren A, Palmieri M, Day F, Li S, Tsui C, Lipton L, Desai J, Jones IT, McLaughlin S, Ward RL, Hawkins NJ, Ruszkiewicz AR, Moore J, Zhu HJ, Mariadason JM, Burgess AW, Busam D, Zhao Q, Strausberg RL, Gibbs P, Sieber OM. SMAD2, SMAD3 and SMAD4 mutations in colorectal cancer. *Cancer Res* 2013; **73**: 725-735 [PMID: 23139211 DOI: 10.1158/0008-5472.CAN-12-2706]

31 **Ahmed D**, Eide PW, Eilertsen IA, Danielsen SA, Eknæs M, Hektoen M, Lind GE, Lothe RA. Epigenetic and genetic features of 24 colon cancer cell lines. *Oncogenesis* 2013; **2**: e71 [PMID: 24042735 DOI: 10.1038/oncsis.2013.35]

32 **Tremblay E**, Auclair J, Delvin E, Levy E, Ménard D, Pshezhetsky AV, Rivard N, Seidman EG, Sinnett D, Vachon PH, Beaulieu JF. Gene expression profiles of normal proliferating and differentiating human intestinal epithelial cells: a comparison with the Caco-2 cell model. *J Cell Biochem* 2006; **99**: 1175-1186 [PMID: 16795037 DOI: 10.1002/jcb.21015]

33 **Moore PS**, Sipos B, Orlandini S, Sorio C, Real FX, Lemoine NR, Gress T, Bassi C, Klöppel G, Kalthoff H, Ungefroren H, Löhr M, Scarpa A. Genetic profile of 22 pancreatic carcinoma cell lines. Analysis of K-ras, p53, p16 and DPC4/Smad4. *Virchows Arch* 2001; **439**: 798-802 [PMID: 11787853 DOI: 10.1007/s004280100474]

34 **Shah RN**, Ibbitt JC, Alitalo K, Hurst HC. FGFR4 overexpression in pancreatic cancer is mediated by an intronic enhancer activated by HNF1alpha. *Oncogene* 2002; **21**: 8251-8261 [PMID: 12447688 DOI: 10.1038/sj.onc.1206020]

35 **Guo Y**, Ziesch A, Hocke S, Kampmann E, Ochs S, De Toni EN, Göke B, Gallmeier E. Overexpression of heat shock protein 27 (HSP27) increases gemcitabine sensitivity in pancreatic cancer cells through S-phase arrest and apoptosis. *J Cell Mol Med* 2015; **19**: 340-350 [PMID: 25331547 DOI: 10.1111/jcmm.12444]

36 **Liu T**, Ye YW, Zhu AL, Yang Z, Fu Y, Wei CQ, Liu Q, Zhao CL, Wang GJ, Zhang XF. Hyperthermia combined with 5-fluorouracil promoted apoptosis and enhanced thermotolerance in human gastric cancer cell line SGC-7901. *Onco Targets Ther* 2015; **8**: 1265-1270 [PMID: 26064061 DOI: 10.2147/OTT.S78514]

37 **Kudo M**, Asao T, Hashimoto S, Kuwano H. Closed continuous hyperthermic peritoneal perfusion model in mice with peritoneal dissemination of colon 26. *Int J Hyperthermia* 2004; **20**: 441-450 [PMID: 15204523 DOI: 10.1080/02656730310001637352]

38 **Kirstein MN**, Root SA, Moore MM, Wieman KM, Williams BW, Jacobson PA, Marker PH, Tuttle TM. Exposure-response relationships for oxaliplatin-treated colon cancer cells. *Anticancer Drugs* 2008; **19**: 37-44 [PMID: 18043128 DOI: 10.1097/CAD.0b013e3282f07791]

39 **Ferraro G**, Pica A, Russo Krauss I, Pane F, Amoresano A, Merlino A. Effect of temperature on the interaction of cisplatin with the model protein hen egg white lysozyme. *J Biol Inorg Chem* 2016; **21**: 433-442 [PMID: 27040953 DOI: 10.1007/s00775-016-1352-0]

40 **Zhang XL**, Shi HJ, Wang JP, Tang HS, Wu YB, Fang ZY, Cui SZ, Wang LT. MicroRNA-218 is upregulated in gastric cancer after cytoreductive surgery and hyperthermic intraperitoneal chemotherapy and increases chemosensitivity to cisplatin. *World J Gastroenterol* 2014; **20**: 11347-11355 [PMID: 25170221 DOI: 10.3748/wjg.v20.i32.11347]

41 **Muenyi CS**, States VA, Masters JH, Fan TW, Helm CW, States JC. Sodium arsenite and hyperthermia modulate cisplatin-DNA damage responses and enhance platinum accumulation in murine metastatic ovarian cancer xenograft after hyperthermic intraperitoneal chemotherapy (HIPEC). *J Ovarian Res* 2011; **4**: 9 [PMID: 21696631 DOI: 10.1186/1757-2215-4-9]

42 **Okayama T**, Kokura S, Ishikawa T, Adachi S, Hattori T, Takagi T, Handa O, Naito Y, Yoshikawa T. Antitumor effect of pretreatment for colon cancer cells with hyperthermia plus geranylgeranylacetone in experimental metastasis models and a subcutaneous tumor model of colon cancer in mice. *Int J Hyperthermia* 2009; **25**: 141-149 [PMID: 19337914 DOI: 10.1080/02656730802631783]

43 **Yoo J**, Lee YJ. Effect of hyperthermia and chemotherapeutic agents on TRAIL-induced cell death in human colon cancer cells. *J Cell Biochem* 2008; **103**: 98-109 [PMID: 17520700 DOI: 10.1002/jcb.21389]

44 **Vertrees RA**, Das GC, Popov VL, Coscio AM, Goodwin TJ, Logrono R, Zwischenberger JB, Boor PJ. Synergistic interaction of hyperthermia and Gemcitabine in lung cancer. *Cancer Biol Ther* 2005; **4**: 1144-1153 [PMID: 16138007 DOI: 10.4161/cbt.4.10.2074]

45 **Adachi S**, Kokura S, Okayama T, Ishikawa T, Takagi T, Handa O, Naito Y, Yoshikawa T. Effect of hyperthermia combined with

gemcitabine on apoptotic cell death in cultured human pancreatic cancer cell lines. *Int J Hyperthermia* 2009; **25**: 210-219 [PMID: 19437237 DOI: 10.1080/02656730802657036]

46 **Kirui DK**, Celia C, Molinaro R, Bansal SS, Cosco D, Fresta M, Shen H, Ferrari M. Mild hyperthermia enhances transport of liposomal gemcitabine and improves in vivo therapeutic response. *Adv Healthc Mater* 2015; **4**: 1092-1103 [PMID: 25721343 DOI: 10.1002/adhm.201400738]

47 **Loggie BW**, Thomas P. Gastrointestinal Cancers With Peritoneal Carcinomatosis: Surgery and Hyperthermic Intraperitoneal Chemotherapy. *Oncology* (Williston Park) 2015; **29**: 515-521 [PMID: 26178339]

48 **Ferraretto A**, Gravaghi C, Donetti E, Cosentino S, Donida BM, Bedoni M, Lombardi G, Fiorilli A, Tettamanti G. New methodological approach to induce a differentiation phenotype in Caco-2 cells prior to post-confluence stage. *Anticancer Res* 2007; **27**: 3919-3925 [PMID: 18225551]

49 **Ahmed K**, Tabuchi Y, Kondo T. Hyperthermia: an effective strategy to induce apoptosis in cancer cells. *Apoptosis* 2015; **20**: 1411-1419 [PMID: 26354715 DOI: 10.1007/s10495-015-1168-3]

P- Reviewer: Caboclo JL, Zhu YL **S- Editor**:Gong ZM
L- Editor: A **E- Editor**: Ma YJ

World Journal of Gastroenterology

Submit a Manuscript: http://www.f6publishing.com

World J Gastroenterol 2018 March 14; 24(10): 1084-1092

DOI: 10.3748/wjg.v24.i10.1084

ISSN 1007-9327 (print) ISSN 2219-2840 (online)

ORIGINAL ARTICLE

Basic Study

Sex disparity in viral load, inflammation and liver damage in transgenic mice carrying full hepatitis B virus genome with the W4P mutation in the preS1 region

Seoung-Ae Lee, So-Young Lee, Yu-Min Choi, Hong Kim, Bum-Joon Kim

Seoung-Ae Lee, So-Young Lee, Yu-Min Choi, Hong Kim, Bum-Joon Kim, Department of Microbiology and Immunology, Biomedical Sciences, Liver Research Institute and Cancer Research Institute, Seoul National University, College of Medicine, Seoul 110799, South Korea

ORCID number: Seoung-Ae Lee (0000-0002-4451-8165); So-Young Lee (0000-0002-9638-893X); Yu-Min Choi (0000-0003-4709-3155); Hong Kim (0000-0003-1383-6803); Bum-Joon Kim (0000-0003-0085-6709).

Author contributions: Kim BJ conceived this research and participated in its design and coordination; Lee SA performed the experiments; Lee SY, Choi YM and Kim H analyzed and interpreted the data; Kim BJ contributed the reagents, materials and analysis tools.

Supported by the Korea Health Technology R&D Project through the Korea Health Industry Development Institute and the Ministry of Health and Welfare, South Korea, No. HI14C0955.

Conflict-of-interest statement: There was no conflict of interest.

Data sharing statement: No additional data are available.

Manuscript source: Unsolicited manuscript

Correspondence to: Bum-Joon Kim, PhD, Professor, Department of Biomedical Sciences, Microbiology and Immunology, and Liver Research Institute, Seoul National University College of Medicine, 103, Daehak-ro, Jongno-gu, Seoul 110799, South Korea. kbumjoon@snu.ac.kr
Telephone: +82-2-7408316
Fax: +82-2-7430881

Received: January 11, 2018
Peer-review started: January 11, 2018
First decision: January 25, 2018
Revised: January 31, 2018
Accepted: February 9, 2018
Article in press: February 9, 2018
Published online: March 14, 2018

Abstract

AIM

To study sex disparity in susceptibility to hepatocellular carcinoma (HCC), we created a transgenic mouse model that expressed the full hepatitis B virus (HBV) genome with the W4P mutation.

METHODS

Transgenic mice were generated by transferring the pHY92-1.1x-HBV-full genome plasmid (genotype A2) into C57Bl/6N mice. We compared serum levels of hepatitis B surface antigen (HBsAg), interleukin (IL)-6, and the liver enzymes alanine aminotransferase (ALT) and aspartate transaminase (AST), as well as liver histopathological features in male and female transgenic (W4P TG) mice and in nontransgenic littermates of 10 mo of age.

RESULTS

W4P TG males exhibited more pronounced hepatomegaly, significantly increased granule generation in liver tissue, elevated HBsAg expression in the liver and serum, and higher serum ALT and IL-6 levels compared

to W4P TG females or littermate control groups.

CONCLUSION

Together, our data indicate that the W4P mutation in preS1 may contribute to sex disparity in susceptibility to HCC by causing increased HBV virion replication and enhanced IL-6-mediated inflammation in male individuals. Additionally, our transgenic mouse model that expresses full HBV genome with the W4P mutation in preS1 could be effectively used for the studies of the progression of liver diseases, including HCC.

Key words: Hepatitis B virus; W4P mutation of preS1; Transgenic mice; Hepatocellular carcinoma

Core tip: With the development of hepatitis B virus (HBV) vaccine, the rate of chronic HBV infection has dramatically declined worldwide. However, the incidence of hepatocellular carcinoma (HCC), which is characterized by poor prognosis and low survival rate, is on the rise. Predominance in males is a representative global epidemiological characteristic of HCC. Recently, we introduced the novel W4P substitution into the preS1 region, which associated with HCC and notably occurred exclusively in male patients. Our study in the nude mouse xenograft model indicated that the W4P mutation likely contributed to IL-6-dependent HCC progression, particularly in male individuals. Here, to gain further insight into the role of this mutation in HBV-induced liver inflammation, we created transgenic mice carrying the full HBV genome with this mutation. Of note, our data showed that W4P transgene males of 10 mo of age, but not W4P transgene females, spontaneously developed liver damage due to IL-6-mediated liver inflammation, further supporting the previous finding regarding the contribution of the W4P mutation to sex disparity in susceptibility to HCC. Furthermore, our results prove the utility of the developed W4P transgene mouse model for research into the mechanisms of HBV-caused liver diseases.

Lee SA, Lee SY, Choi YM, Kim H, Kim BJ. Sex disparity in viral load, inflammation and liver damage in transgenic mice carrying full hepatitis B virus genome with the W4P mutation in the preS1 region. *World J Gastroenterol* 2018; 24(10): 1084-1092 Available from: URL: http://www.wjgnet.com/1007-9327/full/v24/i10/1084.htm DOI: http://dx.doi.org/10.3748/wjg.v24.i10.1084

INTRODUCTION

Hepatitis B virus (HBV) infection causes a wide range of chronic infectious diseases, including chronic hepatitis, liver cirrhosis and hepatocellular carcinoma (HCC). In 2010, the number of patients in which HBV infection was the main cause of death was reported to be 786000 worldwide[1,2].

The incidence of chronic HBV infection in children has been considerably decreased by the successful development of antiHBV vaccine[3-5]. Nevertheless, the high risk of liver cirrhosis (LC) and HCC is still a problem in adult HBV carriers. The five-year cumulative risk of HCC progression is approximately 10%-17% in LC patients, and disease progression from chronic hepatitis B to LC is expected in 12%-20% of patients in 5 years[6-8]. HBV genotype C2, which is predominant in Asia, is associated with a particularly significant risk of HCC compared to that conferred by HBVs of other genotypes[9-11]. The correlation between HBV infection and sex disparity in susceptibility to HCC has been well documented. However, the mechanism by which HBV causes cancer development is still unresolved. Premature termination of HBV X protein (HBx), which results in truncated hepatitis B surface antigen (HBsAg), or mutations, particularly deletions, in the preS region of large-surface proteins (LHBs) have been reported to be associated with HCC progression[12-15].

Prevalence in males is one of the remarkable global epidemiological characteristics of HCC, as approximately 3-5 times more cases of HCC are observed in men than in women[16-18]. The sex disparity is more prominent in HBV-related HCC than in hepatitis C virus-related HCC, suggesting the presence of an HBV infection-related factor that determines HCC male predominance[19,20]. It has been reported that high expression levels of both androgen and active androgen receptor gene alleles increase the risk of HCC in male patients with chronic hepatitis B due to the interaction between HBx and androgen axis[21-23].

HCC development is likely affected not only by the HBx-androgen axis interactions but also by a tumor-protective effect of estrogen. In particular, it has been suggested that taking contraceptives or postmenopausal hormone therapy associated with long-term exposure to estrogen reduces the risk of HCC in female patients[24]. In addition, it has been reported that estrogen receptor α-mediated inhibition of interleukin (IL)-6 production had an essential role in inhibiting carcinogenesis in a mouse model of HCC induced chemically by diethylnitrosamine[25,26].

On the basis of differential time courses of HCC development and disease severity in wild-type (WT) individuals and in individuals with LHB mutations, it has been proposed that mutated LHBs lead to carcinogenesis by inducing endoplasmic reticulum stress pathway or by altering transactivating capacity of hepatocytes[27-29].

In a molecular epidemiological study, we have previously found that the W4P mutation in the preS1 start region is associated with HCC development in male but not female patients[30]. In addition, our further cell-based and nude mouse xenograft model studies supported the notion that the W4P mutation likely induced HCC progression in an IL-6-dependent manner

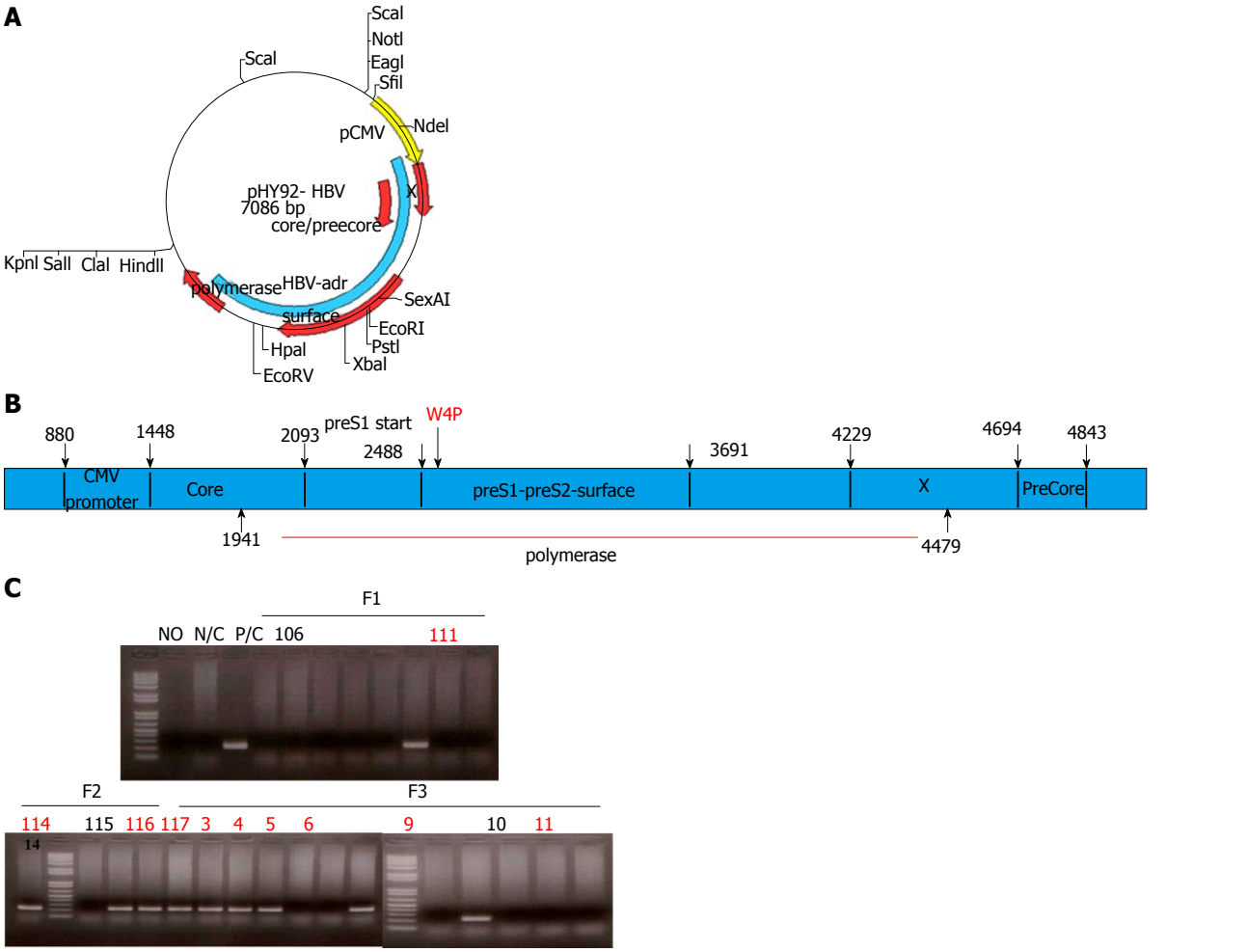

Figure 1 Construction of the W4P TG mice expressing pHY92-1.1x the HBV full genome with the preS1 W4P mutation and the screening of the constructed W4P TG mice. A: A plasmid map of pHY92 vector containing a copy of the 1.1x-unit length HBV genome under the control of a CMV promoter; B: The HBV full genome construct with a W4P missense mutation in the preS1 region; C: Screening of the constructed W4P TG mice by PCR targeting the preS1 region. CMV: Cytomegalovirus; HBV: Hepatitis B virus.

in male patients[31]. Here, to gain further insight into the role of this mutation in the sex disparity of HBV-induced liver inflammation, we created transgenic (TG) mice carrying the full HBV genome with the W4P mutation and evaluated HBV virion replication and IL-6-mediated inflammation in male and female TG and WT individuals.

MATERIALS AND METHODS

Generation of the full-length HBV genome construct with the prS1 W4P mutation using site-directed mutagenesis

The mutant full-length HBV genome construct carrying the W4P mutation in the preS1 region (hereafter, pHY92-W4P) was generated by site-directed mutagenesis of the WT pHBV-1.1x vector (hereafter, pHY92-WT) (Genotype A, GenBank No. AF305422), which was kindly provided by Yang *et al*[32]. The mutagenesis was performed using the forward primer W4P-F (5′- AACAAGAGCTACGCATGGGAGGTCCGT CATCAAAACCTC-3′) and the reverse primer W4P-R (5′-GAGGTTTTGATGACGGACCT CCCATGCTGTAGCTCTTGTT-3′) located from 2473 bp and 2513 bp. Site-directed mutagenesis of the full HBV genome was performed as described[33].

TG mice

To generate W4P TG mice, fertilized C57BL/6N embryos and HBV full genome with the W4P mutation were co-microinjected into one-cell embryo in accordance with the standard microinjection procedures for TG mouse production (Macrogen, Seoul, Korea). Genotyping of TG mice was conducted by PCR and viral DNA samples obtained from tail vein bleeds were screened using the primers PreS-F (5′-GGGTCACCATATTCTTGGGAA-3′) and PreS-R (5′-CGAATGCTCCCRCTCCTAC-3). The mice were housed in a specific pathogen-free laboratory animal center. The TG mice were crossed with B6D2F1/J mice (The Jackson Laboratory, Bar Harbor, ME, United States) and the HBV-expressing offspring mice, as well as their littermates, were used in this study. All animal experiments were conducted following United States' National Institutes of Health guidelines for housing and care of laboratory animals

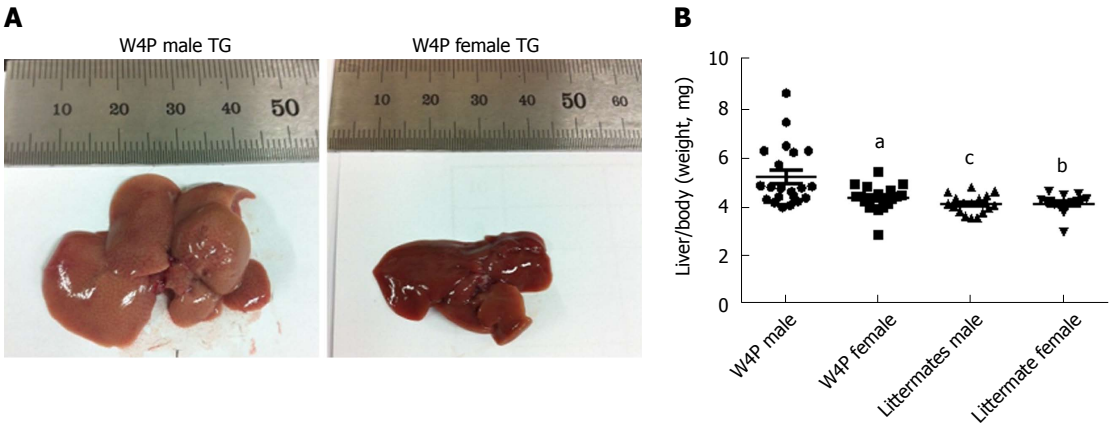

Figure 2 Increased hepatomegaly in the W4P male TG mice. A: *In situ* view of liver of W4P TG male mice and W4P TG female mice at 10 mo of age; B: Liver weight ratio against the total body weight (mg) in W4P mutant mice (males: 24 mice; females: 18 mice) and nonTG littermates (males: 17 mice; females: 15 mice) at 10 mo of age ($^{a}P < 0.05$, $^{b}P < 0.01$, and $^{c}P < 0.001$ *vs* W4P male, one-way ANOVA.

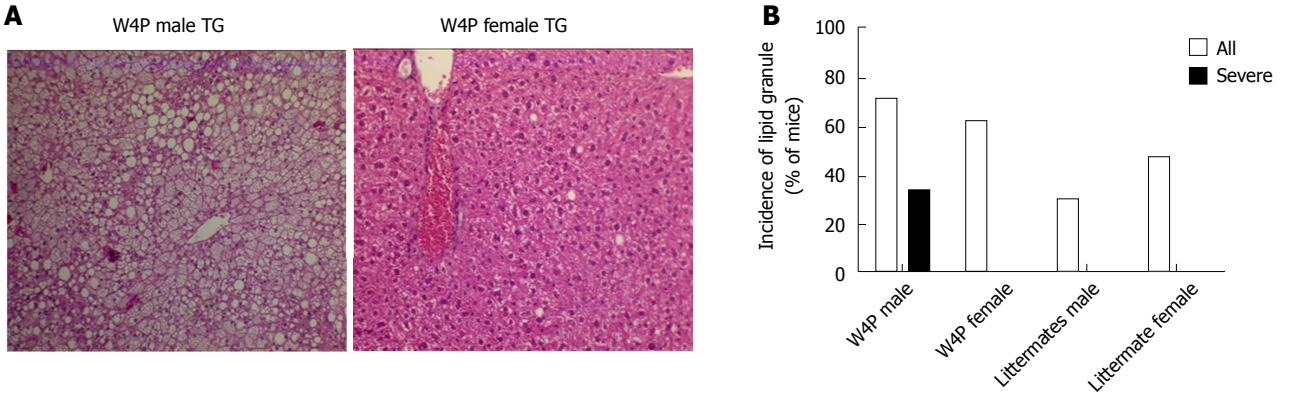

Figure 3 Increased generation of lipid droplets in W4P male TG mice. A: Comparison of generated lipid droplets in the liver section by hematoxylin-eosin staining (× 200); B: Incidence of lipid droplets in W4P mutant mice (males: 24 mice; females: 18 mice) and non TG littermates (males: 17 mice; females: 15 mice) at 10 mo of age.

and in accordance with the protocol approved by the Institutional Animal Care and Use Committee (IAUAC) of the Seoul National University College of Medicine (Protocol No. SNU-111025).

Enzyme-linked immunosorbent assay

Serum HBsAg levels in male and female W4P TG mice and their WT littermates were determined by enzyme-linked immunosorbent assay (ELISA) using a commercial Bioelisa HBsAg color kit (Biokit, Barcelona, Spain) according to the procedures provided by the manufacturer. The amount of secreted IL-6 was determined by a mIL-6 ELISA kit (eBioscience, San Diego, CA, United States). Serum levels of alanine aminotransferase (ALT) and aspartate transaminase (AST) were determined at the Seoul National University Hospital Biomedical Research Institute facility.

Hematoxylin and eosin staining and immunohistochemistry

Liver samples were fixed with 4% paraformaldehyde in phosphate-buffered saline and embedded in paraffin. Tissue sections were stained with hematoxylin and eosin at the Seoul National University Hospital Biomedical Research Institute facility. Immunohistochemical staining with an anti-preS1 monoclonal antibody (Aprogen, Daejeon, South Korea) was also performed. Deparaffinized sections were heated in citrate buffer (Zytomed, Berlin, Germany) to accomplish antigen retrieval. Endogenous peroxidase was blocked with peroxidase blocking solution (Zytomed). An anti-preS1 antibody was applied as the primary antibody followed by the application of the avidin-biotin complex method to detect the primary antibody. Peroxidase activity was visualized by a 3,3'-diaminobenzidine substrate kit (Zytomed) with hematoxylin (Wako, Osaka, Japan) as counterstain.

Statistical analysis

All ELISA assays in this study were repeated at least three times, and the results were expressed as the mean percentage ± standard deviation, or as the median (± range). For continuous variables, separate one-way analyses of variance were used to determine

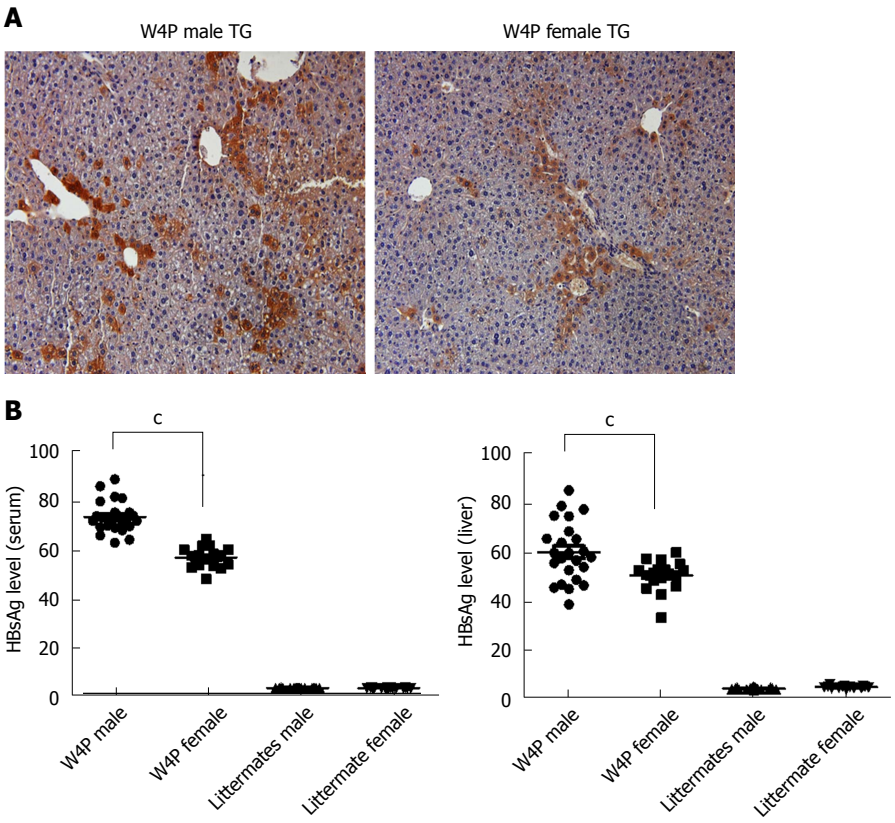

Figure 4 Increased secreted HBsAg level and liver LHBs in W4P male TG mice. A: Comparison of LHBs level in liver section by IHC analysis using anti-preS1 antibodies between W4P TG male and female mice (× 200); B: Comparison of HBsAg level in the liver and serum from W4P mutant mice (males: 24 mice; females: 18 mice) and nonTG littermates (males: 17 mice; females: 15 mice) at 10 mo of age ($^{c}P < 0.001$ *vs* W4P male, one-way ANOVA). HBsAg: Hepatitis B surface antigen; IHC: Immunohistochemistry; LHBs: Large-surface proteins.

if there was a significant difference by using the Bartlett's test. All statistical analyses were conducted with a significance level of $\alpha = 0.05$ ($P < 0.05$).

RESULTS

Construction of TG mice harboring full HBV genome with the W4P mutation in preS1

TG mice generated on B6D2F1/J background expressed the full-length HBV genome with the W4P mutation in preS1 under the control of the cytomegalovirus (CMV) promoter. For this purpose, we used site-directed mutagenesis of the pHY92 vector containing a copy of the 1.1x-unit length HBV genome under the control of the CMV promoter (genotype A, serotype adw, HBV strain identical to GenBank AF305422), which was provided by Yang *et al*[32], and generated a missense mutation, changing tryptophan to proline (TGG to CCG) at the fourth codon of preS1 (Figure 1A). Comparison of WT and W4P mutant LHB region sequences is shown in Supplementary Figure 1.

To confirm whether TG mice harbored the full HBV genome, the presence of virion DNA and secreted HBsAg in the serum or liver was checked by PCR and ELISA, respectively (Figure 1A).

Increased hepatomegaly and lipid granule content in male W4P TG mice

To check whether there was sex disparity in hepatomegaly, we examined the ratio of the liver weight to total body weight between W4P TG mice (24 males, 18 females) and their nonTG littermates (17 males, 15 females) at 10 mo of age. W4P TG male mice showed a significantly higher liver to total body weight ratio compared to that in mice of the three other groups, including W4P TG female mice and nonTG littermates (male and female mice) (Figure 2). Examination of histological samples stained with hematoxylin and eosin revealed that the incidence of mice generating lipid granules was higher in W4P male mice compared to that in W4P TG female mice and nonTG littermates (Figure 3).

Higher serum levels of HBsAg and increased amounts of LHBs in the livers of male W4P TG mice

Next, to check whether there was sex disparity in HBV production, we determined HBsAg levels in the serum and LHB levels in the livers of W4P TG mice (24 males, 18 females) and their nonTG littermates (17 males, 15 females) at 10 mo of age. W4P TG male mice showed a significantly higher level of HBsAg in the serum

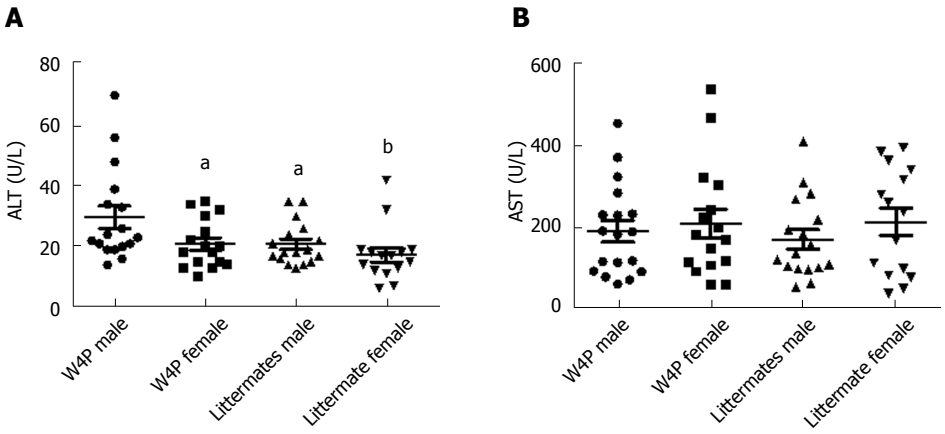

Figure 5 Serum alanine aminotransferase (A) and aspartate transaminase (B) levels in W4P TG mice (males: 24 mice; females: 18 mice) and nonTG littermates (males: 17 mice; females: 15 mice) at 10 mo of age. [a]*P* < 0.05, and [b]*P* < 0.01, *vs* W4P male, one-way ANOVA. ALT: Alanine aminotransferase; AST: Aspartate transaminase.

compared to that in mice from the other three groups. Immunohistochemical staining of the liver samples using an anti-preS1 antibody also showed increased LHB production in W4P TG male mice (Figure 4).

Increased serum levels of ALT and IL-6 in male W4P TG mice

It has been reported previously that the presence of the W4P mutation in the preS1 region sex-dependently affected IL-6 production in the xenograft nude mouse model system, which could be one of the reasons for increased male susceptibility to HCC[31]. Thus, to check whether there was sex disparity in the induction of IL-6-mediated inflammation, we next examined serum IL-6 levels in W4P TG mice (24 males, 18 females) and their nonTG littermates (17 males, 15 females) at 10 mo of age. W4P TG male mice showed significantly higher serum IL-6 levels than did mice of the other three groups (Figure 5). We also checked the levels of liver enzymes in the serum as indicators of liver damage in the four groups of mice. We found that W4P TG male mice had significantly higher serum levels of ALT than mice from the other three groups. However, serum AST levels were not significantly different in the four groups of mice (Figure 6).

DISCUSSION

Increasing evidence has shown sex disparity in the incidence of HBV-associated HCC in a sex hormone-dependent manner. Sex hormones, including androgen and estrogen, likely affect the progression of HBV infection and development of HBV-related HCC *via* their actions on receptor-mediated cell signaling[24-26]. To date, of all HBV proteins, HBx has been most extensively studied as the predominant virus interactor with host cell sex hormone-mediated signaling[22,23]. However, in our recent molecular epidemiologic and cell-based studies, we have demonstrated that LHB harboring the W4P mutation in preS1 could also contribute to the sex disparity of HBV-associated HCC in an IL-6-dependent manner[30,31]. In the present study, we constructed W4P TG mice that expressed the full HBV genome, which can help us to study sex disparity of the progression of liver diseases, including chronic hepatitis, steatohepatitis, cirrhosis and HCC, following chronic HBV infection.

We identified three noteworthy findings supporting the contribution of the W4P mutation in preS1 to liver disease progression in male patients. First, by using the W4P TG mouse model of chronic HBV infection, we found that male W4P TG mice exhibited higher levels of secreted HBsAg and liver LHBs, which was indicative of higher HBV replication than in female W4P TG mice (Figure 4) and is one of the known HCC risk factors[34]. Second, we found that male W4P TG mice showed increased incidence of hepatomegaly and lipid droplets (Figure 3), reflecting the imbalance of metabolic liver homeostasis, which could drive liver pathogenesis, including fatty liver and steatohepatitis, and further promote tumorigenesis. Third, we found that male W4P TG mice had increased IL-6-related liver inflammation and higher serum ALT levels (Figure 5), which were indications of liver damage, compared to those seen in female W4P TG mice.

IL-6 is one of the core stimulators that lead to persistent HBV infection and development of HBV-related HCC. It is also a key cytokine that may be a link to preferential male susceptibility to HCC[25,31]. A previous study that used diethylnitrosamine to evoke HCC showed that estrogen prevented HCC generation in female mice by inhibiting IL-6 production in a Myd88-dependent manner. That observation suggested that inhibition of IL-6 production in liver Kupffer cells by estrogen and estrogen receptor-mediated signaling pathways could be a major molecular mechanism that underlies sex disparity in HBV-associated liver diseases, including HCC[25,26]. Furthermore, increased hepatic IL-6 production also likely plays a pivotal role in the development of nonalcoholic fatty liver disease, nonalcoholic steatohepatitis, and insulin

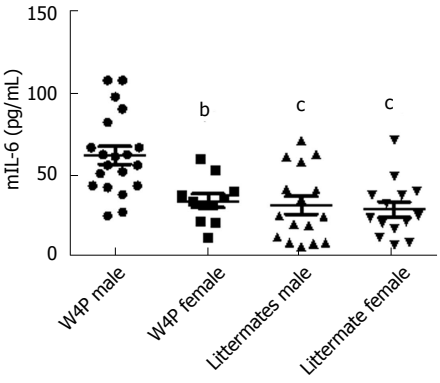

Figure 6 Secreted interleukin-6 levels in the W4P TG mice (males: 24 mice; females: 18 mice) and nonTG littermates (males: 17 mice; females: 15 mice) at 10 mo of age. ($^{a}P < 0.05$, $^{b}P < 0.01$, and $^{c}P < 0.001$ *vs* W4P_male, one-way ANOVA). ALT: Alanine aminotransferase; AST: Aspartate transaminase; IL: Interleukin.

resistance, which are the leading causes of HCC[35-40]. Thus, our W4P TG model showing increased hepatic IL-6 production could provide a novel insight into the relationships between IL-6 production due to an infection caused by an HBV variant on the one hand, and development of nonalcoholic steatohepatitis, type 2 diabetes or HCC on the other hand.

Our study had some limitations. Unfortunately, we did not prove predominant carcinogenesis in males in our W4P TG mice. Therefore, further studies are necessary to demonstrate higher male susceptibility to liver carcinogenesis in our W4P TG mouse model and clarify its mechanism in the future. In addition, the relationships between increased hepatic production of IL-6 in mice expressing HBV genome with the W4P mutation and fat accumulation, increased liver weight and HCC development also remain to be elucidated in the future.

The phenotypes of male W4P TG mice, namely higher levels of IL-6 and ALT in the serum, could provide a technical advantage in drug screening protocols, as it will be possible to analyze not only the inhibition of HBV replication but also the antiinflammatory activity. To the best of our knowledge, this possibility is currently not available in other related TG mouse models.

In conclusion, we created W4P TG mice that constitutively express the full HBV genome with the W4P mutation in preS1 in the present study. Our data using W4P TG mice indicate that this mutation likely contributes to sex disparity in the susceptibility to liver disease, including HCC, leading to increased HBV virion replication and enhanced IL-6-mediated inflammation in male individuals. Additionally, the developed TG mouse model system carrying the full HBV genome with the W4P mutation in preS1 could be effectively used not only in basic research into the mechanisms of liver disease progression in HCC but also for the screening of antiHBV or antiinflammatory drugs.

ARTICLE HIGHLIGHTS

Research background

A remarkable global epidemiological feature of hepatocellular carcinoma (HCC) is its higher incidence in males. Recently, we identified the novel W4P substitution in the preS1 region of hepatitis B virus (HBV) related to HCC that occurs exclusively in male patients. We have also shown that the W4P mutation likely contributed to HCC development, particularly in male patients, in an interleukin (IL)-6-dependent manner.

Research motivation

Studies of sex disparity in the susceptibility to HCC *in vivo* have mainly utilized the chemical agent diethylnitrosamine to induce HCC in mice. However, no transgenic (TG) mouse model system expressing the full HBV genome has yet been available for the study of sex disparity in HBV-related liver diseases.

Research objectives

To gain further insight into the role of the W4P mutation in the preS1 region of HBV on sex disparity of HBV-induced liver inflammatory manifestations, we created a TG mouse that carried the full HBV genome with this mutation and evaluated HBV virion replication and IL-6-mediated inflammation in mutant and wild-type (WT) mice of both sexes.

Research methods

TG mice were generated by transferring the pHY92-1.1x-HBV-full genome plasmid (genotype A2) into C57Bl/6N mice. We compared serum levels of hepatitis B surface antigen (HBsAg), IL-6, and the liver enzymes alanine aminotransferase (ALT) and aspartate transaminase (AST), as well as liver histopathology features in male and female W4P TG mice and their WT littermates.

Research results

Our data showed significantly increased hepatomegaly, enhanced granule generation in liver tissue, higher HBsAg expression in the liver and serum, and higher serum ALT and IL-6 levels in W4P TG males compared to the values of these parameters in W4P TG females or littermate control groups.

Research conclusions

This is the first study that used TG mice to uncover the role of the W4P mutation in HBV preS1 in sex disparity of liver disease progression due to concomitantly increased HBV virion replication and greater IL-6-mediated inflammation in male individuals.

Research perspectives

The obtained results suggest that W4P TG mice developed in this study could be effectively used not only for the basic research into the mechanisms of HBV-associated liver diseases, including HCC, but also for screening antiHBV and antiinflammatory drugs.

REFERENCES

1 **Lee WM**. Hepatitis B virus infection. *N Engl J Med* 1997; **337**: 1733-1745 [PMID: 9392700 DOI: 10.1056/NEJM199712113372406]

2 **Lozano R**, Naghavi M, Foreman K, Lim S, Shibuya K, Aboyans V, Abraham J, Adair T, Aggarwal R, Ahn SY, Alvarado M, Anderson HR, Anderson LM, Andrews KG, Atkinson C, Baddour LM, Barker-Collo S, Bartels DH, Bell ML, Benjamin EJ, Bennett D, Bhalla K, Bikbov B, Bin Abdulhak A, Birbeck G, Blyth F, Bolliger I, Boufous S, Bucello C, Burch M, Burney P, Carapetis J, Chen H, Chou D, Chugh SS, Coffeng LE, Colan SD, Colquhoun S, Colson KE, Condon J, Connor MD, Cooper LT, Corriere M, Cortinovis M, de Vaccaro KC, Couser W, Cowie BC, Criqui MH, Cross M, Dabhadkar KC, Dahodwala N, De Leo D, Degenhardt

L, Delossantos A, Denenberg J, Des Jarlais DC, Dharmaratne SD, Dorsey ER, Driscoll T, Duber H, Ebel B, Erwin PJ, Espindola P, Ezzati M, Feigin V, Flaxman AD, Forouzanfar MH, Fowkes FG, Franklin R, Fransen M, Freeman MK, Gabriel SE, Gakidou E, Gaspari F, Gillum RF, Gonzalez-Medina D, Halasa YA, Haring D, Harrison JE, Havmoeller R, Hay RJ, Hoen B, Hotez PJ, Hoy D, Jacobsen KH, James SL, Jasrasaria R, Jayaraman S, Johns N, Karthikeyan G, Kassebaum N, Keren A, Khoo JP, Knowlton LM, Kobusingye O, Koranteng A, Krishnamurthi R, Lipnick M, Lipshultz SE, Ohno SL, Mabweijano J, MacIntyre MF, Mallinger L, March L, Marks GB, Marks R, Matsumori A, Matzopoulos R, Mayosi BM, McAnulty JH, McDermott MM, McGrath J, Mensah GA, Merriman TR, Michaud C, Miller M, Miller TR, Mock C, Mocumbi AO, Mokdad AA, Moran A, Mulholland K, Nair MN, Naldi L, Narayan KM, Nasseri K, Norman P, O'Donnell M, Omer SB, Ortblad K, Osborne R, Ozgediz D, Pahari B, Pandian JD, Rivero AP, Padilla RP, Perez-Ruiz F, Perico N, Phillips D, Pierce K, Pope CA 3rd, Porrini E, Pourmalek F, Raju M, Ranganathan D, Rehm JT, Rein DB, Remuzzi G, Rivara FP, Roberts T, De León FR, Rosenfeld LC, Rushton L, Sacco RL, Salomon JA, Sampson U, Sanman E, Schwebel DC, Segui-Gomez M, Shepard DS, Singh D, Singleton J, Sliwa K, Smith E, Steer A, Taylor JA, Thomas B, Tleyjeh IM, Towbin JA, Truelsen T, Undurraga EA, Venketasubramanian N, Vijayakumar L, Vos T, Wagner GR, Wang M, Wang W, Watt K, Weinstock MA, Weintraub R, Wilkinson JD, Woolf AD, Wulf S, Yeh PH, Yip P, Zabetian A, Zheng ZJ, Lopez AD, Murray CJ, AlMazroa MA, Memish ZA. Global and regional mortality from 235 causes of death for 20 age groups in 1990 and 2010: a systematic analysis for the Global Burden of Disease Study 2010. *Lancet* 2012; **380**: 2095-2128 [PMID: 23245604 DOI: 10.1016/S0140-6736(12)61728-0]

3 **Chang MH**, Chen TH, Hsu HM, Wu TC, Kong MS, Liang DC, Ni YH, Chen CJ, Chen DS; Taiwan Childhood HCC Study Group. Prevention of hepatocellular carcinoma by universal vaccination against hepatitis B virus: the effect and problems. *Clin Cancer Res* 2005; **11**: 7953-7957 [PMID: 16278421 DOI: 10.1158/1078-0432.CCR-05-1095]

4 **Lavanchy D**. Worldwide epidemiology of HBV infection, disease burden, and vaccine prevention. *J Clin Virol* 2005; **34** Suppl 1: S1-S3 [PMID: 16461208 DOI: 10.1016/S1386-6532(05)00384-7]

5 **Liang X**, Bi S, Yang W, Wang L, Cui G, Cui F, Zhang Y, Liu J, Gong X, Chen Y, Wang F, Zheng H, Wang F, Guo J, Jia Z, Ma J, Wang H, Luo H, Li L, Jin S, Hadler SC, Wang Y. Reprint of: Epidemiological serosurvey of Hepatitis B in China--declining HBV prevalence due to Hepatitis B vaccination. *Vaccine* 2013; **31** Suppl 9: J21-J28 [PMID: 23948229 DOI: 10.1016/j.vaccine.2013.08.012]

6 **Lavanchy D**. Hepatitis B virus epidemiology, disease burden, treatment, and current and emerging prevention and control measures. *J Viral Hepat* 2004; **11**: 97-107 [PMID: 14996343 DOI: 10.1046/j.1365-2893.2003.00487.x]

7 **Hui CK**, Leung N, Yuen ST, Zhang HY, Leung KW, Lu L, Cheung SK, Wong WM, Lau GK; Hong Kong Liver Fibrosis Study Group. Natural history and disease progression in Chinese chronic hepatitis B patients in immune-tolerant phase. *Hepatology* 2007; **46**: 395-401 [PMID: 17628874 DOI: 10.1002/hep.21724]

8 **Liaw YF**, Chu CM. Hepatitis B virus infection. *Lancet* 2009; **373**: 582-592 [PMID: 19217993 DOI: 10.1016/S0140-6736(09)60207-5]

9 **McMahon BJ**. The influence of hepatitis B virus genotype and subgenotype on the natural history of chronic hepatitis B. *Hepatol Int* 2009; **3**: 334-342 [PMID: 19669359 DOI: 10.1007/s12072-008-9112-z]

10 **Schaefer S**. Hepatitis B virus taxonomy and hepatitis B virus genotypes. *World J Gastroenterol* 2007; **13**: 14-21 [PMID: 17206751 DOI:10.3748/wjg.v13.i1.14]

11 **Croagh CM**, Desmond PV, Bell SJ. Genotypes and viral variants in chronic hepatitis B: A review of epidemiology and clinical relevance. *World J Hepatol* 2015; **7**: 289-303 [PMID: 25848459 DOI: 10.4254/wjh.v7.i3.289]

12 **Wang C**, Teng Z, Zhu Y, Zhao AZ, Sun C. Associations between pre-S deletion mutation of hepatitis B virus and risk of hepatocellular carcinoma in the Asian population: a meta-analysis. *Med Sci Monit* 2015; **21**: 1072-1077 [PMID: 25868851 DOI: 10.12659/MSM.894058]

13 **Mun HS**, Lee SA, Jee Y, Kim H, Park JH, Song BC, Yoon JH, Kim YJ, Lee HS, Hyun JW, Hwang ES, Kook YH, Kim BJ. The prevalence of hepatitis B virus preS deletions occurring naturally in Korean patients infected chronically with genotype C. *J Med Virol* 2008; **80**: 1189-1194 [PMID: 18461612 DOI: 10.1002/jmv.21208]

14 **Pollicino T**, Cacciola I, Saffioti F, Raimondo G. Hepatitis B virus PreS/S gene variants: pathobiology and clinical implications. *J Hepatol* 2014; **61**: 408-417 [PMID: 24801416 DOI: 10.1016/j.jhep.2014.04.041]

15 **Iwamoto M**, Watashi K, Tsukuda S, Aly HH, Fukasawa M, Fujimoto A, Suzuki R, Aizaki H, Ito T, Koiwai O, Kusuhara H, Wakita T. Evaluation and identification of hepatitis B virus entry inhibitors using HepG2 cells overexpressing a membrane transporter NTCP. *Biochem Biophys Res Commun* 2014; **443**: 808-813 [PMID: 24342612 DOI: 10.1016/j.bbrc.2013.12.052]

16 **Jemal A**, Bray F, Center MM, Ferlay J, Ward E, Forman D. Global cancer statistics. *CA Cancer J Clin* 2011; **61**: 69-90 [PMID: 21296855 DOI: 10.3322/caac.20107]

17 **Prieto J**. Inflammation, HCC and sex: IL-6 in the centre of the triangle. *J Hepatol* 2008; **48**: 380-381 [PMID: 18093689 DOI: 10.1016/j.jhep.2007.11.007]

18 **Mittal S**, El-Serag HB. Epidemiology of hepatocellular carcinoma: consider the population. *J Clin Gastroenterol* 2013; **47** Suppl: S2-S6 [PMID: 23632345 DOI: 10.1097/MCG.0b013e3182872f29]

19 **Liu WC**, Liu QY. Molecular mechanisms of gender disparity in hepatitis B virus-associated hepatocellular carcinoma. *World J Gastroenterol* 2014; **20**: 6252-6261 [PMID: 24876746 DOI: 10.3748/wjg.v20.i20.6252]

20 **Wang SH**, Chen PJ, Yeh SH. Gender disparity in chronic hepatitis B: Mechanisms of sex hormones. *J Gastroenterol Hepatol* 2015; **30**: 1237-1245 [PMID: 25708186 DOI: 10.1111/jgh.12934]

21 **Yu MW**, Yang YC, Yang SY, Cheng SW, Liaw YF, Lin SM, Chen CJ. Hormonal markers and hepatitis B virus-related hepatocellular carcinoma risk: a nested case-control study among men. *J Natl Cancer Inst* 2001; **93**: 1644-1651 [PMID: 11698569 DOI: 10.1093/jnci/93.21.1644]

22 **Chiu CM**, Yeh SH, Chen PJ, Kuo TJ, Chang CJ, Chen PJ, Yang WJ, Chen DS. Hepatitis B virus X protein enhances androgen receptor-responsive gene expression depending on androgen level. *Proc Natl Acad Sci* 2007; **104**: 2571-2578 [PMID: 17259306 DOI: 10.1073/pnas.0609498104]

23 **Bouchard MJ**, Wang L, Schneider RJ. Activation of focal adhesion kinase by hepatitis B virus HBx protein: multiple functions in viral replication. *J Virol* 2006; **80**: 4406-4414 [PMID: 16611900 DOI: 10.1128/JVI.80.9.4406-4414.2006]

24 **Lam CM**, Yong JL, Chan AO, Ng KK, Poon RT, Liu CL, Lo CM, Fan ST. Better survival in female patients with hepatocellular carcinoma: oral contraceptive pills related? *J Clin Gastroenterol* 2005; **39**: 533-539 [PMID: 15942442 DOI: 10.1097/01.mcg.0000165670.25272.46]

25 **Naugler WE**, Sakurai T, Kim S, Maeda S, Kim K, Elsharkawy AM, Karin M. Gender disparity in liver cancer due to sex differences in MyD88-dependent IL-6 production. *Science* 2007; **317**: 121-124 [PMID: 17615358 DOI: 10.1126/science.1140485]

26 **Yeh SH**, Chen PJ. Gender disparity of hepatocellular carcinoma: the roles of sex hormones. *Oncology* 2010; **78** Suppl 1: 172-179 [PMID: 20616601 DOI: 10.1159/000315247]

27 **Wang HC**, Huang W, Lai MD, Su IJ. Hepatitis B virus pre-S mutants, endoplasmic reticulum stress and hepatocarcinogenesis. *Cancer Sci* 2006; **97**: 683-688 [PMID: 16863502 DOI: 10.1111/j.1349-7006.2006.00235.x]

28 **Hsieh YH**, Su IJ, Wang HC, Chang WW, Lei HY, Lai MD, Chang WT, Huang W. Pre-S mutant surface antigens in chronic

hepatitis B virus infection induce oxidative stress and DNA damage. *Carcinogenesis* 2004; **25**: 2023-2032 [PMID: 15180947 DOI: 10.1093/carcin/bgh207]

29 **Caselmann WH**, Meyer M, Kekulé AS, Lauer U, Hofschneider PH, Koshy R. A trans-activator function is generated by integration of hepatitis B virus preS/S sequences in human hepatocellular carcinoma DNA. *Proc Natl Acad Sci* 1990; **87**: 2970-2974 [PMID: 2158099 DOI: 10.1073/pnas.87.8.2970]

30 **Lee SA**, Kim KJ, Kim DW, Kim BJ. Male-specific W4P/R mutation in the pre-S1 region of hepatitis B virus, increasing the risk of progression of liver diseases in chronic patients. *J Clin Microbiol* 2013; **51**: 3928-3936 [PMID: 24025913 DOI: 10.1128/JCM.01505-13]

31 **Lee SA**, Kim H, Won YS, Seok SH, Na Y, Shin HB, Inn KS, Kim BJ. Male-specific hepatitis B virus large surface protein variant W4P potentiates tumorigenicity and induces gender disparity. *Mol Cancer* 2015; **14**: 23 [PMID: 25645622 DOI: 10.1186/s12943-015-0303-7]

32 **Yang H**, Westland C, Xiong S, Delaney WE 4th. In vitro antiviral susceptibility of full-length clinical hepatitis B virus isolates cloned with a novel expression vector. *Antiviral Res* 2004; **61**: 27-36 [PMID: 14670591 DOI: 10.1016/j.antiviral.2003.07.003]

33 **Zheng L**, Baumann U, Reymond JL. An efficient one-step site-directed and site-saturation mutagenesis protocol. *Nucleic Acids Res* 2004; **32**: e115 [PMID: 15304544 DOI: 10.1093/nar/gnh110]

34 **Fattovich G**, Stroffolini T, Zagni I, Donato F. Hepatocellular carcinoma in cirrhosis: incidence and risk factors. *Gastroenterology* 2004; **127**: S35-S50 [PMID: 15508101 DOI: 10.1053/j.gastro.2004.09.014]

35 **Haukeland JW**, Damås JK, Konopski Z, Løberg EM, Haaland T, Goverud I, Torjesen PA, Birkeland K, Bjøro K, Aukrust P. Systemic inflammation in nonalcoholic fatty liver disease is characterized by elevated levels of CCL2. *J Hepatol* 2006; **44**: 1167-1174 [PMID: 16618517 DOI: 10.1016/j.jhep.2006.02.011]

36 **Abiru S**, Migita K, Maeda Y, Daikoku M, Ito M, Ohata K, Nagaoka S, Matsumoto T, Takii Y, Kusumoto K, Nakamura M, Komori A, Yano K, Yatsuhashi H, Eguchi K, Ishibashi H. Serum cytokine and soluble cytokine receptor levels in patients with non-alcoholic steatohepatitis. *Liver Int* 2006; **26**: 39-45 [PMID: 16420507 DOI: 10.1111/j.1478-3231.2005.01191.x]

37 **Abdelmalek MF**, Diehl AM. Nonalcoholic fatty liver disease as a complication of insulin resistance. *Med Clin North Am* 2007; **91**: 1125-1149, ix [PMID: 17964913 DOI: 10.1016/j.mcna.2007.06.001]

38 **Grivennikov SI**, Karin M. Inflammatory cytokines in cancer: tumour necrosis factor and interleukin 6 take the stage. *Ann Rheum Dis* 2011; **70** Suppl 1: i104-i108 [PMID: 21339211 DOI: 10.1136/ard.2010.140145]

39 **Michelotti GA**, Machado MV, Diehl AM. NAFLD, NASH and liver cancer. *Nat Rev Gastroenterol Hepatol* 2013; **10**: 656-665 [PMID: 24080776 DOI: 10.1038/nrgastro.2013.183]

40 **Scalera A**, Tarantino G. Could metabolic syndrome lead to hepatocarcinoma via non-alcoholic fatty liver disease? *World J Gastroenterol* 2014; **20**: 9217-9228 [PMID: 25071314 DOI: 10.3748/wjg.v20.i28.9217]

:

P- Reviewer: Bramhall S, Huang C, Kai K, Tarantino G, Tomizawa M

S- Editor: Wang XJ **L- Editor**: Filipodia **E- Editor**: Ma YJ

World Journal of Gastroenterology

Submit a Manuscript: http://www.f6publishing.com

World J Gastroenterol 2018 March 14; 24(10): 1093-1106

DOI: 10.3748/wjg.v24.i10.1093

ISSN 1007-9327 (print) ISSN 2219-2840 (online)

ORIGINAL ARTICLE

Basic Study

Determination of the mitigating effect of colon-specific bioreversible codrugs of mycophenolic acid and aminosugars in an experimental colitis model in Wistar rats

Shakuntala Santosh Chopade, Suneela Sunil Dhaneshwar

Shakuntala Santosh Chopade, Suneela Sunil Dhaneshwar, Department of Pharmaceutical Chemistry, Poona College of Pharmacy, Bharati Vidyapeeth University, Pune 411038, India

ORCID number: Shakuntala Santosh Chopade (0000-0002-3886-6577); Suneela Sunil Dhaneshwar (0000-00c01-7646-642X).

Author contributions: Chopade SS and Dhaneshwar SS equally contributed to the conception and design of the study, acquisition, analysis and interpretation of data, drafted the article and made revisions related to the intellectual content of the manuscript.

Supported by Women Scientist Scheme-A (DST), No. SR/WOS-A/LS-1115/2014.

Institutional animal care and use committee statement: All animal experimentation was approved by the Institutional Animal Ethics Committee (IAEC-approval number: CPCSEA/PCH/15/2014-15) of Poona College of Pharmacy, Bharati Vidyapeeth University, Erandwane, Pune 411038, India.

Conflict-of-interest statement: The authors wish to declare no conflict of interest.

Data sharing statement: There are no additional data available in relation to this manuscript.

ARRIVE guidelines statement: The authors have read the ARRIVE guidelines, and the manuscript was prepared and revised according to the guidelines.

Manuscript source: Invited manuscript

Correspondence to: Suneela Sunil Dhaneshwar, BPharm, PhD, Professor, Department of Pharmaceutical Chemistry, Poona College of Pharmacy, Bharati Vidyapeeth University, Pune 411038, India. suneeladhaneshwar@rediffmail.com
Telephone:+91-20-25437237
Fax: +91-20-25439382

Received: December 11, 2017
Peer-review started: December 12, 2017
First decision: December 27, 2017
Revised: December 31, 2017
Accepted: January 24, 2018
Article in press: January 24, 2018
Published online: March 14, 2018

Abstract

AIM

To design colon-targeted codrugs of mycophenolic acid (MPA) and aminosugars as a safer option to mycophenolate mofetil (MMF) in the management of inflammatory bowel disease.

METHODS

Codrugs were synthesized by coupling MPA with aminosugars (D-glucosamine and D-galactosamine) using EDCI coupling. The structures were confirmed by infrared radiation, nuclear magnetic resonance, mass spectroscopy and elemental analysis. The release profile of codrugs was extensively studied in aqueous buffers, upper gastrointestinal homogenates, faecal matter and caecal homogenates (*in vitro*) and rat blood (*in vitro*). Anti-colitic activity was assessed in 2,4,6-trinitrobezenesulfonic acid-induced colitis in Wistar rats by the estimation of various demarcating parameters. Statistical evaluation was performed by applying one-way and two-way ANOVA when compared with the disease control.

RESULTS

The prodrugs resisted activation in HCl buffer (pH 1.2) and stomach homogenates of rats with negligible hydrolysis in phosphate buffer (pH 7.4) and intestinal homogenates. Incubation with colon homogenates (*in vitro*) produced 76% to 89% release of MPA emphasizing colon-specific activation of codrugs and the release of MPA and aminosugars at the site of action. In the *in vitro* studies, the prodrug of MPA with D-glucosamine (MGLS) was selected which resulted in 68% release of MPA in blood. *in vitro* studies on MGLS revealed its colon-specific activation after a lag time of 8 h which could be ascribed to the hydrolytic action of N-acyl amidases found in the colon. The synthesized codrugs markedly diminished disease activity score and revived the disrupted architecture of the colon that was comparable to MMF but superior to MPA.

CONCLUSION

The significant attenuating effect of prodrugs and individual aminosugars on colonic inflammation proved that the rationale of the codrug approach is valid.

Key words: Mycophenolic acid; Mutual prodrug; Inflammatory bowel disease; Mycophenolate mofetil

Core tip: Mycophenolic acid (MPA), an immunosuppressant and its morpholinoethyl ester prodrug: mycophenolate mofetil are under investigation for the treatment of inflammatory bowel disease (IBD). Diarrhea and local gut toxicity are their major setbacks. The present work focused on the synthesis of colon-targeted prodrugs wherein MPA was bio-reversibly linked with aminosugars to mask the carboxyl group of MPA responsible for gastrointestinal side effects. The synthesized prodrugs exhibited a significant mitigating effect on 2,4,6-trinitrobezenesulfonic acid-induced colitis in Wistar rats compared to MPA. The absence of pancreatitis, hepatitis and the gastro-sparing nature of the prodrugs emphasize their potential which could be investigated further for the management of IBD.

Choapade SS, Dhaneshwar SS. Determination of the mitigating effect of colon-specific bioreversible codrugs of mycophenolic acid and aminosugars in an experimental colitis model in Wistar rats. *World J Gastroenterol* 2018; 24(10): 1093-1106 Available from: URL: http://www.wjgnet.com/1007-9327/full/v24/i10/1093.htm DOI: http://dx.doi.org/10.3748/wjg.v24.i10.1093

INTRODUCTION

Mycophenolic acid (MPA) was synthesized as a fermentation product of *Penicillium stoloniferum* cultures by Gosio in 1896. Since its discovery, MPA has been the subject of intensive *in vivo* and *in vitro* screening for antifungal[1], antibacterial[2,3] and immunosuppressive activities[4-8]. Currently it is under investigation for the treatment of inflammatory bowel disease (IBD) and rheumatoid arthritis (RA). MPA is a potent, non-competitive, reversible inhibitor of eukaryotic inosine monophosphate dehydrogenase which is necessary for the growth of T cells and B cells. Due to its local gastric irritant side effect, it is being marketed in two forms *i.e.* mycophenolate mofetil (MMF) and mycophenolate sodium (enteric coated) to improve its gastrointestinal tolerance[7] and enhance bioavailability. MMF is an immunosuppressant of choice due to its multifaceted spectrum of activities and the apparent advantage of enhanced oral bioavailability. However, MMF-induced diarrhoea and local gut toxicity lead to poor patient compliance. It is under investigation for the treatment of IBD patients refractory or intolerant to steroids.

Since the isolation of MPA, it has been shown to possess a broad spectrum of activities due to which continuous attempts were made to improve its specificity by replacement of the lactone ring, modification of aromatic substituents, ester or amide derivatization, but these failed to show any benefits in most cases. Various derivatives of MPA, their synthesis and uses in the treatment of autoimmune diseases, psoriasis, inflammatory diseases including IBD, RA, tumors, virus and allograft rejection are described in many United States Patents[9-12]. Hydroxamic acid derivatives of MPA as histone deacetylases at the cellular level have been reported by Batovska *et al*[9]. 4 and 6-substituted derivatives of MPA[10], 5-hexanoic acid side chain derivatives of MPA[11] and a parenteral formulation of MPA, a salt or prodrug[12] thereof have been filed in the last two decades. Recently, Iwaszkiewicz-Grzes *et al*[13] in search of new immunosuppressants, synthesized amino acid derivatives of MPA as methyl esters using EDCI as the coupling reagent. With the exception of MMF, the morpholinoethyl ester prodrug of MPA, there are no reports of any prodrugs in the literature that are designed with the objective of enhancing its efficacy, reducing its effective dose or rendering a gastro-sparing effect.

The routine drug therapy of IBD involves the use of 5-aminosalicylic acid (5-ASA), sulfasalazine, corticosteroids (hydrocortisone, prednisolone, betamethasone, beclometasone and budesonide) and immunosuppressive agents (6-mercaptopurine, azathioprine, methotrexate and cyclosporine), whereas 4-ASA, broad-spectrum antibiotics, MMF, metronidazole, nicotine and thalidomide are other choices available for the treatment of disease or its secondary effects. Short chain fatty acids such as butyric acid are presently under investigation as treatment options for the safer management of IBD. Alternative treatments for IBD involve the use of colestyramine, sodium cromoglycate, bismuth and arsenical salts, methotrexate, lidocaine (lignocaine), sucralfate, new steroid entities, cytoprotective agents, fish oils and human growth hormone. During the last

decade, a huge number of biological agents against tumor necrosis factor-α, as well as many biochemical substances, have been developed for the effective treatment of patients with IBD. Among the new biologic agents, natalizumab is currently in regular use in the United States. Several nutritional deficiencies have been indicated in IBD and there are reports of improvement in the symptoms by taking daily supplements of nutraceuticals like vitamin A and carotenoids, vitamin E, vitamin C, vitamin K, folic acid, calcium, iron, selenium, zinc, magnesium and copper. Patients with active ulcerative colitis (UC) have a reduction in the amounts of obligate anaerobes, facultative organisms and micro-aerobes, when compared to UC patients in remission. Supplementation with probiotics is considered an effective option in UC. Leukocytapheresis has shown satisfactory results in steroid-refractory patients with UC. Unfractionated heparin and low molecular weight heparins (LMWH) have been used in patients with active UC with encouraging results. Microbes and microbial products including eggs of helminths seem to reduce disease activity in patients with UC or Crohn's disease[14].

5-ASA and its colon-targeted prodrug sulphasalazine, are associated with various serious side effects including ulcerogenicity, hypersensitivity, skin rash, blood disorders, pancreatitis and hepatitis. Corticosteroids and immunosuppressants are also known to produce many serious side effects so there is an urgent need for steroid-sparing, non-nephrotoxic, safe anti-inflammatory agents to treat inflammatory diseases such as IBD, RA, psoriasis and organ transplantations[14-18].

The present work was focused on exploring colon-targeting prodrugs of MPA for their possible application in the management of IBD. For the study, aminosugars such as D-galactosamine and D-glucosamine were selected as promoieties. An extensive literature review revealed that aminosugars play a vital role in resisting chemical attack and improving the tenacity of colon mucus. Moreover, glucosamine is involved in the biosynthesis of glucosaminoglycans and intestinal mucus. Colonic mucus is distinguished from mucus in the proximal intestine not only by its greater sialylation but also by its marked degree of sulphation[19]. The mucin molecule bristles with oligosaccharide side chains, the initial sugar of which is always N-acetyl galactosamine O-linked onto serine or threonine in the protein core. Onto this initial galactosamine may be attached up to 10 or more sugar moieties which can include N-acetyl glucosamine, galactose, N-acetyl galactosamine, fucose or the acid sugar sialic acid (usually as N-acetyl neuraminic acid). Alterations in sialylation and sulphation of mucins and O-acetylation of the mucin sialic acids could all have important effects on the resistance of mucus to bacterial enzymatic attack leading to colorectal cancer and IBD. Clamp and colleagues demonstrated that in UC and Crohn's disease, the oligosaccharide side chain of mucin is greatly shortened[20]. Therefore, we thought of linking glucosamine and galactosamine with MPA which when released in the colon would help to retain the architecture of mucin and form a protective layer on the colon mucosa. In addition to this, the polyhydroxy nature of these aminosugars would increase the hydrophilicity of MPA to such an extent that absorption of the intact prodrug in the upper gastrointestinal tract (GIT) would be minimized assuring efficient delivery to the site of action.

In the present study, we synthesized colon-specific mutual prodrugs involving the formation of a covalent amide linkage between MPA and aminosugars (glucosamine and galactosamine) in such a manner that upon oral administration the linkage remains intact in the upper GIT, but releases MPA in the colon through enzymatic activation[14,21]. Site-specific drug delivery through site-specific prodrug activation may be accomplished by the utilization of specific enzymes secreted by the colonic microflora such as N-acyl amidases. The present work was aimed at the rational design, pharmacokinetic and pharmacodynamic comparison of colon-targeting, mutual prodrugs of MPA with the marketed prodrug MMF.

MATERIALS AND METHODS

Mycophenolate sodium was generously gifted by Emcure Pharmaceuticals Pvt. Ltd., Pune, India. D-(+)-glucosamine hydrochloride and D-(+)-galactosamine hydrochloride were purchased from Sigma-Aldrich, St. Louis, United States and Himedia Laboratories Pvt. Ltd., Nashik, India, respectively. All other chemicals used in the synthesis were purchased from Merck Speciality Pvt. Ltd., Mumbai, India. The reactions were monitored on TLC, which was performed on pre-coated silica gel plates-60 F264 (Merck). Nuclear magnetic resonance (NMR) spectra were recorded on a NMR Varian Mercury 400 MHz at SAIF, Panjab University, Chandigarh, India. The IR spectra were recorded on a Jasco, V-530 FTIR in potassium bromide (anhydrous IR grade). A Jasco V530, UV-Visible double-beam spectrophotometer was used for determination of aqueous solubility and partition coefficient. The partition coefficient was determined in n-octanol/distilled water, whereas aqueous solubility was determined in distilled water at room temperature (25 ± 1 ℃). *In vitro* and *in vivo* studies were carried out using HPLC. Before analysis, the mobile phase was filtered through a 0.45 μm membrane filter and degassed using a sonicator. Sample solutions were also filtered through the same system. The HPLC system consisted of a pump (Jasco PU-1580, Serial No. B179460677), with an autosampler injector (Jasco AS-1555) and a UV/VIS detector (Jasco UV 1575, Serial No. A083360681). Data were incorporated using Jasco Borwin version 1.5. The Waters Xterra RP 18 (4.6 mm I.D. × 150 mmL; Part No. 186000442) column along with a Hypersil guard column were used in the reversed phase partition chromatographic condition. The system was used in an air-conditioned HPLC laboratory atmosphere (20 ±

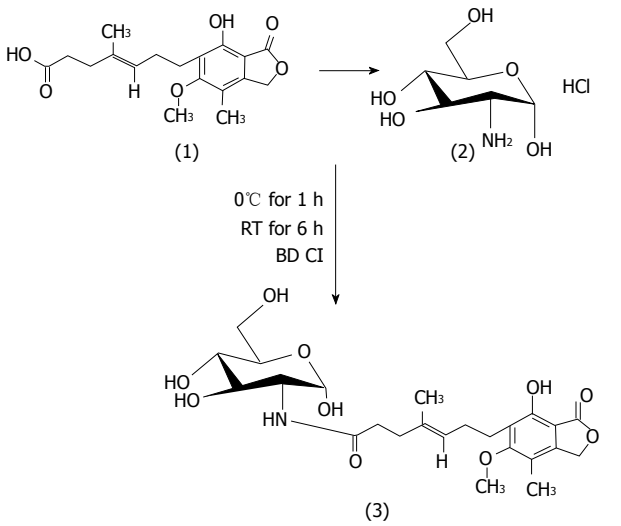

Figure 1 Scheme of synthesis. (1) Mycophenolic acid: (2) D-glucosamine and (3) Prodrug of mycophenolic acid and D-glucosamine.

1 ℃). The column was monitored for UV absorbance at a detection wavelength of 225 nm for estimation of both prodrugs. All kinetic studies were carried out in triplicate. The K values from the plots were calculated separately and the average K and SD values were determined. Histopathological studies of the colon, liver and pancreas were carried out at PRADO Pathology Laboratory, Pune. The pathologist was unaware of the experimental protocols. The histopathological sections were stained with haematoxylin and eosin. Colour microphotographs of the sections were captured on a Nikon optical microscope, Eclipse E-200, with resolution 10 × 40 ×, and a trinocular camera at Poona College of Pharmacy, Pune.

Synthesis

MPA (1 mol) in DMF was reacted with EDCI (2 mol) at 0 ℃. The reaction was continued for 1 h until the MPA-EDCI activated complex was formed. Then in a separate beaker, the aminosugar (1.2 mol/L) in methanol was mixed with 2 drops of triethylamine until basic to litmus and the resulting solution was added to the MPA-EDCI activated complex and stirred at room temperature for 6 h. After completion of the reaction, the solution was poured into 15 mL of cold water and extracted with ethyl acetate. The organic layer was separated and dried with sodium sulphate, filtered and concentrated. The crude product was purified by preparative chromatography using chloroform:methanol:glacial acetic acid (90 V:9 V:1 V). The structures of the synthesized prodrugs (MPA with D-glucosamine: MGLS and MPA with D-galactosamine: MGAS) were established by spectroscopic methods. The scheme of synthesis[13] is presented in Figure 1.

In vitro stability and release studies

In vitro release profiling of the synthesized prodrugs was carried out in aqueous buffers (0.05 mol/L HCl buffer pH 1.2 and 0.05 mol/L phosphate buffer pH 7.4), faecal matter and tissue homogenates of the upper GIT and colon of male Wistar rats by a validated HPLC method. The R_t values for MPA, MGAS and MGLS were 5.9, 9.7 and 11.6, respectively. Concentrations of the parent drug and prodrugs were calculated by equations generated from their respective calibration curves. All the kinetic studies were carried out in triplicate and their standard deviation was calculated.

Aqueous buffers

Prodrug (50 mg) was introduced into 100 mL of HCl buffer in a flask which was kept in a constant temperature bath at 37 ± 1 ℃ under continuous stirring and 2 mL aliquots were withdrawn at different time intervals (0-180 min), each time reloading with an equal volume of fresh buffer. The aliquots were filtered through a membrane filter (0.45 μm) and directly estimated by HPLC at 225 nm using phosphate buffer (pH 4.5):acetonitrile (40 V:60 V) as mobile phase. The same procedure as described above was followed to study the release kinetics of prodrugs in 0.05 mol/L phosphate buffer pH 7.4.

Upper GIT homogenates

Wistar rats (250 g) were anesthetized by ether, sacrificed and then midline incisions were made. Sections of stomach, small intestine and colon were collected separately, homogenized using a Remi overhead homogenizer and diluted to half concentration with isotonic HCl buffer (pH 1.2) for stomach homogenates and with isotonic phosphate buffer (pH 7.4) for small intestinal homogenates and colon homogenates. To each Eppendorf tube, 0.8 mL of prodrug solution (1 mg/mL) and 0.2 mL of homogenate solution were added and incubated at 37 ± 1 ℃. Subsequently, at 15 min intervals for the first 1 h and then hourly for the next 3 h (stomach homogenates), 7 h (small intestinal homogenates) and 10 h (colon homogenates), the Eppendorf tubes were withdrawn and mixed in a vortex mixer, centrifuged at 10000 rpm for 10 min and the supernatants were filtered through a membrane filter (0.45 μm). The filtrate (20 μL) was injected into the HPLC system and the amount of MPA released estimated by the UV detector using the same mobile phase as above at 225 nm.

Faecal matter and caecal homogenate

To a 0.1 mL suspension of fresh rat faecal matter and caecal homogenate (homogenised and diluted with phosphate buffer pH 7.4), prodrug solution (0.9 mL) was added and the tubes were incubated at 37 ± 1 ℃. The samples were removed from the incubator at predetermined time intervals over a period of 13 h and the same procedure was followed for analysis as mentioned in the above section.

Table 1 Doses of test and standard compounds

Groups	Dose[1] (mg/kg)
HC	0.9% saline (1 mL)
MPA	18.5
MMF	25.0
MGLS	28.5
MGAS	28.5
D- Glucosamine	12.4
D- Galactosamine	12.4
MPA + GL	18.5 + 12.4
MPA + GA	18.5 + 12.4

[1]All doses were calculated on an equimolar basis to the dose of MPA. HC: Healthy control; MPA: Mycophenolic acid; MMF: Mycophenolate mofetil; MGLS: Prodrug of MPA and D-glucosamine; MGAS: Prodrug of MPA and D-galactosamine; MPA + GL: Physical mixture of MPA and D-glucosamine; MPA + GA: Physical mixture of MPA and D-galactosamine.

In vivo pharmacokinetics

Of the two prodrugs, MGLS was selected for *in vivo* study. All the experimental procedures and protocols used for the *in vivo* release studies were reviewed and approved by the Institutional Animal Ethical Committee (IAEC) of Poona College of Pharmacy, Pune (CPCSEA/PCH/15/2014-15) and were in accordance with the guidelines of the Committee for the purpose of Control and Supervision of Experiment on Animals (CPCSEA), Government of India.

Male Wistar rats fasted for 24 h (average weight 200-230 g; 12-15 wk; *n* = 6/group) were provided with only water *ad libitum*. The retro-orbital bleeding technique was used to withdraw blood from the rats (1 mL) and this was considered the zero hour reading. Then an oral dose of MGLS prodrug (28.53 mg/kg) in 1.0 mL of physiological saline was administered and blood samples were collected in EDTA tubes at 15 min intervals for 1 h and then on an hourly basis until the 11th hour and finally at the 24th hour. The EDTA tubes were centrifuged at 5000 rpm at 0-5 ℃ for 10 min. The supernatant solution of centrifuged blood was added to the Eppendorf tube and 0.9 mL of methanol was added for immediate plasma precipitation. All the solutions were then vortexed for 2 min, centrifuged at 10000 rpm for 5 min at 0-5 ℃, filtered through a membrane filter and analysed by HPLC.

Faeces and urine were collected from metabolic cages, pooled together as 24 h samples, diluted 100- and 10-fold, respectively, with isotonic phosphate buffer solution pH (7.4) and then the same procedure was followed as described above.

Pharmacological evaluation

Induction of colitis: To induce inflammation in rat colon, all the groups except the healthy control group were catheterized using a rubber cannula (8 cm intra-rectal) and 0.25 mL of 2,4,6-trinitrobezenesulfonic acid (TNBS) (100 mg/kg of body weight in 50% v/v ethanol solution) was administered after light narcotizing with ether. The animals were then maintained in a vertical position for 30 s and returned to their cages. The rats were housed without treatment for 3 d to maintain the development of a full inflammatory bowel disease model. The animals received standard and test compounds orally, once daily for five continuous days. The doses of prodrugs were calculated on an equimolar basis to MPA and are shown in Table 1. The healthy control and colitis control groups were given only saline instead of free drug or prodrug[22].

During the course of 11 d, three parameters were observed; weight loss, stool consistency and rectal bleeding. Anti-colitic activity was estimated by assessment of the disease activity score rate[23] (Table 3). As previously applied by Krawisz *et al*[24], the disease activity score was determined by calculating the average of the above three parameters for each group on each day in the range of 0 (healthy) to 4 (maximal activity of colitis). On the 11th day the animals were sacrificed by isoflurane anaesthesia and their colon/body weight ratio was calculated using dissected sections of colon. Anti-colitic activity of the prodrugs was compared with MPA and MMF as standards. Rat stomach, colon, liver and pancreas were dissected. Gastric ulcers were scanned and the ulcer index was calculated by scoring the ulcers as per the method reported by Cioli *et al*[25] (1979). Specimens of colon, liver and pancreas were fixed in formalin for histopathological analysis.

Statistical analysis

All data were expressed as mean ± SEM; (*n* refers to the number of animals in each group). For the disease activity score rate, statistical differences between groups were calculated by two-way ANOVA followed by Bonferroni's test, whereas statistical analysis of ulcerogenic activity was carried out using one-way ANOVA followed by the Dunnett's *post- hoc* test. Differences were considered significant at $P < 0.001$-0.05.

RESULTS

Aqueous solubility and partition coefficient

The aqueous solubility was determined experimentally and was found to be 0.42 mg/mL and 0.21 mg/mL for MGLS and MGAS, respectively. Log *P* in n-octanol/distilled water was found to be 2.1 and 2.3, respectively.

Spectral analysis

Structures of the synthesized prodrugs were confirmed by IR, NMR, mass spectroscopy and elemental analysis.

Amide prodrug of MPA and D-glucosamine

MGLS: (E)-N-((2S, 3R, 4R, 5S)-tetrahydro-2,4,5-trihydroxy-6-(hydroxymethyl)-2H-pyran-3-yl)-7-1,3-dihydro-7-hydroxy-5-methoxy-4-methyl-1-oxoiso-benzofuran-6-yl)-4-methylhept-4-enamide, M.P: 78 ℃ (uncorrected), R_f 0.42; chloroform: methanol: glacial acetic acid (90:9:1; v/v/v), Aq. sol.: 0.42 mg/mL,

Table 2 Results of in vitro release in different incubation media

Prodrug	Incubation media							
	Aqueous buffers pH 1.2 and pH 7.4	Stomach and intestinal homogenates	Colon homogenate				Faecal matter	
			K ± SD (min^{-1})[1]	$t_{1/2}$ (min)	% Prodrug hydrolysed	% MPA released	% Prodrug hydrolysed	% MPA released
MGLS	Stable	1.30%	0.0025 ± 0.000978	275	92.6	86.7	63	54
MGAS	Stable	14-19%	0.000108 ± 0.00001	305	79.15	76.4	47	52

[1]Average of six readings, follows first-order kinetics. MGLS: Prodrug of mycophenolic acid and D-glucosamine; MGAS: Prodrug of mycophenolic acid and D-galactosamine.

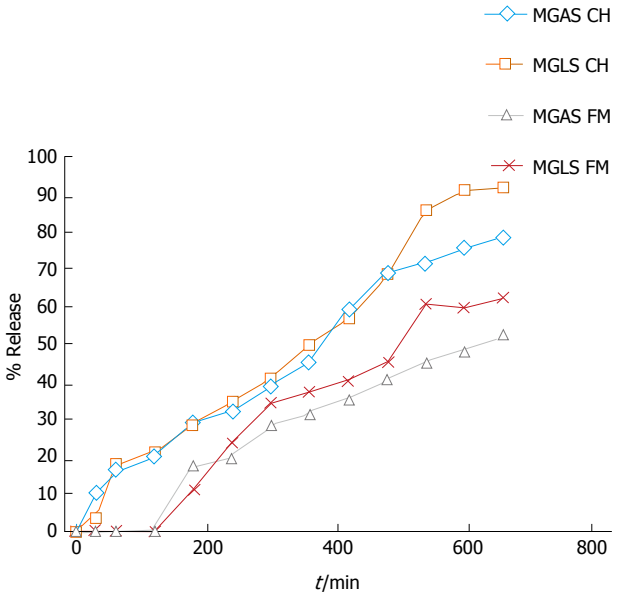

Figure 2 *In vitro* release of mycophenolic acid from prodrugs in different incubation media. MPA: Mycophenolic acid; MGLS: Prodrug of MPA and D-glucosamine; CH: Colon homogenate; FM: Faecal matter.

Log P_{oct}: 2.1, FTIR (anhydrous KBr; cm^{-1}): 3530 (OH stretch), 3284 (NH stretch sec. amide), 3048 (C=C stretch aromatic ring), 1765 (C=O stretch ester), 1698 (C=O stretch sec. amide), 1536 (C=C bend aromatic ring), 1133 (C-O stretch ester), ^{1}H NMR ($CDCl_3$; 400MHz) MPA backbone : δ 1.71 [s,3H] C-CH_3 , 1.80-1.89 [t, 2H] C-CH_2, 2.33-2.38 [q, 2H]-CH_2, 2.50 [s, 3H] -CH_3 Ar-H, 2.59-2.63 [m, 4H] O=C-CH_2 and Ar-CH_2, 3.71 [t, 3H] -OCH_3, 3.77-3.78 [d, H] = CH, 5.20 [s, 2H] lactone ring, 5.26 [s, H] -OH glucosamine backbone: 2.1 [s, 2H] -OH tetrahydropyran, 2.17-2.22 [t, 2H] -OH group tetrahydropyran, 3.06-3.36 [m, 5H]-CH, 3.79-3.82 [d, H]-CH2-OH, 9.2 [s, H] -NH sec. amide, ^{13}C NMR (400 MHz, $CDCl_3$): δ 11.00, 11.40, 14.42, 16.06, 22.34, 25.74, 34.09, 60.41, 68.65, 78.31, 78.64, 78.84, 78.97, 106.63, 115.71, 122.16, 122.82, 123.14, 133.29, 145.03, 162.60, 170.53, Mass: m/z M+1: 496. 99, (molecular weight: 495.52), Elemental analysis: calculated for $C_{24}H_{33}NO_{10}$; C, 58.17; H, 6.71; N, 2.83. Found: C, 58.24; H, 6.72; N, 2.82.

Amide prodrug of MPA and D-galactosamine

MGAS: (E)-N-((2S, 3R, 4R, 5R)-tetrahydro-2,4,5-trihydroxy-6-(hydroxymethyl)-2H-pyran-3-yl)-7-(1,3-dihydro-7-hydroxy-5-methoxy-4-methyl-1-oxoisobenzofuran-6-yl)-4-methylhept-4-enamide. M.P: 80 ℃ (uncorrected), R_f 0.41; chloroform: methanol: glacial acetic acid (90:9:1; v/v/v), Aq. sol.: 0.21 mg/mL, Log P_{oct}: 2.3, FTIR (anhydrous KBr ; cm^{-1}): 3652 (OH stretch) , 3284 (NH stretch sec. amide group), 2997 (C=C stretch aromatic), 1765 (C=O stretch ester), 1698 (C=O stretch sec. amide), 1536 (C=C bend aromatic), 1132 (C-O stretch ester), ^{1}H NMR ($CDCl_3$; 400MHz) MPA backbone : δ 1.88 [s, 3H] =C-CH_3, 2.09 [s, 3H] Ar-CH_3 , 2.17-2.20 [m, 4H]-CH_2-CH_2-, 2.29-2.36 [q, 2H]=C-CH_2, 2.59-2.70 [t, 2H]Ar-CH_2, 3.1 6[s, 3H] -OCH_3 , 5.13 [t, 1H] =C-H, 5.14 [s, 2H] lactone ring, 5.29 [s, 1H] OH group, galactosamine backbone: 1.79 [s, 1H] -OH tetrahydropyran, 2.50-2.52 [s, 3H] -OH tetrahydropyran , 3.20-3.38 [m, 7H] C-H tetrahydropyran ring, 9.1 [s, 1H] -NH sec. amide, ^{13}C NMR (400 MHz, $CDCl_3$, δ ppm): 11.01, 14.46, 15.82, 22.35, 32.15, 34.09, 34.80, 51.02, 60.49, 60.93, 68.59, 78.53, 78.86, 79.19, 106.81, 115.83, 122.21, 123.05, 133.06, 145.46, 152.73, 162.54, 170.24, 172.75, Mass: m/z M+2 497. 09, (molecular weight: 495.52), Elemental analysis: calculated for $C_{24}H_{33}NO_{10}$; C, 58.17; H, 6.71; N, 2.83. Found: C, 58.21; H, 6.72; N, 2.82.

In vitro stability study

In vitro release kinetics are an important tool in understanding the behaviour of prodrugs with respect to their stability and ability to release drugs under *in vitro* conditions that simulate those in the body with respect to pH and enzymes. For the *in vitro* study, prodrugs were incubated at 37 ℃ in aqueous buffers at pH 1.2 and 7.4 representing the pH of stomach and small intestine, respectively. The prodrugs were also incubated with homogenates of stomach and small intestine at 37 ℃ and the release of MPA was studied. Approximately 1%-3% and 14%-19% release of MPA was observed in homogenates of stomach and small intestine, respectively, suggesting negligible hydrolysis by peptidases in the upper GIT. MGLS and MGAS showed 63% and 52% release of MPA in rat faecal matter, respectively, and 87% and 76% release in colon homogenate, respectively (Figure 2). The half-lives of MGLS and MGAS were found to be 275 min and 305

Table 3 Disease activity score rate

Groups	Days										
	1	2	3	4	5	6	7	8	9	10	11
HC	0	0	0	0	0	0	0	0	0	0	0
DC	0	0.67 ± 1.15	0.87 ± 1.50	2.53 ± 0.50	2.63 ± 0.65	2.63 ± 0.65	2.97 ± 0.85	3.12 ± 1.80	3.22 ± 1.70	3.23 ± 2.00	3.30 ± 2.0
MMF	0	0.33 ± 0.58	0.67 ± 1.15	1.07 ± 1.29	1.53 ± 0.50	2.53 ± 0.0	2.10 ± 0.85	1.07 ± 0.51	0.73 ± 0.81	0.23 ± 0.68	0[c]
MPA	0	0.43 ± 0.75	0.67 ± 1.15	2.50 ± 0.17	2.63 ± 0.35	2.63 ± 0.35	2.33 ± 0.58	1.97 ± 0.65	1.63 ± 0.91	0.97 ± 0.85	0.77 ± 0.68[c]
MGLS	0	0.33 ± 0.58	0.33 ± 0.58	1.77 ± 0.40	1.97 ± 0.65	2.53 ± 1.08	1.73 ± 1.03	1.06 ± 0.50	0.63 ± 0.65	0.33 ± 0.17	0[c]
MGAS	0	0.33 ± 0.58	0.43 ± 0.75	1.53 ± 0.81	2.10 ± 0.17	2.33 ± 0.58	1.73 ± 1.03	0.93 ± 0.58	0.73 ± 0.81	0.50 ± 0.35	0.30 ± 0.1[c]
GL	0	0.33 ± 0.58	0.67 ± 1.15	2.1 ± 0.85	2.3 ± 0.89	2.53 ± 0.50	2.1 ± 0.85	1.73 ± 0.75	1.40 ± 0.17	1.20 ± 0.40	1.02 ± 0.2[b]
GA	0	0.43 ± 0.75	0.67 ± 1.15	2.17 ± 0.75	2.53 ± 0.50	2.53 ± 0.52	2.33 ± 0.58	2.10 ± 0.85	1.50 ± 1.01	1.39 ± 1.00	1.30 ± 0.4[b]
GL + MPA	0	0.33 ± 0.58	0.33 ± 0.58	1.83 ± 0.68	2.17 ± 0.75	2.17 ± 0.75	1.87 ± 0.51	1.30 ± 0.70	0.93 ± 0.58	0.53 ± 0.50	0.40 ± 0.35[c]
GA + MPA	0	0.33 ± 0.58	0.667 ± 1.15	1.97 ± 0.65	1.97 ± 0.654	2.3 ± 0.89	1.77 ± 0.51	1.17 ± 0.51	0.73 ± 0.23	0.53 ± 0.50	0.40 ± 0.35[c]

Average of six readings; two-way ANOVA followed by Bonferroni's Test, statistical significance considered at [c]$P < 0.001$ *vs* Disease control. HC: Healthy control; DC: Disease control; MMF: Mycophenolate mofetil; MPA: Mycophenolic acid; MGLS: Prodrug of MPA and D-glucosamine; MGAS: Prodrug of MPA and D-galactosamine; GL: D-glucosamine; GA: D-galactosamine; GL+MPA: Physical mixture of D-glucosamine and MPA; GA + MPA oral: Physical mixture of D-galactosamine and MPA.

min in rat colon homogenates and 523 min and 641 min in rat faecal matter following first order kinetics (Table 2).

In vivo kinetics

MGLS was selected as a representative of the two synthesized prodrugs to study *in vivo* behaviour which was compared with standard MPA. The study was carried out by oral administration of 28.53 mg/kg MGLS and 18.5 mg/kg plain MPA in male Wistar rats housed in metabolic cages. The blood samples were withdrawn by retro-orbital puncture at pre-set time intervals. Urine/faeces samples were collected at various time intervals and pooled together over a period of 24 h. The release pattern of the prodrug was determined by injecting these biological samples into the HPLC system using the newly developed and validated method. After oral administration, MPA appeared in the blood after 1 h, reached a maximum at 7 h (68%) and then gradually declined with disappearance at 24 h. After administration of MGLS, neither MPA nor intact prodrug was observed until 6 h. At 7 h, MGLS was observed in the blood. MGLS showed 70% concentration at 10 h. MPA was observed in the blood at 10 h and reached 68% at 13 h. The concentration of MPA and MGLS started to decline in the blood and was negligible at 24 h (Figure 3).

Pharmacological evaluation

The TNBS model efficiently imitates both acute and chronic colitis resembling human UC[26]. All animals in each group were examined for stool consistency, rectal bleeding and weight loss for 11 d to determine the disease activity score. On the 11th day, all animals were sacrificed and the colon/body weight ratio was calculated to quantify inflammation (Figure 5). The mitigating effect of synthesized prodrugs as well as standards was evaluated for disease activity score rate and colon/body weight ratio in the TNBS-induced experimental colitis model in Wistar rats[24,27]. The results for disease activity score, colon/body weight ratio and ulcerogenic activity are shown in Table 3, Figures 5 and 6, respectively, while photomicrographs of rat colon, pancreas, and liver are shown in Figures 7-9, respectively.

DISCUSSION

Aqueous solubility and partition coefficient

Two mutual latentiated amide derivatives (MGLS and MGAS) of MPA were synthesized with aminosugars D-glucosamine and D-galactosamine, respectively. As anticipated, the outcomes of physico-chemical characterisation revealed that the aqueous solubility of MPA (practically insoluble in water) was significantly improved with

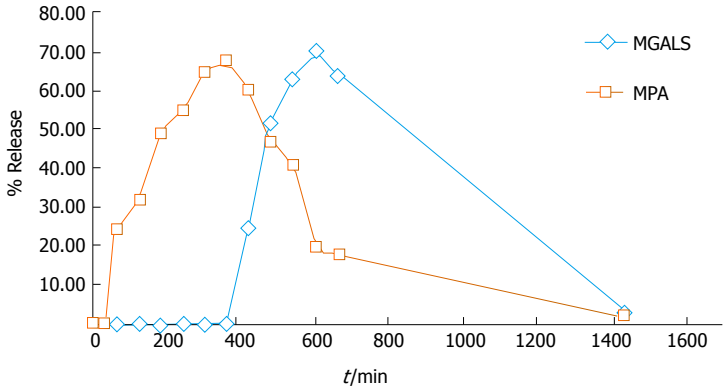

Figure 3 ***In vivo*** **kinetics.** MPA: Mycophenolic acid; MGLS: Prodrug of MPA and D-glucosamine.

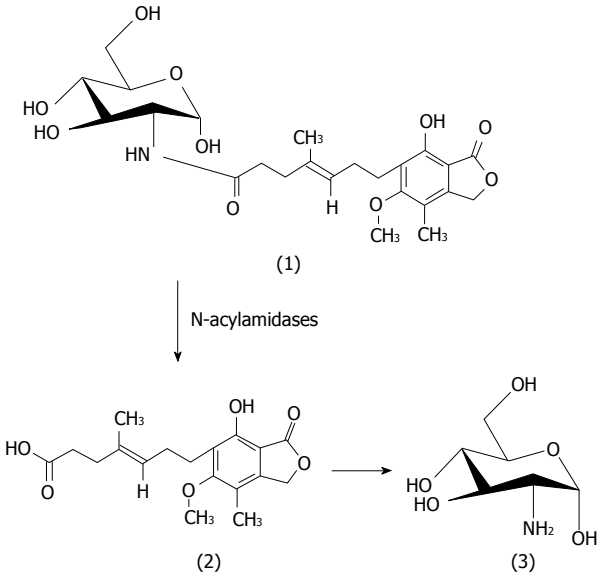

Figure 4 Mode of activation of mycophenolic acid and D-glucosamine prodrug. (1) MGLS prodrug; (2) Mycophenolic acid; and (3) D-glucosamine. MPA: Mycophenolic acid; MGLS: Prodrug of MPA and D-glucosamine.

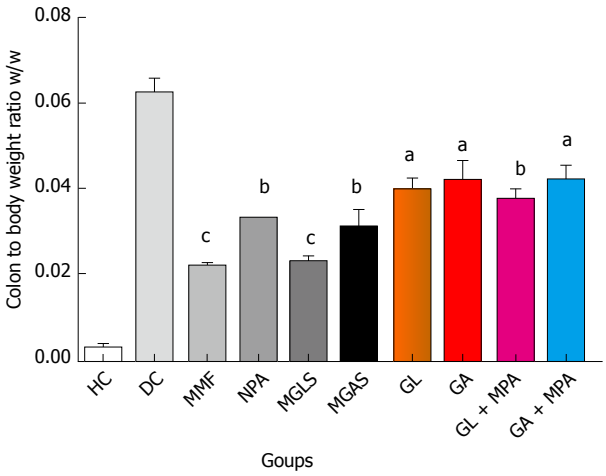

Figure 5 Colon to body weight ratio. Average of six readings; One-way ANOVA followed by Dunnett's Multiple Comparison Test, statistical significance considered at $^{a}P < 0.05$, $^{b}P < 0.01$, $^{c}P < 0.001$ *vs* Disease control. HC: Healthy control; DC: Disease control; MMF: Mycophenolate mofetil; MPA: Mycophenolic acid; MGLS: Prodrug of MPA and D-glucosamine; MGAS: Prodrug of MPA and D-galactosamine; GL: D-glucosamine; GA: D-galactosamine; GL + MPA: Physical mixture of D-glucosamine and MPA; GA + MPA oral: Physical mixture of D-galactosamine and MPA.

a corresponding decrease in the partition coefficient (2.8) in prodrugs. This feature would minimize trans-cellular absorption of prodrugs, thus facilitating their passage directly to the colon. Increased aqueous solubility was attributed to the polyhydroxy nature of the aminosugars.

Spectral study

The IR spectra showed characteristic 2 amide stretches at 3284 and 3283 and C=O stretches of amide at 1698 and 1700 cm^{-1}. ^{1}H NMR of both prodrugs showed characteristic chemical shifts for protons of amide between δ 5 to 8. ^{13}C NMR showed all the relevant chemical shifts as per number of anticipated carbon atoms present in the prodrugs. Disappearance of C=O stretch and OH stretch of carboxylic acid confirmed the formation of an amide bond between MPA and the aminosugars.

The outcomes of ^{1}H NMR and ^{13}C NMR spectral

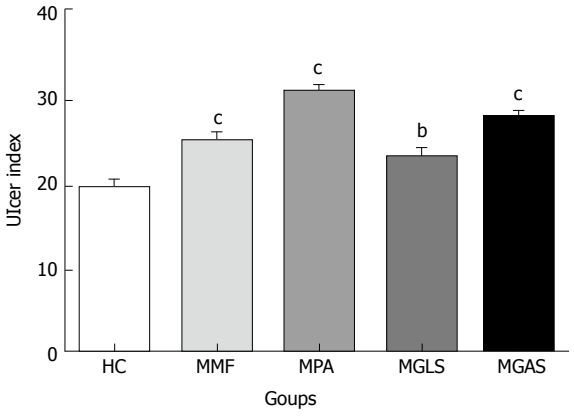

Figure 6 Results of ulcerogenic activity. Average of six readings; One-way ANOVA followed by Dunnett's Multiple Comparison Test, statistical significance considered at $^{b}P < 0.01$, $^{c}P < 0.001$ *vs* Healthy control. HC: Healthy control; MMF: Mycophenolate mofetil; MPA: Mycophenolic acid; MGLS: Prodrug of MPA and D-glucosamine; MGAS: Prodrug of MPA and D-galactosamine.

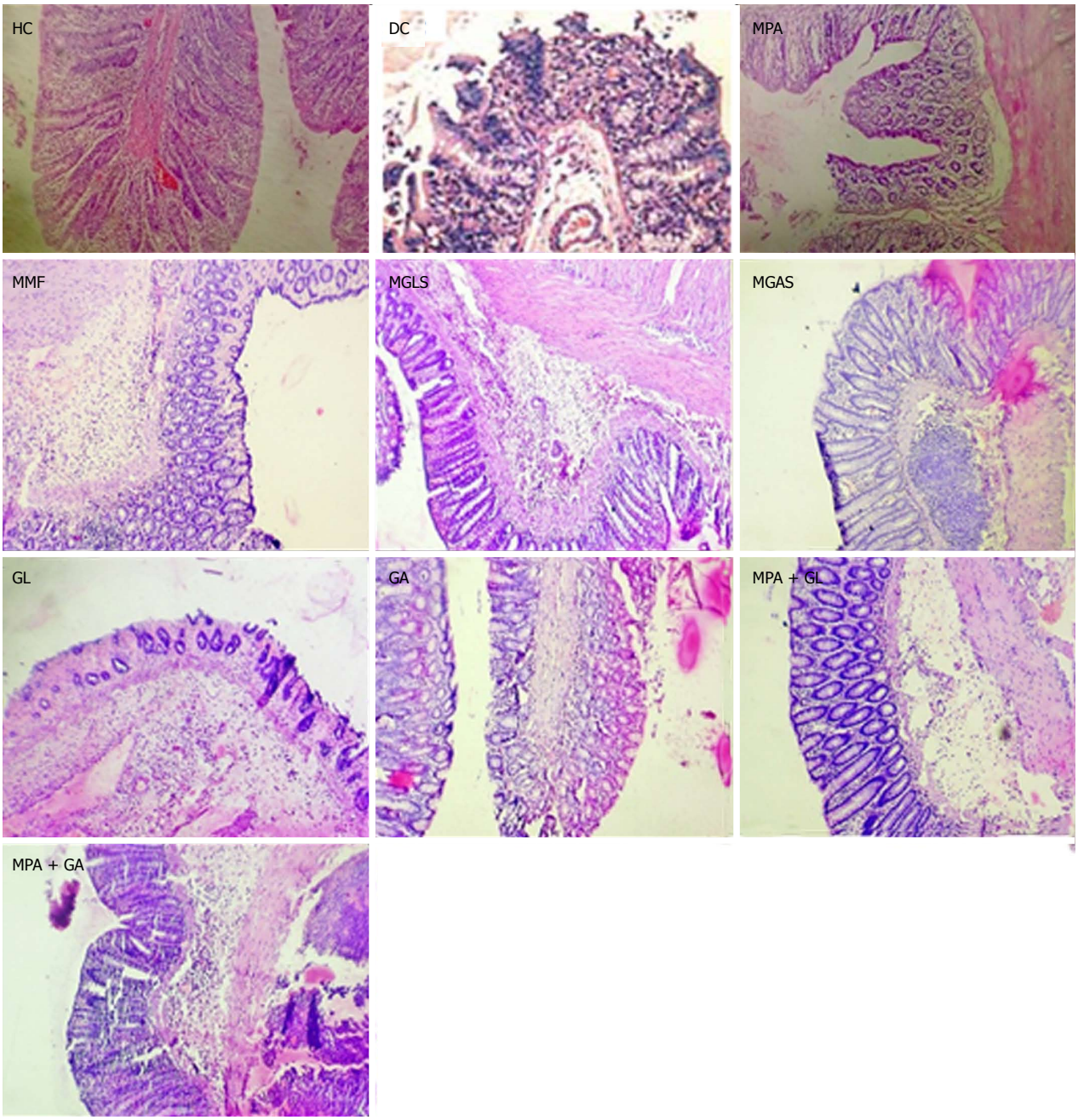

Figure 7 Photomicrographs of colon. HC: Healthy control showing normal architecture of colon mucosa; DC: Disease control showing severe haemorrhage in submucosa with infiltration of inflammatory cells; MPA: MPA showing mild infiltration of inflammatory cells and mild degeneration of epithelium lining; MMF: Showing mild infiltration of inflammatory cells and mild degeneration of epithelium lining; MGLS: Prodrug of MPA and D-glucosamine; MGAS: Prodrug of MPA and D-galactosamine showing mild infiltration of inflammatory cells; GL: D-glucosamine showing mild infiltration of inflammatory cells; GA: D-galactosamine showing mild infiltration of inflammatory cells; MPA + GL: Physical mixture of D-glucosamine and MPA showing mild infiltration of inflammatory cells; MPA + GA: Physical mixture of D-galactosamine and MPA showing mild infiltration of inflammatory cells and mild degeneration of epithelium lining.

studies supported the formation of MGLS and MGAS prodrugs. The results of elemental analysis and mass spectroscopy revealed that the calculated molecular weights of the prodrugs were in accordance with their predicted molecular weights.

In vitro stability study

The aim of the present work was to achieve colon-targeted drug delivery of MPA through its site-specific activation in the colon by resident microflora. The *in vitro* studies showed that the prodrugs were stable in aqueous buffers at pH 1.2 and 7.4 over a period of 3 h and 7 h, respectively, confirming that the prodrugs were not released in the upper GIT. Further studies revealed that both prodrugs exhibited faster activation in colon homogenates as compared to faecal content which was attributed to greater microbial populations in the colon than in faeces. The release of MPA from prodrugs in rat colon homogenates and faecal matter confirmed their colon-specific activation.

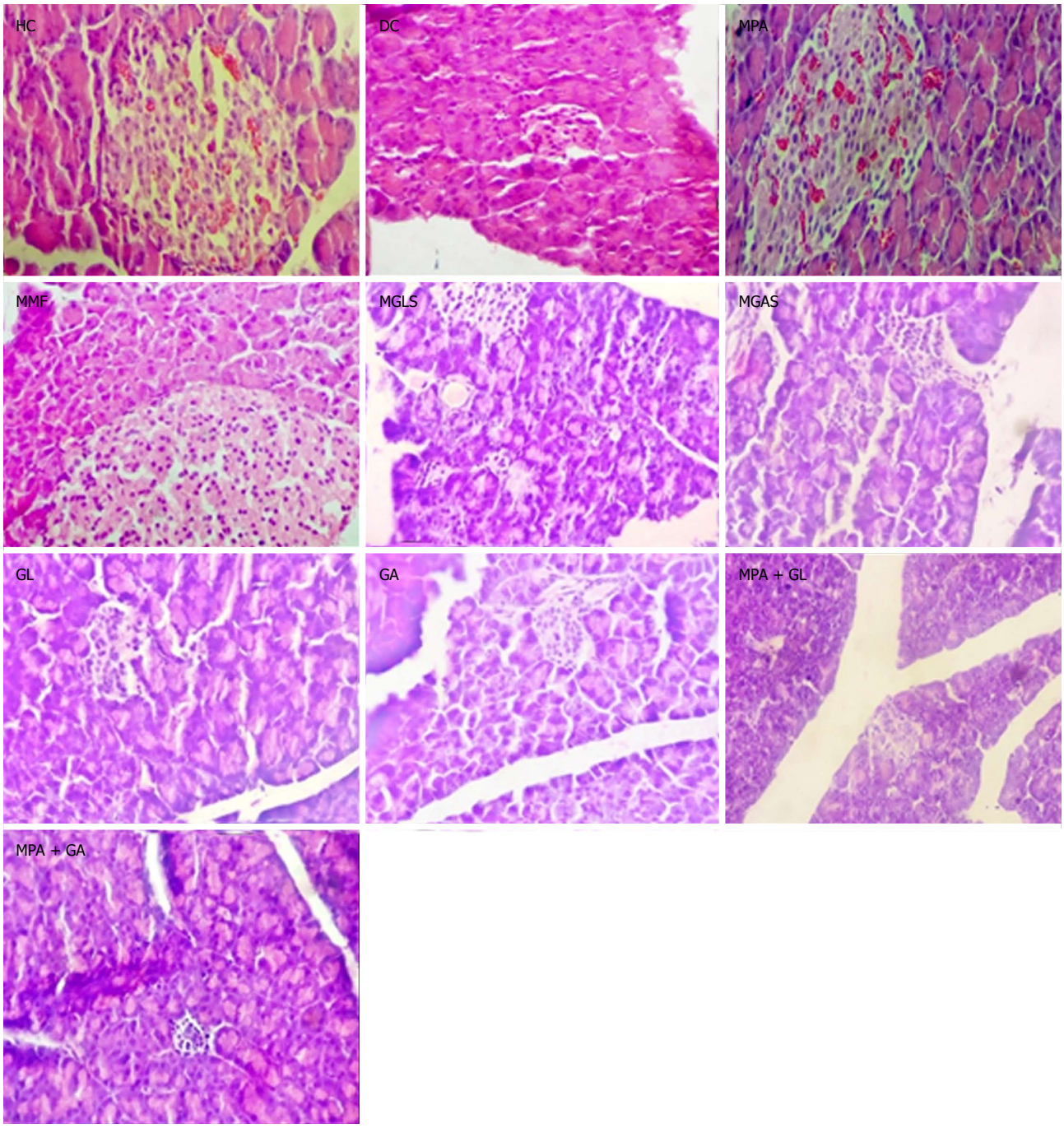

Figure 8 Photomicrographs of pancreas. HC: Healthy control; DC: Disease control; MMF: Mycophenolate mofetil; MPA: Mycophenolic acid; MGLS: Prodrug of MPA and D-glucosamine; MGAS: Prodrug of MPA and D-galactosamine; GL: D-glucosamine; GA: D-galactosamine; GL + MPA: Physical mixture of D-glucosamine and MPA; GA + MPA oral: Physical mixture of D-galactosamine and MPA. DC group showing reduced number and size of islets of Langerhans while all other groups showed normal pancreas architecture without evidence of pancreatitis.

In vivo kinetic study

The *in vivo* study indicated quick absorption of MPA in the upper GIT. In contrast, when MGLS was administered, neither MPA nor intact prodrug was observed until 6 h indicating that prodrug was not absorbed from the stomach and remained intact there. MGLS was observed in the blood at 7 h indicating minimal absorption through the small intestine. The concentration of MGLS consistently increased in the blood reaching a maximum of 70% at 10 h indicating its absorption from the large intestine (colonic mucosa) into the systemic circulation. MPA was observed in the blood at 10 h indicating hydrolysis of MGLS to MPA in the large intestine which was due to its high lipophilicity and it may have transversed the colonic mucosa into the systemic circulation. MPA concentration reached 68% at 13 h. The concentration of MPA and MGLS started to decline in the blood and was negligible at 24 h (Figure 3). The *in vivo* release profile clearly indicated that activation of the prodrug was pH-

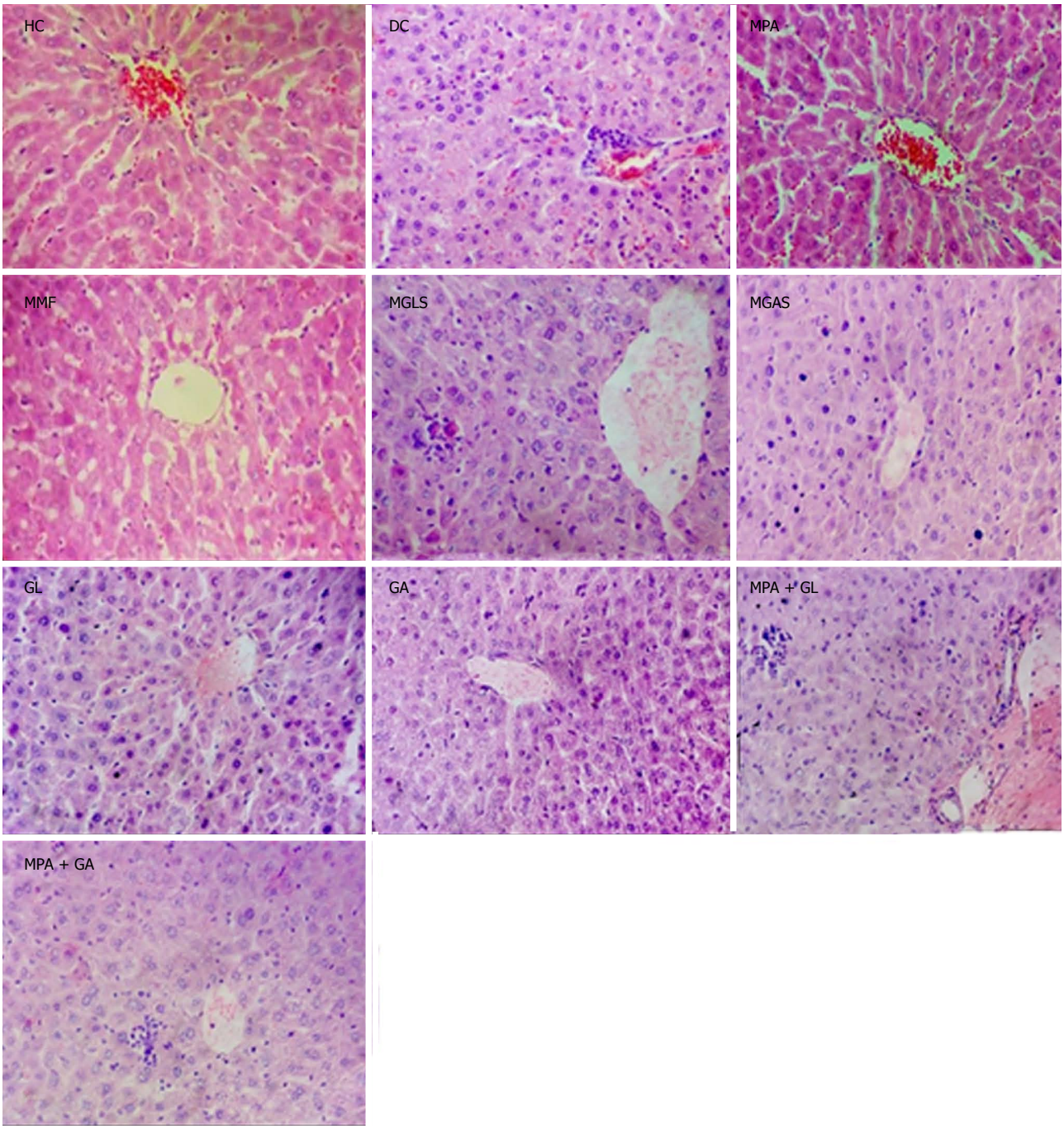

Figure 9 Photomicrographs of liver. HC: Healthy control; DC: Disease control showing minimal degeneration of hepatocytes and congestion of blood vessels; MPA: MPA showing normal liver architecture; MMF: MMF Showing normal liver architecture; MGLS: Prodrug of MPA and D-glucosamine showing minimal infiltration of inflammatory cells; MGAS: Prodrug of MPA and D-galactosamine showing mild infiltration of inflammatory cells; GL: D-Glucosamine showing minimal infiltration of inflammatory cells; GA: D-galactosamine showing minimal infiltration of inflammatory cells; MPA + GL: Physical mixture of D-glucosamine and MPA showing minimal infiltration of inflammatory cells; MPA + GA: Physical mixture of D-galactosamine and MPA showing mild infiltration of inflammatory cells.

dependent (pH 7.4) and by N-acyl amidase present in the colon (Figure 4). The 24 h pooled faeces and urine samples also showed peaks of prodrug and MPA, which confirmed that the prodrug passed through the entire length of the GIT and hence appeared in the faeces; thus, the objective of targeting MPA to the colon was achieved. Moreover, the systemic availability of MPA at high concentration at 13 h revealed that MGLS can be used effectively for the treatment of inflammatory diseases associated with the circadian rhythm such as rheumatoid arthritis.

Pharmacological evaluation

An approximately 11 d TNBS-induced colitis model was used for the pharmacological evaluation. The anti-colitic activity of prodrugs was compared with MMF and MPA. Up to the 5th day the disease activity score increased rapidly and consistently for all TNBS-treated groups

(Table 3). From day 6 to day 10, standard MMF and MPA, prodrugs, carriers and physical mixtures were administered orally to the animals. Full-blown colonic inflammation was demonstrated by the high disease activity score (3.30 ± 2.0) in the colitis control group. Prodrug-treated groups showed a marked decrease in disease activity score rate (99%-100%) that was comparable with the MMF-treated groups. The results of the animal study showed that the disease activity-lowering effect of both prodrugs was significantly superior to MPA (77%), individual carriers (61%-69%) and physical mixtures (88%). Overall, the maximum decrease in colon/body weight ratio was observed in the prodrug-treated groups indicating their significant protective effect on colon inflammation, which was significantly better than MMF and MPA. The lowering effect of carriers and physical mixtures was also better than that of both standards.

Microscopic characterisation of a colon section was performed by considering the following four important parameters, mucosal distortion, inflammation, fibrosis and cryptitis (Figure 7). The colitis control showed severe erosion with absence of the mucosal layer, goblet cell depletion, distorted crypt architecture, lymphocytic infiltration, and thickening of the muscularis mucosa. The lamina propria was also infiltrated with leukocytes. Due to the destruction of crypts, normal mucosal architecture was totally lost. Treatment with the synthesized prodrugs resulted in a marked decrease in the extent and severity of colonic damage (Figure 7) with normal morphology and mild lymphocytic infiltration, which may have been due to activation of T lymphocytes triggered by immune-stimulation of D-glucosamine as well as D-galactosamine as reported by Sadeghi *et al*[28], while the colon of animals treated with a physical mixture of MPA and aminosugars, appeared congested with ulcerated mucosa. MGLS and MGAS proved to be better than the physical mixtures as they were able to release MPA and aminosugars locally in the colon in effective concentrations, thus having a protective effect, while MPA and aminosugars administered orally were unable to reach the colon in required concentrations to mitigate colonic inflammation.

All groups except DC exhibited normal pancreas morphology (Figure 8). Mild infiltration of inflammatory cells in the liver was observed in the groups treated orally with prodrugs and physical mixtures (Figure 9).

The synthesized prodrugs resulted in substantial lowering of ulcer indices as compared to MMF and MPA (Figure 6). These results were consistent with their stability in upper GIT homogenates.

In conclusion, in the present study carrier-linked codrug platforms were successfully designed for efficient colon-specific transport of MPA in order to investigate their potential in mitigating local inflammation in the colon induced by TNBS. Tethering aminosugars to MPA as promoieties resulted in a significant outcome in terms of a marked protective effect compared to MPA without the perpetual diarrhoea observed with MMF therapy. The gastro-sparing nature of the prodrugs and the absence of adverse effects on the pancreas and liver make them promising candidates which should be exploited further as mainstream therapy in the management of IBD.

ARTICLE HIGHLIGHTS

Research background

Defects in the innate immune system are key factors in the pathogenesis of inflammatory bowel disease (IBD). The most commonly used immunomodulators are azathioprine (AZA) or 6-mercaptopurine; however, approximately 10% of patients exhibit intolerance to these drugs, resulting in either withdrawal or prescription of an alternative immunomodulator. Discovered by Gosio in 1893, mycophenolic acid (MPA) was the first antibiotic to be synthesized in a pure and crystalline form. It was used as an immunosuppressant to prevent rejection in organ transplantation, but poor oral bioavailability of MPA was an issue of serious concern. To overcome this setback, mycophenolate mofetil (MMF), the only marketed prodrug of MPA was introduced in 1995 (Trade name: Cellcept) which was used in the treatment of refractory Crohn's disease. Unfortunately MMF also induced GI side effects such as diarrhoea and local gut toxicity leading to poor patient compliance. The role of MMF as an immunomodulator in managing IBD is yet to be fully defined. It is reported in the literature that it may represent a promising treatment for inducing and maintaining remission in IBD patients intolerant of thiopurines. It may be of more value and relevance in ulcerative colitis, as few alternative proven therapies are available.

Hence, it is necessary to design novel colon-targeted prodrugs of MPA with improved bioavailability, lower gastrointestinal (GI) side effects and enhanced efficacy. Many derivatives of MPA have been patented but none has cleared the clinical trials. Therefore, in the present study, colon-specific mutual prodrugs were synthesized by the formation of a covalent amide linkage between MPA and aminosugars. To confirm attainment of an effective concentration of MPA in the colon, *in vivo* pharmacokinetic studies were performed. A 2,4,6-trinitrobezenesulfonic acid (TNBS)-induced colitis model in Wistar rats was used for biological screening of prodrugs and to confirm their mitigating effect on colonic inflammation. The present study underlines the potential of colon-targeting co-therapy of IBD using a novel strategy of delivering MPA with aminosugars simultaneously at the site of action without causing the GIT distress associated with MMF therapy.

Research motivation

Immunosuppressants such as AZA are an inherent constituent of therapy for 50% of patients with Crohn's disease (CD) who develop steroid-dependent or refractory disease. MMF is of proven efficacy and safety in transplantation and in some autoimmune disorders. It has been reported that both AZA and MMF are effective in inducing remission, but AZA seems to be more effective in maintaining remission while onset of the therapeutic effect is delayed less under MMF treatment. Both drugs have steroid-sparing potential, which is delayed under AZA. It seems that AZA is still the immunosuppressant of choice in chronic active CD, but MMF is a reasonable alternative in patients who do not tolerate AZA. One of the major side effects of MMF is gastric distress and diarrhoea that may worsen the symptoms of IBD. The morpholino moiety in MMF is implicated in these side effects. This particular observation inspired us to design codrugs of MPA; replacing the morpholino moiety of MMF with aminosugars which could help to maintain the integrity of the colonic mucosal wall. It was envisaged that these prodrugs might find applicability in those cases of CD which are intolerant to AZA.

Research objectives

The main objectives of this work were to minimize gastric discomfort caused by MMF, and improve the bioavailability and efficacy of MPA in the management of IBD. As gastric side effects are known to be caused by the morpholino moiety of MMF, replacing this moiety with nontoxic aminosugars may have a mitigating effect on inflammation, a stabilizing effect on the colonic mucosal layer and the requisite hydrophilic nature that would impart the desired aqueous solubility to MPA ensuring its efficient delivery to the colon. As anticipate,

effective targeting of MPA to the colon using glucosamine and galactosamine as carriers was achieved due to enhanced aqueous solubility of the prodrugs and a resistant amide linkage between MPA and the aminosugars. MMF-related diarrhoea was not evident in the prodrug-treated groups, which was one of the important objectives of the present study. Site-specific delivery of MPA resulted in improved bioavailability of MPA. Future research should be directed at investigating the potential of these prodrugs on refractory CD and for inducing and maintaining remission in IBD patients intolerant of thiopurines.

Research methods

A clean, single step synthesis of target codrugs was achieved through optimization of the EDCI coupling reaction to avoid complex purification procedures. The synthesized compounds were extensively characterized by spectral analysis. New HPLC methods were developed and validated for simultaneous estimation of MPA and aminosugars in the presence of intact codrugs in order to study the release profiles of codrugs in buffers of various pH, homogenates of gastro-intestinal tract, faecal matter, rat blood, urine and faeces. The TNBS-induced experimental colitis model was optimized to investigate the mitigating effect of codrugs of MPA and aminosugars in comparison to standard drugs (MPA and MMF) and physical mixtures (MPA plus aminosugars) to prove the codrug hypothesis. All data were analysed using relevant statistical tests.

Research results

Colon-targeted release of MPA, absence of gastric distress, diarrhoea, maintenance of the integrity of colonic mucosa by released aminosugars and a significant marked amelioration of TNBS-induced colitis in Wistar rats as compared to MPA were the promising outcomes of this study. These codrugs should be explored further as an alternative to MMF for inducing and maintaining remission in IBD patients, those intolerant to thiopurines as well as those with refractory CD.

A comparative analysis of efficacy of these codrugs against the established anticolitics such as aminosalicylates and corticosteroids is required. In addition, screening of combinations of these prodrugs with established therapies would help to prove their potential in the management of IBD. Acute toxicity and estimation of various pro-inflammatory mediators such as interleukins, tumour necrosis factor-α and myeloperoxidase enzyme are several studies which are underway.

Research conclusions

In the present work, the morpholino moiety of MMF was replaced by novel aminosugars which were tethered with MPA as a literature review revealed that glucosamine and galactosamine play a vital role in resisting chemical attack and improving the tenacity of colon mucus. The novel strategy of codrug therapy proved to be beneficial in terms of lowering the disease activity, colon to body weight ratio and markedly improving the degenerated colon morphology induced by TNBS. MMF-related gut toxicity and diarrhoea were not evident with these codrugs, which was a very promising outcome. This study underlined the utility of aminosugars in maintaining the integrity of colonic mucosa and supported the significant role of an abnormal immune response in the pathophysiology of IBD. These codrugs have the potential to be screened further to determine their efficacy in refractory CD and in the induction and maintenance of IBD remission in patients who are intolerant to thiopurines or MMF.

Research perspectives

A mutual prodrug approach was proven to be superior to physical mixtures of two active drugs *i.e.*, MPA and aminosugars in this study as the efficacy of the codrugs was found to be significantly better than physical mixtures. There is a scope to explore the possibility of conjugation of other nontoxic, biocompatible carrier moieties and established drugs with MPA for a synergistic advantage over administering them in the form of a physical combination.

ACKNOWLEDGEMENTS

The authors are grateful to Department of Science and Technology, New Delhi (DST- WOS-A) for financial assistance to carry out this project and Emcure Pharmaceuticals Pvt. Ltd. Pune, Maharashtra for providing a gift sample of mycophenolate sodium. The authors would like to thank Dr. K.R. Mahadik, Principal, Poona College of Pharmacy, Pune for providing the necessary facilities to carry out the work.

REFERENCES

1 **Hohenleutner U**, Mohr VD, Michel S, Landthaler M. Mycophenolate mofetil and cyclosporin treatment for recalcitrant pyoderma gangrenosum. *Lancet* 1997; **350**: 1748 [PMID: 9413469 DOI: 10.1016/S0140-6736(05)63571-4]

2 **Wilkins WH**. Investigation into the production of bacteriostatic substances by fungi; preliminary examination of the fifth 100 species, all basidiomycetes, mostly of the wood-destroying type. *Br J Exp Pathol* 1946; **27**: 140-142 [PMID: 20995642]

3 **Abraham EP.** The Antibiotics. In: Florkin M, Stotz EH. Comprehensive Biochemistry. Oxford: Sir William Dunn School of Pathology, University of Oxford (Great Britain), **1963**: 181-224 [DOI: 10.1016/B978-1-4831-9711-1.50022-3]

4 **Wilasrusmee C**, Da Silva M, Singh B, Siddiqui J, Bruch D, Kittur S, Wilasrusmee S, Kittur DS. Morphological and biochemical effects of immunosuppressive drugs in a capillary tube assay for endothelial dysfunction. *Clin Transplant* 2003; **17** Suppl 9: 6-12 [PMID: 12795661 DOI: 10.1034/j.1399-0012.17.s9.1.x]

5 **Mitsui A**, Suzuki S. Immunosuppressive effect of mycophenolic acid. *J Antibiot* (Tokyo) 1969; **22**: 358-363 [PMID: 5345678 DOI: 10.7164/antibiotics.22.358]

6 **Eugui EM**, Almquist SJ, Muller CD, Allison AC. Lymphocyte-selective cytostatic and immunosuppressive effects of mycophenolic acid in vitro: role of deoxyguanosine nucleotide depletion. *Scand J Immunol* 1991; **33**: 161-173 [PMID: 1826793 DOI: 10.1111/j.1365-3083.1991.tb03746.x]

7 **Eugui EM**, Mirkovich A, Allison AC. Lymphocyte-selective antiproliferative and immunosuppressive effects of mycophenolic acid in mice. *Scand J Immunol* 1991; **33**: 175-183 [PMID: 2017655 DOI: 10.1111/j.1365-3083.1991.tb03746.x]

8 **Cioli V**, Putzolu S, Rossi V, Corradino C. A toxicological and pharmacological study of ibuprofen guaiacol ester (AF 2259) in the rat. *Toxicol Appl Pharmacol* 1980; **54**: 332-339 [PMID: 6968463 DOI: 10.1016/0041-008X(80)90203-3]

9 **Batovska DI**, Kim DH, Mitsuhashi S, Cho YS, Kwon HJ, Ubukata M. Hydroxamic acid derivatives of mycophenolic acid inhibit histone deacetylase at the cellular level. *Biosci Biotechnol Biochem* 2008; **72**: 2623-2631 [PMID: 18838793 DOI: 10.1271/bbb.80303]

10 **Patterson JW,** inventor. Syntex (USA) Inc., assignee. 4 and 6-substituted derivatives of MPA. United States patent No.5,554,612. 1996

11 **Morgans J,** inventor. Syntex (USA) Inc., assignee. 5-hexanoic acid side chain derivatives of MPA. United States patent No. 5,633,279. 1997

12 **Ahlheim M,** inventor**.** Parenteral formulation of mycophenolic acid, a salt or prodrug thereof. United States Patent No. 20060189683 A1. 2006

13 **Iwaszkiewicz-Grzes D**, Cholewinski G, Kot-Wasik A, Trzonkowski P, Dzierzbicka K. Synthesis and biological activity of mycophenolic acid-amino acid derivatives. *Eur J Med Chem* 2013; **69**: 863-871 [PMID: 24121309 DOI: 10.1016/j.ejmech.2013.09.026]

14 **Dhaneshwar SS**, Vadnerkar G. Rational design and development of colon-specific prodrugs. *Curr Top Med Chem* 2011; **11**: 2318-2345 [PMID: 21671865 DOI: 10.2174/156802611797183249]

15 **Jung YJ**, Lee JS, Kim YM. Synthesis and in vitro/in vivo evaluation of 5-aminosalicyl-glycine as a colon-specific prodrug of 5-aminosalicylic acid. *J Pharm Sci* 2000; **89**: 594-602 [PMID: 10756325 DOI: 10.1002/(SICI)1520-

6017(200005)89:53.0.CO;2-8]
16 **Jung YJ**, Kim HH, Kong HS, Kim YM. Synthesis and properties of 5-aminosalicyl-taurine as a colon-specific prodrug of 5-aminosalicylic acid. *Arch Pharm Res* 2003; **26**: 264-269 [PMID: 12735682 DOI: 10.1007/BF02976953]
17 **Kim H**, Huh J, Jeon H, Choi D, Han J, Kim Y, Jung Y. N,N'-Bis(5-aminosalicyl)-L-cystine is a potential colon-specific 5-aminosalicylic acid prodrug with dual therapeutic effects in experimental colitis. *J Pharm Sci* 2009; **98**: 159-168 [PMID: 18399548 DOI: 10.1002/jps.21404]
18 **Nagpal D,** Singh R, Gairola, N, Bodhankar SL, Dhaneshwar SS. Mutual azo prodrug of 5-aminosalicylic acid for colon targeted drug delivery: synthesis, kinetic studies and pharmacological evaluation. *Ind J Pharm Sci* 2006; **68**: 171-178 [DOI: 10.4103/0250-474X.25710]
19 **Rhodes JM**. Colonic mucus and mucosal glycoproteins: the key to colitis and cancer? *Gut* 1989; **30**: 1660-1666 [PMID: 2693227 DOI: 10.1136/gut.30.12.1660]
20 **Clamp JR**, Fraser G, Read AE. Study of the carbohydrate content of mucus glycoproteins from normal and diseased colons. *Clin Sci* (Lond) 1981; **61**: 229-234 [PMID: 7261546 DOI: 10.1042/cs0610229]
21 **Dhaneshwar S**, Gautam H. Exploring novel colon-targeting antihistaminic prodrug for colitis. *J Physiol Pharmacol* 2012; **63**: 327-337 [PMID: 23070081]
22 **Yamada Y**, Marshall S, Specian RD, Grisham MB. A comparative analysis of two models of colitis in rats. *Gastroenterology* 1992; **102**: 1524-1534 [PMID: 1314749 DOI: 10.1016/0016-5085(92)91710-L]
23 **Hartmann G**, Bidlingmaier C, Siegmund B, Albrich S, Schulze J, Tschoep K, Eigler A, Lehr HA, Endres S. Specific type IV phosphodiesterase inhibitor rolipram mitigates experimental colitis in mice. *J Pharmacol Exp Ther* 2000; **292**: 22-30 [PMID: 10604928]
24 **Krawisz JE**, Sharon P, Stenson WF. Quantitative assay for acute intestinal inflammation based on myeloperoxidase activity. Assessment of inflammation in rat and hamster models. *Gastroenterology* 1984; **87**: 1344-1350 [PMID: 6092199]
25 **Cioli V**, Putzolu S, Rossi V, Scorza Barcellona P, Corradino C. The role of direct tissue contact in the production of gastrointestinal ulcers by anti-inflammatory drugs in rats. *Toxicol Appl Pharmacol* 1979; **50**: 283-289 [PMID: 505458 DOI: 10.1016/0041-008X(79)90153-4]
26 **Ajuebor MN**, Hogaboam CM, Kunkel SL, Proudfoot AE, Wallace JL. The chemokine RANTES is a crucial mediator of the progression from acute to chronic colitis in the rat. *J Immunol* 2001; **166**: 552-558 [PMID: 11123336 DOI: 10.4049/jimmunol.166.1.552]
27 **Barbier M**, Cherbut C, Aubé AC, Blottière HM, Galmiche JP. Elevated plasma leptin concentrations in early stages of experimental intestinal inflammation in rats. *Gut* 1998; **43**: 783-790 [PMID: 9824605 DOI: 10.1136/gut.43.6.783]
28 **Sadeghi B**, Hagglund H, Remberger M, Al-Hashmi S, Hassan Z, Abedi-Valugerdi M, Hassan M. Glucosamine Activates T Lymphocytes in Healthy Individuals and may Induce GVHD/GVL in Stem Cell Transplanted Recipients. *Open Transplant J* 2011; **5**: 1-7 [DOI: 10.2174/18744184011050.10001]

P- Reviewer: Gassler N, Mijandrusic-Sincic B, Sergi CM
S- Editor: Wang JL **L- Editor**: Webster JR **E- Editor**: Ma YJ

World Journal of Gastroenterology

Submit a Manuscript: http://www.f6publishing.com

World J Gastroenterol 2018 March 14; 24(10): 1107-1119

DOI: 10.3748/wjg.v24.i10.1107

ISSN 1007-9327 (print) ISSN 2219-2840 (online)

ORIGINAL ARTICLE

Basic Study

Maturity of associating liver partition and portal vein ligation for staged hepatectomy-derived liver regeneration in a rat model

Yi-Fan Tong, Ning Meng, Miao-Qin Chen, Han-Ning Ying, Ming Xu, Billy Lu, Jun-Jie Hong, Yi-Fan Wang, Xiu-Jun Cai

Yi-Fan Tong, Ning Meng, Han-Ning Ying, Ming Xu, Jun-Jie Hong, Yi-Fan Wang, Xiu-Jun Cai, Department of General Surgery, Sir Run Run Shaw Hospital, School of Medicine, Zhejiang University, Hangzhou 310000, Zhejiang Province, China

Ning Meng, Department of General Surgery, Second Hospital, School of Medicine, Hangzhou Normal University, Hangzhou 310000, Zhejiang Province, China

Miao-Qin Chen, Department of Biological Treatment Research Center, Sir Run Run Shaw Hospital, School of Medicine, Zhejiang University, Hangzhou 310000, Zhejiang Province, China

Billy Lu, National Center for Advancing Translational Science/ National Institutes of Health (NIH), Rickville 20850, American Samoa

ORCID number: Yi-Fan Tong (0000-0001-9028-5756); Ning Meng (0000-0001-8334-1801); Miao-Qin Chen (0000-0001-9479-3574); Han-Ning Ying (0000-0001-6026-580X); Ming Xu (0000-0003-0339-3332); Billy Lu (0000-0001-8369-8157); Jun-Jie Hong (0000-0002-6286-415X); Yi-Fan Wang (0000-0002-8828-4268); Xiu-Jun Cai (0000-0002-3615-4680).

Author contributions: Tong YF, Meng N, Chen MQ, Ying HN and Xu M contributed equally to this work; Cai XJ, Wang YF and Tong YF designed research; Tong YF, Chen MQ and Xu M performed research; Meng N and Ying HN contributed new reagents or analytic tools; Tong YF and Chen MQ analyzed data; Tong YF and Meng N wrote the paper; Lu B, Hong JJ and Cai XJ revised and supervised the study and revised the paper; all authors have read and approved the final version to be published.

Supported by the Major Scientific and Technological Project of Zhejiang Province, China, No. 2015C03026.

Institutional review board statement: This study was reviewed and approved by the Ethical Committees for Human Subjects at Zhejiang University, China, Institutional Review Board.

Institutional animal care and use committee statement: All animal experiments were conducted in accordance with policies of Institutional Animal Care and Use Committee (IACUC) of the School of Medicine, Zhejiang University, China. Specific protocols used in this study were approved by School of Medicine, Zhejiang University IACUC.

Conflict-of-interest statement: The authors declared no conflicts of interest was included in the study.

Data sharing statement: Technical appendix, statistical code, and dataset available from the corresponding author at srrsh_cxj@zju.edu.cn. Participants gave informed consent for data sharing.

ARRIVE guidelines statement: The authors have read the ARRIVE guidelines, and the manuscript was prepared and revised according to the ARRIVE guidelines.

Manuscript source: Unsolicited manuscript

Corresponding to: Xiu-Jun Cai, FRSC, MD, Professor, Surgeon, Department of General Surgery, Sir Run Run Shaw Hospital, School of Medicine, Zhejiang University, Qingchun East Road No.3, Hangzhou 310016, Zhejiang Province, China. srrsh_cxj@zju.edu.cn
Telephone: +86-571-86006605
Fax: +86-571-86006605

Received: December 28, 2017

Peer-review started: December 29, 2017
First decision: January 17, 2018
Revised: February 4, 2018
Accepted: February 9, 2018
Article in press: February 9, 2018
Published online: March 14, 2018

Abstract

AIM

To establish a rat model for evaluating the maturity of liver regeneration derived from associating liver partition and portal vein ligation for staged hepatectomy (ALPPS).

METHODS

In the present study, ALPPS, partial hepatecotmy (PHx), and sham rat models were established initially, which were validated by significant increase of proliferative markers including Ki-67, proliferating cell nuclear antigen, and cyclin D1. In the setting of accelerated proliferation in volume at the second and fifth day after ALPPS, the characteristics of newborn hepatocytes, as well as specific markers of progenitor hepatic cell, were identified. Afterwards, the detection of liver function followed by cluster analysis of functional gene expression were performed to evaluate the maturity.

RESULTS

Compared with PHx and sham groups, the proliferation of FLR was significantly higher in ALPPS group (P = 0.023 and 0.001 at second day, P = 0.034 and P < 0.001 at fifth day after stage I). Meanwhile, the increased expression of proliferative markers including Ki-67, proliferating cell nuclear antigen, and cyclin D1 verified the accelerated liver regeneration derived from ALPPS procedure. However, ALPPS-induced Sox9 positive hepatocytes significantly increased beyond the portal triad, which indicated the progenitor hepatic cell was potentially involved. And the characteristics of ALPPS-induced hepatocytes indicated the lower expression of hepatocyte nuclear factor 4 and anti-tryptase in early proliferative stage. Both suggested the immaturity of ALPPS-derived liver regeneration. Additionally, the detection of liver function and functional genes expression confirmed the immaturity of renascent hepatocytes derived in early stage of ALPPS-derived liver regeneration.

CONCLUSION

Our study revealed the immaturity of ALPPS-derived proliferation in early regenerative response, which indicated that the volumetric assessment overestimated the functional proliferation. This could be convincing evidence that the stage Ⅱ of ALPPS should be performed prudently in patients with marginally adequate FLR, as the ALPPS-derived proliferation in volume lags behind the functional regeneration.

Key words: Associating liver partition and portal vein ligation for staged hepatectomy; Liver regeneration; Hepatic progenitor cell; Function; Immature

Core tip: Despite the rapid proliferation of future liver remnant induced by associating liver partition and portal vein ligation for staged hepatectomy (ALPPS), the high mortality and morbidity rates have remained alarming. A plausible reason was the functional proliferation lagged behind the increase in volume. In this study, a rat model was established to evaluate the maturity of ALPPS-derived hepatocytes. Through the identification of hepatic characteristics, detection of liver function, and analysis of functional gene expression, we revealed the immaturity of ALPPS-derived proliferation in early regenerative response, which indicated that the volumetric assessment overestimated the functional proliferation. And clinically, the stage Ⅱ of ALPPS should be performed prudently in patients with marginally adequate FLR, as the ALPPS-derived proliferation in volume lags behind the functional regeneration.

Tong YF, Meng N, Chen MQ, Ying HN, Xu M, Lu B, Hong JJ, Wang YF, Cai XJ. Maturity of associating liver partition and portal vein ligation for staged hepatectomy-derived liver regeneration in a rat model. *World J Gastroenterol* 2018; 24(10): 1107-1119 Available from: URL: http://www.wjgnet.com/1007-9327/full/v24/i10/1107.htm DOI: http://dx.doi.org/10.3748/wjg.v24.i10.1107

INTRODUCTION

Given its increasing incidence, liver tumor is one of the most life-threatening diseases worldwide[1]. Despite the development in a variety of therapies based on the property of tumor (*e.g.,* transcatheter arterial chemoembolization, chemotherapy, molecular targeting therapy, *etc.*) in recent decades, surgery remains the only curative treatment for patients with primary or metastatic hepatic malignancies[2,3]. Although the remarkable regenerative capacity of the liver permits the extended hepatectomy in clinic, postoperative liver failure caused by small-for-size syndrome (SFSS) represents the most common cause of death after hepatectomy[4]. To address this issue, a novel innovation called associating liver partition and portal vein ligation for staged hepatectomy (ALPPS) has been invented. This technique induces the accelerated growth of future liver remnant (FLR) within transient period through integrating the portal vein occlusion and parenchymal transection[5-8].

However, some experts caution the feasibility and safety of such procedure, and the initial enthusiasm for ALPPS also was tempered because of high morbidity and mortality[9-12]. The improvement of technology and accumulation of experience has decreased the mortality rate to less than 10%, but this remains too high[8].

A rational possibility is that volumetric assessment overestimates the functional proliferation. Given the development of induced pluripotent stem cell technique and the illustration of the roadmap determining the fate of diverse cells, the mechanism of hepatocyte differentiation has been elucidated gradually through the lineage tracing method[13]. Basic research has elucidated that it takes about 8 to 10 d for a hepatoblast to mature into a hepatocyte[14]. In this setting, within a short interval period of ALPPS procedure, the maturity of induced hepatocytes has to be queried. Clinically, the interval time between two stages of ALPPS is usual one or two weeks. Additionally, several studies also have shown that there is a distinct delay in functional gain compared to volumetric increase in ALPPS[15,16]. Therefore, the functional quality of hypertrophic response derived from ALPPS procedure, not just volumetric assessment of the FLR, should be performed to time the stage Ⅱ.

Despite the establishment of several ALPPS animal studies with remarkable growth in volume, none of models were dedicated to evaluating functional proliferation. Thus, the aim of study was to establish a rat model mimicking ALPPS procedure to assess the maturity of ALPPS-derived liver regeneration functionally and volumetrically. This might be of great value in timing the stage Ⅱ of ALPPS and improving its safety clinically.

MATERIALS AND METHODS

Study design

The protocol of this study was reviewed and approved by the animal ethics committee of the Zhejiang University, Hangzhou, China. All experiments were performed in accordance with relevant approved guidelines and regulations. In the present study, male Sprague-Dawley rats, weighing 180 to 230 g from experimental animal center of Zhejiang province, Hangzhou, China, were used. All the rats were housed in a restricted access room with controlled temperature (23 ℃) and a light/dark (12 h:12 h) cycle, and had free access to food and water before and after treatment. Initially, a preliminary study was simply performed to screen the feasible models (n = 5, each group). The sham group was adopted as negative control and the appropriate PHx model was regarded as a positive control. Then, the volumetric and functional liver regeneration of three groups, ALPPS group, PHx group, and sham group were compared in this study.

Definition of different groups

According to the results of preliminary study, the ALPPS, PHx, and sham groups were defined as experimental, positive, and negative control groups in this study. ALPPS group: ligation of the portal vein belonging to left lateral, right, caudate lobes, and transection of parenchyma of middle lobe. PHx group: removal of left lateral, right and caudate lobes. Sham group: Open and close the abdominal cavity.

Surgical procedure

All rats were fasted 8 h before operation. Under the general anesthesia with 8% of chloral hydrate (5.0 mL/kg) by intra-abdominal injection, the abdominal transverse incision was adopted. For the ALPPS procedure, dissection of the left lateral lobe followed by ligation of the portal vein supplying the corresponding lobe with 5-0 silk were performed while artery and biliary duct branches were maintained. Then, the same procedure was conducted in the portal branches of the right and caudate lobes, respectively. The parenchyma was partitioned by 5-0 silks along with the ischemic demarcation line of the middle lobe. Five days after stage Ⅰ, the stage Ⅱ was performed, in which the deportalization lobes were removed (n = 5). For the PHx model, the left lateral, right, and caudate lobes were removed after corresponding hepatic pedicle were ligated with 3-0 silks. And for sham group, opening followed by closing the abdominal cavity was performed (Figure 1A).

Previously, several studies indicated the ALPPS procedure was divided into early (1-3 d after stage Ⅰ) and later stage (4-7 d after stage Ⅰ) generally[17-21]. Therefore in our study, the rats were sacrificed on the second and fifth day after operation. The specimen was collected for subsequent research. Each group at different time points contained six rats. Half of them were used for evaluating the efficiency of proliferation, and the other three rats were used for primary hepatocyte isolation and subsequent detection of hepatic function.

RNA extraction, reverse transcription, quantitative real-time PCR

For RNA extraction, total RNA was extracted from 50 mg of liver specimen by TRIzol reagent (CWBIO, China). 5 μg of RNA were reverse-transcribed by the HiFiScript cDNA Synthesis Kit (CWBIO, China), yielding the complementary DNA template. The quantitative real-time PCR amplification was performed by the ROCHE Light Cycler 480 Ⅱ. The expression of mRNA was shown as fold induction. The primer sequences were listed in Supplement Table 1.

Western blotting

The detection of proteins was performed by standard western blot assays according to the steps below[22]. Total proteins from liver tissues were extracted with RIPA buffer containing protease inhibitors (Beyotime, China) and quantified using the Pierce BCA Protein Assay Kit (Thermo Scientific, United States). About 40 μg of total protein was separated by 10% SDS-PAGE. Samples were transferred to PVDF membranes

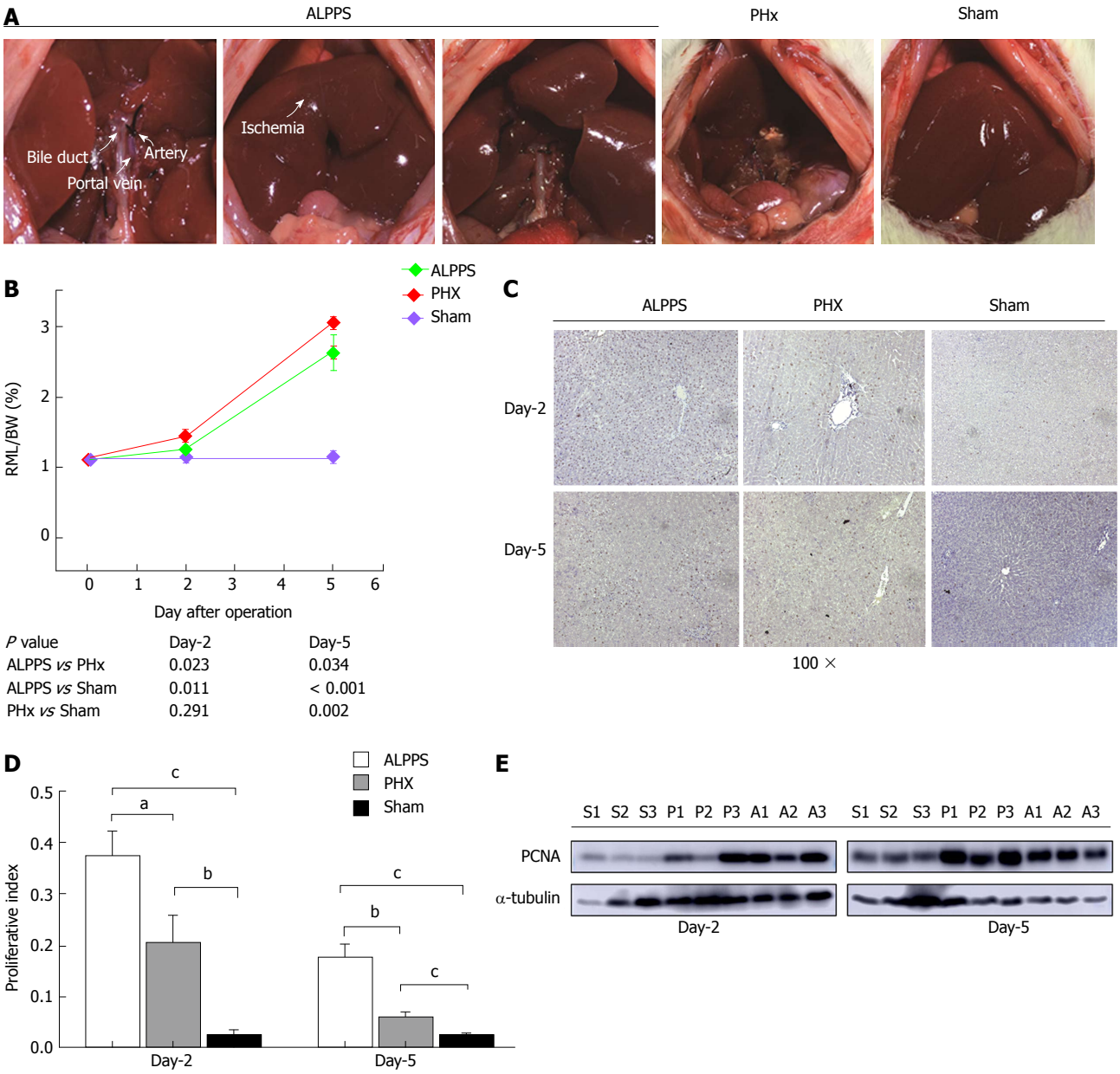

P value	Day-2	Day-5
ALPPS *vs* PHx	0.023	0.034
ALPPS *vs* Sham	0.011	< 0.001
PHx *vs* Sham	0.291	0.002

Figure 1 Establishment of ALPPS model. A: Pictures of ALPPS, PHx, and sham models; B: Proliferation of ALPPS, PHx, and sham models. The X axis represented the day after operation while the Y axis represents the RML/WB (%); C: Representative image (100 ×) of Ki-67 stain by immunohistochemistry of each group at day 2 and 5, respectively; D: Proliferative index of different models, which was calculated by the mean of percentage of Ki-67 positive particle in four random visual fields (200 ×) of IHC stain. $^{a}P < 0.05$, $^{b}P < 0.01$, $^{c}P < 0.001$; E: Protein level of represent expression of PCNA of each group. A: ALPPS; P/PHx: Partial hepatectomy; S: Sham; PCNA: Proliferating cell nuclear antigen; IHC: Immunohistochemistry; RML: Right middle lobe; WB: Body weight.

(Millipore, United States) and incubated overnight at 4 degrees with primary antibodies. The blots were incubated with horseradish peroxidase (HRP)-conjugated secondary antibodies and visualized using the ECL system (Thermo Fisher Scientific, Rochester, NY, United States).

Histological examination

The liver tissues were immersion fixed in 4% formaldehyde overnight. Then, they were embedded, sectioned, dehydrated in ethanol and xylene before being stained with hematoxylin-eosin (HE) immunohistochemistry (IHC). Through the IHC stain, the number of Ki-67 positive hepatocytes were calculated randomly in four visual fields (× 400) and analyzed by Image Pro plus 5.1 (Media Cybernetics, United States), which was presented as the proliferation index. With respect to immunofluorescence, the primary antibody to Sox9 (ab185230) and Albumin (ab106582) were produced from Abcam. The experimental procedure was according to the standard protocol.

Primary hepatocyte isolation and function detection

The protocol for isolation of primary hepatocytes was

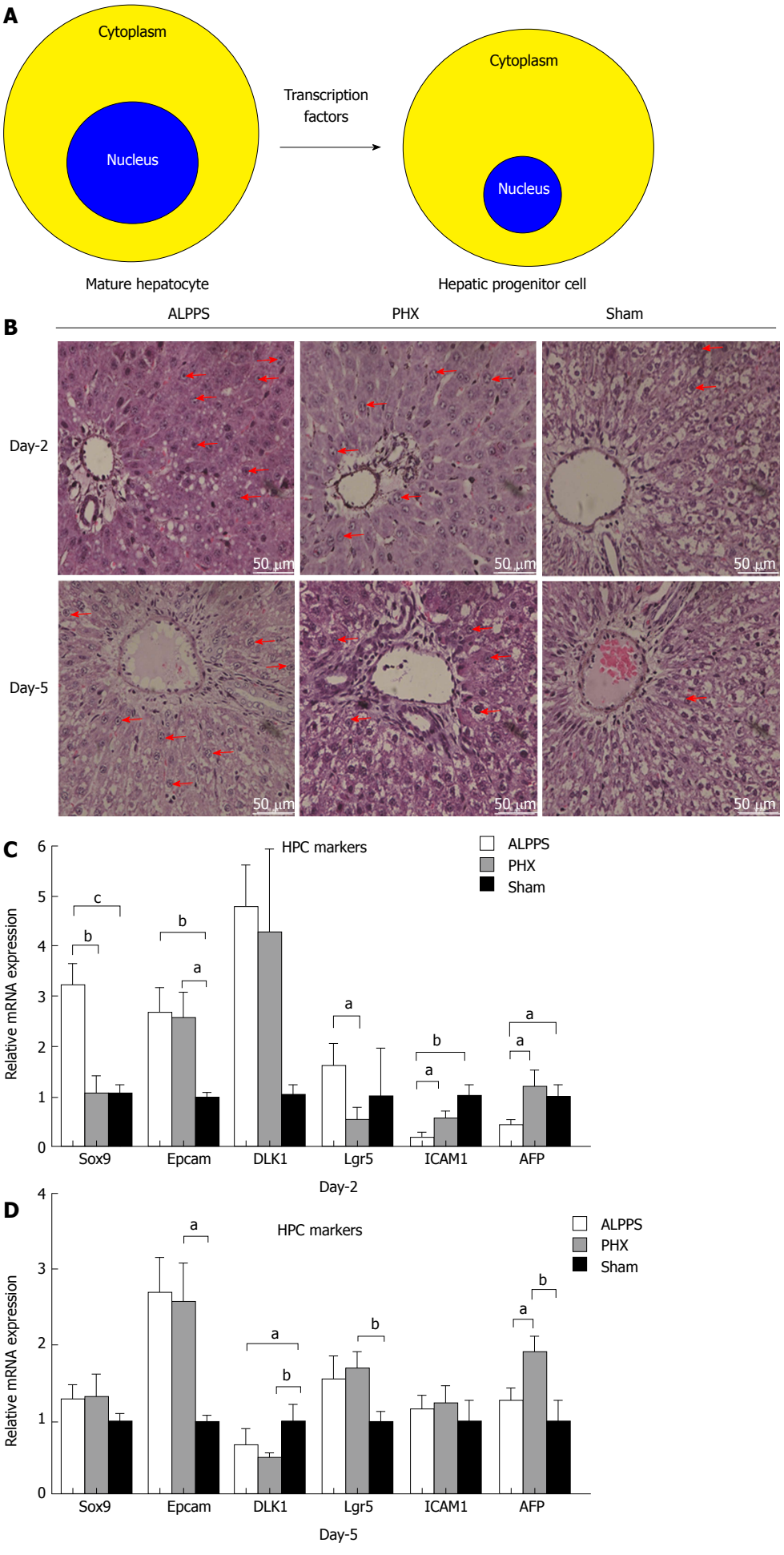
A
Cytoplasm
Nucleus
Transcription factors
Cytoplasm
Nucleus
Mature hepatocyte
Hepatic progenitor cell
B
ALPPS
PHX
Sham
Day-2
Day-5
50 μm
C
HPC markers
ALPPS
PHX
Sham
Relative mRNA expression
Sox9
Epcam
DLK1
Lgr5
ICAM1
AFP
Day-2
D
HPC markers
ALPPS
PHX
Sham
Relative mRNA expression
Sox9
Epcam
DLK1
Lgr5
ICAM1
AFP
Day-5

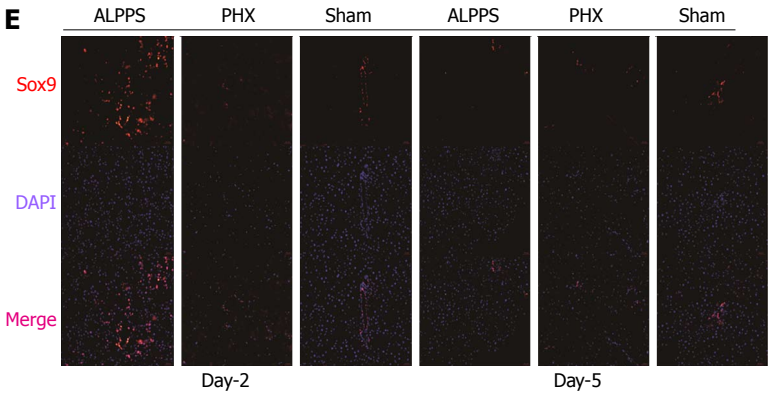

Figure 2 The role of hepatic progenitor cell in associating liver partition and portal vein ligation for staged hepatectomy. A: The schematic of differentiation from hepatic progenitor cell to mature hepatocyte; B: Representative image (400 ×) of HE stain of each group at day 2 and 5, respectively; C: Relative mRNA expression of hepatic progenitor cell markers of each group; D: Immunofluorescence for expression of Sox9 in different groups. $^{a}P < 0.05$, $^{b}P < 0.01$, $^{c}P < 0.001$.

according to three-step collagenase perfusion. Briefly, the liver was perfused through the suprahepatic inferior vena cava with calcium-free buffer (0.5 mmol/L EGTA, 1 × EBSS without Ca^{2+} and Mg^{2+}), followed by the calcium-bearing buffer (10 mmol/L HEPES, 1 × EBSS with Ca^{2+} and Mg^{2+}), and then irrigated with collagenase [0.2 mg/mL collagenase type Ⅳ (Yeasen, China)]. Subsequently, parenchymal cells were purified by 90% Percoll buffer (Sigma) at low speed centrifugation (1000 rpm, 10 min). After the cells were cultured in DMEM medium with 10% FBS for 8 h, PAS stain, OilRed stain, and detection of urea nitrogen were performed following the manufacturer's instructions (Solarbio, China). In the indocyanine green (ICG) uptake assay, hepatocytes were cultured with 1 mg/mL ICG (Tianyi, China) at 37 ℃ for 90 min and washed with PBS three times.

Statistical analysis

The data were expressed as a mean with standard deviation or a percentage. Correspondingly, Student *t*-test or χ^2 test was used to analyze the difference. Significance was considered when a two-tailed *P* value was less than 0.05. Statistical analysis was performed using SPSS, version 22.0 for Windows (IBM Corporation, Armonk, NY, United States).

RESULTS

Establishment of rat models

To establish a feasible positive control model, various PHx models with different extensions of hepatectomy were compared (Supplement Figure 1). The mortality of extended PHx group (removal of left lateral, left middle, right and caudate lobes, $n = 5$), which presented the same extension of stage Ⅱ of ALPPS, was 80%. Compared with extended PHx model (removal left lateral, left middle, right and caudate lobes) and minor PHx model (only removal left lateral), the medium PHx group (removal of left lateral, right and caudate lobes) presented an acceptable mortality (20%) and triggered a remarkable proliferation of FLR. It was therefore determined as positive control group in this study.

Compared with extended PHx group, no rat in ALPPS group which induces rapid hepatic proliferation (removal of left lateral, left middle, right and caudate lobes) died both in stage Ⅳ and Ⅱ. (0% *vs* 80%, $P = 0.053$). As the preservation of portal vein of right middle lobe (RLM) in each group, the liver regeneration was assessed by the ratio of RLM weight to body weight (BW). The mean RML/BW of ALPPS, PHx, sham groups were 1.44% ± 0.04%, 1.24% ± 0.09%, 1.14% ± 0.11% on the second day after operation, and 3.06% ± 0.11%, 2.63% ± 0.39%, 1.13% ± 0.10% on the fifth day after operation, respectively (Figure 1B). Compared with sham group, the proliferation of PHx group was remarkably induced in later stage ($P = 0.002$). However, in the ALPPS group, the hypertrophic response was more active than that of the PHx groups in whole course ($P = 0.023$ and $P = 0.034$). To further confirm the regenerative response, the staining of Ki-67 followed by the calculation of proliferation index of different groups were compared (Figure 1C and D). The expression of PCNA, a classical marker for cell proliferation, was detected by western blotting. Apparently, up-regulated expression of PCNA in the ALPPS group appeared earlier than that in PHx group (Figure 1E).

Thus, these results indicated PHx procedure could trigger liver regeneration, but a stronger regenerative response was activated by ALPPS procedure.

The characteristics of induced hepatocytes

As suggested by previous studies showing that the progenitor hepatic cell (HPC) differentiated into mature hepatocyte by the regulation of hepatic transcription factors (Figure 2A), we found that the hepatocytes in ALPPS and PHx presented a larger nucleus around the portal triad in both early and late stages (Figure 2B). These special hepatoctyes, we suspected, might be immature HPC. To verify this hypothesis, classical markers of hepatic progenitor cell were detected (Figure 2C). Compared with sham group, several markers, including Sox9 and Epcam were significantly increased at mRNA level ($P < 0.001$ and $P = 0.002$), especially in early proliferative stage. Furthermore, we checked

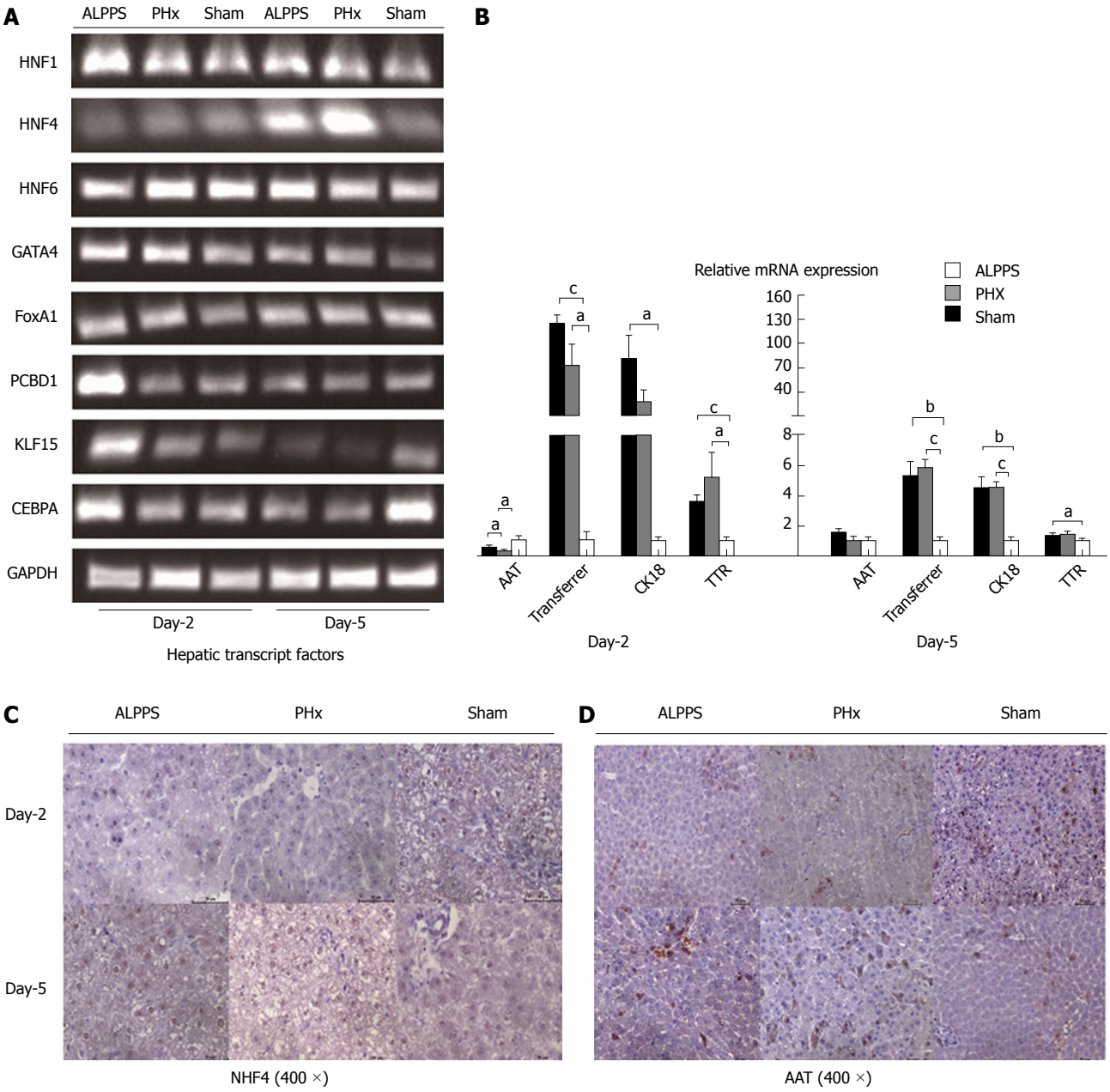

Figure 3 Characteristics of induced hepatocytes. A: The expression of hepatic transcription factors in different groups at each time point at RNA level; B: Relative mRNA expression of mature hepatocyte markers; C: Detection of HNF4 and AAT content by immunohistochemistry procedure of each group at day 2 and 5, respectively. $^{a}P < 0.05$, $^{b}P < 0.01$, $^{c}P < 0.001$.

the expression of Sox9 at protein level, and found it remarkable that the Sox9-positive hepatocytes were widespread beyond the portal traid on second day after ALPPS procedure (Figure 2D). These might imply the activation of HPC in early regenerative response, which was in accordance with the powerful regenerative capacity of HPC from literature reports[23]. As suggested by expression of HPC special markers, the maturity of induced liver hypertrophy either by ALPPS or conventional PHx procedure seemed comparable in later stage of proliferation. And thereby, we inferred the ALPPS-derived liver regeneration might be not completely mature in early phase. Meanwhile, a delay of functional proliferation was indicated in comparison of PHx-derived liver regeneration.

To clarify the above-mentioned inference from the other side, we detected the expression of well-known markers of mature hepatocytes (Figure 3A). Several transcription factors (*e.g.*, HNF1, HNF4, GATA4, FoxA1, *etc*) had been demonstrated to regulate the lineage reprogramming of fibroblasts into hepatocytes *in vitro*[24]. In this study, the HNF4 was delayed up-regulation on the fifth day of ALPPS and PHx groups, suggesting the process of differentiation of hepatocyte remained activated even in later phase. To measure the expression of HNF4 at protein level, the IHC stain was performed, which presented a negative result in early stage but a positive result in later stage of hypertrophic

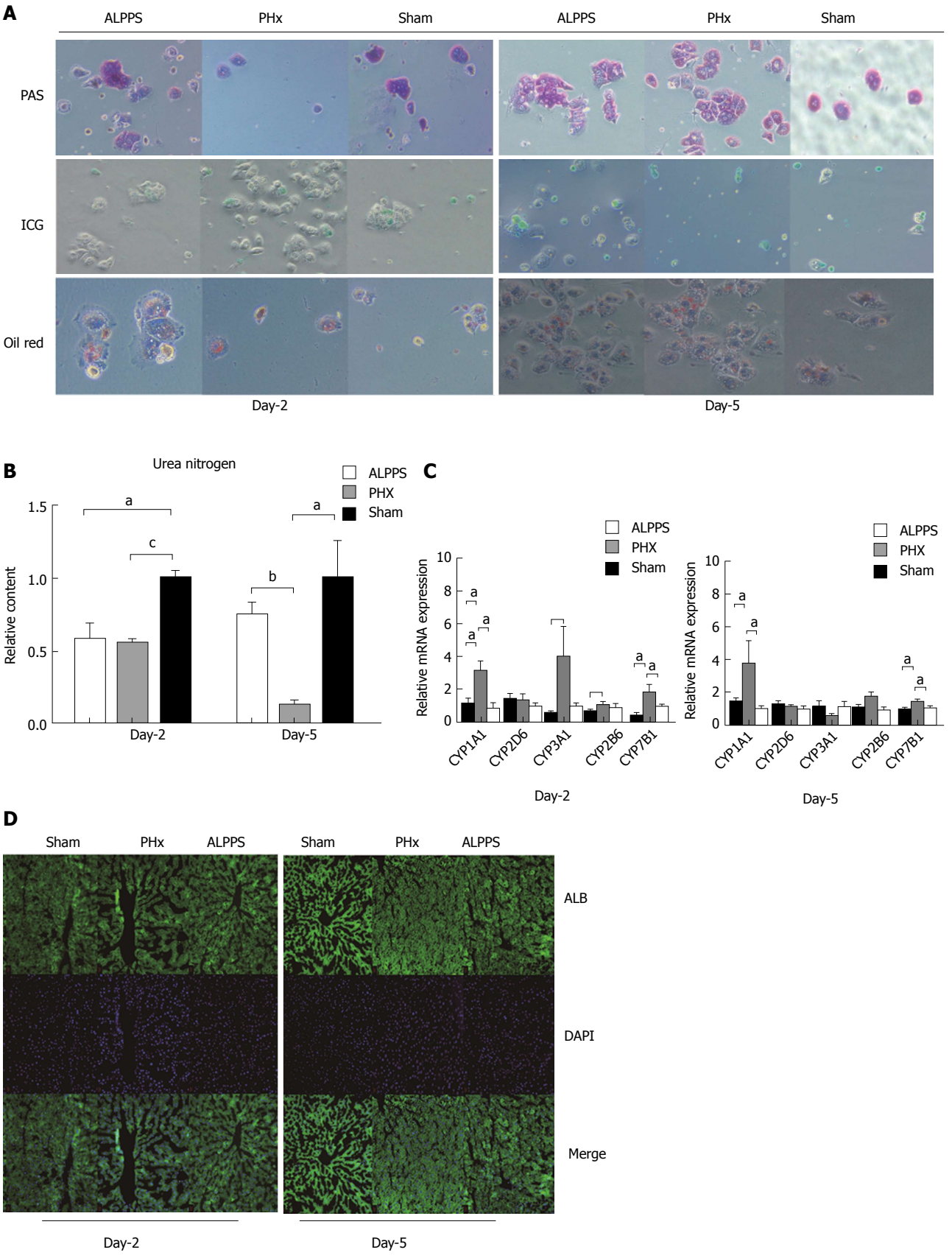

Figure 4 Hepatocytes function. A: Glycogen storage was assayed by PAS staining; Fat storage was assayed by OilRed staining; ICG uptake in cells of different groups (green staining); B: P450Y enzymes expression at RNA level; C: The synthesis of Urea nitrogen of ALPPS, PHx, sham groups at each time point; D: The protein level of albumin expression was measured by Immunofluorescence. A: ALPPS; P/PHx: Partial hepatectomy; S: Sham. $^{a}P < 0.05$, $^{b}P < 0.01$, $^{c}P < 0.001$.

response (Figure 3C). Similarly, functional proteins in the cytoplasm were detected. We found that in the initial

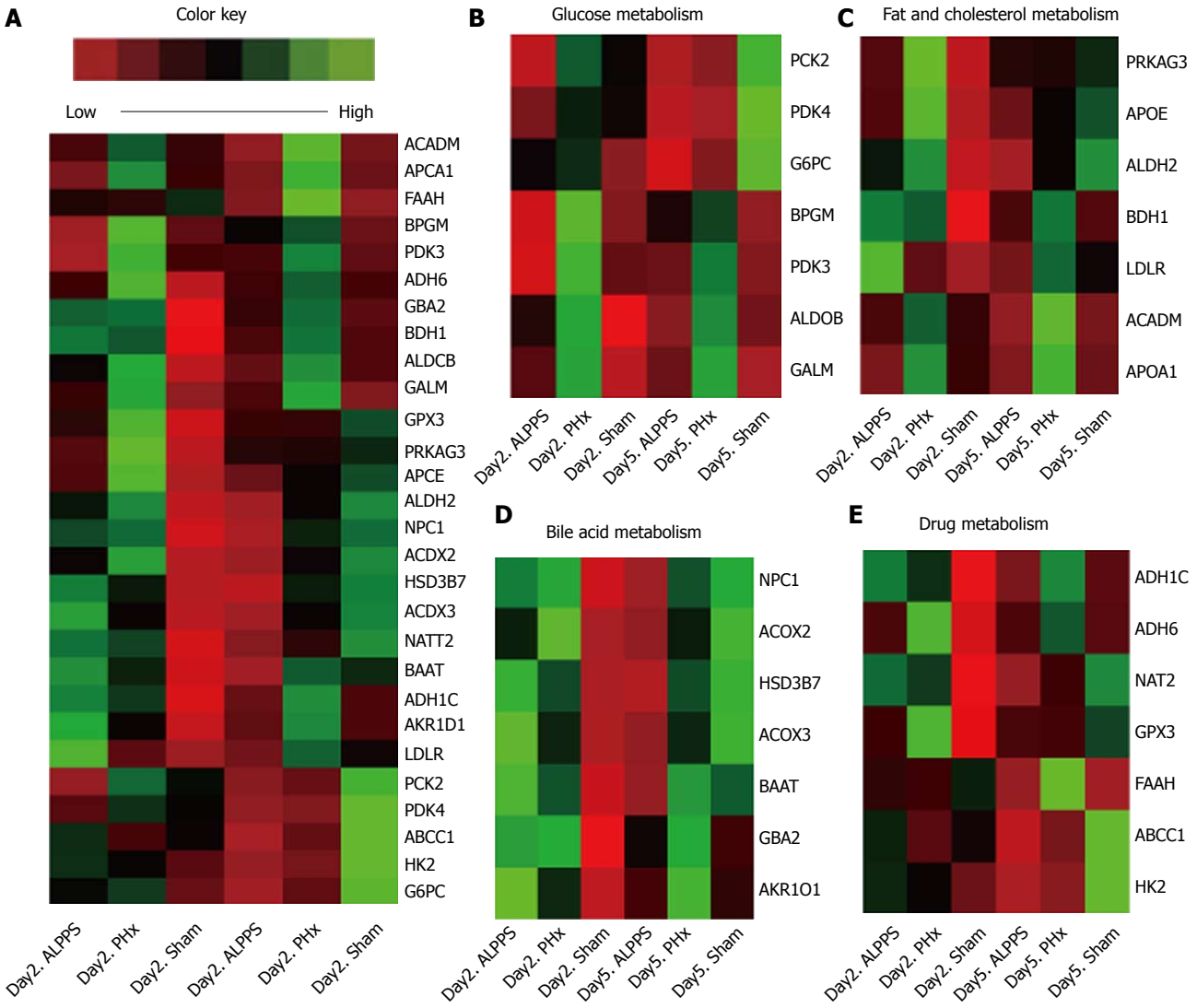

Figure 5 Cluster analysis of different expression of functional genes. The color key represented the abundance expression of indicated genes (Compared with corresponding sham group at each time point). A: The overall cluster analysis of expression of functional genes; B: Glucose metabolism associated functional genes; C: Fat and cholesterol metabolism associated functional genes; D: Bile acid metabolism associated functional genes; E: Drug metabolism associated functional genes.

process of regeneration, the expression of anti-tryptase (AAT) was relatively reduced even in the setting of the increase in amount of hepatocytes (Figure 3B and D).

Taken together, compared with intrinsic hepatocyte in sham group, the immaturity of newborn hepatocytes in early proliferative response of ALPPS and PHx group were elucidated. Among, the differentiation of hepatocyte in ALPPS group appeared to be more prolonged than that in PHx group through the analysis of characteristics of induced hepatocyte.

Detection of hepatocyte function

Given the proliferation in volume and the immaturity of the induced hepatocyte, the functional regeneration had to be naturally questioned. Despite the complexity of induced liver regeneration, an elaborate detection of hepatocyte function was performed as shown below. By primary hepatocyte isolation, the PAS stain, OilRed stain, ICG stain, and synthesis of urea nitrogen of each group in early and later stages were conducted (Figure 4A). As a result, a comparable capacity of glycogen synthesis and fat metabolism was presented between groups, even in the early stage of proliferation. Nevertheless, compared with sham group on the second day after operation, the PHx group had a decreased capability of ICG up-take. Furthermore, the ALPPS group showed a more inferior capacity of ingestion of ICG. Moreover, an insufficiency of urea nitrogen synthesis of hypertrophic groups existed in the whole course of liver regeneration (Figure 4B). With respect to the metabolism, the P450Y enzyme system was the most representative substance. In comparison of PHx group, the expression of CYP3A1 and CYP2B6 in ALPPS group was suppressed on the second day and the expression of CYP1A1 and CYP7B1 was down-regulated in both stages (Figure 4C). But in terms of expression of albumin, no inter-group discrepancy was clarified (Figure 4D).

In this section, we found that the ALPPS-derived

liver regeneration postponed the functional maturity in aspects of ICG up-take, synthesis of urea nitrogen, and expression of P450Y enzyme in the early stage of proliferation.

Cluster analysis of different expression of functional genes

As seen from above, because the ALPPS-derived liver regeneration might be not completely mature in early stage, cluster analysis of different expression of functional genes was therefore performed. All expression of functional genes were summarized in Figure 5A and Supplement Table 2. In the initial stage of liver regeneration, almost all functional genes were up-regulated and were accompanied by an increase in the amount of hepatocyte, which either was induced by ALPPS or PHx procedure. Intriguingly, although the PAS stain showed comparable capacity of synthesis of glycogen in ALPPS and PHx groups, the cluster analysis indicated a relatively low expression of genes in regard to glycogen metabolism. Until the later stage of proliferation, almost all genes had relatively lower expression in the ALPPS group (Figure 5B-E).

Together, these results suggested the expression of functional genes in hepatocytes derived from ALPPS procedure were relatively lower, even in the later stage of proliferation.

DISCUSSION

Based on the first ALPPS Consensus Meeting held in Hamburg in February 2015, the timing of stage Ⅱ was recommended until the FLR reached 40% in liver with cirrhosis or 25% to 30% in normal liver[25,26]. Nevertheless, the incidence of postoperative hepatic failure remains up to 31% even when sufficient FLR volumes were achieved[27]. A rational explanation is the fact that rapid increase in volume derived from ALPPS lags behind the functional proliferation. And thereby, the timing of stage Ⅱ could be better addressed and the rate of mortality could be minimized more efficiently on the basis of functional evaluation. Till now, several technologies including ICG disappearance rate, fluorodeoxyglucose imaging, and 99mTc-mebrofenin hepatobiliary scintigraphy (HBS) had been established[28,29]. Among them, the widespread application of HBS is of great help in the assessment of functional maturity before and after hepatectomy, even in the ALPPS procedure[8]. However, the functional maturity in the process of liver regeneration is too complicated to be determined by merely the uptake and excretory function. For instance, the synthesis of urea nitrogen and albumin, vitality of P450Y enzyme, and fat metabolism are vital parameters in the assessment of liver function. Clinically, it is quite difficult to recruit adequate recipients to fulfill the study of functional detection in ALPPS procedure. Thus, we conducted a rat model mimicking ALPPS procedure to evaluate the functional proliferation, which could be of great help in clinical decision-making.

As suggested by previous results presenting that the volumetric proliferation of FLR could be induced in patients who underwent ALPPS procedure, it was remarkable that the right middle lobe in our rat model was rapidly hypertrophic through the same manipulation. Nonetheless, we found that the newborn hepatocytes for liver restoration remained poorly characterized. First of all, our study revealed that in ALPPS and PHx models, of the majority of cells with a large ratio of nucleus to cytoplasm appeared enriched around the portal vein. In addition, a significant up-regulation of Sox9 on the second day after ALPPS and subsequent decrease in the later stage indicated the potential role of HPC in triggering the activation of regeneration[30]. Based on previous reports, the HPC, a stem-like cell around the portal triads, presented a dramatic capacity to restore liver function and replenish liver mass in liver regeneration[31-33]. Thus, we inferred that the activity of HPC promoted the accelerated liver restoration. To clarify the immaturity of newborn hepatocyte, we detected several transcription factors associated with the destiny of hepatocytes, and found that the peak of HNF4, which plays a critical role in regulating the expression of differentiation-related genes and maintenance of liver function in mammals, was postponed[34-36]. Meanwhile, the inferior expression of AAT was manifested on the second day of ALPPS and PHx groups, which supported the immaturity of hepatocytes. To sum up, the induced hepatocytes were still in the process of differentiation, which suggested the induced-hepatocytes were defective functionally in early regenerative response.

To further evaluate the maturity of neonatal hepatocytes, function detection was performed. In this section, a mild inefficiency of ICG uptake capacity was presented in ALPPS group in early stage. And the insufficient synthesis of P450Y enzymes indicated a deficient capacity of ALPPS-derived hepatocyte in early stage. As seen from the above, the metabolic function is not recovered in early stage of ALPPS procedure. Hence, for patients with biliary obstruction or disorder of renal function, the accumulation of detrimental substances always aggravates the burden of detoxification, and thereby induces the hepatic failure theoretically. Correspondingly, the patients with hilar cholangiocarcinoma or gallbladder cancer, always combined with biliary obstruction, presented a higher mortality and morbidity clinically. Intriguingly, the cluster analysis of different genes expression revealed a paradoxical result. The lower abundance of functional genes relevant to glycogen metabolism presented an insufficiency of synthesis in the ALPPS group, even though the PAS stain presented a comparable capacity in terms of glycogen synthesis. Moreover, relatively low expression of genes in regards to fat, cholesterol, bile acid, and drugs in later stage reminded us that liver

function of hepatocytes derived from ALPPS procedure lagged behind the increase in liver volume. Taken together, the assessment of ICG clearance and hepatic metabolites could improve the comprehensiveness of liver functional evaluation, avoiding the process by which the volumetric increase overestimates the functional gain in liver.

In the present study, we demonstrated that the liver regeneration derived from ALPPS was not completely mature in early stage, but the functional proliferation was mainly completed on the fifth day after ALPPS. Besides, the 0% of mortality after stage Ⅱ indirectly clarified both volumetric and functional regeneration were achieved. Nevertheless, whether the results could be generalized to clinical patients are warranted definitely. To begin with, a majority of ALPPS procedure are performed in patients with diseased liver (*e.g.,* fibrosis, non-alcoholic steatohepatitis, post-chemotherapy, *etc*). Given that the capacity of liver regeneration was attenuated in the diseased liver, the maturity has to be queried subsequently. In this setting, the timing of stage Ⅱ should be prolonged as well. Additionally, the rate of metabolism is apparently faster in rats than in humans. The optimal time to perform stage Ⅱ in human is still controversial, despite that extended hepatecotmy was performed smoothly with an interval time of five days in rat. Theoretically, the species-specific characteristics and inconsecutive observation point time could contribute to a confounding effect on the conclusion.

Given the mechanism of ALPPS-derived liver regeneration is scarce, our follow-up work will verify the hypothesis that the dramatic capacity of regeneration is derived from HPC by lineage tracing method (Sox9-Cre-GFP mouse)[32]. Despite these limitations, our study revealed the immaturity of ALPPS-derived proliferation in early regenerative response, which indicated the volumetric assessment overestimated the functional proliferation. This could be a convincing evidence that the stage Ⅱ of ALPPS should be performed prudently in patients with marginally adequate FLR, as the ALPPS-derived proliferation in volume lags behind the functional regeneration.

ARTICLE HIGHLIGHTS

Research background

Associating liver partition and portal vein ligation for staged hepatectomy (ALPPS) has been increasingly popular worldwide recently. However, the high mortality makes surgeons reconsider the difference between functional and volumetric proliferation in ALPPS-derived liver regeneration. In this study, we therefore establish a rat model to mimic the ALPPS, exploring whether the functional proliferation lags behind the hypertrophy in volume.

Research motivation

This was a preliminary study with regard to the maturity of ALPPS-derived liver regeneration. On the basis of developing a rat model, we found the volumetric assessment overestimated the functional proliferation in ALPPS procedure, which indicated the stage II of ALPPS should be performed prudently in patients with marginally adequate future liver remnant.

Research objectives

This study was to evaluate the maturity of ALPPS-derived liver regeneration. In our rat model, the postponed maturity in function might be an important reason for high mortality of ALPPS even when the adequate future liver remnant was achieved before stage II of ALPPS. Likewise, the functional proliferation should be performed to time the stage II of ALPPS clinically.

Research methods

In this study, ALPPS, partial hepatectomy (PHx) and sham models were conducted. The ratio of right middle lobe to body weight as well as proliferative markers were used for assessing the liver regeneration. Morphological changes by HE stain and detection of specific markers of progenitor or mature hepatocytes were adopted to identify the characteristics of newborn hepatocytes. Eventually, the liver function in vivo and vitro was measured, followed by the cluster analysis of expression of functional genes to detect the maturity of liver regeneration from different models.

Research results

By establishment of ALPPS, PHx and sham models, we demonstrated that ALPPS could induce an accelerated proliferative response. However, the characteristics of newborn hepatocytes seemed to be not mature completely. Sox9 positive hepatocyte, as well as different expression of other specific markers, indicated the potential role of progenitor hepatic cell in ALPPS-derived regeneration. Parts of limited liver function and different expression of functional genes supported the above-mentioned immaturity in ALPPS-induced proliferation.

Research conclusions

As the mortality remains unsatisfactory even in patients with adequate future liver remnant after stage I of ALPPS, this study presented the immaturity of ALPPS-derived proliferation in early regenerative response, which indicated that the volumetric assessment overestimated the functional proliferation. To the best of our knowledge, this is the first study to evaluate the maturity of ALPPS-derived liver regeneration in a rat model. Meanwhile, Sox9 positive hepatocyte indicated the potential role of hepatic progenitor cell in the ALPPS rather than conventional PHx model. Therefore, a more detailed research about the hepatic progenitor cell promotes the ALPPS-derived liver regeneration and its mechanism would be done in our next work.

Research perspectives

The stage II of ALPPS should be performed prudently in patients with marginally adequate future liver remnant, as the ALPPS-derived proliferation in volume lags behind the functional regeneration. By the way, as the hepatic progenitor cell might be an important role in ALPPS-derived liver regeneration, our future work is to further demonstrate the fate of Sox9 positive hepatocyte with ALPPS procedure and its underlying mechanism by lineage tracing method.

ACKNOWLEDGEMENTS

Thanks to Professor Li-jian Hui, PhD, Laboratory of Molecular Cell Biology, Institute of Biochemistry and Cell Biology, Shanghai Institutes for Biological Sciences, Chinese Academy for Sciences, for guidance of primary hepatocyte isolation.

REFERENCES

1 **Torre LA**, Bray F, Siegel RL, Ferlay J, Lortet-Tieulent J, Jemal A. Global cancer statistics, 2012. *CA Cancer J Clin* 2015; **65**: 87-108 [PMID: 25651787 DOI: 10.3322/caac.21262]

2 **Zhong BY**, Ni CF, Chen L, Zhu HD, Teng GJ. Early Sorafenib-related Biomarkers for Combination Treatment with Transarterial Chemoembolization and Sorafenib in Patients with Hepatocellular Carcinoma. *Radiology* 2017; **284**: 583-592 [PMID: 28263701 DOI: 10.1148/radiol.2017161975]

3 **Tong Y**, Li Z, Liang Y, Yu H, Liang X, Liu H, Cai X. Postoperative adjuvant TACE for patients of hepatocellular carcinoma in AJCC stage I: friend or foe? a propensity score analysis. *Oncotarget* 2017; **8**: 26671-26678 [PMID: 28460456 DOI: 10.18632/oncotarget.15793]

4 **Langiewicz M**, Schlegel A, Saponara E, Linecker M, Borger P, Graf R, Humar B, Clavien PA. Hedgehog pathway mediates early acceleration of liver regeneration induced by a novel two-staged hepatectomy in mice. *J Hepatol* 2017; **66**: 560-570 [PMID: 27771454 DOI: 10.1016/j.jhep.2016.10.014]

5 **Olthof PB**, Coelen RJS, Wiggers JK, Groot Koerkamp B, Malago M, Hernandez-Alejandro R, Topp SA, Vivarelli M, Aldrighetti LA, Robles Campos R, Oldhafer KJ, Jarnagin WR, van Gulik TM. High mortality after ALPPS for perihilar cholangiocarcinoma: case-control analysis including the first series from the international ALPPS registry. *HPB* (Oxford) 2017; **19**: 381-387 [PMID: 28279621 DOI: 10.1016/j.hpb.2016.10.008]

6 **Lang H**, de Santibanes E, Clavien PA. Outcome of ALPPS for perihilar cholangiocarcinoma: case-control analysis including the first series from the international ALPPS registry. *HPB* (Oxford) 2017; **19**: 379-380 [PMID: 28262523 DOI: 10.1016/j.hpb.2017.01.024]

7 **Chan ACY**, Chok K, Dai JWC, Lo CM. Impact of split completeness on future liver remnant hypertrophy in associating liver partition and portal vein ligation for staged hepatectomy (ALPPS) in hepatocellular carcinoma: Complete-ALPPS versus partial-ALPPS. *Surgery* 2017; **161**: 357-364 [PMID: 27596751 DOI: 10.1016/j.surg.2016.07.029]

8 **Linecker M**, Björnsson B, Stavrou GA, Oldhafer KJ, Lurje G, Neumann U, Adam R, Pruvot FR, Topp SA, Li J, Capobianco I, Nadalin S, Machado MA, Voskanyan S, Balci D, Hernandez-Alejandro R, Alvarez FA, De Santibañes E, Robles-Campos R, Malagó M, de Oliveira ML, Lesurtel M, Clavien PA, Petrowsky H. Risk Adjustment in ALPPS Is Associated With a Dramatic Decrease in Early Mortality and Morbidity. *Ann Surg* 2017; **266**: 779-786 [PMID: 28806301 DOI: 10.1097/SLA.0000000000002446]

9 **Olthof PB**, Huiskens J, Wicherts DA, Huespe PE, Ardiles V, Robles-Campos R, Adam R, Linecker M, Clavien PA, Koopman M, Verhoef C, Punt CJ, van Gulik TM, de Santibanes E. Survival after associating liver partition and portal vein ligation for staged hepatectomy (ALPPS) for advanced colorectal liver metastases: A case-matched comparison with palliative systemic therapy. *Surgery* 2017; **161**: 909-919 [PMID: 28038862 DOI: 10.1016/j.surg.2016.10.032]

10 **Sun Z**, Tang W, Sakamoto Y, Hasegawa K, Kokudo N. A systematic review and meta-analysis of feasibility, safety and efficacy of associating liver partition and portal vein ligation for staged hepatectomy (ALPPS) versus two-stage hepatectomy (TSH). *Biosci Trends* 2015; **9**: 284-288 [PMID: 26559020 DOI: 10.5582/bst.2015.01139]

11 **Bertens KA**, Hawel J, Lung K, Buac S, Pineda-Solis K, Hernandez-Alejandro R. ALPPS: challenging the concept of unresectability--a systematic review. *Int J Surg* 2015; **13**: 280-287 [PMID: 25496851 DOI: 10.1016/j.ijsu.2014.12.008]

12 **Schadde E**, Schnitzbauer AA, Tschuor C, Raptis DA, Bechstein WO, Clavien PA. Systematic review and meta-analysis of feasibility, safety, and efficacy of a novel procedure: associating liver partition and portal vein ligation for staged hepatectomy. *Ann Surg Oncol* 2015; **22**: 3109-3120 [PMID: 25448799 DOI: 10.1245/s10434-014-4213-5]

13 **Han X**, Yu H, Huang D, Xu Y, Saadatpour A, Li X, Wang L, Yu J, Pinello L, Lai S, Jiang M, Tian X, Zhang F, Cen Y, Fujiwara Y, Zhu W, Zhou B, Zhou T, Ouyang H, Wang J, Yuan GC, Duan S, Orkin SH, Guo G. A molecular roadmap for induced multi-lineage trans-differentiation of fibroblasts by chemical combinations. *Cell Res* 2017; **27**: 386-401 [PMID: 28128194 DOI: 10.1038/cr.2017.17]

14 **Chaudhari P**, Tian L, Deshmukh A, Jang YY. Expression kinetics of hepatic progenitor markers in cellular models of human liver development recapitulating hepatocyte and biliary cell fate commitment. *Exp Biol Med* (Maywood) 2016; **241**: 1653-1662 [PMID: 27390263 DOI: 10.1177/1535370216657901]

15 **Truant S**, Baillet C, Deshorgue AC, El Amrani M, Huglo D, Pruvot FR. Contribution of hepatobiliary scintigraphy in assessing ALPPS most suited timing. *Updates Surg* 2017; **69**: 411-419 [PMID: 28795384 DOI: 10.1007/s13304-017-0481-5]

16 **Stockmann M**, Bednarsch J, Malinowski M, Blüthner E, Pratschke J, Seehofer D, Jara M. Functional considerations in ALPPS - consequences for clinical management. *HPB* (Oxford) 2017; **19**: 1016-1025 [PMID: 28844397 DOI: 10.1016/j.hpb.2017.07.010]

17 **Shi H**, Yang G, Zheng T, Wang J, Li L, Liang Y, Xie C, Yin D, Sun B, Sun J, Wang H, Pan S, Jiang H, Lau W, Liu L. A preliminary study of ALPPS procedure in a rat model. *Sci Rep* 2015; **5**: 17567 [PMID: 26631552 DOI: 10.1038/srep17567]

18 **Wei W**, Zhang T, Zafarnia S, Schenk A, Xie C, Kan C, Dirsch O, Settmacher U, Dahmen U. Establishment of a rat model: Associating liver partition with portal vein ligation for staged hepatectomy. *Surgery* 2016; **159**: 1299-1307 [PMID: 26879073 DOI: 10.1016/j.surg.2015.12.005]

19 **Schlegel A**, Lesurtel M, Melloul E, Limani P, Tschuor C, Graf R, Humar B, Clavien PA. ALPPS: from human to mice highlighting accelerated and novel mechanisms of liver regeneration. *Ann Surg* 2014; **260**: 839-846; discussion 846-847 [PMID: 25379855 DOI: 10.1097/SLA.0000000000000949]

20 **Linecker M**, Kambakamba P, Reiner CS, Linh Nguyen-Kim TD, Stavrou GA, Jenner RM, Oldhafer KJ, Björnsson B, Schlegel A, Györi G, Schneider MA, Lesurtel M, Clavien PA, Petrowsky H. How much liver needs to be transected in ALPPS? A translational study investigating the concept of less invasiveness. *Surgery* 2017; **161**: 453-464 [PMID: 27814957 DOI: 10.1016/j.surg.2016.08.004]

21 **Almau Trenard HM**, Moulin LE, Padín JM, Stringa P, Gondolesi GE, Barros Schelotto P. Development of an experimental model of portal vein ligation associated with parenchymal transection (ALPPS) in rats. *Cir Esp* 2014; **92**: 676-681 [PMID: 25064517 DOI: 10.1016/j.ciresp.2013.11.005]

22 **Wang Y**, Zhou Y, Tao F, Chai S, Xu X, Yang Y, Yang Y, Xu H, Wang K. N-myc downstream regulated gene 1(NDRG1) promotes the stem-like properties of lung cancer cells through stabilized c-Myc. *Cancer Lett* 2017; **401**: 53-62 [PMID: 28456659 DOI: 10.1016/j.canlet.2017.04.031]

23 **Huang P**, He Z, Ji S, Sun H, Xiang D, Liu C, Hu Y, Wang X, Hui L. Induction of functional hepatocyte-like cells from mouse fibroblasts by defined factors. *Nature* 2011; **475**: 386-389 [PMID: 21562492 DOI: 10.1038/nature10116]

24 **Nishikawa T**, Bell A, Brooks JM, Setoyama K, Melis M, Han B, Fukumitsu K, Handa K, Tian J, Kaestner KH, Vodovotz Y, Locker J, Soto-Gutierrez A, Fox IJ. Resetting the transcription factor network reverses terminal chronic hepatic failure. *J Clin Invest* 2015; **125**: 1533-1544 [PMID: 25774505 DOI: 10.1172/JCI73137]

25 **Oldhafer KJ**, Stavrou GA, van Gulik TM; Core Group. ALPPS--Where Do We Stand, Where Do We Go?: Eight Recommendations From the First International Expert Meeting. *Ann Surg* 2016; **263**: 839-841 [PMID: 26756771 DOI: 10.1097/SLA.0000000000001633]

26 **Cai X**, Tong Y, Yu H, Liang X, Wang Y, Liang Y, Li Z, Peng S, Lau WY. The ALPPS in the Treatment of Hepatitis B-Related Hepatocellular Carcinoma With Cirrhosis: A Single-Center Study and Literature Review. *Surg Innov* 2017; **24**: 358-364 [PMID: 28689487 DOI: 10.1177/1553350617697187]

27 **Schadde E**, Raptis DA, Schnitzbauer AA, Ardiles V, Tschuor C, Lesurtel M, Abdalla EK, Hernandez-Alejandro R, Jovine E, Machado M, Malago M, Robles-Campos R, Petrowsky H, Santibanes ED, Clavien PA. Prediction of Mortality After ALPPS Stage-1: An Analysis of 320 Patients From the International ALPPS Registry. *Ann Surg* 2015; **262**: 780-785; discussion 785-786 [PMID: 26583666 DOI: 10.1097/SLA.0000000000001450]

28 **Olthof PB**, Coelen RJS, Bennink RJ, Heger M, Lam MF, Besselink MG, Busch OR, van Lienden KP, van Gulik TM. 99mTc-mebrofenin hepatobiliary scintigraphy predicts liver failure following major liver resection for perihilar cholangiocarcinoma. *HPB* (Oxford) 2017; **19**: 850-858 [PMID: 28687148 DOI:

10.1016/j.hpb.2017.05.007]
29 **Serenari M**, Collaud C, Alvarez FA, de Santibañes M, Giunta D, Pekolj J, Ardiles V, de Santibañes E. Interstage Assessment of Remnant Liver Function in ALPPS Using Hepatobiliary Scintigraphy: Prediction of Posthepatectomy Liver Failure and Introduction of the HIBA Index. *Ann Surg* 2017; Epub ahead of print [PMID: 28121683 DOI: 10.1097/SLA.0000000000002150]
30 **Itoh T**. Stem/progenitor cells in liver regeneration. *Hepatology* 2016; **64**: 663-668 [PMID: 27227904 DOI: 10.1002/hep.28661]
31 **Li D**, Li W, Hui L. Hybrid hepatocyte: A newly identified player for regeneration in hepatic injuries. *Hepatology* 2016; **64**: 2244-2246 [PMID: 27641691 DOI: 10.1002/hep.28837]
32 **Font-Burgada J**, Shalapour S, Ramaswamy S, Hsueh B, Rossell D, Umemura A, Taniguchi K, Nakagawa H, Valasek MA, Ye L, Kopp JL, Sander M, Carter H, Deisseroth K, Verma IM, Karin M. Hybrid Periportal Hepatocytes Regenerate the Injured Liver without Giving Rise to Cancer. *Cell* 2015; **162**: 766-779 [PMID: 26276631 DOI: 10.1016/j.cell.2015.07.026]
33 **Iacob R**, Rüdrich U, Rothe M, Kirsch S, Maasoumy B, Narain N, Verfaillie CM, Sancho-Bru P, Iken M, Popescu I, Schambach A, Manns MP, Bock M. Induction of a mature hepatocyte phenotype in adult liver derived progenitor cells by ectopic expression of transcription factors. *Stem Cell Res* 2011; **6**: 251-261 [PMID: 21474405 DOI: 10.1016/j.scr.2011.02.002]
34 **Zhu S**, Rezvani M, Harbell J, Mattis AN, Wolfe AR, Benet LZ, Willenbring H, Ding S. Mouse liver repopulation with hepatocytes generated from human fibroblasts. *Nature* 2014; **508**: 93-97 [PMID: 24572354 DOI: 10.1038/nature13020]
35 **Mederacke I**, Hsu CC, Troeger JS, Huebener P, Mu X, Dapito DH, Pradere JP, Schwabe RF. Fate tracing reveals hepatic stellate cells as dominant contributors to liver fibrosis independent of its aetiology. *Nat Commun* 2013; **4**: 2823 [PMID: 24264436 DOI: 10.1038/ncomms3823]
36 **Friedman SL**, Sheppard D, Duffield JS, Violette S. Therapy for fibrotic diseases: nearing the starting line. *Sci Transl Med* 2013; **5**: 167sr1 [PMID: 23303606 DOI: 10.1126/scitranslmed.3004700]

P- Reviewer: Campos RR, Starlinger P **S- Editor**: Gong ZM
L- Editor: A **E- Editor**: Ma YJ

World Journal of Gastroenterology

Submit a Manuscript: http://www.f6publishing.com

World J Gastroenterol 2018 March 14; 24(10): 1120-1133

DOI: 10.3748/wjg.v24.i10.1120

ISSN 1007-9327 (print) ISSN 2219-2840 (online)

ORIGINAL ARTICLE

Basic Study

Proteinase-activated receptor 2 promotes tumor cell proliferation and metastasis by inducing epithelial-mesenchymal transition and predicts poor prognosis in hepatocellular carcinoma

Liang Sun, Pi-Bao Li, Yan-Fen Yao, Ai-Yuan Xiu, Zhi Peng, Yu-Huan Bai, Yan-Jing Gao

Liang Sun, Qilu Hospital of Shandong University, Jinan 250012, Shandong Province, China

Liang Sun, Pi-Bao Li, Yan-Fen Yao, Department of Critical Care Medicine, Shandong Traffic Hospital, Jinan 250000, Shandong Province, China

Ai-Yuan Xiu, Zhi Peng, Yu-Huan Bai, Yan-Jing Gao, Department of Gastroenterology, Qilu Hospital of Shandong University, Jinan 250012, Shandong Province, China

ORCID number: Liang Sun (0000-0003-0308-8426); Pi-Bao Li (0000-0003-3944-5106); Yan-Fen Yao (0000-0002-5633-9172); Ai-Yuan Xiu (0000-0002-5009-8961); Zhi Peng (0000-0002-9612-5064); Yu-Huan Bai (0000-0002-2848-4639); Yan-Jing Gao (0000-0001-8153-3754).

Author contributions: Sun L and Gao YJ designed the research; Sun L, Xiu AY and Peng Z performed the research; Li PB and Bai YH contributed new reagents or analytic tools; Sun L and Yao YF analyzed the data; Sun L wrote the paper.

Supported by Jinan College Innovation Plan, No. 26010105081333; and Shandong Social Development Plan, No. 26010104011343.

Institutional animal care and use committee statement: The use and care of experimental animals were approved by the Institutional Animal Care and Use Committee, Qilu Hospital of Shandong University.

Conflict-of-interest statement: The authors declare that they have no competing interests.

Data sharing statement: No additional data are available.

Manuscript source: Unsolicited manuscript

Correspondence to: Yan-Jing Gao, PhD, Chief Doctor, Professor, Department of Gastroenterology, Qilu Hospital of Shandong University, No. 107, West Wenhua Road, Jinan 250012, Shandong Province, China. gaoyanjing@sdu.edu.cn
Telephone: +86-531-86927544

Received: December 8, 2017
Peer-review started: December 8, 2017
First decision: December 20, 2017
Revised: December 29, 2017
Accepted: January 24, 2018
Article in press: January 24, 2018
Published online: March 14, 2018

Abstract

AIM

To clarify the role of proteinase-activated receptor 2 (PAR2) in hepatocellular carcinoma, especially in the process of metastasis.

METHODS

PAR2 expression levels were assessed by qRT-PCR and immunohistochemistry (IHC) in patient tissues and in hepatocellular carcinoma cell lines SMMC-7721 and HepG2. Cell proliferation and metastasis were assessed both *in vitro* and *in vitro*. Immunoblotting was carried out to monitor the levels of mitogen-activated protein kinase (MAPK) and epithelial-mesenchymal transition

markers.

RESULTS

The prognosis was significantly poorer in patients with high PAR2 levels than in those with low PAR2 levels. Patients with high PAR2 levels had advanced tumor stage (P = 0.001, chi-square test), larger tumor size (P = 0.032, chi-square test), and high microvascular invasion rate (P = 0.037, chi-square test). The proliferation and metastasis ability of SMMC-7721 and HepG2 cells was increased after PAR2 overexpression, while knockdown of PAR2 decreased the proliferation and metastasis ability of SMMC-7721 and HepG2 cells. Knockdown of PAR2 also inhibited hepatocellular carcinoma tumor cell growth and liver metastasis in nude mice. Mechanistically, PAR2 increased the proliferation ability of SMMC-7721 and HepG2 cells *via* ERK activation. Activated ERK further promoted the epithelial-mesenchymal transition of these cells, which endowed them with enhanced migration and invasion ability.

CONCLUSION

These data suggest that PAR2 plays an important role in the proliferation and metastasis of hepatocellular carcinoma. Therefore, targeting PAR2 may present a favorable target for treatment of this malignancy.

Key words: Hepatocellular carcinoma; Proteinase-activated receptor 2; Epithelial-mesenchymal transition

Core tip: The role of proteinase-activated receptor 2 (PAR2) in tumor progression especially metastasis of hepatocellular carcinoma and how it is regulated are still unclear. In this study, we found that PAR2 was upregulated in hepatocellular carcinoma (HCC) tumor tissues and related with poor prognosis in HCC patients. In addition, we proved that PAR2 could not only promote the proliferation and metastasis ability of SMMC-7721 and HepG2 cells *in vitro*, but also promoted xenograft tumor growth and HCC cell liver metastasis *in vivo*. These effects were mediated by the activation of ERK, which further induced epithelial-mesenchymal transition of HCC cells.

Sun L, Li PB, Yao YF, Xiu AY, Peng Z, Bai YH, Gao YJ. Proteinase-activated receptor 2 promotes tumor cell proliferation and metastasis by inducing epithelial-mesenchymal transition and predicts poor prognosis in hepatocellular carcinoma. *World J Gastroenterol* 2018; 24(10): 1120-1133 Available from: URL: http://www.wjgnet.com/1007-9327/full/v24/i10/1120.htm DOI: http://dx.doi.org/10.3748/wjg.v24.i10.1120

INTRODUCTION

Hepatocellular carcinoma (HCC) is one of the most common malignancies worldwide[1,2]. Surgical resection is the main strategy for treating this deadly malignancy[3]. Unfortunately, intrahepatic and extrahepatic metastases often occur in progressive and recurrent patients, thus leading to a poor prognosis[4]. Metastasis is a comprehensive process that facilitates cancer cell transition from a primary lesion to a metastatic focus. Many intrinsic cellular characteristics and extrinsic microenvironmental factors influence the metastatic potential of HCC cells[5]. However, the underlying mechanisms that facilitate this process remain largely unknown, therefore, it is critical to identify new targets for these patients to improve their prognosis.

Proteinase-activated receptor 2 (PAR2) is a member of the G-protein coupled receptor 1 family[6]. PAR2 downstream signaling is mediated through several signaling pathways such as intracellular calcium, phospholipase C (PLC), mitogen-activated protein kinase (MAPK), Rho, and I-kappaB kinase/NF-kappaB[7,8]. It is also transactivated by cleaved F2R/PAR1[9]. PAR2 is known to regulate physiological responses such as vasoregulation, cell growth, inflammation, and nociception[10,11]. However, there is growing evidence that PAR2 also has an important role in tumors, especially in tumors of epithelial origin[12-15]. PAR2 is expressed in HCC tissues and multiple HCC cell lines, where it promotes cancer cell migration and invasion through different signaling pathways including $[Ca^{2+}]_i$ mobilization, Src, Met, and p42/p44 MAPK[16,17]. PAR2 also participates in tumor initiation, self-renewal, and metastasis by regulating $CD47^+$ HCC stem cells[18]. Moreover, PAR2 in hepatic stellate cells (HSCs) plays an important role in promoting HCC growth through mediating migration and secretion of pro-angiogenic and pro-mitotic factors[19]. In addition, TF/VIIa/PAR2 signaling is involved in mTOR mediated autophagy in HCC[20]. Collectively, these data suggest an important role for PAR2 in HCC progression. However, the role of PAR2 in HCC metastasis and the underlying mechanism are poorly understood.

Epithelial-mesenchymal transition (EMT) and its intermediate states have been identified as crucial drivers of organ fibrosis and tumor progression[21,22]. EMT is thought to be activated in cancer cells to allow for dissociation from the primary tumor and intravasation into blood vessels[23,24]. However, the impact of PAR2-associated EMT in cancer metastasis is still poorly understood. Based on these findings, we sought to investigate the relationship between PAR2 expression and HCC prognosis and the underlying mechanisms of the EMT in HCC.

MATERIALS AND METHODS

Patients

Cancer tissue sections were obtained with informed consent from 60 HCC patients undergoing radical resection between 2010 and 2012 at Qilu Hospital of Shandong University. Ethical consent was granted from

the Institutional Ethics Committee, Qilu Hospital of Shandong University.

Immunohistochemistry and evaluation of PAR2 expression

Immunohistochemistry (IHC) was performed using a standard immunoperoxidase staining method. Rabbit anti-PAR2 antibody (#6976) was purchased from Cell Signaling Technology (Danvers, United States). PAR2 expression in HCC tissues was evaluated using a method described previously[25]. The scoring of PAR2 immunohistochemical staining was performed as follows: the degree of staining [yellow (1) and brown (2)] and the percentage of area staining positive [< 50% (1) and > 50% (2)]. The final score was the product of the two parameters, and the samples were grouped as high (2-4 point) or low PAR2 expression (1). Two experienced pathologists evaluated the staining for PAR2.

Cell culture

HepG2 and SMMC-7721 cells were cultured at 37 ℃ in a humidified atmosphere containing 5% CO_2. Cells were cultured in DMEM (Gibco, NY, United States) supplemented with 10% fetal bovine serum (FBS; Gibco, NY, United States), 100 U/mL penicillin, and 100 μg/mL streptomycin (Hyclone, UT, United States).

Cell proliferation analysis

The cell counting kit 8 (CCK8) assay (Tongren Chemical Research Institute, Kyushu, Japan) was used to measure cell proliferation. HepG2 and SMMC-7721 cells in the exponential growth phase were seeded into a 96-well plate at 1000 cells per well with five replicates. DMEM medium containing 10% FBS was used to culture the cells. At 6, 24, 48, 72, 96, or 120 h after plating the cells, 100 μL of DMEM containing 10 μL of CCK-8 solution was added into each well. The wells were then incubated for 2 h at 37 ℃, and the absorbance was measured at 450 nm. The absorbance at 6 h of each group was designated as baseline.

Colony formation assay

Cells were seeded in 6-well plates (500 cells per well) and cultured for 2 wk. The generated colonies were fixed with 4% paraformaldehyde and then stained with 5% crystal violet dye (Sigma, MO, United States). The total number of colonies in each well was manually counted.

Cell invasion and migration assays

Cell invasion and migration assays were carried out using a 24-well plate and 8-μm polyethylene terephthalate membrane filters (Costar, MA, United States). Serum-free medium (200 μL) containing 3 × 10^4 HepG2 and SMMC-7721 cells was added to the upper chambers, which contained either uncoated (for migration assay) or matrigel coated (for invasion assay) membranes. Each inferior chamber was filled with 600 μL of medium containing 10% FBS. After 16 h of incubation, the filters were taken out, fixed with 4% paraformaldehyde for 30 min, and stained with crystal violet dye for 30 min. Then, the remaining cells on the upper sides of the filters were removed using cotton swabs. Migrated or invaded cells in four randomly chosen fields (× 100 magnification) per well were counted.

Wound healing assay

HepG2 and SMMC-7721 cells were seeded into 6-well plates and grown to 90% confluence. Then, the confluent cell monolayers were scraped with a 10 μL pipette tip to create wounds. The cellular debris was removed and cells were cultured in FBS-free medium. Pictures were taken under a microscope (Leica) at 0, 24, and 48 h. The difference in wound width represents the migration ability.

Plasmid construction and transfection

The coding region of PAR2 was cloned into a pcDNA3.1(+) plasmid at *EcoR* I and *Xho* I sites; this is referred to as pcDNA3.1-PAR2. Empty control and pcDNA3.1-PAR2 vectors were transfected into HepG2 and SMMC-7721 cells using Lipofectamine 2000 (Thermo, United States) according to the manufacturer's instructions. Primer sequences for vector construction were as follows: forward, 5′-GGAATTCTCGGGGCTTCCAGGAGGA-3′ and reverse, 5′-CCGCTCGAGTTCCCATCTGAGGACCTGG-3′.

Lentivirus-mediated RNA interference

pLKO.1 vector encoding shRNA targeting human PAR2 was purchased from Sigma (MISSION shRNA lentivirus-mediated transduction system, SHCLNG-NM_005242). To generate lentivirus that expressed shRNA, HEK293T cells were cultured in DMEM (Gibco, NY, United States) supplemented with 10% FBS (Gibco, NY, United States). Using polyethyleneimine, we transfected cells transiently with pLKO.1-derived plasmids combined with pRev, pEnv-VSV-G, and pMDLg. Retrovirus particles were collected from the media after 12, 24, and 48 h[19]. HepG2 and SMMC-7721 cells were infected three times with the retrovirus particles with 8.0 μg/mL polybrene. At 48 h after the transduction, transduced cells were selected using 2.0 μg/mL puromycin for one week. The efficiency of the shRNA knockdown was measured *via* quantitative real-time RT-PCR and immunoblot analysis.

RNA extraction and quantitative real-time PCR

Total RNA was extracted from cultured cells using Trizol reagent (Takara, Japan). cDNA was synthesized from at most 1 μg of total RNA (Takara, Japan). RNA expression was measured by qRT-PCR using SYBR-Green (Takara, Japan) according to the manufacturer's guidelines. Primers for PAR2 were: forward, 5′-GATGGCACATCCCACGTCACT-3′ and reverse, 5′-TTGGCAAACCCACCACAAACAC-3′. GAPDH was used as

Table 1 Immunohistochemical score for proteinase-activated receptor 2 in hepatocellular carcinoma

Score	Patient number
1	22
2	15
4	23

an endogenous control.

Immunoblot analysis

Rabbit anti-PAR2, anti-ERK, anti-phospho-ERK, anti-E-cadherin, anti-N-cadherin, and anti-GAPDH antibodies were obtained from Cell Signaling Technology (Danvers, United States). Cell lysates were prepared in RIPA buffer (Sigma-Aldrich, MO, United States) where equal quantities of cellular proteins were separated by sodium dodecyl sulfate-polyacrylamide gel electrophoresis and transferred onto polyvinylidene difluoride membranes. The membranes were blocked with skimmed milk, incubated with a primary antibody, washed with TBST three times, and then incubated with a secondary antibody (Cell Signaling Technology, GA, United States). After the secondary antibody incubation, the membranes were washed three more times with TBST, and the proteins were visualized by enhanced chemiluminescence (Millipore, MA, United States). GADPH was used as the internal loading control.

Experimental animals

Male Balb/c nude mice (aged 4 wk with an initial body weight of 20 ± 2 g) were purchased from Shanghai SLAC Laboratory Animal Co., Ltd. (Shanghai, China). The mice were housed at a temperature of 25 ± 2 ℃ and a relative humidity of 70% ± 5% under natural light/dark conditions for 1 wk and allowed free access to food and water. The animal experiments were performed in strict accordance with international ethical guidelines and the National Institutes of Health Guide for the Care and Use of Laboratory Animals. The protocols were approved by the Institutional Animal Care and Use Committee, Qilu Hospital of Shandong University.

Tumor xenograft model

HepG2 or SMMC-7721 cells (2×10^6) suspended in 100 μL of normal saline were subcutaneously injected into the axillae of the nude mice (4 wk). Tumor growth was monitored every week and tumor volume was calculated as follows: tumor volume = $4\pi/3 \times (\text{width}/2)^2 \times (\text{length}/2)$, in which the length and width are the longest and shortest diameters, respectively. Four weeks after injection, the mice were sacrificed and the tumors were dissected and weighed.

Tumor metastasis model

HepG2 and SMMC-7721 cells (2×10^6) suspended in 100 μL of normal saline were injected into the spleen of nude mice (4 wk) followed by a splenectomy 3 min later; the mice were monitored every 3 d after the procedure. After the 4th week, the mice were sacrificed and their livers were dissected. The liver tumor was weighed and tumor number on each liver was counted.

Table 2 Clinicopathological characteristics of hepatocellular carcinoma patients according to proteinase-activated receptor 2 expression

Clinicopathological variable	PAR2 expression		
	Low	High	*P* value
All cases	22	38	
Gender			
Male	16	28	0.832
Female	6	10	
Age (yr)			
< 60	10	22	0.352
⩾ 60	12	16	
TNM stage			
Early (Ⅰ-Ⅱ)	16	12	0.001[a]
Late (Ⅲ-Ⅳ)	6	26	
Tumor size (cm)			
Small (⩽ 5)	15	15	0.032[a]
Large (> 5)	7	23	
Microvascular invasion			
Present	5	21	0.037[a]
Absent	17	17	
HBsAg			
Negative	3	7	0.632
Positive	19	31	
Serum AFP level (ng/mL)			
< 400	18	25	0.154
⩾ 400	4	13	

[a]*P* < 0.05. PAR2: Proteinase-activated receptor 2; HBsAg: Hepatitis B surface antigen; AFP: Alpha-fetoprotein.

Statistical analysis

All assays were done in triplicate. The data are shown as mean ± SD. To compare the mean values between the two groups, the independent Student's *t*-test was used. To compare the mean values among more than two groups, two-way ANOVA was used. Fisher's exact test was used to compare tumor metastatic rate in the two groups. A Pearson χ^2 test was adopted to analyze the clinicopathological variables according to PAR2 expression. For survival analysis, Kaplan-Meier method and log-rank test were used. $P < 0.05$ was considered statistically significant.

RESULTS

The expression level of PAR2 correlates with TNM stage, tumor size, microvascular invasion, and patients' overall survival and disease-free survival

To determine whether PAR2 plays an important role in HCC progression, the expression level of PAR2 in patients' tumor tissues was detected by IHC. PAR2 was mainly located on the plasma membrane (Figure 1A). The patient distribution of PAR2 IHC score is shown in Table 1. Patients were divided into PAR2 high and PAR2 low groups according to the IHC score (Figure

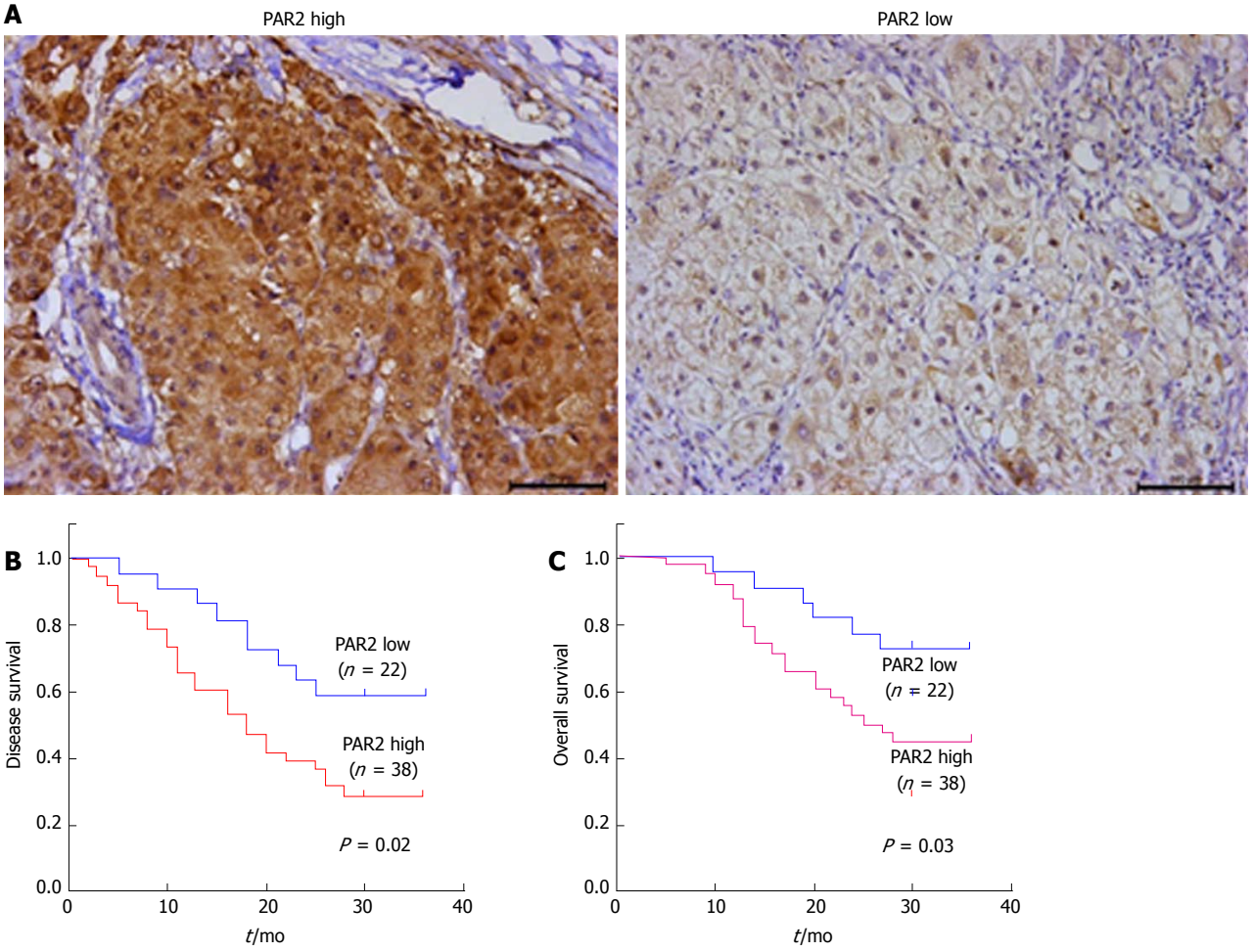

Figure 1 The expression level of proteinase-activated receptor 2 predicts overall survival and disease-free survival in hepatocellular carcinoma patients. A: Immunohistochemical staining for proteinase-activated receptor 2 (PAR2) in hepatocellular carcinoma (HCC) tissues, and the expression level of PAR2 was divided into high (left) and low (right); B: Disease-free survival in HCC patients correlated with PAR2 expression; C: Overall survival in HCC patients correlated with PAR2 expression.

1A). Patients with high PAR2 levels had advanced tumor stage (P = 0.001, chi-square test), larger tumor size (P = 0.032, chi-square test), and high microvascular invasion rate (P = 0.037, chi-square test; Table 2). Patients with high PAR2 expression levels had significantly shorter overall survival (OS) and disease-free survival (DFS) than those with low PAR2 expression levels (P = 0.02 and P = 0.03, respectively; Figure 1B and C). Multivariate Cox regression analysis further revealed that PAR2 was an independent prognostic marker for the OS of HCC patients (hazard ratio = 1.814; P = 0.041) (Table 3). These data suggest that PAR2 is associated with tumor growth and invasion; it can also predict the prognosis of HCC patients.

PAR2 is stably knocked down by lentiviral-mediated RNAi and transiently overexpressed by plasmid transfection

To determine whether PAR2 is essential for HCC carcinogenesis, the expression of PAR2 was stably knocked down using lentiviral-mediated shRNA in HepG2 and SMMC-7721 cells. The PAR2 knockdown is referred to as shPAR2, while the negative control is referred to as shNC. The PAR2 RNA and protein levels both decreased in shPAR2 knockdown cells (Figure 2A and B). To overexpress PAR2, its coding region was amplified and inserted into the pcDNA3.1 (+) plasmid. After transfecting cells with empty pcDNA3.1 or pcDNA3.1-PAR2 using Lipofectamine 2000, PAR2 was transiently overexpressed in pcDNA3.1-PAR2 cells (Figure 2C and D).

PAR2 promotes proliferation of HCC cells

CCK8 and colony formation assays were used to uncover the role of PAR2 in promoting HCC cell proliferation. Cell viability and proliferation were dramatically reduced after PAR2 knockdown (Figure 3A and B), but increased after PAR2 overexpression (Figure 3C and D). The same results were also observed using a colony formation assay (Figure 3E and F). These results demonstrate that PAR2 could promote the proliferation

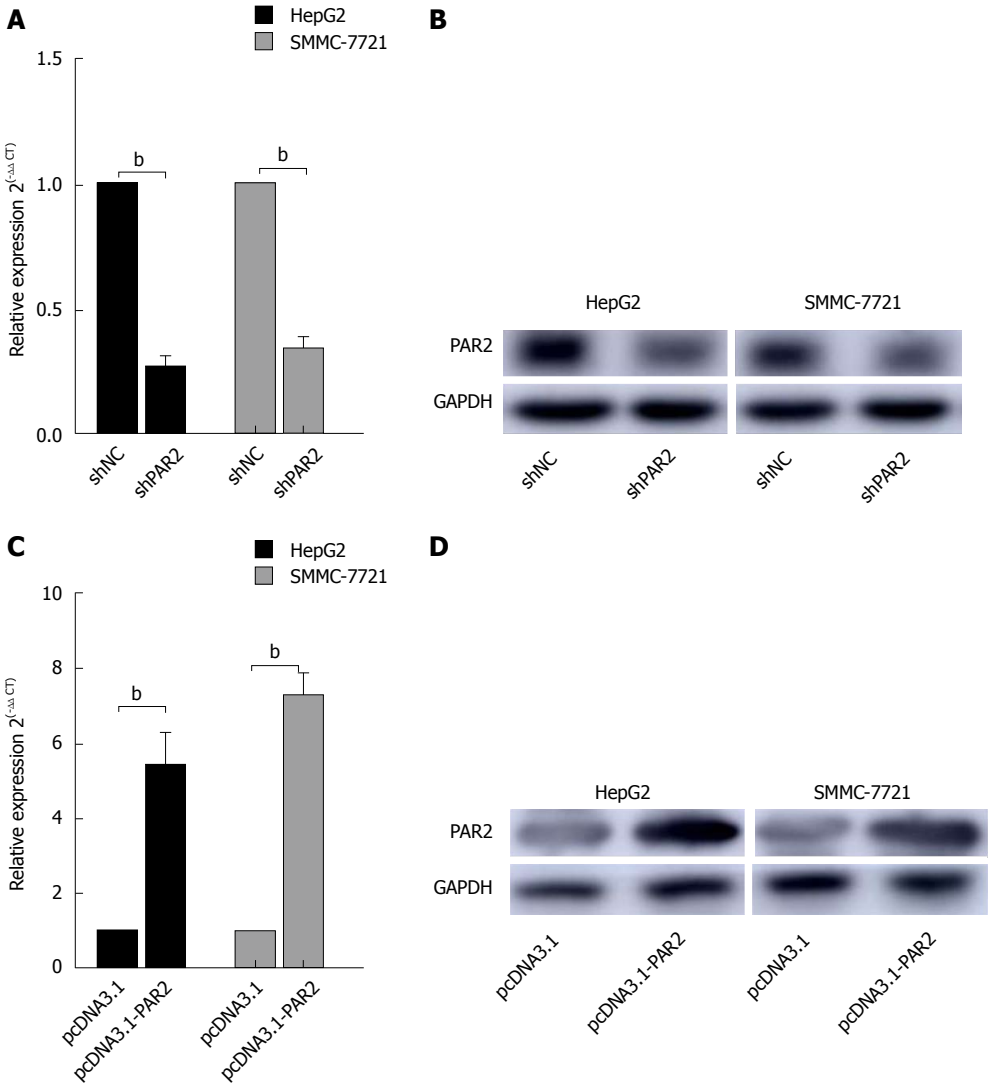

Figure 2 Proteinase-activated receptor 2 knockdown and overexpression. A: qRT-PCR analysis of the proteinase-activated receptor 2 (PAR2) mRNA expression levels in HepG2 and SMMC-7721 cells with PAR2 knockdown; B: Immunoblot analysis of the protein levels of PAR2 in HepG2 and SMMC-7721 cells with PAR2 knockdown; C: The RNA expression levels of PAR2 in HepG2 and SMMC-7721 cells with PAR2 overexpression were measured by qRT-PCR; D: The protein levels of PAR2 in HepG2 and SMMC-7721 cells with PAR2 overexpression were measured by immunoblot analysis. $^{b}P < 0.01$.

Table 3 Multivariate analysis of the association of prognosis with clinicopathological variables and proteinase-activated receptor 2 expression in hepatocellular carcinoma patients

Clinicopathological variable	Hazard ratio	*P* value
Gender (male *vs* female)	0.214	0.672
Age (< 60 *vs* ⩾ 60)	0.126	0.763
TNM stage (Ⅰ-Ⅱ *vs* Ⅲ-Ⅳ)	4.292	0.016[a]
Tumor size (⩽ 5 cm *vs* >5 cm)	2.193	0.034[a]
Microvascular invasion (present vs absent)	2.499	0.029[a]
HBsAg (negative *vs* positive)	1.072	0.092
Serum AFP level (< 400 ng/mL *vs* ⩾ 400 ng/mL)	3.688	0.023[a]
PAR2 expression (high *vs* low)	1.814	0.041[a]

[a]$P < 0.05$. HBsAg: Hepatitis B surface antigen; AFP: Alpha-fetoprotein; PAR2: Proteinase-activated receptor 2.

ability of HCC cells.

PAR2 promotes HCC cell invasion and migration

Metastasis often occurs in HCC patients and the results shown in Table 1 suggest that PAR2 is associated with tumor microvascular invasion. To determine whether PAR2 could promote HCC cell migration and invasion, transwells with or without matrigel coating were used to measure cell migration *in vitro*. As shown in Figure 4A and B, the migration and invasion abilities of HepG2 and SMMC-7721 cells were reduced after PAR2 knockdown, but increased after overexpression. These results were also verified using a wound healing assay (Figure 4C and D). The wound healing assay showed that the migration rate of shPAR2 cells was significantly slower than that of the control shNC cells. Also, the migration rate of pcDNA3.1-PAR2 cells was faster than that of the control pcDNA3.1 cells. These data suggest that PAR2 can influence the process of HCC cell invasion and migration.

PAR2 knockdown inhibits tumor growth in nude mice

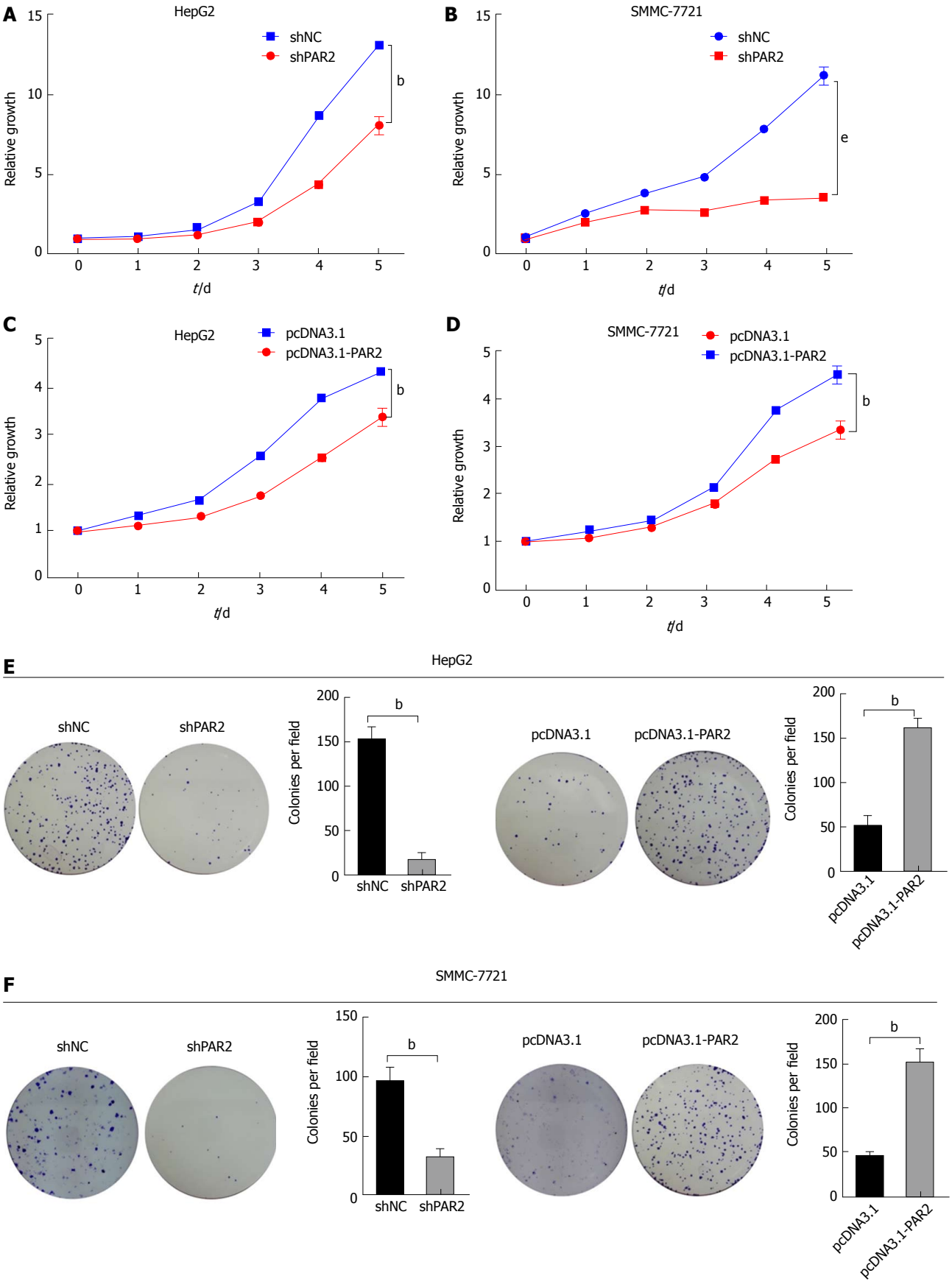

Figure 3 Proteinase-activated receptor 2 promotes proliferation of hepatocellular carcinoma cells. A-D: CCK8 assay in HepG2 and SMMC-7721 cells; E and F: Colony formation assay in HepG2 and SMMC-7721 cells. The colony number in each field was counted. $^{b}P < 0.01$, $^{e}P < 0.001$.

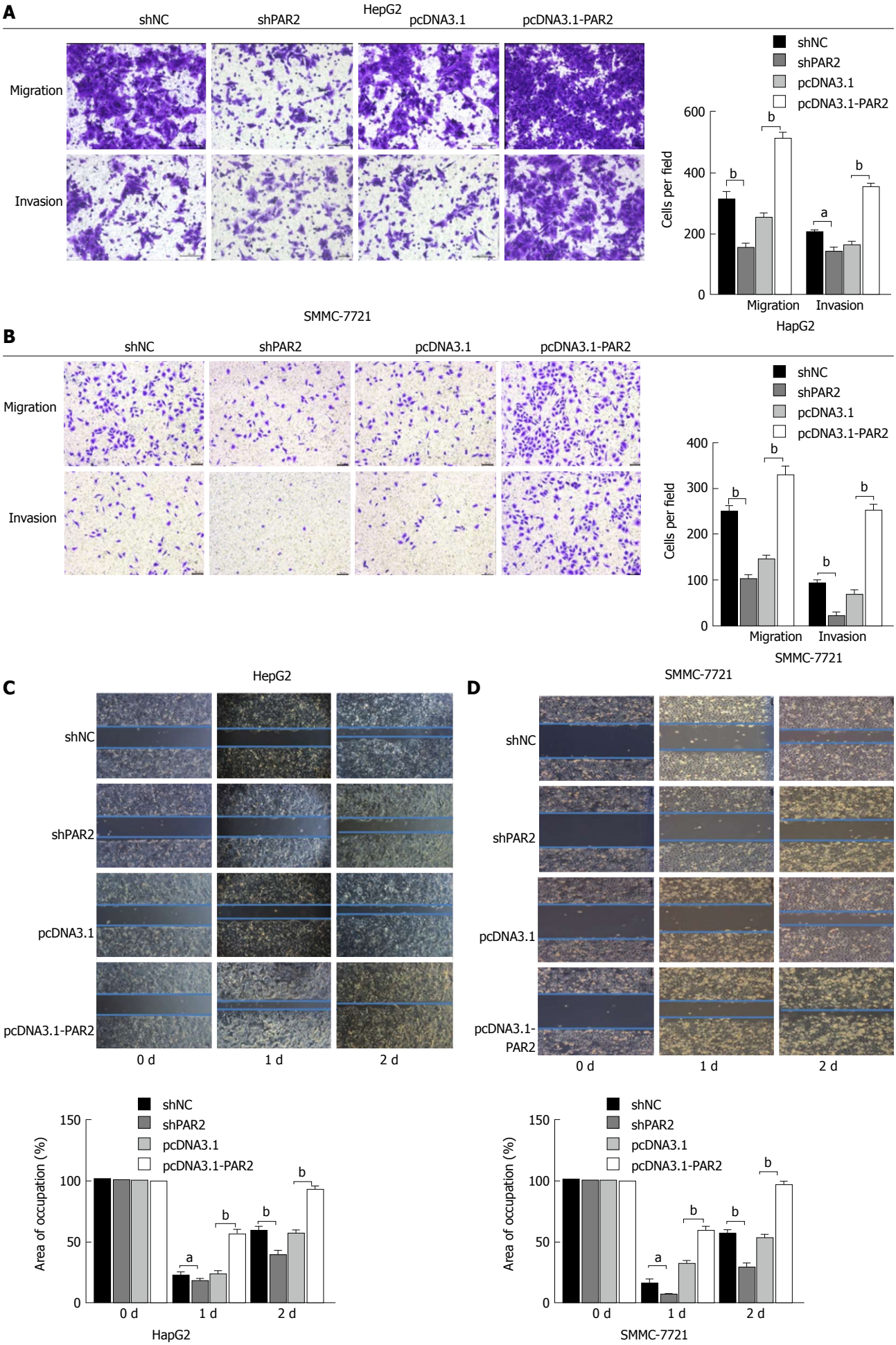
A
HepG2
shNC
shPAR2
pcDNA3.1
pcDNA3.1-PAR2
Migration
Invasion
Cells per field
600
400
200
0
b
a
Migration
Invasion
HapG2
SMMC-7721
B
shNC
shPAR2
pcDNA3.1
pcDNA3.1-PAR2
Migration
Invasion
Cells per field
400
300
200
100
0
SMMC-7721
C
HepG2
shNC
shPAR2
pcDNA3.1
pcDNA3.1-PAR2
0 d
1 d
2 d
Area of occupation (%)
150
100
50
0
HapG2
D
SMMC-7721
shNC
shPAR2
pcDNA3.1
pcDNA3.1-PAR2
0 d
1 d
2 d
Area of occupation (%)
SMMC-7721

Figure 4 Proteinase-activated receptor 2 promotes hepatocellular carcinoma cell invasion and migration *in vitro*. A and B: Transwell assays with or without matrigel coating were performed in HepG2 and SMMC-7721 cells. Cell number in each field was counted; C and D: Wound healing assays were performed in HepG2 and SMMC-7721 cells and the pictures were taken every 24 h ($^{a}P < 0.05$, $^{b}P < 0.01$).

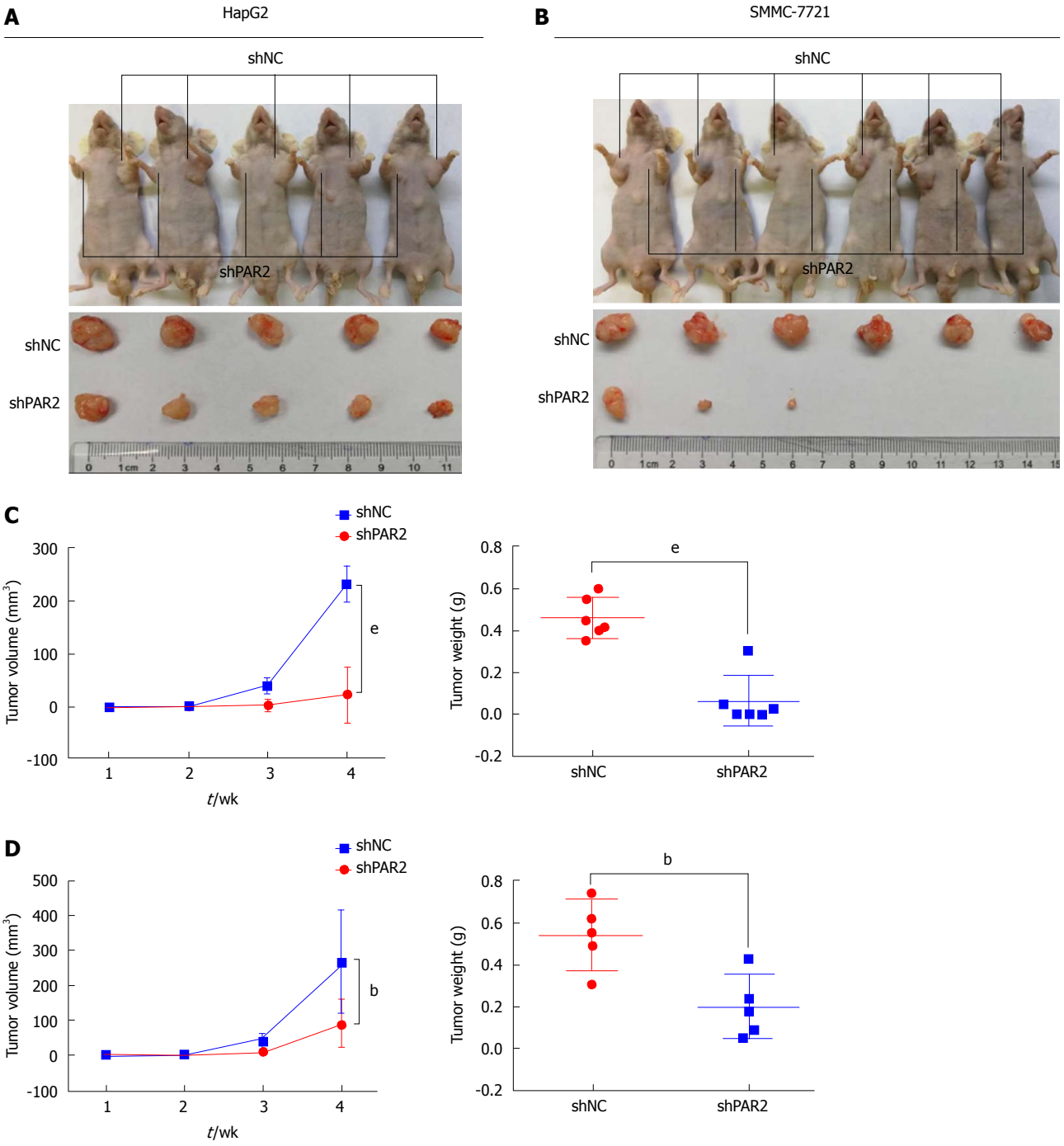

Figure 5 Proteinase-activated receptor 2 knockdown inhibits tumor growth in nude mice. A and B: Subcutaneous xenografts of HepG2 and SMMC-7721 cells in nude mice growing for 4 wk; C and D: Tumor volumes were measured every week and tumor weights were tested at the end. $^{b}P < 0.01$, $^{e}P < 0.001$.

To further confirm the role of PAR2 in promoting cell proliferation *in vivo*, HepG2 and SMMC-7721 cells with stable knockdown of either PAR2 or NC were subcutaneously injected into nude mice to make tumor xenografts. After 4 wk, tumors from the NC groups were much larger than those from the shPAR2 groups for both HepG2 and SMMC-7721 cells (Figure 5A and B). Tumor weights from the NC groups were much greater than those of the shPAR2 groups (Figure 5C and D). These data suggest that PAR2 knockdown could dramatically inhibit tumor growth *in vivo*.

PAR2 knockdown inhibits tumor metastasis in nude mice

Intrahepatic metastasis is the most common mode of HCC metastasis[26]. To determine whether PAR2 could

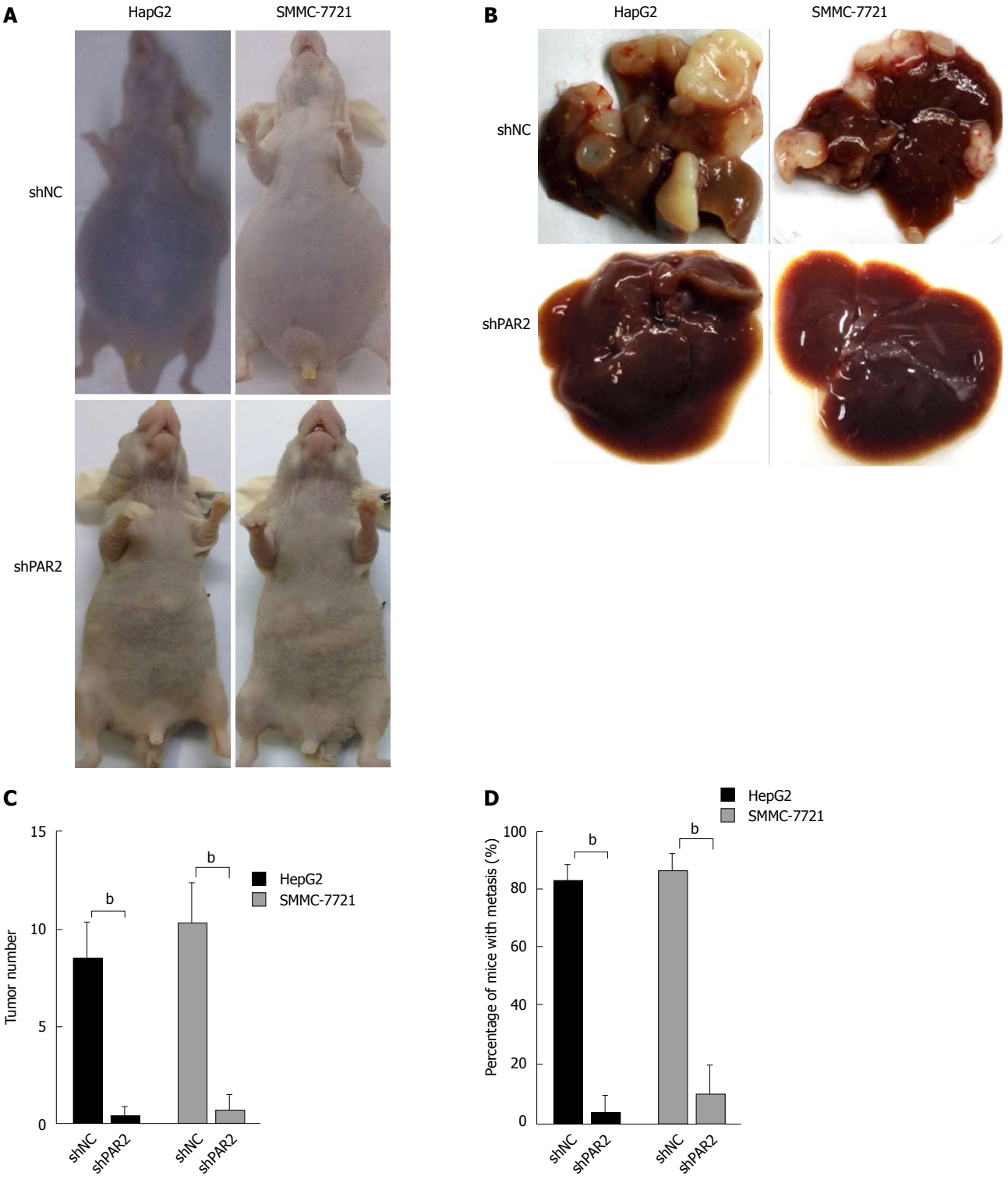

Figure 6 Proteinase-activated receptor 2 knockdown inhibits tumor metastasis in nude mice. A: HepG2 and SMMC-7721 cells were injected into the spleen of nude mice to form liver metastases. The appearance of mice after 4 wk is shown; B: Tumors grown on the liver; C: Tumor number on each liver was counted; D: Percentage of mice with liver metastases (n = 10 per group). $^{b}P < 0.01$.

facilitate tumor metastasis *in vivo*, a mouse model was established that mimics the process of tumor metastasis to the liver. HepG2 and SMMC-7721 cells stably expressing shPAR2 or shNC were injected into the spleen of nude mice, and then a splenectomy was performed. This allows the tumor cells to circulate into the liver through the portal vein, thus forming liver metastases. After 4 wk, ascites and liver tumors grew in the mice of the shNC groups (Figure 6A), the maximum body weight that increased due to ascites was no more than 10% of the body weight in age-matched shPAR2 group. The mice in both groups were sacrificed and

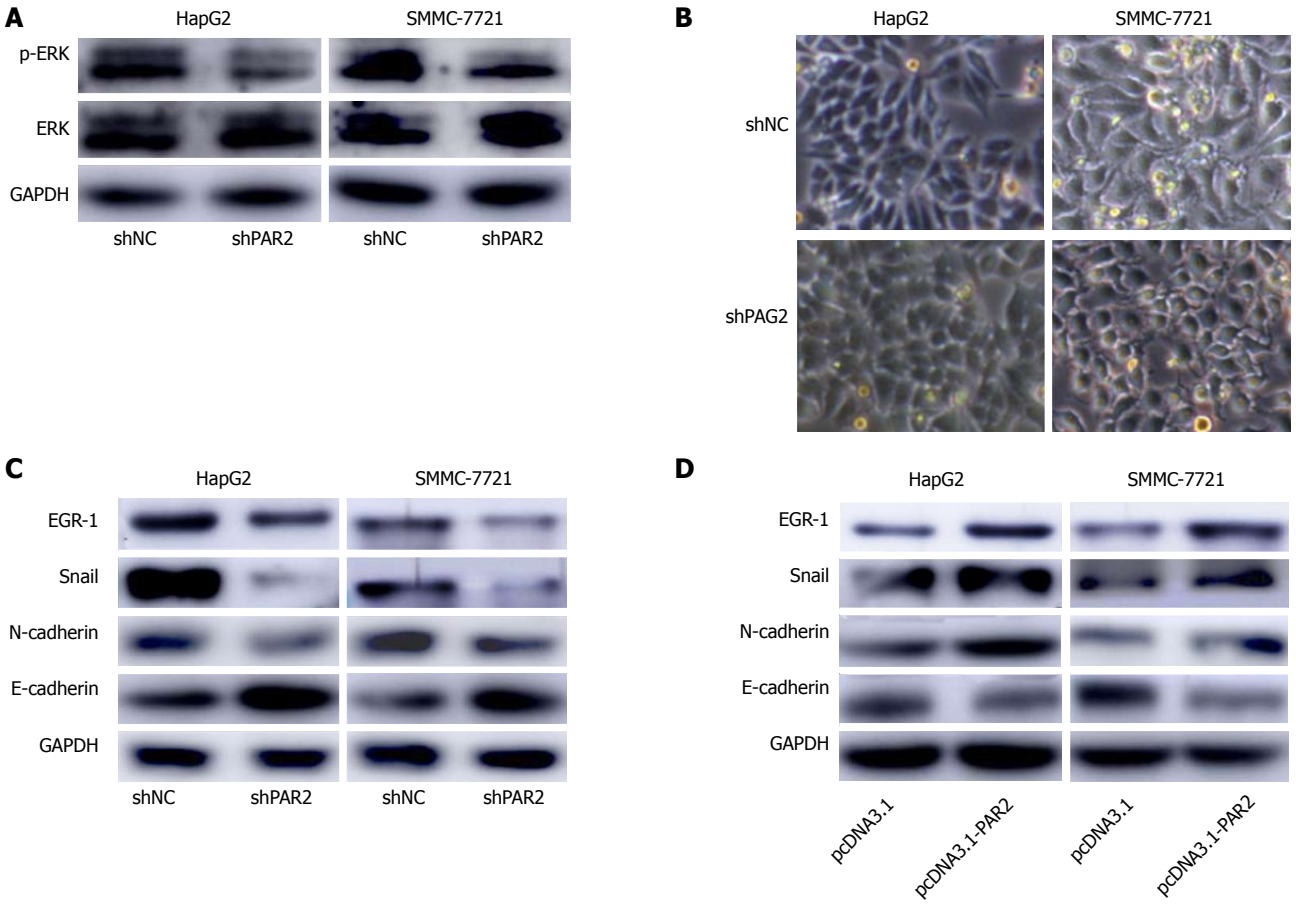

Figure 7 Proteinase-activated receptor 2 mediates the activation of ERK and further induces epithelial-mesenchymal transition. A: The protein levels of ERK and p-ERK in HepG2 and SMMC-7721 cells; B: The morphological changes in HepG2 and SMMC-7721 cells after proteinase-activated receptor 2 knockdown; C and D: The protein levels of EGR-1, Snail, E-cadherin, and N-cadherin in HepG2 and SMMC-7721 cells. GAPDH was selected as an endogenous control.

the tumor volumes of the shNC groups were much larger than those in the shPAR2 groups (Figure 6B). Livers in the shNC group also had a higher number of tumors compared to the shPAR2 groups (Figure 6C). There was almost no liver metastasis observed in the shPAR2 groups (Figure 6D). From this metastasis model, it appears that PAR2 is necessary for HCC intrahepatic metastasis. PAR2 knockdown could inhibit the colonization of HCC cells on the liver.

PAR2 mediates the activation of ERK to promote cell proliferation and induces EMT to promote metastasis

PAR2 is reported to activate ERK to promote HCC cell proliferation[16]; these results were confirmed in HepG2 and SMMC-7721 cells (Figure 7A), but the downstream mechanisms that facilitate metastasis are unclear. EMT is a common mechanism of cancer metastasis, and it is reported that activated ERK can activate EGR-1[27]. As a transcription factor, EGR-1 induces Snail expression to inhibit E-cadherin expression, thus inducing EMT[27-29]. Interestingly, after knockdown of PAR2, HepG2 and SMMC-7721 cells showed obvious morphological changes toward an epithelial phenotype (Figure 7B). Therefore, we measured EGR-1, Snail, and the EMT markers E-cadherin and N-cadherin expression in shNC and shPAR2 cells through immunoblot analysis. As shown in Figure 7C, the epithelial marker E-cadherin was upregulated while EGR-1, Snail, and the mesenchymal marker N-cadherin were downregulated when PAR2 was knocked down. After transient overexpression of PAR2, E-cadherin was downregulated, and EGR-1, Snail, and N-cadherin were upregulated (Figure 7D). These results demonstrate that PAR2 participates in the process of EMT and promotes HCC cell metastasis.

DISCUSSION

HCC is one of the most lethal malignancies worldwide, especially in China[4]. Although many genes and signaling pathways have been found to participate in HCC carcinogenesis[30-33], the prognosis of the patients is still unsatisfactory, therefore it is urgent to uncover more genes responsible for the development of HCC. The focus of this work was PAR2, which is evident for its important role in the development of tumors, especially of epithelial origin[12-15]. PAR2 is known to promote proliferation, migration, and invasion of HCC cells. Unfortunately, the underlying mechanism of PAR2 activity in HCC metastasis is unclear and few *in*

vivo studies have been carried out elucidating its role in tumor development. Additionally, the association between PAR2 and clinicopathological variables of HCC patients has not been analyzed; this work addressed those questions.

In the clinical association study, expression levels of PAR2 were analyzed in 60 HCC patients by immunohistochemistry. Patients with high PAR2 expression levels tended to have advanced tumor stage, larger tumor size, and high microvascular invasion rate, indicating that PAR2 plays an important role in the development of HCC. Additionally, patients with high PAR2 expression levels had shorter OS and DFS, implying that PAR2 could serve as a biomarker to predict the prognosis of HCC patients.

Because PAR2 is associated with tumor size and microvascular invasion, the role of PAR2 in HCC proliferation and invasion was investigated. PAR2 was stably knocked down using shRNA or transiently overexpressed in HepG2 and SMMC-7721 cells. CCK8 and colony forming assays were used to measure *in vitro* cell proliferation. These assays showed that PAR2 knockdown inhibited cell proliferation and colony formation ability, while overexpression of PAR2 presented adverse effects. From transwell and wound healing assays, PAR2 was shown to promote tumor cell migration and invasion. These *in vitro* experiments indicated that PAR2 plays an important role in tumorigenesis and the development of HCC cells.

Two mouse models were used to explore the role of PAR2 in HCC progression *in vivo*. From a subcutaneous xenograft model, it was determined that knockdown of PAR2 could inhibit tumor growth to a great extent. From the liver metastasis model, PAR2 was shown to help HCC cells plant onto the liver and form metastatic foci. These *in vivo* data provide solid evidence that PAR2 promotes HCC cell proliferation, invasion, and migration.

After knockdown of PAR2, morphological changes toward an epithelial phenotype were observed in HepG2 and SMMC-7721 cells. EMT is an important step in tumor progression and plays a critical role during cancer invasion and metastasis. During EMT, cells lose their epithelial qualities and acquire mesenchymal features[21] such as increased expression of mesenchymal-related markers (such as N-cadherin), and reduced expression of epithelial-related markers (such as E-cadherin)[28]. It is reported that the function of PAR2 is mediated by activating MAPK proteins such as ERK[16]; ERK activation by PAR2 was verified in this study. Interestingly, it is reported that activated ERK can induce EMT through EGR-1 and Snail[28,29], therefore the expression levels of EGR-1, Snail, E-cadherin, and N-cadherin were monitored through immunoblot analysis in HepG2 and SMMC-7721 cells. PAR2 knockdown resulted in higher levels of E-cadherin and lower levels of N-cadherin, while overexpression of PAR2 reduced the levels of E-cadherin and increased the levels of N-cadherin. This implies that PAR2 can promote EMT in HCC cells through activating ERK, at least in part. As we all know, PAR2 is activated *via* its N-terminal cleavage by several proteases such as serine proteases[34], but which protease is responsible for PAR2 activation in HCC is still not clear. This is a very interesting direction in the following study. Recently, some growth factors such as HGF were reported to be responsible for EMT in HCC. Whether HGF participates in PAR2-induced EMT could be further investigated based on this study[27,35].

Collectively, this study comprehensively investigated the role of PAR2 in HCC progression *in vitro*, *in vivo,* and in clinical samples for the first time. PAR2 could promote HCC cell proliferation, invasion, and migration by activating ERK and thus inducing EMT. These findings highlight the potential role of PAR2 in directing the diagnosis, treatment, and prognosis of HCC.

ARTICLE HIGHLIGHTS

Research background

Hepatocellular carcinoma (HCC) is one of the most common malignancies worldwide. Metastasis often occurs in HCC patients, thus leading to a poor prognosis. It is urgent for us to find out molecules that are responsible for HCC metastasis to improve the prognosis of HCC patients.

Research motivation

Proteinase-activated receptor 2 (PAR2) is reported to be responsible for HCC development, but the underlying mechanism is unclear. Figuring out the detailed mechanisms for PAR2-induced metastasis of HCC could give us more options for HCC treatment.

Research objectives

Although the role of PAR2 in HCC has been reported, the underlying mechanism for PAR2-induced metastasis is more important. Therefore, we aimed to find out the downstream signaling for PAR2-induced HCC metastasis. This could help us to find targets for HCC treatment.

Research methods

PAR2 expression levels were assessed by qRT-PCR and immunohistochemistry in patient tissues. Cell proliferation was investigated by CCK8 and colony formation assays *in vitro* and tumor xenograft *in vivo*. HCC cell metastasis was assessed by transwell and wound healing assays *in vitro* and intrasplenic injection of HCC cells in mice *in vivo*. Immunoblotting was carried out to monitor the levels of mitogen-activated protein kinases and epithelial-mesenchymal transition (EMT) markers to figure out the underlying mechanisms for PAR2. This is the first time to analyze the correlation between PAR2 expression and HCC clinicopathological characteristics. Also, it is the first for us to investigate the underlying mechanism for PAR2-mediated HCC metastasis. What's more, we proved the role of PAR2 in HCC proliferation and metastasis using an animal model.

Research results

The prognosis of patients with high PAR2 levels was poorer than those with low PAR2 levels. Patients with high PAR2 levels had advanced tumor stage, larger tumor size, and high microvascular invasion rate. The proliferation and metastasis ability of SMMC-7721 and HepG2 cells was increased after PAR2 overexpression, while knockdown of PAR2 decreased the proliferation and metastasis ability of SMMC-7721 and HepG2 cells. Knockdown of PAR2 also inhibited HCC tumor cell growth and liver metastasis in nude mice. Mechanistically, PAR2 increased the proliferation ability of SMMC-7721 and HepG2 cells *via* ERK activation. Activated ERK further promoted the epithelial-mesenchymal transition of these cells with the help of EGR-1 and Snail, which endowed them with enhanced migration and invasion ability.

Research conclusions

In this study, we found that PAR2 was upregulated in HCC tumor tissues and related with poor prognosis in HCC patients. In addition, we proved that PAR2 could not only promote the proliferation and metastasis ability of SMMC-7721 and HepG2 cells *in vitro*, but also promoted xenograft tumor growth and HCC cell liver metastasis *in vivo*. These effects were mediated by the activation of ERK, which further induced EMT by EGR-1 and Snail of HCC cells. Therefore, targeting PAR2 may present a favorable anticancer target for treatment.

Research perspectives

As we all know, PAR2 is activated *via* its N-terminal cleavage by several proteases such as serine proteases, but which protease is responsible for PAR2 activation in HCC is still not clear. This is a very interesting direction in the following study. Recently, some growth factors such as HGF were reported to be responsible for EMT in HCC. Whether HGF participates in PAR2-induced EMT could be further investigated based on this study.

REFERENCES

1 **Bruix J**, Reig M, Sherman M. Evidence-Based Diagnosis, Staging, and Treatment of Patients with Hepatocellular Carcinoma. *Gastroenterology* 2016; **150**: 835-853 [PMID: 26795574 DOI: 10.1053/j.gastro.2015.12.041]

2 **Ye JZ**, Chen JZ, Li ZH, Bai T, Chen J, Zhu SL, Li LQ, Wu FX. Efficacy of postoperative adjuvant transcatheter arterial chemoembolization in hepatocellular carcinoma patients with microvascular invasion. *World J Gastroenterol* 2017; **23**: 7415-7424 [PMID: 29151695 DOI: 10.3748/wjg.v23.i41.7415]

3 **Feng LH**, Dong H, Lau WY, Yu H, Zhu YY, Zhao Y, Lin YX, Chen J, Wu MC, Cong WM. Novel microvascular invasion-based prognostic nomograms to predict survival outcomes in patients after R0 resection for hepatocellular carcinoma. *J Cancer Res Clin Oncol* 2017; **143**: 293-303 [PMID: 27743138 DOI: 10.1007/s00432-016-2286-1]

4 **Chan SL**, Wong VW, Qin S, Chan HL. Infection and Cancer: The Case of Hepatitis B. *J Clin Oncol* 2016; **34**: 83-90 [PMID: 26578611 DOI: 10.1200/JCO.2015.61.5724]

5 **Fidler IJ**. The pathogenesis of cancer metastasis: the 'seed and soil' hypothesis revisited. *Nat Rev Cancer* 2003; **3**: 453-458 [PMID: 12778135 DOI: 10.1038/nrc1098]

6 **Nystedt S**, Emilsson K, Wahlestedt C, Sundelin J. Molecular cloning of a potential proteinase activated receptor. *Proc Natl Acad Sci USA* 1994; **91**: 9208-9212 [PMID: 7937743 DOI: 10.1073/pnas.91.20.9208]

7 **Ossovskaya VS**, Bunnett NW. Protease-activated receptors: contribution to physiology and disease. *Physiol Rev* 2004; **84**: 579-621 [PMID: 15044683 DOI: 10.1152/physrev.00028.2003]

8 **Grab DJ**, Garcia-Garcia JC, Nikolskaia OV, Kim YV, Brown A, Pardo CA, Zhang Y, Becker KG, Wilson BA, de A Lima AP, Scharfstein J, Dumler JS. Protease activated receptor signaling is required for African trypanosome traversal of human brain microvascular endothelial cells. *PLoS Negl Trop Dis* 2009; **3**: e479 [PMID: 19621073 DOI: 10.1371/journal.pntd.0000479]

9 **Lin H**, Trejo J. Transactivation of the PAR1-PAR2 heterodimer by thrombin elicits β-arrestin-mediated endosomal signaling. *J Biol Chem* 2013; **288**: 11203-11215 [PMID: 23476015 DOI: 10.1074/jbc.M112.439950]

10 **Weithauser A**, Rauch U. Role of protease-activated receptors for the innate immune response of the heart. *Trends Cardiovasc Med* 2014; **24**: 249-255 [PMID: 25066486 DOI: 10.1016/j.tcm.2014.06.004]

11 **Weithauser A**, Bobbert P, Antoniak S, Böhm A, Rauch BH, Klingel K, Savvatis K, Kroemer HK, Tschope C, Stroux A, Zeichhardt H, Poller W, Mackman N, Schultheiss HP, Rauch U. Protease-activated receptor-2 regulates the innate immune response to viral infection in a coxsackievirus B3-induced myocarditis. *J Am Coll Cardiol* 2013; **62**: 1737-1745 [PMID: 23871888 DOI: 10.1016/j.jacc.2013.05.076]

12 **Kanemaru A**, Yamamoto K, Kawaguchi M, Fukushima T, Lin CY, Johnson MD, Camerer E, Kataoka H. Deregulated matriptase activity in oral squamous cell carcinoma promotes the infiltration of cancer-associated fibroblasts by paracrine activation of protease-activated receptor 2. *Int J Cancer* 2017; **140**: 130-141 [PMID: 27615543 DOI: 10.1002/ijc.30426]

13 **Quanjun D**, Qingyu Z, Qiliang Z, Liqun X, Jinmei C, Ziquan L, Shike H. Effect and mechanism of PAR-2 on the proliferation of esophageal cancer cells. *Eur Rev Med Pharmacol Sci* 2016; **20**: 4688-4696 [PMID: 27906434]

14 **Zeeh F**, Witte D, Gädeken T, Rauch BH, Grage-Griebenow E, Leinung N, Fromm SJ, Stölting S, Mihara K, Kaufmann R, Settmacher U, Lehnert H, Hollenberg MD, Ungefroren H. Proteinase-activated receptor 2 promotes TGF-β-dependent cell motility in pancreatic cancer cells by sustaining expression of the TGF-β type I receptor ALK5. *Oncotarget* 2016; **7**: 41095-41109 [PMID: 27248167 DOI: 10.18632/oncotarget.9600]

15 **Schaffner F**, Versteeg HH, Schillert A, Yokota N, Petersen LC, Mueller BM, Ruf W. Cooperation of tissue factor cytoplasmic domain and PAR2 signaling in breast cancer development. *Blood* 2010; **116**: 6106-6113 [PMID: 20861457 DOI: 10.1182/blood-2010-06-289314]

16 **Kaufmann R**, Oettel C, Horn A, Halbhuber KJ, Eitner A, Krieg R, Katenkamp K, Henklein P, Westermann M, Böhmer FD, Ramachandran R, Saifeddine M, Hollenberg MD, Settmacher U. Met receptor tyrosine kinase transactivation is involved in proteinase-activated receptor-2-mediated hepatocellular carcinoma cell invasion. *Carcinogenesis* 2009; **30**: 1487-1496 [PMID: 19546160 DOI: 10.1093/carcin/bgp153]

17 **Kaufmann R**, Mussbach F, Henklein P, Settmacher U. Proteinase-activated receptor 2-mediated calcium signaling in hepatocellular carcinoma cells. *J Cancer Res Clin Oncol* 2011; **137**: 965-973 [PMID: 21125404 DOI: 10.1007/s00432-010-0961-1]

18 **Lee TK**, Cheung VC, Lu P, Lau EY, Ma S, Tang KH, Tong M, Lo J, Ng IO. Blockade of CD47-mediated cathepsin S/protease-activated receptor 2 signaling provides a therapeutic target for hepatocellular carcinoma. *Hepatology* 2014; **60**: 179-191 [PMID: 24523067 DOI: 10.1002/hep.27070]

19 **Mußbach F**, Ungefroren H, Günther B, Katenkamp K, Henklein P, Westermann M, Settmacher U, Lenk L, Sebens S, Müller JP, Böhmer FD, Kaufmann R. Proteinase-activated receptor 2 (PAR2) in hepatic stellate cells - evidence for a role in hepatocellular carcinoma growth in vivo. *Mol Cancer* 2016; **15**: 54 [PMID: 27473374 DOI: 10.1186/s12943-016-0538-y]

20 **Chen KD**, Wang CC, Tsai MC, Wu CH, Yang HJ, Chen LY, Nakano T, Goto S, Huang KT, Hu TH, Chen CL, Lin CC. Interconnections between autophagy and the coagulation cascade in hepatocellular carcinoma. *Cell Death Dis* 2014; **5**: e1244 [PMID: 24853422 DOI: 10.1038/cddis.2014.212]

21 **Nieto MA**, Huang RY, Jackson RA, Thiery JP. EMT: 2016. *Cell* 2016; **166**: 21-45 [PMID: 27368099 DOI: 10.1016/j.cell.2016.06.028]

22 **Lamouille S**, Xu J, Derynck R. Molecular mechanisms of epithelial-mesenchymal transition. *Nat Rev Mol Cell Biol* 2014; **15**: 178-196 [PMID: 24556840 DOI: 10.1038/nrm3758]

23 **De Craene B**, Berx G. Regulatory networks defining EMT during cancer initiation and progression. *Nat Rev Cancer* 2013; **13**: 97-110 [PMID: 23344542 DOI: 10.1038/nrc3447]

24 **Chua KN**, Poon KL, Lim J, Sim WJ, Huang RY, Thiery JP. Target cell movement in tumor and cardiovascular diseases based on the epithelial-mesenchymal transition concept. *Adv Drug Deliv Rev* 2011; **63**: 558-567 [PMID: 21335038 DOI: 10.1016/j.addr.2011.02.003]

25 **Pinheiro C**, Longatto-Filho A, Scapulatempo C, Ferreira L, Martins S, Pellerin L, Rodrigues M, Alves VA, Schmitt F, Baltazar F. Increased expression of monocarboxylate transporters 1, 2, and 4 in colorectal carcinomas. *Virchows Arch* 2008; **452**: 139-146 [PMID: 18188595 DOI: 10.1007/s00428-007-0558-5]

26 **Kudo M**. Early detection and curative treatment of early-stage hepatocellular carcinoma. *Clin Gastroenterol Hepatol* 2005; **3**: S144-S148 [PMID: 16234064 DOI: 10.1016/S1542-3565(05)00712-3]

27 **Grotegut S**, von Schweinitz D, Christofori G, Lehembre F. Hepatocyte growth factor induces cell scattering through

MAPK/Egr-1-mediated upregulation of Snail. *EMBO J* 2006; **25**: 3534-3545 [PMID: 16858414 DOI: 10.1038/sj.emboj.7601213]

28 **Waerner T**, Alacakaptan M, Tamir I, Oberauer R, Gal A, Brabletz T, Schreiber M, Jechlinger M, Beug H. ILEI: a cytokine essential for EMT, tumor formation, and late events in metastasis in epithelial cells. *Cancer Cell* 2006; **10**: 227-239 [PMID: 16959614 DOI: 10.1016/j.ccr.2006.07.020]

29 **Cai L**, Ye Y, Jiang Q, Chen Y, Lyu X, Li J, Wang S, Liu T, Cai H, Yao K, Li JL, Li X. Epstein-Barr virus-encoded microRNA BART1 induces tumour metastasis by regulating PTEN-dependent pathways in nasopharyngeal carcinoma. *Nat Commun* 2015; **6**: 7353 [PMID: 26135619 DOI: 10.1038/ncomms8353]

30 **Weiler SME**, Pinna F, Wolf T, Lutz T, Geldiyev A, Sticht C, Knaub M, Thomann S, Bissinger M, Wan S, Rössler S, Becker D, Gretz N, Lang H, Bergmann F, Ustiyan V, Kalin TV, Singer S, Lee JS, Marquardt JU, Schirmacher P, Kalinichenko VV, Breuhahn K. Induction of Chromosome Instability by Activation of Yes-Associated Protein and Forkhead Box M1 in Liver Cancer. *Gastroenterology* 2017; **152**: 2037-2051.e22 [PMID: 28249813 DOI: 10.1053/j.gastro.2017.02.018]

31 **Nakagawa H**, Mizukoshi E, Kobayashi E, Tamai T, Hamana H, Ozawa T, Kishi H, Kitahara M, Yamashita T, Arai K, Terashima T, Iida N, Fushimi K, Muraguchi A, Kaneko S. Association Between High-Avidity T-Cell Receptors, Induced by α-Fetoprotein-Derived Peptides, and Anti-Tumor Effects in Patients With Hepatocellular Carcinoma. *Gastroenterology* 2017; **152**: 1395-1406.e10 [PMID: 28188748 DOI: 10.1053/j.gastro.2017.02.001]

32 **Schneider AT**, Gautheron J, Feoktistova M, Roderburg C, Loosen SH, Roy S, Benz F, Schemmer P, Büchler MW, Nachbur U, Neumann UP, Tolba R, Luedde M, Zucman-Rossi J, Panayotova-Dimitrova D, Leverkus M, Preisinger C, Tacke F, Trautwein C, Longerich T, Vucur M, Luedde T. RIPK1 Suppresses a TRAF2-Dependent Pathway to Liver Cancer. *Cancer Cell* 2017; **31**: 94-109 [PMID: 28017612 DOI: 10.1016/j.ccell.2016.11.009]

33 **Fortin J**, Mak TW. Targeting PI3K Signaling in Cancer: A Cautionary Tale of Two AKTs. *Cancer Cell* 2016; **29**: 429-431 [PMID: 27070694 DOI: 10.1016/j.ccell.2016.03.020]

34 **Cattaruzza F**, Amadesi S, Carlsson JF, Murphy JE, Lyo V, Kirkwood K, Cottrell GS, Bogyo M, Knecht W, Bunnett NW. Serine proteases and protease-activated receptor 2 mediate the proinflammatory and algesic actions of diverse stimulants. *Br J Pharmacol* 2014; **171**: 3814-3826 [PMID: 24749982 DOI: 10.1111/bph.12738]

35 **Gui Y**, Khan MGM, Bobbala D, Dubois C, Ramanathan S, Saucier C, Ilangumaran S. Attenuation of MET-mediated migration and invasion in hepatocellular carcinoma cells by SOCS1. *World J Gastroenterol* 2017; **23**: 6639-6649 [PMID: 29085209 DOI: 10.3748/wjg.v23.i36.6639]

P- Reviewer: Midorikawa Y, Vij M, Ilangumaran S, Sakaguchi T
S- Editor: Gong ZM **L- Editor**: Wang TQ **E- Editor**: Ma YJ

World Journal of Gastroenterology

Submit a Manuscript: http://www.f6publishing.com

World J Gastroenterol 2018 March 14; 24(10): 1134-1143

DOI: 10.3748/wjg.v24.i10.1134

ISSN 1007-9327 (print) ISSN 2219-2840 (online)

ORIGINAL ARTICLE

Retrospective Cohort Study

Budd-Chiari syndrome in China: A 30-year retrospective study on survival from a single center

Wei Zhang, Qiao-Zheng Wang, Xiao-Wei Chen, Hong-Shan Zhong, Xi-Tong Zhang, Xu-Dong Chen, Ke Xu

Wei Zhang, Xu-Dong Chen, Department of Interventional Radiology, Shenzhen People's Hospital, the Second Affiliated Hospital of Jinan University, Shenzhen 518020, Guangdong Province, China

Wei Zhang, Qiao-Zheng Wang, Xiao-Wei Chen, Hong-Shan Zhong, Xi-Tong Zhang, Ke Xu, Department of Radiology, The First Affiliated Hospital of China Medical University, Shenyang 110001, Liaoning Province, China

Wei Zhang, Xiao-Wei Chen, Hong-Shan Zhong, Ke Xu, Key Laboratory of Diagnostic Imaging and Interventional Radiology of Liaoning Province, The First Affiliated Hospital of China Medical University, Shenyang 110001, Liaoning Province, China

ORCID number: Wei Zhang (0000-0003-2179-6821); Qiao-Zheng Wang (0000-0003-3512-3118); Xiao-Wei Chen (0000-0002-7839-7584); Hong-Shan Zhong (0000-0002-6150-6115); Xi-Tong Zhang (0000-0003-2519-9047); Xu-Dong Chen (0000-0002-3789-0495); Ke Xu (0000-0001-7587-822X).

Author contributions: Zhang W, Xu K and Chen XD designed the research; Xu K, Zhang XD and Zhong HS performed the research; Zhang W, Wang QZ and Chen XW analyzed the data; Zhang W wrote the paper; Wang QZ, Chen XW, Zhong HS, Zhang XT, Chen XD and Xu K critically revised the manuscript for important intellectual content.

Institutional review board statement: This study was reviewed and approved by the Research Ethics Committee of Faculty of Medicine, The First Affiliated Hospital of China Medical University Institutional Review Board.

Informed consent statement: All study participants provided written informed consent for personal and medical data collection prior to study enrollment and each patient agreed to management *via* written consent.

Conflict-of-interest statement: The authors declare that there are no conflicts of interest regarding the publication of this paper.

Data sharing statement: The technical appendix, statistical code, and dataset are available from the corresponding author at kexu@vip.sina.com. The participants gave informed consent for the data sharing.

STROBE statement: The authors have read the STROBE Statement-checklist of items, and the manuscript was prepared and revised according to the STROBE Statement-checklist of items.

Manuscript source: Unsolicited manuscript

Correspondence to: Ke Xu, MD, PhD, Professor, Department of Radiology and Key Laboratory of Diagnostic Imaging and Interventional Radiology of Liaoning Province, the First Affiliated Hospital of China Medical University, 155 Nanjing Bei Street, Shenyang 110001, Liaoning Province, China. kexu@vip.sina.com
Telephone: +86-24-83282730
Fax: +86-24-83282629

Received: December 8, 2017
Peer-review started: December 8, 2017
First decision: December 20, 2017
Revised: January 2, 2018
Accepted: January 24, 2018
Article in press: January 24, 2018
Published online: March 14, 2018

Abstract

AIM

To investigate 30-year treatment outcomes associated with Budd-Chiari syndrome (BCS) at a tertiary hospital in China.

METHODS
A total of 256 patients diagnosed with primary BCS at our tertiary hospital between November 1983 and September 2013 were followed and retrospectively studied. Cumulative survival rates and cumulative mortality rates of major causes were calculated by Kaplan-Meier analysis, and the independent predictors of survival were identified using a Cox regression model.

RESULTS
Thirty-four patients were untreated; however, 222 patients were treated by medicine, surgery, or interventional radiology. Forty-four patients were lost to follow-up; however, 212 patients were followed, 67 of whom died. The symptom remission rates of treated and untreated patients were 81.1% (107/132) and 46.2% (6/13), respectively (P = 0.009). The cumulative 1-, 5-, 10-, 20-, and 30-year survival rates of the treated patients were 93.5%, 81.6%, 75.2%, 64.7%, and 58.2%, respectively; however, the 1-, 5-, 10-, 20-, and 30-year survival rates of the untreated patients were 70.8%, 70.8%, 53.1%, 0%, and unavailable, respectively (P = 0.007). Independent predictors of survival for treated patients were gastroesophageal variceal bleeding (HR = 3.043, 95%CI: 1.363-6.791, P = 0.007) and restenosis (HR = 4.610, 95%CI: 1.916-11.091, P = 0.001). The cumulative 1-, 5-, 10-, 20-, and 30-year mortality rates for hepatocellular carcinoma were 0%, 2.6%, 3.5%, 8%, and 17.4%, respectively.

CONCLUSION
Long-term survival is satisfactory for treated Chinese patients with BCS. Hepatocellular carcinoma is a chronic complication and should be monitored with long-term follow-up.

Key words: Budd-Chiari syndrome; Chinese; Survival; Interventional radiology

Core tip: This is the first study to evaluate interventional treatment outcomes of Chinese Budd-Chiari syndrome (BCS) patients with more than 20-year follow-up, and the cumulative 20-year survival rate was 69.5% for patients treated by interventional radiological procedures. The cumulative 1-, 5-, 10-, and 20-year survival rates for untreated BCS patients were 70.8%, 70.8%, 53.1%, and 0%, respectively. Restenosis and gastroesophageal variceal bleeding were critical factors for predicting long-term survival. Long-term follow-up to monitor the chronic complications of BCS should not be less than 10 years, and deaths greatly increase after 10-year follow-up, especially those of patients who died from hepatocellular carcinoma.

Zhang W, Wang QZ, Chen XW, Zhong HS, Zhang XT, Chen XD, Xu K. Budd-Chiari syndrome in China: A 30-year retrospective study on survival from a single center. *World J Gastroenterol* 2018; 24(10): 1134-1143 Available from: URL: http://www.wjgnet.com/1007-9327/full/v24/i10/1134.htm DOI: http://dx.doi.org/10.3748/wjg.v24.i10.1134

INTRODUCTION

Budd-Chiari syndrome (BCS) is a rare disease defined as hepatic venous outflow tract obstruction at any level from small hepatic veins (HVs) to the junction of the inferior vena cava (IVC) and right atrium in the absence of right heart failure or constrictive pericarditis[1]. An obstruction that originates from endoluminal lesions (*i.e.*, thrombosis, webs, and endophlebitis) is considered primary BCS[2]. Western and Asian patients exhibit different characteristics regarding the nature and level of obstructive lesions; therefore, clinical presentations and treatment strategies are also different in these groups[3]. In Western countries, where hepatic thrombosis is the major obstructive lesion of BCS, a step-wise therapeutic strategy aimed at minimizing invasiveness has been advocated and proven to be effective[4,5]. The most widely used treatment modalities are anticoagulation and trans-jugular intra-hepatic porto-systemic shunt (TIPS)[5,6]. However, for Asian patients, especially Chinese patients, the predominant obstructive lesions are membranous and segmental obstructions of the supra-hepatic or retro-hepatic portion of the IVC, and the most used treatment modalities are interventional re-canalization and surgery[7-11].

Till the year 2014, more than 20000 cases of BCS have been published in China[12], since the first Chinese case was reported in 1957[13]. According to a recent literature survey study, interventional radiological procedures (mainly percutaneous re-canalization) have become the most common treatment option[14], and their outcomes are good or excellent[10,15,16]. However, outcomes from more than 10-year follow-up are scarcely reported[10,15-20]. Ten years may not be long enough for long-term outcome observations in Chinese patients with BCS characterized by insidious onset and chronic development[21,22]. The aim of this study was to retrospectively analyze the 30-year follow-up outcomes of BCS patients at our center and to evaluate their long-term survival and its related predictors.

MATERIALS AND METHODS

Study design and case selection

This retrospective case series study was approved by the ethics committee of our hospital. All patients were informed about the benefits and related risks before treatment, and they provided written informed consent. Medical records of 410 patients treated between November 1983 and September 2013 with an admission diagnosis of BCS were identified in

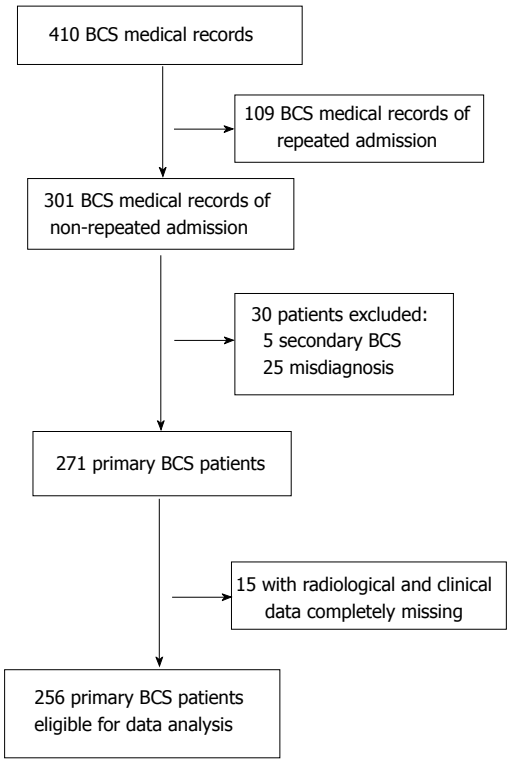

Figure 1 Flow chart of case selection. BCS: Budd-Chiari syndrome.

our hospitalization register system. There were 172 records from 63 patients that represented repeated hospitalizations; only the primary hospitalization medical records were enrolled. Thirty records were excluded, including 5 for secondary BCS and 25 for misdiagnoses of BCS. For the remaining 271 primary BCS records, 15 were not qualified for statistical analysis due to missing laboratory and imaging investigation data. Finally, 256 patients were eligible for our study. A flow chart of case selection is shown in Figure 1.

Diagnosis and classification

BCS was diagnosed by color Doppler ultrasonography, computed tomography, magnetic resonance imaging, and/or venography of HVs and the IVC. BCS patients were classified into three groups according to the obstruction site of the hepatic venous outflow tract: (1) IVC type, manifesting as obstruction of the IVC with at least one patent HV; (2) HV type, manifesting as obstruction of the three main HVs; and (3) combined type, manifesting as obstruction of both the IVC and three main HVs[10]. Patients were considered symptomatic when they had any one of the following manifestations: abdominal pain, abdominal distention, ascites, esophageal and gastric varicose bleeding, encephalopathy, or lower-extremity edema.

Treatment

In this case series, 34 patients were untreated (did not receive any regular treatments) due to technical contraindications (n = 9), poverty (n = 10), or relatively mild symptoms (n = 15), and 222 patients received treatment. Treatment modalities used for BCS patients included medical treatments, surgical operations, and interventional radiological procedures. Medical treatments included anticoagulation, diuretics, paracentesis and reinfusion of ascites, and albumin infusion. Surgical operations included cavoatrial shunting, radical resection, meso-cavo-atrial shunting, splenopneumopexy, and splenocaval shunting and were performed as described in a previous study[23]. Interventional radiological procedures included percutaneous intravascular catheter-directed thrombolysis, percutaneous transluminal angioplasty (PTA) with or without stent implantation, and TIPS, and the techniques were described in our previous studies[10,24]. Technical success of the interventional radiological procedures (mostly percutaneous recanalization) was defined as the recanalization of hepatic venous outflow tract obstruction as demonstrated by venography[10].

Data collection and follow-up

Baseline data were extracted from the medical records before treatment, including demographic data, clinical presentations, laboratory test results, and imaging data. Patients were followed until death, the end of this study (December 31, 2014), or the last outpatient visit date if the patient was lost to follow-up. Symptom remission was defined as complete remission or substantial partial remission of the main symptoms that the patients complained about most urgently. Patients were examined by color Doppler ultrasonography, computed tomography, or magnetic resonance imaging at their local hospitals for restenosis evaluation, and the results were confirmed by venography at our hospital. Follow-up data were obtained from medical records or by telephone interview of the patients themselves or their family members.

Statistical analysis

Categorical variables are expressed as absolute numbers (or frequencies, if indicated) and were compared using the chi-square or Fisher's exact test. Continuous variables are summarized as medians and ranges and were compared by using the independent sample t-test or one-way analysis of variance. Cumulative survival rates and cumulative mortalities associated with major causes were analyzed using Kaplan-Meier curves and compared by the log-rank test. The Cox regression model was employed for the analysis of factors related to survival. Variables reaching statistical significance ($P < 0.05$) in the univariate analysis were incorporated into a multivariate analysis as covariates. Two-tailed P-values less than 0.05 were considered statistically significant. All statistical calculations were performed using SPSS 21.0 package (SPSS Inc, Chicago, IL, United States).

RESULTS

Characteristics of patients

Two hundred and fifty-six patients with confirmed diagnoses of primary BCS were analyzed, including 153 males and 103 females with a median age of 41 (range,

Table 1 Baseline characteristics of the 256 patients

	Medicine	Surgery	Intervention	Untreated
Total number	30	14	178	34
Demographic data				
Sex				
Male	16	4	109	24
Female	14	10	69	10
Age (yr)[1]	36 (7-74)	35 (24-47)	41 (14-80)	44.5 (14-66)
Duration of symptoms				
≤ 1 mo	5	0	28	7
1-6 mo	7	2	35	12
≥ 6 mo	18	12	115	15
Clinical manifestations				
Abdominal distention	24	12	82	15
Abdominal wall varicosis	12	13	105	16
Lower-extremity edema	17	13	104	17
Gastroesophageal variceal bleeding	8	3	26	4
Hepatic encephalopathy	0	0	0	2
Laboratory tests[1,2]				
Hemoglobin level (g/L)	133 (64-172)	149 (101-176)	130.5 (30-180)	134 (80-180)
Platelet count (× 10^9/L)	130 (49-479)	92 (47-160)	108.5 (33-603)	139.5 (50-341)
Alanine transaminase level (× ULN)	0.6 (0.2-7.6)	0.6 (0.3-1.6)	0.6 (0.2-28)	0.7 (0.3-3.6)
Albumin level (g/L)	34.5 (13.1-54)	36 (22-41)	37.4 (16.7-57.7)	35 (16-58)
Total bilirubin level (μmol/L)	26.2 (6-146.2)	28.6 (17.1-68.4)	26 (7-292)	24.9 (6.1-168)
International normalized ratio	1.4 (0.9-1.9)	1.3 (1.1-1.7)	1.3 (0.9-2.9)	1.3 (0.9-1.8)
Creatinine level (μmol/L)	106.3 (85-341)	74 (71-77)	74.1 (30-254)	75 (29.6-146)
Blood urea nitrogen level (mmol/L)	5.3 (1.8-26.6)	5.1 (2.5-18.6)	5.3 (2.5-39.1)	5.6 (3.6-11.8)
Imaging features				
Type of obstruction				
HV	9	0	25	10
IVC	3	2	41	9
Com	18	12	112	15
Pattern of IVC obstruction				
No obstruction	7	0	25	10
Membranous	14	8	108	15
Segmental	8	4	36	4
Long segmental	1	2	9	5
Ascites	17	9	85	14
AHV compensation	1	3	34	4
IVC thrombosis	11	5	57	14
Portal vein thrombosis	1	0	3	3
Prognostic index				
Child-Pugh score[1,2]	7 (5-9)	6 (5-7)	7 (5-12)	6 (5-11)
Child-Pugh class[2]				
A	3	1	59	6
B	6	1	61	4
C	0	0	6	1

[1]Data are shown as median with range in parentheses; [2]Data are incomplete because some laboratory tests were not performed prior to the year 2000. Except where indicated, data are shown as number of patients. ULN: Upper limit of normal; HV: Hepatic vein; IVC: Inferior vena cava; Com: Combination; AHV: Accessory hepatic vein.

7-80) years. The baseline characteristics of the 256 patients are shown in Table 1 according to treatment modality. Furthermore, the patients were divided into two groups according to whether they received treatment or not, and their baseline characteristics were compared. The treated and untreated groups had statistically significant differences in the presentation of hepatic encephalopathy (P = 0.017), the pattern of IVC obstruction (P = 0.016), and portal vein thrombosis (P = 0.047).

Treatment

Except for 34 untreated patients, 222 patients received treatment, including 30 treated by medicine, 14 by surgery, and 178 by interventional radiology. Detailed information is presented in Table 2 for the 14 patients treated by surgical operations and the 178 patients treated by interventional procedures. For the patients treated by interventional radiology, the procedures were successful in 172 (96.6%) patients and failed in 6 patients due to diffuse HV obstruction (n = 4) and long segments (more than 5 cm) of IVC obstruction (n = 2). For the patients who experienced procedure-related complications, one died of disseminated intravascular coagulation 6 h after PTA, one died of severe hemoptysis of bronchiectasis 72 h after thrombolysis, one had stent fracture and was treated by implantation of an additional stent, and the other patients were

Table 2 Detailed information on surgical operations and interventional procedures

Department	Operations/procedures	No.	Complications
Surgery	Cavoatrial shunt	10	Hemorrhagic shock (n = 1)
	Radical resection	1	
	Meso-cavo-atrial shunt	1	Acute hepatic failure (n = 1)
	Splenopneumopexy	1	
	Splenocaval shunt	1	
Interventional radiology	Technic failure	6	
	PTA	96	Abdominal pain (n = 4), DIC (n = 1)
	PTA combined with stent	69	Abdominal pain (n = 2), Stent fracture (n = 1), Supraventricular tachycardia (n = 2)
	TIPS	7	
	Catheter directed thrombolysis	19[1]	Hematuria (n = 2), Hemoptysis (n = 1)

[1]The total number of patients treated by interventional procedures was 178, and the 19 patients treated by catheter directed thrombolysis were repeatedly counted among the patients treated by PTA (n = 5) and PTA combined with stent implantation (n = 14). PTA: Percutaneous transluminal angioplasty; TIPS: Transjugular intrahepatic portosystemic shunt; DIC: Disseminated intravascular coagulation.

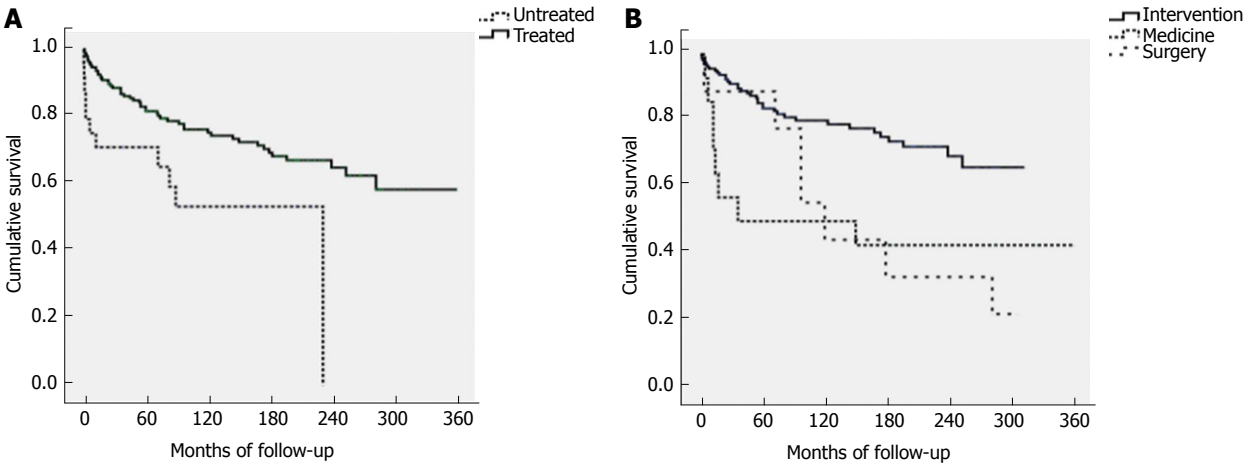

Figure 2 Survival rates of Budd-Chiari syndrome patients. A: Comparison of cumulative survival rates of Budd-Chiari syndrome (BCS) between the 188 treated patients and 24 untreated patients. Treated patients had significantly better long-term survival than untreated patients (P = 0.007); B: Comparison of cumulative survival rates of BCS among different treatment modalities. Patients treated by interventional radiology had significantly better long-term survival than patients treated by medicine or surgery (P = 0.002).

given symptomatic treatment.

Follow-up

Forty-four patients were lost to follow-up, and 212 patients were followed with a median period of 89 (0.2-360) mo; 67 of the followed patients died, with a median follow-up period of 28 (0.2-289) mo. The deaths of five patients who suffered from intracranial hemorrhage induced by hypertension (n = 1), cholangiocarcinoma (n = 1), disseminated intravascular coagulation (n = 1), accidental death (n = 1), and hemoptysis (n = 1) were not considered to be related to BCS. Detailed follow-up information is shown in Table 3. Regarding the remission of symptoms, symptoms were relieved in 107 out of 132 living patients in the treated group, and the overall remission rate was 81.1%; for the untreated group, 6 out of the 13 living patients were relieved of symptoms, and the remission rate was 46.2%. The difference between these two groups was statistically significant (P = 0.009). Furthermore, the comparison of loss rates between these two groups was not significantly different (P = 0.052). It was notable that the loss rate of the untreated group was 29.4% (10/34), which was higher than 20%.

Survival

The cumulative 1-, 5-, 10-, 20-, and 30-year survival rates of the 188 treated patients were 93.5%, 81.6%, 75.2%, 64.7%, and 58.2%, respectively; for the 24 untreated patients, the 1-, 5-, 10-, 20-, and 30-year survival rates were 70.8%, 70.8%, 53.1%, 0%, and unavailable, respectively. The difference in cumulative survival rates between these two groups was statistically significant (P = 0.007) (Figure 2A). Regarding the different treatment modalities, the cumulative 1-, 5-, 10-, 20-, and 30-year survival rates of patients treated by interventional radiology were 95.7%, 85.3%, 80.2%, 69.5%, and unavailable, respectively; the 1-, 5-, 10-, 20-, and 30-year rates of patients treated by medicine were 85.7%, 50%, 50%, 50%, and 50%, respectively; and the 1-, 5-, 10-, 20-, and 30-year rates of patients treated by surgery were 88.9%, 88.9%, 44.4%, 33.3%, and unavailable, respectively. The difference in cumulative survival rates among these three treatment

Table 3 Follow-up results of 256 Budd-Chiari syndrome patients

Treatment	Total	Lost	Death	Remission	Non-remission/progression
Medicine	30	16	Variceal bleeding (n = 4), liver or multiple organ failure (n = 3), and hepatocellular carcinoma (n = 1)	3	Abdominal distention (n = 3)
Surgery	14	5	Liver or multiple organ failure (n = 3), hepatocellular carcinoma (n = 1), variceal bleeding (n = 1), anastomotic infection (n = 1), and hepatic encephalopathy (n = 1)	1	Abdominal distention (n = 1)
Interventional radiology					
Technic failure	6	0	Liver or multiple organ failure (n = 3)	1	Abdominal distention (n = 1) and lower-extremity edema (n = 1)
PTA	96	6	Liver or multiple organ failure (n = 8), hepatocellular carcinoma (n = 5), variceal bleeding (n = 3), cholangiocarcinoma (n = 1), intracranial hemorrhage induced by hypertension (n = 1), DIC (n = 1), and accidental death (n = 1)	57	Abdominal distention (n = 7), lower-extremity edema (n = 4), and lower-extremity varix (n = 2)
PTA combined with stent placement	69	5	Liver or multiple organ failure (n = 7), hepatocellular carcinoma (n = 3), variceal bleeding (n = 2), hepatic encephalopathy (n = 2), and hemoptysis (n = 1)	44	Abdominal distention (n = 3), lower-extremity edema (n = 1), and muscle wasting (n = 1)
TIPS	7	2	Liver or multiple organ failure (n = 2), and variceal bleeding (n = 1)	1	Jaundice (n = 1)
Untreated	34	10	Liver or multiple organ failure (n = 7), variceal bleeding (n = 1), hepatocellular carcinoma (n = 1), hepatic encephalopathy (n = 1), and chronic leukemia (n = 1)	6	Abdominal distention (n = 4), muscle wasting (n = 2), and lower-extremity edema (n = 1)

PTA: Percutaneous transluminal angioplasty; TIPS: Transjugular intrahepatic portosystemic shunt; DIC: Disseminated intravascular coagulation.

modalities was statistically significant (P = 0.002) (Figure 2B). The factors related to survival, excluding the five deaths unrelated to BCS, were analyzed in the treated patients. In univariate analysis, the predictors of survival included gastroesophageal variceal bleeding, a high level of alanine transaminase, ascites, and restenosis. In multivariate analysis, the independent predictors of survival were gastroesophageal variceal bleeding (HR = 3.043, 95%CI: 1.363-6.791, P = 0.007) and restenosis (HR = 4.610, 95%CI: 1.916-11.091, P = 0.001) (Table 4).

Cumulative mortalities of major causes

For the treated patients, the major causes of death were liver or multiple organ failure (n = 26), gastroesophageal variceal bleeding (n = 11), and hepatocellular carcinoma (HCC) (n = 10), which accounted for more than 80% of the total deaths (83.9%). The median survival time was 37.5 (1-239) mo for patients who died of liver or multiple organ failure, 48 (4-150) mo for patients who died of gastroesophageal variceal bleeding, and 122.5 (14-282) mo for patients who died of HCC. The difference in survival times across these three groups was statistically significant (P = 0.016). The cumulative 1-, 5-, 10-, 20-, and 30-year mortality rates for liver or multiple organ failure were 4.4%, 10.1%, 14.5%, 20.5%, and 20.5%, respectively (Figure 3A); the 1-, 5-, 10-, 20-, and 30-year mortality rates for gastroesophageal variceal bleeding were 0.5%, 5.3%, 7.3%, 8.5%, and 8.5%, respectively (Figure 3B); and the 1-, 5-, 10-, 20-, and 30-year mortality rates for HCC were 0%, 2.6%, 3.5%, 8%, and 17.4%, respectively (Figure 3C).

DISCUSSION

To the best of our knowledge, the present study is the first large case series that evaluated interventional treatment outcomes of Chinese BCS patients with more than 20-year follow-up. We assume that most Chinese BCS patients are characterized by insidious onset and chronic development[22,25,26]; therefore, a relatively long time is needed to observe long-term outcomes. However, the follow-up time span that can be defined as "long-term follow-up" is still debatable. According to our study, we found that deaths greatly increased after 10-year follow-up, especially those of patients who died of HCC. Therefore, we suggest that the long-term follow-up span should not be less than 10 years for Chinese BCS patients.

In the present study, patients were retrospectively divided into a treated group and an untreated group according to whether the patients received treatment or not. Less than half of the patients who did not receive any regular treatments (medicine, surgery, or interventional radiology) had intermittent, spontaneous relief of clinical symptoms, and none survived for more than 20 years. These findings were very interesting because the follow-up results might reflect the natural outcomes of Chinese BCS patients. According to our

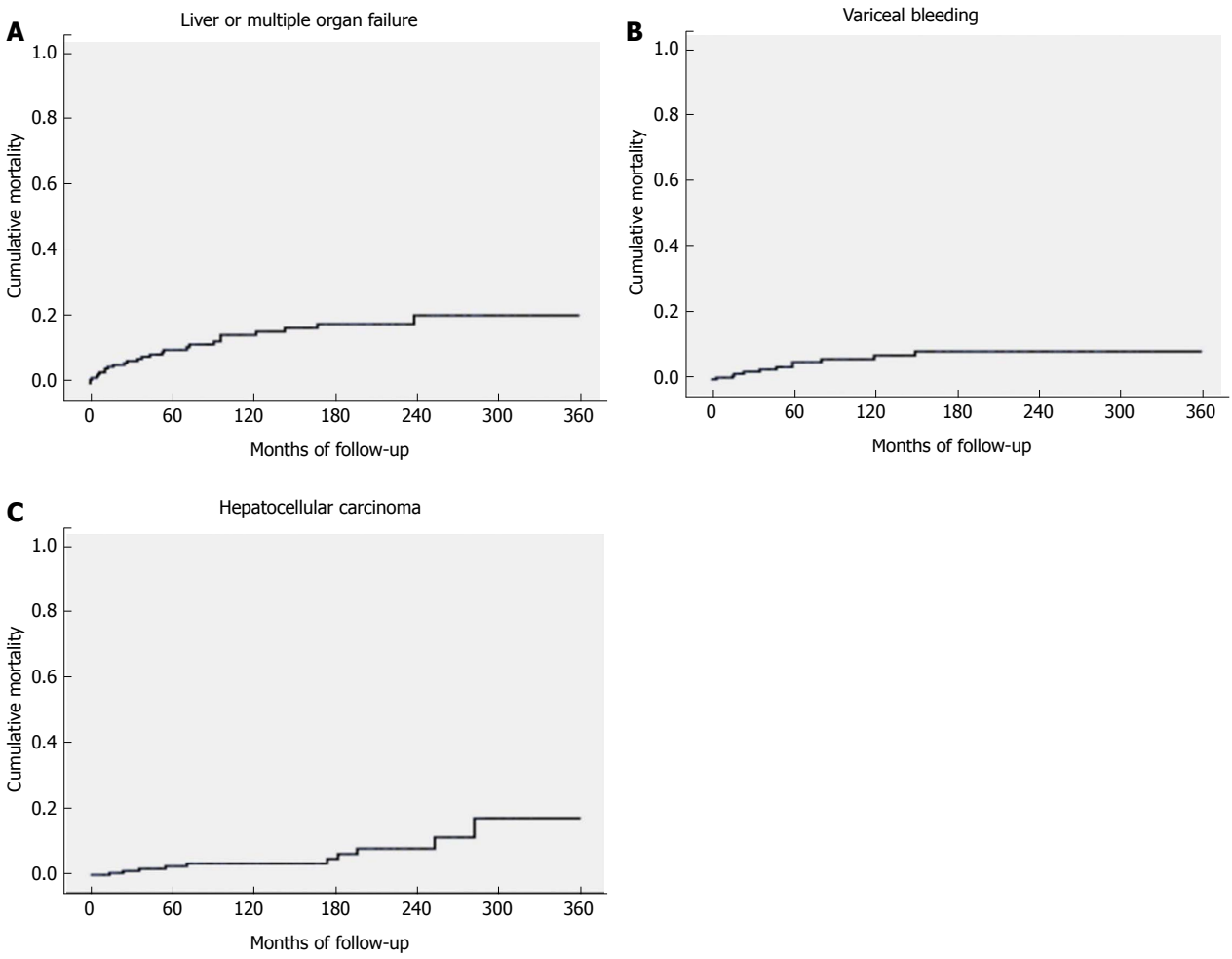

Figure 3 Cumulative mortality rates of Budd-Chiari syndrome. A: Cumulative mortality rates of Budd-Chiari syndrome (BCS) patients who died of liver or multiple organ failure; B: Cumulative mortality rates of BCS patients who died of gastroesophageal variceal bleeding; C: Cumulative mortality rates of BCS patients who died of hepatocellular carcinoma.

results, the natural survival of Chinese BCS patients seemed to be better than that of Western patients, for whom it was estimated that 90% of untreated patients would die within 3 years[2,27]. The follow-up results also suggested that timely intervention was crucial for the survival of BCS patients, even if their symptoms could be spontaneously intermittently relieved. It was noteworthy that the loss rate was higher than 20% for untreated patients; therefore, the findings that reflected the natural outcomes of Chinese BCS patients should be carefully interpreted.

The cumulative survival rates of the treated group were better than those of the untreated group. However, some baseline characteristics between these two groups were different (the presentation of hepatic encephalopathy and portal vein thrombosis was higher in the untreated group than in the treated group, indicating a more serious condition). For the patients treated by interventional radiology, the cumulative 1-, 5-, 10-, and 20-year survival rates were 95.7%, 85.3%, 80.2%, and 69.5%, respectively. The cumulative 1-, 5-, and 10-year survival rates were excellent and comparable to the results recently reported from a systematic review, which found that the median 1-, 5-, and 10-year survival rates were 93%, 83%, and 73% after interventional radiological treatments, respectively[28]. The cumulative 20-year survival rate of patients treated by intervention radiology was significantly better than that of patients treated by medicine or surgery (69.5% *vs* 50% or 33.3%, respectively), which supported wide future use of interventional radiological procedures as a treatment modality. Furthermore, the cumulative 20- and 30-year survival rates of the treated patients were 64.7% and 58.2%, which were satisfying for such a rare disease with chronic history. Of note, the actual survival rates of patients treated by medicine and surgery in our study were influenced by the high ratio of patients lost to follow-up (more than 50%) and should be cautiously interpreted.

According to previous studies, the causes of death of BCS patients mainly included liver failure, gastroesophageal bleeding, HCC, hepatic encephalopathy, and chronic leukemia[5,10,29]. The present study demonstrated that the major cause of death was liver or multiple organ failure, which accounted for 46% (26/56) of the total deaths of treated patients,

Table 4 Univariate and multivariate analyses of the predictors of survival for treated patients

Variable	Univariate analysis			Multivariate analysis		
	HR	95%CI	*P* value	HR	95%CI	*P* value
Sex (Male/Female)	0.558	0.297-1.050	0.071			
Age	0.992	0.968-1. 017	0.550			
History of BCS since first presentation	0.994	0.987-1.000	0.055			
Abdominal distention (Yes/No)	0.943	0.531-1.643	0.813			
Abdominal wall varicosis (Yes/No)	0.819	0.461-1.457	0.497			
Gastroesophageal variceal bleeding (Yes/No)	2.928	1.647-5.270	< 0.001	3.043	1.363-6.791	0.007
Lower-extremity edema (Yes/No)	1.318	0.757-2.294	0.330			
Hemoglobin level	0.994	0.983-1.005	0.311			
Platelet count	1.002	0.998-1.006	0.308			
Alanine transaminase level	1.003	1.001-1.005	0.005	1.002	0.999-1.005	0.274
Albumin level	0.975	0.928-1.024	0.307			
Total bilirubin level	1.007	0.997-1.017	0.183			
INR	1.280	0.367-4.468	0.699			
Creatinine level	1.005	0.991-1.019	0.489			
Blood urea nitrogen level	1.049	0.971-1.133	0.225			
Ascites (Yes/No)	2.108	1.205-3.686	0.009	1.849	0.812-4.213	0.143
Accessory hepatic vein (Yes/No)	2.126	0.842-5.366	0.110			
Associated IVC thrombosis (Yes/No)	1.000	0.553-1.809	0.999			
Restenosis (Yes/No)	5.309	2.378-11.852	< 0.001	4.610	1.916-11.091	0.001
Child-Pugh score	1.108	0.852-1.440	0.444			

HR: Hazard ratio; BCS: Budd-Chiari syndrome; INR: International normalized ratio; IVC: Inferior vena cava.

and this proportion was relatively high compared with results from previous studies[5,6,10]. We explored the possible reasons for this relatively higher occurrence of liver or multiple organ failure by further calculating its cumulative mortality and found that liver or multiple organ failure occurred more frequently within 5 years after primary treatments, which was longer than the 2-year time-frame reported in a previous study[5]. One possible explanation is that for Chinese BCS patients, the chronic development course may allow formation of HV collateral circulation or accessory HV compensation, which might slow down the occurrence of liver failure but simultaneously increases the number of patients who are prone to liver failure.

Another major cause of death that we focused on was HCC. It occurred in 10 of the 188 treated patients, and the median time of survival was 122.5 (14-282) mo, which indicated that it was a chronic complication of BCS. This result agreed with previous studies and demonstrated that HCC was a chronic complication of BCS and mostly occurred over a relatively long time[30-32]. A recent study demonstrated that the cumulative incidence of HCC was 3.5% at 10 years, and the risk factors related to HCC development were liver cirrhosis, combined IVC and HV block, and long-segment IVC block. The authors found that association of these three events with occurrence of HCC would indicate that degree and extent of outflow obstruction, and presence of advanced degree of fibrosis suggesting prolonged hepatic congestion with resultant parenchymal loss were associated with HCC development[33].

In our study, 10 patients experienced HCC and died during 30-year follow-up, and this incidence was higher than that in the above mentioned study (8 out of 413 patients during 20-year follow-up). In addition, we further calculated the cumulative mortality of HCC and found that the cumulative 1-, 5-, 10-, 20-, and 30-year mortality rates were 0%, 2.6%, 3.5%, 8%, and 17.4%, respectively. This result also demonstrated that the incidence and number of patients who died of HCC progressively increased over time, which is consistent with the results of the above mentioned study.

One major limitation of our study was its retrospective nature. Some of the earlier original data (especially before the year 2000) were not recorded or lost. In addition, although a regular follow-up schedule was established and we tried our best to stay in contact with all BCS patients, approximately 17% (44/256) of the total patients were lost to follow-up, and this proportion was even higher (more than 50%) in patients treated by medicine or surgery. One possible explanation is that most of the lost patients were admitted in a relatively early period (before 2002) when follow-up was very difficult, especially for patients in poverty or remote regions. Another limitation was that the baseline data of patients treated by different modalities were inhomogeneous; thus, subgroup analysis was inappropriate.

In conclusion, the long-term survival of Chinese BCS patients was satisfactory for treated patients, especially for patients treated by interventional procedures. Restenosis and gastroesophageal variceal bleeding were critical factors for predicting long-term survival. Long-term follow-up should not be less than 10 years to monitor the chronic complications of HCC.

ARTICLE HIGHLIGHTS

Research background

Budd-Chiari syndrome (BCS) is a rare disease. For Asian patients, especially Chinese patients, the predominant obstructive lesions are membranous and

segmental obstructions of the supra-hepatic or retro-hepatic portion of the inferior vena cava. Till the year 2014, more than 20000 cases of BCS have been published in China, and interventional radiological procedures (mainly percutaneous re-canalization) have become the most common treatment option. However, outcomes from more than 10-year follow-up are scarcely reported for Chinese BCS patients.

Research motivation

As Chinese BCS patients are characterized by insidious onset and chronic development, ten years may not be long enough for long-term outcome observations. We want to find the 20-year and 30-year survival rates at our single center, which may represent the Chinese BCS population to a certain extent. Furthermore, for the chronic complications, such as hepatocellular carcinoma, the incidence and mortality of Chinese BCS patients are still unknown, and we are very interested in these issues.

Research objectives

The objectives were to analyze a 30-year follow-up outcome Chinese BCS patients in a single Chinese center, specifically, to find the 20-year and 30-year cumulative survival rates for the different treatment modalities applied in our center; to find the factors related to long-term survival; and to calculate the cumulative mortalities of major causes.

Research methods

We retrospectively analyzed a 30-year follow-up outcome of BCS patients at our center. Medical records of 410 patients treated between November 1983 and September 2013 with an admission diagnosis of BCS were identified in our hospitalization register system. Only the primary hospitalization medical records were enrolled. Finally, 256 patients were eligible for our study. In this case series, 34 patients were untreated (did not receive any regular treatments) and 222 patients received treatment, including 30 treated by medicine, 14 by surgery, and 178 by interventional radiology. Patients were followed until the end of this study (December 31, 2014). Symptom remission was defined as complete remission or substantial partial remission of the main symptoms that the patients complained about most urgently. Patients were examined by color Doppler ultrasonography, computed tomography, or magnetic resonance imaging for restenosis evaluation, and the results were confirmed by venography at our hospital. Cumulative survival rates and cumulative mortalities associated with major causes were analyzed. The Cox regression model was employed for the analysis of factors related to survival. Variables reaching statistical significance in the univariate analysis were incorporated into a multivariate analysis as covariates. $P < 0.05$ was considered statistically significant.

Research results

About 212 patients (44 were lost to follow-up) were followed with a median time of 89 (0.2-360) mo; 67 of the followed patients died, with a median follow-up period of 28 (0.2-289) mo. A statistically significant difference was found in cumulative survival rates between these two groups. A statistically significant difference was also found in cumulative survival rates among these three treatment modalities. The independent predictors of survival were gastroesophageal variceal bleeding and restenosis. For the treated patients, the major causes of death were liver or multiple organ failure, gastroesophageal variceal bleeding, and hepatocellular carcinoma (HCC), which accounted for more than 80% of the total deaths.

Research conclusions

The present study is the first large case series that evaluated interventional treatment outcomes of Chinese BCS patients with more than 20-year follow-up, to the best of our knowledge. We suggest that the long-term follow-up span should not be less than 10 years for Chinese BCS patients. Less than half of the patients had intermittent, spontaneous relief of clinical symptoms, and none survived for more than 20 years. Restenosis and gastroesophageal variceal bleeding were critical factors for predicting the long-term survival. To monitor the chronic complications of BCS such as HCC, long-term follow-up should not be less than 10 years.

Research perspectives

In future studies, prospective and multi-center research should be encouraged to overcome the high rate of loss and to do the subgroup analysis.

REFERENCES

1 **European Association for the Study of the Liver**. EASL Clinical Practice Guidelines: Vascular diseases of the liver. *J Hepatol* 2016; **64**: 179-202 [PMID: 26516032 DOI: 10.1016/j.jhep.2015.07.040]

2 **Valla DC**. Primary Budd-Chiari syndrome. *J Hepatol* 2009; **50**: 195-203 [PMID: 19012988 DOI: 10.1016/j.jhep.2008.10.007]

3 **Valla DC**. Hepatic venous outflow tract obstruction etiopathogenesis: Asia versus the West. *J Gastroenterol Hepatol* 2004; **19**: S204-S211 [DOI: 10.1111/j.1440-1746.2004.03642.x]

4 **Plessier A**, Sibert A, Consigny Y, Hakime A, Zappa M, Denninger MH, Condat B, Farges O, Chagneau C, de Ledinghen V, Francoz C, Sauvanet A, Vilgrain V, Belghiti J, Durand F, Valla D. Aiming at minimal invasiveness as a therapeutic strategy for Budd-Chiari syndrome. *Hepatology* 2006; **44**: 1308-1316 [PMID: 17058215 DOI: 10.1002/hep.21354]

5 **Seijo S**, Plessier A, Hoekstra J, Dell'era A, Mandair D, Rifai K, Trebicka J, Morard I, Lasser L, Abraldes JG, Darwish Murad S, Heller J, Hadengue A, Primignani M, Elias E, Janssen HL, Valla DC, Garcia-Pagan JC; European Network for Vascular Disorders of the Liver. Good long-term outcome of Budd-Chiari syndrome with a step-wise management. *Hepatology* 2013; **57**:1962-1968 [PMID: 23389867 DOI: 10.1002/hep.26306]

6 **Darwish Murad S**, Plessier A, Hernandez-Guerra M, Fabris F, Eapen CE, Bahr MJ, Trebicka J, Morard I, Lasser L, Heller J, Hadengue A, Langlet P, Miranda H, Primignani M, Elias E, Leebeek FW, Rosendaal FR, Garcia-Pagan JC, Valla DC, Janssen HL; EN-Vie (European Network for Vascular Disorders of the Liver). Etiology, management, and outcome of the Budd-Chiari syndrome. *Ann Intern Med* 2009; **151**: 167-175 [PMID: 19652186 DOI: 10.7326/0003-4819-151-3-200908040-00004]

7 **Okuda K**, Kage M, Shrestha SM. Proposal of a new nomenclature for Budd-Chiari syndrome: hepatic vein thrombosis versus thrombosis of the inferior vena cava at its hepatic portion. *Hepatology* 1998; **28**: 1191-1198 [PMID: 9794901 DOI: 10.1002/hep.510280505]

8 **Wang ZG**, Zhang FJ, Yi MQ, Qiang LX. Evolution of management for Budd-Chiari syndrome: a team's view from 2564 patients. *ANZ J Surg* 2005; **75**: 55-63 [PMID: 15740519 DOI: 10.1111/j.1445-2197.2005.03135.x]

9 **Dilawari JB**, Bambery P, Chawla Y, Kaur U, Bhusnurmath SR, Malhotra HS, Sood GK, Mitra SK, Khanna SK, Walia BS. Hepatic outflow obstruction (Budd-Chiari syndrome). Experience with 177 patients and a review of the literature. *Medicine* (Baltimore) 1994; **73**: 21-36 [PMID: 8309360]

10 **Han G**, Qi X, Zhang W, He C, Yin Z, Wang J, Xia J, Xu K, Guo W, Niu J, Wu K, Fan D. Percutaneous recanalization for Budd-Chiari syndrome: an 11-year retrospective study on patency and survival in 177 Chinese patients from a single center. *Radiology* 2013; **266**: 657-667 [PMID: 23143028 DOI: 10.1148/radiol.12120856]

11 **Rathod K**, Deshmukh H, Shukla A, Popat B, Pandey A, Gupte A, Gupta DK, Bhatia SJ. Endovascular treatment of Budd-Chiari syndrome: Single center experience. *J Gastroenterol Hepatol* 2017; **32**: 237-243 [PMID: 27218672 DOI: 10.1111/jgh.13456]

12 **Zhang W**, Qi X, Zhang X, Su H, Zhong H, Shi J, Xu K. Budd-Chiari Syndrome in China: A Systematic Analysis of Epidemiological Features Based on the Chinese Literature Survey. *Gastroenterol Res Pract* 2015; **2015**: 738548 [PMID: 26504461 DOI: 10.1155/2015/738548]

13 **Shenyang Branch of Internal Medicine Institute of Chinese Medical Association and Department of Pathology of Shenyang Medical College**. Discussion of clinical pathology: case No. 32. *Zhonghua Nei Ke Za Zhi* 1957; **5**: 166-169

14 **Qi XS**, Ren WR, Fan DM, Han GH. Selection of treatment modalities for Budd-Chiari Syndrome in China: a preliminary

survey of published literature. *World J Gastroenterol* 2014; **20**: 10628-10636 [PMID: 25132785 DOI: 10.3748/wjg.v20.i30.10628]
15 **Tripathi D**, Sunderraj L, Vemala V, Mehrzad H, Zia Z, Mangat K, West R, Chen F, Elias E, Olliff SP. Long-term outcomes following percutaneous hepatic vein recanalization for Budd-Chiari syndrome. *Liver Int* 2017; **37**: 111-120 [PMID: 27254473 DOI: 10.1111/liv.13180]
16 **Zhang QQ**, Xu H, Zu MH, Gu YM, Shen B, Wei N, Xu W, Liu HT, Wang WL, Gao ZK. Strategy and long-term outcomes of endovascular treatment for Budd-Chiari syndrome complicated by inferior vena caval thrombosis. *Eur J Vasc Endovasc Surg* 2014; **47**: 550-557 [PMID: 24560649 DOI: 10.1016/j.ejvs.2014.01.014]
17 **Zhang CQ**, Fu LN, Xu L, Zhang GQ, Jia T, Liu JY, Qin CY, Zhu JR. Long-term effect of stent placement in 115 patients with Budd-Chiari syndrome. *World J Gastroenterol* 2003; **9**: 2587-2591 [PMID: 14606103 DOI: 10.3748/wjg.v9.i11.2587]
18 **Qiao T**, Liu CJ, Liu C, Chen K, Zhang XB, Zu MH. Interventional endovascular treatment for Budd-Chiari syndrome with long-term follow-up. *Swiss Med Wkly* 2005; **135**: 318-326 [PMID: 16034686 DOI: 2005/21/smw-10947]
19 **Meng X**, Lv Y, Zhang B, He C, Guo W, Luo B, Yin Z, Fan D, Han G. Endovascular Management of Budd-Chiari Syndrome with Inferior Vena Cava Thrombosis: A 14-Year Single-Center Retrospective Report of 55 Patients. *J Vasc Interv Radiol* 2016; **27**: 1592-1603 [PMID: 27397618 DOI: 10.1016/j.jvir.2016.04.019]
20 **Ding PX,** Li Z, Zhang SJ, Han XW, Wu Y, Wang ZG, Fu MT. Outcome of the Z-expandable metallic stent for Budd-Chiari syndrome and segmental obstruction of the inferior vena cava. *Eur J Gastroenterol Hepatol* 2016; **28**: 972-979 [PMID: 27172449 DOI: 10.1097/MEG.0000000000000640]
21 **Zhang XM**, Li QL. Etiology, treatment, and classification of Budd-Chiari syndrome. *Chin Med J* (Engl) 2007; **120**: 159-161[PMID: 17335663]
22 **Cheng D**, Xu H, Lu ZJ, Hua R, Qiu H, Du H, Xu X, Zhang J. Clinical features and etiology of Budd-Chiari syndrome in Chinese patients: a single-center study. *J Gastroenterol Hepatol* 2013; **28**: 1061-1067 [PMID: 23425079 DOI: 10.1111/jgh.12140]
23 **Wang ZG**, Jones RS. Budd-Chiari syndrome. *Curr Probl Surg* 1996; **33**: 83-211 [PMID: 8595784 DOI: 10.1016/S0011-3840(96)80001-3]
24 **Xu K**, Feng B, Zhong H, Zhang X, Su H, Li H, Zhao Z, Zhang H. Clinical application of interventional techniques in the treatment of Budd-Chiari syndrome. *Chin Med J* (Engl) 2003; **116**: 609-615 [PMID: 12875733]
25 **Dang X**, Li L, Xu P. Research status of Budd-Chiari syndrome in China. *Int J Clin Exp Med* 2014; **7**: 4646-4652 [PMID: 25663961]
26 **Fan JG**, Wang FS. Difference of Budd-Chiari syndrome between West and China. *Hepatology* 2014; **62**: 657 [PMID: 25476406 DOI: 10.1002/hep.27627]
27 **Tavill AS**, Wood EJ, Kreel L, Jones EA, Gregory M, Sherlock S. The Budd-Chiari syndrome: correlation between hepatic scintigraphy and the clinical, radiological, and pathological findings in nineteen cases of hepatic venous outflow obstruction. *Gastroenterology* 1975; **68**: 509-518 [PMID: 1112452]
28 **Qi X**, Ren W, Wang Y, Guo X, Fan D. Survival and prognostic indicators of Budd-Chiari syndrome: a systematic review of 79 studies. *Expert Rev Gastroenterol Hepatol* 2015; **9**: 865-875 [PMID: 25754880 DOI: 10.1586/17474124.2015.1024224]
29 **Eapen CE**, Velissaris D, Heydtmann M, Gunson B, Olliff S, Elias E. Favourable medium term outcome following hepatic vein recanalisation and/or transjugular intrahepatic portosystemic shunt for Budd Chiari syndrome. *Gut* 2006; **55**: 878-884 [PMID: 16174658 DOI: 10.1136/gut.2005.071423]
30 **Moucari R**, Rautou PE, Cazals-Hatem D, Geara A, Bureau C, Consigny Y, Francoz C, Denninger MH, Vilgrain V, Belghiti J, Durand F, Valla D, Plessier A. Hepatocellular carcinoma in Budd-Chiari syndrome: characteristics and risk factors. *Gut* 2008; **57**: 828-835 [PMID: 18218675 DOI: 10.1136/gut.2007.139477]
31 **Ren W**, Qi X, Yang Z, Han G, Fan D. Prevalence and risk factors of hepatocellular carcinoma in Budd-Chiari syndrome: a systematic review. *Eur J Gastroenterol Hepatol* 2013; **25**: 830-841 [PMID: 23411869 DOI: 10.1097/MEG.0b013e32835eb8d4]
32 **Sakr M**, Abdelhakam SM, Dabbous H, Hamed A, Hefny Z, Abdelmoaty W, Shaker M, El-Gharib M, Eldorry A. Characteristics of hepatocellular carcinoma in Egyptian patients with primary Budd-Chiari syndrome. *Liver Int* 2017; **37**: 415-422 [PMID: 27507647 DOI: 10.1111/liv.13219]
33 **Paul SB**, Shalimar, Sreenivas V, Gamanagatti SR, Sharma H, Dhamija E, Acharya SK. Incidence and risk factors of hepatocellular carcinoma in patients with hepatic venous outflow tract obstruction. *Aliment Pharmacol Ther* 2015; **41**: 961-971 [PMID: 25809735 DOI: 10.1111/apt.13173]

P- Reviewer: Elsiesy H, Gad EH, Garbuzenko DV, Tahiri MJT
S- Editor: Wang JL **L- Editor**: Wang TQ **E- Editor**: Ma YJ

World Journal of Gastroenterology

Submit a Manuscript: http://www.f6publishing.com

World J Gastroenterol 2018 March 14; 24(10): 1144-1151

DOI: 10.3748/wjg.v24.i10.1144

ISSN 1007-9327 (print) ISSN 2219-2840 (online)

ORIGINAL ARTICLE

Retrospective Study

Risk factors of electrocoagulation syndrome after esophageal endoscopic submucosal dissection

Dae Won Ma, Young Hoon Youn, Da Hyun Jung, Jae Jun Park, Jie-Hyun Kim, Hyojin Park

Dae Won Ma, Young Hoon Youn, Da Hyun Jung, Jae Jun Park, Jie-Hyun Kim, Hyojin Park, Department of Internal Medicine, Gangnam Severance Hospital, Yonsei University College of Medicine, Seoul 06273, South Korea

ORCID number: Dae Won Ma (0000-0002-0321-1140); Young Hoon Youn (0000-0002-0071-229X); Da Hyun Jung (0000-0001-6668-3113); Jae Jun Park (0000-0001-5297-5414); Jie-Hyun Kim (0000-0002-9198-3326); Hyojin Park (0000-0002-5759-5135).

Author contributions: All authors helped to perform their research; Ma DW substantial contributions to conception and design, or analysis and interpretation of data and drafting the article or revising it critically for important intellectual content; Youn YH substantial contributions to conception and design, final approval of the version to be published and agreement to be accountable for all aspects of the work; Jung DH, Park JJ, Kim JH and Park H revising the article critically for important intellectual content.

Supported by Basic Science Research Program through the National Research Foundation of Korea (NRF) funded by the Ministry of Science and ICT, No. NRF-2015R1C1A1A01054352.

Institutional review board statement: The Institutional Review Board of Gangnam Severance Hospital approved this study (3-2017-0163).

Informed consent statement: Patients were not required to give informed consent the study because the analysis used anonymous clinical data that were obtained after each patient agreed to treatment by written consent.

Conflict-of-interest statement: All authors declare no conflicts-of-interest related to this article.

Manuscript source: Unsolicited manuscript

Correspondence to: Young Hoon Youn, MD, PhD, Professor, Department of Internal Medicine, Gangnam Severance Hospital, Yonsei University College of Medicine, 211 Eonjuro, Gangnam-gu, Seoul 06273, South Korea. dryoun@yuhs.ac
Telephone: +82-2-20193453
Fax: +82-2-34633882

Received: January 15, 2018
Peer-review started: January 15, 2018
First decision: January 16, 2018
Revised: January 22, 2018
Accepted: January 29, 2018
Article in press: January 29, 2018
Published online: March 14, 2018

Abstract

AIM

To investigate post endoscopic submucosal dissection electrocoagulation syndrome (PEECS) of the esophagus.

METHODS

We analyzed 55 consecutive cases with esophageal endoscopic submucosal dissection for superficial esophageal squamous neoplasms at a tertiary referral hospital in South Korea. Esophageal PEECS was defined as "mild" meeting one of the following criteria without any obvious perforation: fever (≥ 37.8 ℃), leukocytosis (> 10800 cells/μL), or regional chest pain more than 5/10 points as rated on a numeric pain intensity scale. The grade of PEECS was determined as "severe" when meet two or more of above criteria.

RESULTS

We included 51 cases without obvious complications

in the analysis. The incidence of mild and severe esophageal PEECS was 47.1% and 17.6%, respectively. Risk factor analysis revealed that resected area, procedure time, and muscle layer exposure were significantly associated with PEECS. In multivariate analysis, a resected area larger than 6.0 cm^2 (OR = 4.995, 95%CI: 1.110-22.489, P = 0.036) and muscle layer exposure (OR = 5.661, 95%CI: 1.422-22.534, P = 0.014) were independent predictors of esophageal PEECS. All patients with PEECS had favorable outcomes with conservative management approaches, such as intravenous hydration or antibiotics.

CONCLUSION

Clinicians should consider the possibility of esophageal PEECS when the resected area exceeds 6.0 cm^2 or when the muscle layer exposure is noted.

Key words: Electrocoagulation; Endoscopic submucosal dissection; Esophageal neoplasm; Syndrome

Core tip: A number of patients experience fever, chest pain, and/or a systemic inflammatory response after esophageal endoscopic submucosal dissection, even in the absence of obvious perforation. Post endoscopic submucosal dissection electrocoagulation syndrome which is characterized by fever, leukocytosis, and chest pain has been found to be a relatively common condition after esophageal endoscopic submucosal dissection. It more frequently occurs when the resection area is wide (OR = 4.995) or when there is muscle layer damage (OR = 5.661), but it is restored without significant sequelae by conservative treatment.

Ma DW, Youn YH, Jung DH, Park JJ, Kim JH, Park H. Risk factors of electrocoagulation syndrome after esophageal endoscopic submucosal dissection. *World J Gastroenterol* 2018; 24(10): 1144-1151 Available from: URL: http://www.wjgnet.com/1007-9327/full/v24/i10/1144.htm DOI: http://dx.doi.org/10.3748/wjg.v24.i10.1144

INTRODUCTION

With the development of endoscopic imaging technology and the increase in early endoscopic surveillance, the incidence of superficial esophageal neoplasm (SEN) has increased substantially[1,2]. Endoscopic resection has been considered to be a feasible procedure for SEN because of its minimal invasiveness and the fact that it does not compromise organ function[3,4]. Endoscopic submucosal dissection (ESD) is an endoscopic resection method that enables high rates of en bloc resection regardless of tumor size and consequently reduces local recurrence[5,6]. However, esophageal ESD is a more difficult procedure to perform than gastric ESD. The technical resectability of the lesion is affected by various applied techniques, the expertise of the endoscopist, and the location and/or features of the lesion[1,6].

Well-known complications of esophageal ESD include perforation (0%-6.9%), bleeding (0%-5.2%), and post-procedural stricture (0%-17.2%)[1,4,7-10]. However, post ESD electrocoagulation syndrome (PEECS) can be also a common complication of ESD[11,12]. PEECS is characterized by localized abdominal pain, rebound tenderness, fever, and signs of peritoneal irritation without frank perforation after gastric or colorectal ESD. Several previous studies analyzed PEECS after gastric or colonic ESD, but PEECS after esophageal ESD has not been studied yet[12,13]. Actually, some patients demonstrate clinical signs of PEECS after esophageal ESD associated with fever, chest pain and leukocytosis, despite the absence of perforation. However, the possibility of PEECS in the esophagus has received little attention. As far as we know, no studies have yet been conducted on PEECS in the esophagus, and we tried to investigate this new study. Therefore, we aimed to evaluate the incidence and risk factors of PEECS in the esophagus.

MATERIALS AND METHODS

Patients and tumors

We retrospectively analyzed prospectively collected database of patients who underwent esophageal ESD for superficial esophageal squamous neoplasms between March 2009 and December 2016 at Gangnam Severance Hospital, Seoul, South Korea. The analyzed demographic data and clinicopathologic features included patient age, sex, comorbidities, smoking and alcohol history, gross appearance of the tumor, location of the tumor, histological type, invasion depth, circumferential extension of the tumor, area of resection, degree of exposure of the muscularis propria, procedure time, systemic inflammatory response markers (*e.g.*, leukocyte count and body temperature), administration of antibiotics, and hospitalization period. The gross appearance of the tumor was categorized according to the Paris classification system[14]. Tumor histology was assigned according to the Japanese Classification of Esophageal Carcinoma scheme[15]. Tumor location was classified according to the guidelines of the American Joint Committee on Cancer[16]. The resected specimen was assumed to have an elliptical shape. Therefore, the resected area was calculated using the major and minor specimen axes, both of which were measured by a pathologist. The procedure time for ESD was defined as the time from circumferential marking to the retrieval of the resected specimens by an endoscope. Proper muscle layer exposure was defined as when the fine texture of the muscle fibers of muscularis propria was clearly exposed and visible endoscopically due to deep submucosal dissection (Figure 1). Patients who underwent multiple esophageal ESD were excluded in this study.

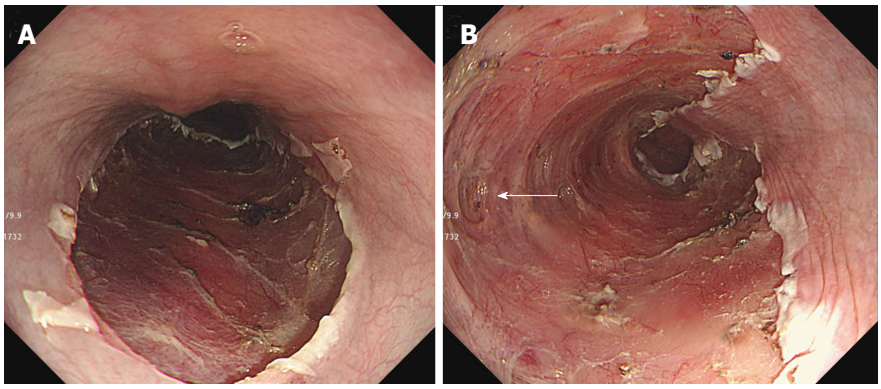

Figure 1 Proper muscle layer exposure during endoscopic submucosal dissection in esophagus. A: Absent; B: Present.

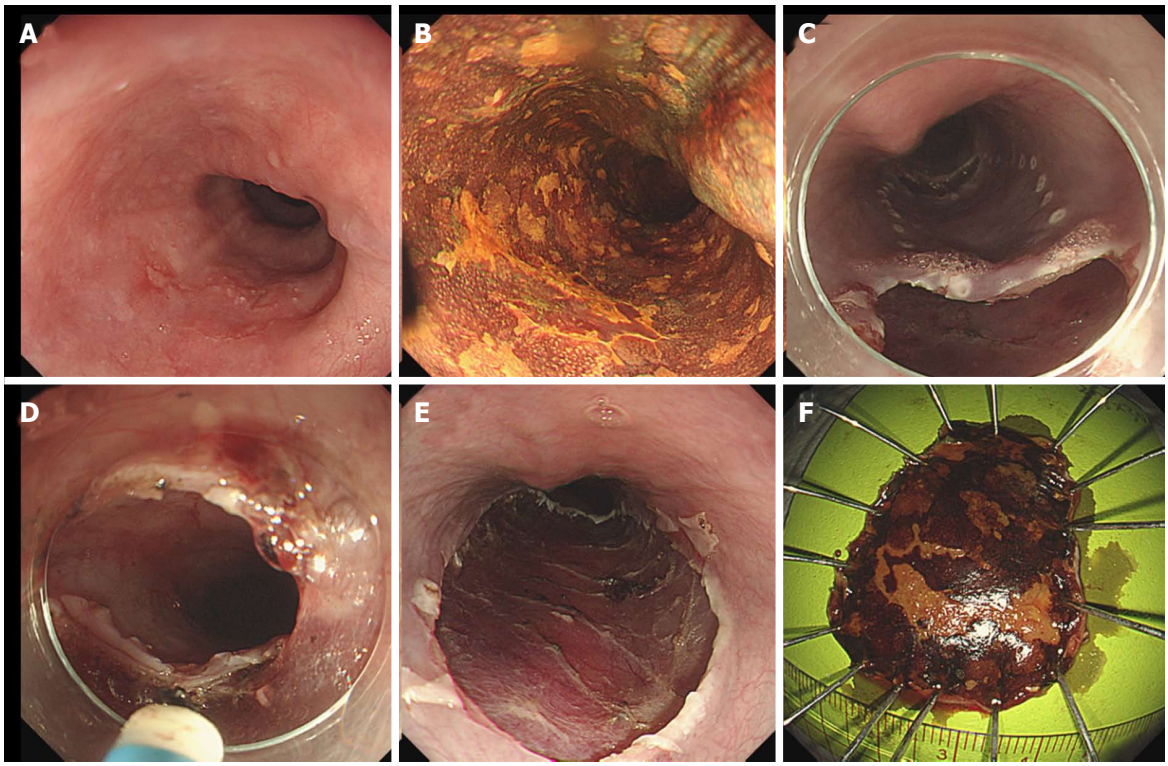

Figure 2 Endoscopic submucosal dissection of a superficial esophageal neoplasm. A and B: A flat erythematous lesion that is unstained with Lugol's solution; C and D: Endoscopic submucosal dissection is made with a dual-knife after local submucosal injection; E and F: The lesion is completely resected.

PEECS was defined as meeting following criteria: fever (≥ 37.8 ℃), leukocytosis (> 10800 counts/μL), or regional chest pain greater than 5/10 points as assessed on a numeric pain rating scale within 24 h after ESD[11,12]. Patients indicated the intensity of current, best, and worst pain levels on a scale of 0 (no pain) to 10 (worst pain imaginable)[17]. If one of the criteria was met, it was defined as mild PEECS and defined as severe PEECS if two or more criteria were met. Patients who had ESD complications such as overt perforation or bleeding were excluded from the analyses. Overt perforation was defined as radiographic evidence of free air, mediastinal emphysema, or subcutaneous emphysema after the procedure. Massive bleeding was defined as bleeding that led to the termination of the procedure. Patients with other defined infections such as pneumonia were also excluded. The Institutional Review Board (IRB) of Gangnam Severance Hospital approved this study (3-2017-0163). We received a consent exemption from the IRB. Patients records and information was anonymized

ESD procedures

All ESD procedures were performed by two expert ESD endoscopists (Y.Y.H. and J.K.). Patients were moderately sedated with midazolam and propofol while ESD was performed. A video endoscope with a water-jet function (GIF-HQ290, GIF-Q260J; Olympus, Tokyo, Japan) was used. A disposable distal transparent cap (D-201-11804; Olympus) was mounted on the tip of

Table 1 Baseline patient and tumor characteristics *n* (%)

Characteristic	Value (*n* = 51)
Number of patients	51
Sex	
Male	46 (90.2)
Female	5 (9.8)
Age, mean ± SD, yr	63.6 ± 9.4
Comorbidity	
Hypertension	21 (41.2)
Diabetes mellitus	7 (13.7)
Chronic kidney disease	1 (2.0)
Smoker	42 (82.4)
Alcohol consumption	40 (78.4)
Gross appearance of tumor	
Polypoid	1 (2.0)
Elevated	8 (15.7)
Flat	40 (78.4)
Depressed	2 (3.9)
Location of tumor	
Upper third of esophagus	3 (5.9)
Middle third of esophagus	20 (39.2)
Lower third of esophagus	24 (47.1)
Esophagogastric junction	4 (7.8)
Circumferential extension, median (IQR), %	40 (30-60)
Pathology of tumor	
Dysplasia	14 (27.5)
Squamous cell carcinoma	37 (72.5)
Invasion depth of tumor	
Mucosa	38 (74.5)
Submucosa	13 (25.5)
Resected area, median (IQR), cm^2	4.5 (2.9-8.2)
Procedure time, median (IQR), min	40 (27-69)
Muscle layer exposure	
Absent	27 (52.9)
Present	24 (47.1)
En bloc resection	51 (100)
Antibiotics use	23 (45.1)
Post procedure BT, mean ± SD, ℃	36.6 ± 0.5
Post procedure WBC, median (IQR), counts/μL	10800 (9340-12600)
Post procedure pain scale score, median (IQR)	5 (3-6)
Duration of hospitalization, median (IQR), d	4 (3-6)
Post ESD electrocoagulation syndrome	
Absent	18 (35.3)
Mild	24 (47.1)
Severe	9 (17.6)

SD: Standard deviation; IQR: Interquartile range; BT: Body temperature; WBC: White blood cell.

the endoscope in all cases. To identify the target lesion, chromoendoscopy with Lugol's stain or narrow band imaging with magnification was used. The area around the lesion was marked with electrical coagulation. A mixture of 10% glycerol solution and 0.005 mg/mL epinephrine was injected through a 25-gauge needle into the submucosal layer under the lesion. In some cases, hyaluronic acid (Endo-Mucoup; BMI Korea, Jeju, South Korea) was added to the mixture. An endoscopic carbon dioxide regulation unit (UCR, Olympus, Tokyo, Japan) was used for the insufflation. A dual knife (KD-650Q; Olympus) or an IT-knife 2 (KD-610L; Olympus) was used to perform the submucosal dissection with the Swift coagulation mode of an electrosurgical generator (VIO 300D; Erbe Elektromedizin GmbH, Tübingen, Germany). Hemostatic forceps (Coagrasper, FD-410LR; Olympus) with a soft coagulation mode (60-W output) were used to control bleeding during the procedure (Figure 2).

After ESD, the patients were closely observed to detect any adverse events. Intravenous proton pump inhibitors and oral sucralfate were administered to each patient to prevent procedure-related bleeding. Chest and abdominal X-rays were taken immediately at the end of the procedure and the following morning to identify any leakage of luminal air or pneumonic consolidation. On the day following the procedure, complete blood cell count was performed to evaluate the leukocytosis. If any aspiration or minute perforation was suspected during ESD, prophylactic antibiotics were administered to the patients. In the absence of evidence of complications such as bleeding or perforation, a clear liquid diet was served the following morning and the patient was discharged in two or three days.

Statistical analysis

Categorical data were analyzed using Fisher's exact test or the χ^2 test. Student's *t*-test or the Mann-Whitney *U* test was used for analysis of quantitative data. Receiver operating characteristic (ROC) curve analysis was performed to find the optimal cutoff values of quantitative data such as resected area and procedure time. In the univariate analysis to determine independent risk factors for PEECS, variables with $P < 0.05$ were considered statistically significant and were added to the multivariate logistic regression. All statistical analysis was performed using SPSS software, version 18.0 for Windows (SPSS, Chicago, IL, United States).

RESULTS

We obtained data from 55 consecutive patients with SEN treated by ESD at Gangnam Severance Hospital. Among them, 4 patients were excluded because of procedure-related complication (3 cases of perforation, 1 case of bleeding). Thus, 51 patients were enrolled in our study. Table 1 shows the patient and tumor baseline characteristics. Most of the patients were male (46, 90.2%), and the mean age was 63.6 years. According to the Paris classification scheme, the tumors of 40 patients (78.4%) had type 0-IIb gross appearance. There were 14 patients (27.5%) who had dysplasia and 37 patients (72.5%) who had squamous cell carcinoma. Regarding tumor invasion depth, 38 cases (74.5%) had mucosal invasion and 13 cases (25.5%) had submucosal invasion. More than half of the patients had no muscle fiber exposure after the procedure (52.9%). The median resected area was 4.5 cm^2 (range 0.8-17.6) and the median procedure time was 40 minutes (range 17-167). The median WBC after the procedure was 10800 cells/uL. There were 2 patients who had a fever (≥ 37.8 ℃) without any obvious evidence of infection. There were 8 patients (15.7%) who had severe pain (≥ 6 points) after ESD. As a result, 24 patients

Table 2 Univariate analysis of risk factors for post endoscopic submucosal dissection electrocoagulation syndrome *n* (%)

	No PEECS (*n* = 18)	PEECS (*n* = 33)	*P* value
Male sex,	17 (94.4)	29 (87.9)	0.451
Age, mean ± SD, yr	63.6 ± 11.2	63.6 ± 8.5	0.977
Comorbidity			0.769
Absent	9 (50.0)	19 (57.6)	
Present	9 (50.0)	14 (42.4)	
Gross appearance			0.933
Flat	14 (77.8)	26 (78.8)	
Non-flat	4 (22.2)	7 (21.2)	
Location			0.378
Upper and middle	10 (55.6)	13 (39.4)	
Lower and EGJ	8 (44.4)	20 (60.6)	
Circumferential extension, median (IQR), %	35 (30-42.5)	40 (30-60)	0.164
Pathology			0.487
Dysplasia	6 (33.3)	8 (24.2)	
Squamous cell carcinoma	12 (66.7)	25 (75.8)	
Invasion depth			0.082
Mucosa	16 (88.9)	22 (66.7)	
Submucosa	2 (11.1)	11 (33.3)	
Resected area			0.035
< 6.0 cm^2	15 (83.3)	17 (51.5)	
⩾ 6.0 cm^2	3 (16.7)	16 (48.5)	
Procedure time			0.026
< 25 min	7 (38.9)	4 (12.1)	
⩾ 25 min	11 (61.1)	29 (87.9)	
Muscle layer exposure			0.018
Absent	14 (77.8)	13 (39.4)	
Present	4 (22.2)	20 (60.6)	
Hospitalization period, mean (IQR), d	3.5 (3-4)	5 (4-6)	0.007
Antibiotics use			0.020
No	14 (77.8)	14 (42.4)	
Yes	4 (22.2)	19 (57.6)	

PEECS: Post endoscopic submucosal dissection electrocoagulation syndrome; SD: Standard deviation; EGJ: Esophagogastric junction; IQR: Interquartile range.

(47.1%) developed mild PEECS and 9 patients (17.6%) developed severe PEECS during the post-ESD period.

There were several significant differences between patients with *vs* patients without PEECS. Patients with PEECS had a relatively larger resection area, a longer mean procedure time, a more often incidence of proper muscle layer exposure, a more prolonged hospitalization period, and a more frequent administration of antibiotics. However, patient-related factors (sex, age, comorbidity) and tumor-related factors (gross appearance, tumor location, tumor histology, tumor invasion depth) were not significantly associated with the development of PEECS (Table 2). Also, ESD learning curve did not show statistically significant relationship with PEECS. The difference in PEECS incidence among the operators was not statistically significant (55.8% *vs* 50%, $P = 0.529$). Multivariate analysis revealed that a resection area larger than 6.0 cm^2 (OR = 4.995, 95%CI: 1.110-22.489, $P = 0.036$) and a present of muscle layer exposure (OR = 5.661, 95%CI: 1.422-22.534, $P = 0.014$) were independent risk factors for PEECS (Table 3). We did not include hospitalization period and antibiotics use in the multivariate analysis, because these factors are considered as consequence of the PEECS rather than cause. No patient diagnosed with PEECS required additional surgery and all patients diagnosed with PEECS spontaneously recovered with intravenous hydration and antibiotics.

DISCUSSION

While ESD is a feasible and effective method for the treatment of SEN, it is a technically difficult procedure and its complications remain a problem[18]. Pain, bleeding, and perforation are common acute complications after esophageal ESD[19]. In addition to major complications, various minor complications may accompany this procedure. These complications, such as chest discomfort, nausea, vomiting, and pyrexia, tend to occur frequently in the postesophageal ESD period. We define esophageal PEECS as a condition accompanied by fever, systemic inflammatory response and chest pain after ESD without such perforation. There have been previous studies on PEECS for Gastric ESD and Colonic ESD[13,20]. The present study is the first to focus on PEECS in the esophagus, which was characterized by fever, leukocytosis, or regional chest pain.

The incidence of esophageal PEECS in this study was higher (60.8%) than the incidence of PEECS in the colon in previous studies[11,12]. This relatively high incidence may have several explanations. Firstly, the esophagus lacks a serosal membrane, unlike other gastrointestinal

Table 3 Multivariate logistic regression analysis of risk factors for post endoscopic submucosal dissection electrocoagulation syndrome

Factor	OR (95%CI)	*P* value
Procedure time		0.379
≤ 25 min	Reference	
> 25 min	2.032 (0.419-9.868)	
Resected area		0.036
≤ 6.0 cm^2	Reference	
> 6.0 cm^2	4.995 (1.110-22.489)	
Muscle layer exposure		0.014
Absent	Reference	
Present	5.661 (1.422-22.534)	

tract organs. Instead of a serosal membrane, the esophagus has a unique structure called adventitia, which is composed of loose connective tissue. Due to the lack of a serosal layer in the esophageal wall, the esophagus might be more susceptible to PEECS than the colon. Moreover, many important organs surround the esophagus, such as the aorta and the bronchus. We propose that these anatomical differences may affect the development of esophageal PEECS. Secondly, although we proposed a definition of esophageal PEECS for this study, a definitive definition of PEECS has not yet been established. While the definition of post polypectomy coagulation syndrome was first published in the 1980s, the criteria were ambiguous and no exact value has been proposed[21]. Moreover, previous studies on gastric or colorectal PEECS also used slightly different definitions[11-13]. These discrepancies may affect relatively high incidence of the PEECS.

In this study, 2 risk factors - resection area and muscle layer exposure - were identified for PEECS in esophageal ESD. These findings are slightly different from previous studies. For instance, polyp size and location were found to be risk factors of post polypectomy electrocoagulation syndrome in the colon[22,23]. For colorectal PEECS, female sex, tumor location, piecemeal resection, tumor size, and procedure time have been identified as risk factors[11,12]. In gastric ESD, tumor size, location, and procedure time have been identified as risk factors for PEECS[13]. While sex differences might influence pain perception, most of the patients with SEN were male[6,17,18,24]. Therefore, it is difficult to identify differences in the incidence of PEECS due to sex based on the data in the present study. In colon ESD, PEECS has been shown to be more common in the right colon than the left colon because of anatomical differences[12,23]. However, unlike the colon, anatomical variation according to the location in the esophagus did not significantly affect the occurrence of PEECS.

PEECS occurred more often with wide resection areas, most likely because the wide area meant that more electric cauterization was required[11,12]. Also, the muscle layer exposure affected the development of PEECS in this study. In colon ESD, superficial damage of the muscularis propria does not significantly influence the spread of inflammation[11]. However, the esophagus does not have serosa membrane, and exposure of bare muscle fibers may have an effect on the propagation of inflammatory substances through muscularis propria. For complete resection of the tumor, clinicians usually attempt to dissect the submucosal layer as deeply as possible to the extent that it does not damage the muscular layers of the esophagus. Therefore, muscle layer exposure can occur frequently during the procedure, and it can be expected that it would have a significant impact on the occurrence of PEECS. The longer procedure time, the chance of fluid aspiration to the respiratory tract may increase substantially. Although longer procedure time was significantly associated with PEECS in univariate analysis, the multivariate analysis showed that longer procedure time was not an independent risk factor of esophageal PEECS. Kawata *et al*[25]. reported an incidence of bacteremia after esophageal ESD of 1%. Due to the rare incidence of bacteremia, they did not recommend prophylactic antibiotics for patients who undergo esophageal ESD. In our study, we used antibiotics only when patients were suspected to have complications. All patients with PEECS showed good outcomes without any severe complications. As a result, we suggest that esophageal PEECS is a systemic inflammatory response syndrome caused by electrical burns and transmural penetration of oro-esophageal secretion rather than true infection.

There are several limitations of our study. First, it was a small number and retrospective study that was performed at a single center. Thus, the cut off values we have established need external validation. Furthermore, there may be a recording bias because of retrospective design. Second, assessment of pain felt by patients after ESD may be subjective because pain tolerance can vary according to sex or age[17]. Third, we routinely perform chest and abdomen X-ray examinations after esophageal ESD. A computed tomography (CT) scan might be needed to detect micro perforations accurately after ESD. However, we performed a CT scan only when perforation was suspected on X-ray scans. Even if micro perforations were present, all patients in our study showed improvement with conservative treatment.

This is the first study of PEECS for esophageal lesions. PEECS is a common clinical syndrome characterized by chest pain, leukocytosis, or fever after esophageal ESD. It is another kind of clinical syndrome that is different from systemic inflammatory response syndrome. However, PEECS can be easily controlled by conservative management without surgical intervention when there is no obvious perforation. We found that the incidence of PEECS was high when the resected tumor area exceeded 6.0 cm^2 or when the muscle layer exposure was present. If these risk factors are accompanied, careful attention should be paid to the

potential occurrence of PEECS after esophageal ESD.

ARTICLE HIGHLIGHTS

Research background

A number of patients experience fever, chest pain, and/or a systemic inflammatory response after esophageal endoscopic submucosal dissection (ESD), even in the absence of obvious perforation.

Research motivation

Post ESD electrocoagulation syndrome (PEECS) is known as a common complication after colon ESD. However, there were no studies of PEECS after esophageal ESD.

Research objectives

We aimed to investigate the incidence and risk factors of PEECS in the esophagus.

Research methods

We retrospectively analyzed electronic medical database of patients who underwent esophageal ESD for superficial esophageal squamous neoplasms between March 2009 and December 2016 at single center in South Korea. PEECS was defined as meeting one of following criteria: fever (≥ 37.8 ℃), leukocytosis (> 10800 counts/μL), or regional chest pain greater than 5/10 points as assessed on a numeric pain rating scale within 24 h after ESD.

Research results

As a result, 24 patients (47.1%) developed mild PEECS and 9 patients (17.6%) developed severe PEECS during the post-ESD period. We identified that that a resection area larger than 6.0 cm^2 (OR = 4.995, 95%CI: 1.110-22.489, P = 0.036) and a present of muscle layer exposure (OR 5.661, 95%CI: 1.422-22.534, P = 0.014) were independent risk factors for PEECS. All patients diagnosed with PEECS fully recovered with conservative management, such as intravenous hydration and antibiotics.

Research conclusions

PEECS is not a rare clinical after esophageal ESD. However, PEECS can be easily controlled by conservative management without surgical intervention when there is no obvious perforation. We conclude that the incidence of PEECS is expected to be high when the resected tumor area exceeds 6.0 cm^2 or when the muscle layer exposure is present.

Research perspective

If these risk factors are accompanied, careful attention should be paid to the potential occurrence of PEECS after esophageal ESD. Further large-scale study is needed to validate our research.

REFERENCES

1 **Ono S**, Fujishiro M, Niimi K, Goto O, Kodashima S, Yamamichi N, Omata M. Long-term outcomes of endoscopic submucosal dissection for superficial esophageal squamous cell neoplasms. *Gastrointest Endosc* 2009; **70**: 860-866 [PMID: 19577748 DOI: 10.1016/j.gie.2009.04.044]

2 **Shimizu Y**, Takahashi M, Yoshida T, Ono S, Mabe K, Kato M, Asaka M, Sakamoto N. Endoscopic resection (endoscopic mucosal resection/ endoscopic submucosal dissection) for superficial esophageal squamous cell carcinoma: current status of various techniques. *Dig Endosc* 2013; **25** Suppl 1: 13-19 [PMID: 23480399 DOI: 10.1111/j.1443-1661.2012.01408.x]

3 **Das A**, Singh V, Fleischer DE, Sharma VK. A comparison of endoscopic treatment and surgery in early esophageal cancer: an analysis of surveillance epidemiology and end results data. *Am J Gastroenterol* 2008; **103**: 1340-1345 [PMID: 18510606 DOI: 10.1111/j.1572-0241.2008.01889.x]

4 **Takahashi H**, Arimura Y, Masao H, Okahara S, Tanuma T, Kodaira J, Kagaya H, Shimizu Y, Hokari K, Tsukagoshi H, Shinomura Y, Fujita M. Endoscopic submucosal dissection is superior to conventional endoscopic resection as a curative treatment for early squamous cell carcinoma of the esophagus (with video). *Gastrointest Endosc* 2010; **72**: 255-264, 264.e1-264.e2 [PMID: 20541198 DOI: 10.1016/j.gie.2010.02.040]

5 **Fujishiro M**. Perspective on the practical indications of endoscopic submucosal dissection of gastrointestinal neoplasms. *World J Gastroenterol* 2008; **14**: 4289-4295 [PMID: 18666315 DOI: 10.3748/wjg.14.4289]

6 **Tsujii Y**, Nishida T, Nishiyama O, Yamamoto K, Kawai N, Yamaguchi S, Yamada T, Yoshio T, Kitamura S, Nakamura T, Nishihara A, Ogiyama H, Nakahara M, Komori M, Kato M, Hayashi Y, Shinzaki S, Iijima H, Michida T, Tsujii M, Takehara T. Clinical outcomes of endoscopic submucosal dissection for superficial esophageal neoplasms: a multicenter retrospective cohort study. *Endoscopy* 2015; **47**: 775-783 [PMID: 25826277 DOI: 10.1055/s-0034-1391844]

7 **Hirasawa K**, Kokawa A, Oka H, Yahara S, Sasaki T, Nozawa A, Tanaka K. Superficial adenocarcinoma of the esophagogastric junction: long-term results of endoscopic submucosal dissection. *Gastrointest Endosc* 2010; **72**: 960-966 [PMID: 21034897 DOI: 10.1016/j.gie.2010.07.030]

8 **Ishihara R**, Iishi H, Uedo N, Takeuchi Y, Yamamoto S, Yamada T, Masuda E, Higashino K, Kato M, Narahara H, Tatsuta M. Comparison of EMR and endoscopic submucosal dissection for en bloc resection of early esophageal cancers in Japan. *Gastrointest Endosc* 2008; **68**: 1066-1072 [PMID: 18620345 DOI: 10.1016/j.gie.2008.03.1114]

9 **Kakushima N**, Yahagi N, Fujishiro M, Kodashima S, Nakamura M, Omata M. Efficacy and safety of endoscopic submucosal dissection for tumors of the esophagogastric junction. *Endoscopy* 2006; **38**: 170-174 [PMID: 16479425 DOI: 10.1055/s-2005-921039]

10 **Oyama T**, Tomori A, Hotta K, Morita S, Kominato K, Tanaka M, Miyata Y. Endoscopic submucosal dissection of early esophageal cancer. *Clin Gastroenterol Hepatol* 2005; **3**: S67-S70 [PMID: 16013002 DOI: 10.1016/S1542-3565(05)00291-0]

11 **Yamashina T**, Takeuchi Y, Uedo N, Hamada K, Aoi K, Yamasaki Y, Matsuura N, Kanesaka T, Akasaka T, Yamamoto S, Hanaoka N, Higashino K, Ishihara R, Iishi H. Features of electrocoagulation syndrome after endoscopic submucosal dissection for colorectal neoplasm. *J Gastroenterol Hepatol* 2016; **31**: 615-620 [PMID: 26202127 DOI: 10.1111/jgh.13052]

12 **Jung D**, Youn YH, Jahng J, Kim JH, Park H. Risk of electrocoagulation syndrome after endoscopic submucosal dissection in the colon and rectum. *Endoscopy* 2013; **45**: 714-717 [PMID: 23990482 DOI: 10.1055/s-0033-1344555]

13 **Lee H**, Cheoi KS, Chung H, Park JC, Shin SK, Lee SK, Lee YC. Clinical features and predictive factors of coagulation syndrome after endoscopic submucosal dissection for early gastric neoplasm. *Gastric Cancer* 2012; **15**: 83-90 [PMID: 21761134 DOI: 10.1007/s10120-011-0073-x]

14 . The Paris endoscopic classification of superficial neoplastic lesions: esophagus, stomach, and colon: November 30 to December 1, 2002. *Gastrointest Endosc* 2003; **58**: S33-S43 [PMID: 14652541 DOI: 10.1016/S0016-5107(03)02159-X]

15 **Shimoda T**. Japanese classification of esophageal cancer, the 10th edition--Pathological part. *Nihon Rinsho* 2011; **69** Suppl 6: 109-120 [PMID: 22471004]

16 **Rice TW**, Blackstone EH, Rusch VW. 7th edition of the AJCC Cancer Staging Manual: esophagus and esophagogastric junction. *Ann Surg Oncol* 2010; **17**: 1721-1724 [PMID: 20369299 DOI: 10.1245/s10434-010-1024-1]

17 Pain: clinical manual for nursing practice Pain: clinical manual for nursing practice Margo McCaffery Alexander Beebe Mosby Yearbook UK £17.25 0 7234 1992 2. *Nurs Stand* 1994; **9**: 55 [PMID: 27527475 DOI: 10.7748/ns.9.11.55.s69]

18 **Kim DH**, Jung HY, Gong EJ, Choi JY, Ahn JY, Kim MY, Choi KS, Lee JH, Choi KD, Song HJ, Lee GH, Kim JH, Park YS, Baek S. Endoscopic and Oncologic Outcomes of Endoscopic Resection

for Superficial Esophageal Neoplasm. *Gut Liver* 2015; **9**: 470-477 [PMID: 25473069 DOI: 10.5009/gnl13263]
19 **Isomoto H**, Yamaguchi N, Minami H, Nakao K. Management of complications associated with endoscopic submucosal dissection/endoscopic mucosal resection for esophageal cancer. *Dig Endosc* 2013; **25** Suppl 1: 29-38 [PMID: 23368404 DOI: 10.1111/j.1443-1661.2012.01388.x]
20 **Onogi F**, Araki H, Ibuka T, Manabe Y, Yamazaki K, Nishiwaki S, Moriwaki H. "Transmural air leak": a computed tomographic finding following endoscopic submucosal dissection of gastric tumors. *Endoscopy* 2010; **42**: 441-447 [PMID: 20432207 DOI: 10.1055/s-0029-1244013]
21 Selected papers from the Second International Congress on Colonoscopy and Diseases of the Large Bowel, March 6 to 8, 1980. *Gastrointest Endosc* 1981; **27**: 184-187 [PMID: 7297830 DOI: 10.1016/S0016-5107(81)73190-0]
22 **Cha JM**, Lim KS, Lee SH, Joo YE, Hong SP, Kim TI, Kim HG, Park DI, Kim SE, Yang DH, Shin JE. Clinical outcomes and risk factors of post-polypectomy coagulation syndrome: a multicenter, retrospective, case-control study. *Endoscopy* 2013; **45**: 202-207 [PMID: 23381948 DOI: 10.1055/s-0032-1326104]
23 **Choo WK**, Subhani J. Complication rates of colonic polypectomy in relation to polyp characteristics and techniques: a district hospital experience. *J Interv Gastroenterol* 2012; **2**: 8-11 [PMID: 22586542 DOI: 10.4161/jig.20126]
24 **Park JS**, Youn YH, Park JJ, Kim JH, Park H. Clinical Outcomes of Endoscopic Submucosal Dissection for Superficial Esophageal Squamous Neoplasms. *Clin Endosc* 2016; **49**: 168-175 [PMID: 26867548 DOI: 10.5946/ce.2015.080]
25 **Kawata N**, Tanaka M, Kakushima N, Takizawa K, Imai K, Hotta K, Matsubayashi H, Tsukahara M, Kawamura I, Kurai H, Ono H. The low incidence of bacteremia after esophageal endoscopic submucosal dissection (ESD) obviates the need for prophylactic antibiotics in esophageal ESD. *Surg Endosc* 2016; **30**: 5084-5090 [PMID: 26983438 DOI: 10.1007/s00464-016-4857-2]

P- Reviewer: Hashimoto N, Jani K, Jonaitis LV **S- Editor**: Ma YJ
L- Editor: A **E- Editor**: Ma YJ

World Journal of Gastroenterology

Submit a Manuscript: http://www.f6publishing.com

World J Gastroenterol 2018 March 14; 24(10): 1152-1166

DOI: 10.3748/wjg.v24.i10.1152

ISSN 1007-9327 (print) ISSN 2219-2840 (online)

ORIGINAL ARTICLE

Clinical Practice Study

Progesterone receptor membrane component 1 as a potential prognostic biomarker for hepatocellular carcinoma

Hung-Wen Tsai, Chung-Liang Ho, Shu-Wen Cheng, Yih-Jyh Lin, Chou-Cheng Chen, Pin-Nan Cheng, Chia-Jui Yen, Ting-Tsung Chang, Po-Min Chiang, Shih-Huang Chan, Cheng-Hsun Ho, Shu-Hui Chen, Yi-Wen Wang, Nan-Haw Chow, Jou-Chun Lin

Hung-Wen Tsai, Po-Min Chiang, Institute of Clinical Medicine, National Cheng Kung University Hospital, College of Medicine, National Cheng Kung University, Tainan 70403, Taiwan

Hung-Wen Tsai, Chung-Liang Ho, Shu-Wen Cheng, Yi-Wen Wang, Nan-Haw Chow, Jou-Chun Lin, Department of Pathology, National Cheng Kung University Hospital, College of Medicine, National Cheng Kung University, Tainan 70403, Taiwan

Hung-Wen Tsai, Chung-Liang Ho, Shu-Wen Cheng, Chou-Cheng Chen, Nan-Haw Chow, Jou-Chun Lin, Institute of Basic Medical Sciences, College of Medicine, National Cheng Kung University, Tainan 70403, Taiwan

Hung-Wen Tsai, Ting-Tsung Chang, Center of Infectious Disease and Signaling Research, College of Medicine, National Cheng Kung University, Tainan 70403, Taiwan

Yih-Jyh Lin, Department of Surgery, National Cheng Kung University Hospital, College of Medicine, National Cheng Kung University, Tainan 70403, Taiwan

Pin-Nan Cheng, Chia-Jui Yen, Ting-Tsung Chang, Cheng-Hsun Ho, Department of Internal Medicine, National Cheng Kung University Hospital, College of Medicine, National Cheng Kung University, Tainan 70403, Taiwan

Shih-Huang Chan, Department of Statistics, College of Management, National Cheng Kung University, Tainan 70403, Taiwan

Cheng-Hsun Ho, Research Center of Clinical Medicine, National Cheng Kung University Hospital, College of Medicine, National Cheng Kung University, Tainan 70403, Taiwan

Shu-Hui Chen, Department of Chemistry, College of Sciences, National Cheng Kung University, Tainan 70403, Taiwan

ORCID number: Hung-Wen Tsai (0000-0001-9223-2535); Chung-Liang Ho (0000-0002-4562-5122); Shu-Wen Cheng (0000-0002-8684-4428); Yih-Jyh Lin (0000-0003-0998-3229); Chou-Cheng Chen (0000-0002-4030-8849); Pin-Nan Cheng (0000-0001-9331-9018); Chia-Jui Yen (0000-0001-8744-6248); Ting-Tsung Chang (0000-0002-5073-2678); Po-Min Chiang (0000-0002-4950-9292); Shih-Huang Chan (0000-0002-3666-180X); Cheng-Hsun Ho (0000-0003-4451-2887); Shu-Hui Chen (0000-0003-1871-9366); Yi-Wen Wang (0000-0001-7863-727X); Nan-Haw Chow (0000-0002-0277-1947); Jou-Chun Lin (0000-0002-2358-3670).

Author contributions: Lin JC, Cheng SW, Wang YW and Tsai HW conducted the experiments in this study, analyzed the data, and prepared the manuscript; Tsai HW, Ho CL, Chiang PM and Chow NH performed the pathological analysis; Lin YJ, Cheng PN, Yen CJ and Chang TT provided and analyzed the clinical information; Chen CC performed the TCGA data analysis; Chan SH conducted the statistical analysis; Ho CH and Chen SH performed the mass spectrometry and data analysis; Tsai HW designed the study.

Supported by the Ministry of Science and Technology, No. NSC102-2320-B-006-011., No. MOST103-2320-B-006-021-MY2, and No. MOST105-2320-B-006-033 to Tsai HW; and National Cheng Kung University Hospital, Taiwan, No. NCKUH-10406002 and No. NCKUH-10509001 to Tsai HW.

Institutional review board statement: The study was conducted in accordance with the Declaration of Helsinki and approved by the Human Experiment and Ethics Committee of NCKUH (No. BR-100-117).

Conflict-of-interest statement: The authors declare that they have no competing interests.

Data sharing statement: Technical appendix and study data are available from the corresponding author at hungwen@mail.ncku.edu.tw with the permission of Hung-Wen Tsai. Consent was not obtained but the presented data are anonymized and the risk of identification is low. No additional data are available.

Manuscript source: Unsolicited manuscript

Correspondence to: Hung-Wen Tsai, MD, Associate Professor, Department of Pathology, National Cheng Kung University Hospital, College of Medicine, National Cheng Kung University, 138 Sheng-Li Road, Tainan 70403, Taiwan. hungwen@mail.ncku.edu.tw
Telephone: +886-6-2353535-2635
Fax: +886-6-2766195

Received: December 11, 2017
Peer-review started: December 12, 2017
First decision: December 27, 2017
Revised: January 16, 2018
Accepted: January 24, 2018
Article in press: January 24, 2018
Published online: March 14, 2018

Abstract

AIM

To investigate the clinicopathological significance of progesterone receptor membrane component 1 (PGRMC1) and PGRMC2 in hepatocellular carcinoma (HCC).

METHODS

We performed immunohistochemical staining to evaluate the estrogen receptor (ER), progesterone receptor (PR), PGRMC1, and PGRMC2 in a clinical cohort consisting of 89 paired HCC and non-tumor liver samples. We also analyzed HCC data (n = 373) from The Cancer Genome Atlas (TCGA). We correlated the expression status of PGRMC1 and PGRMC2 with clinicopathological indicators and the clinical outcomes of the HCC patients. We knocked down or overexpressed PGRMC1 in HCC cell lines to evaluate its biological significance in HCC cell proliferation, differentiation, migration, and invasion.

RESULTS

We found that few HCC cases expressed ER (5.6%) and PR (4.5%). In contrast, most HCC cases expressed PGRMC1 (89.9%) and PGRMC2 (100%). PGRMC1 and PGRMC2 exhibited significantly lower expression in tumor tissue than in non-tumor tissue (P < 0.001). Lower PGRMC1 expression in HCC was significantly associated with higher serum alpha-fetoprotein expression (P = 0.004), poorer tumor differentiation (P = 0.045) and liver capsule penetration (P = 0.038). Low PGRMC1 expression was an independent predictor for worse disease-free survival (P = 0.002, HR = 2.384, CI: 1.377-4.128) in our cases, as well as in the TCGA cohort (P < 0.001, HR = 2.857, CI: 1.781-4.584). The expression of PGRMC2 did not relate to patient outcome. PGRMC1 knockdown promoted a poorly differentiated phenotype and proliferation of HCC cells *in vitro*, while PGRMC1 overexpression caused the opposite effects.

CONCLUSION

PGRMC1 is a non-classical hormonal receptor that negatively regulates hepatocarcinogenesis. PGRMC1 down-regulation is associated with progression of HCC and is a poor prognostic indicator.

Key words: Progesterone receptor membrane component 1; Hormonal receptor; Proliferation; Hepatocellular carcinoma; Prognosis

Core tip: Neither estrogen receptor or progesterone receptor are commonly expressed in hepatocellular carcinoma (HCC), implying the existence of other hormone-related events in the pathogenesis of HCC. Most primary HCC cases expressed progesterone receptor membrane component 1 (PGRMC1) (89.9%) in our clinical cohort (n = 89). Down-regulation of PGRMC1 was associated with poor tumor differentiation and worse patient survival. The potential prognostic significance was independently validated by The Cancer Genome Atlas (TCGA) database (n = 373). Knockdown of PGRMC1 promoted proliferation and a poorly differentiated phenotype *in vitro*. Overexpression of PGRMC1 resulted in suppressed proliferation in response to progesterone treatment. PGRMC1 is a prognostic marker and a potential auxiliary therapeutic target for human HCC.

Tsai HW, Ho CL, Cheng SW, Lin YJ, Chen CC, Cheng PN, Yen CJ, Chang TT, Chiang PM, Chan SH, Ho CH, Chen SH, Wang YW, Chow NH, Lin JC. Progesterone receptor membrane component 1 as a potential prognostic biomarker for hepatocellular carcinoma. *World J Gastroenterol* 2018; 24(10): 1152-1166 Available from: URL: http://www.wjgnet.com/1007-9327/full/v24/i10/1152.htm DOI: http://dx.doi.org/10.3748/wjg.v24.i10.1152

INTRODUCTION

The major risk factors for hepatocellular carcinoma (HCC) are chronic liver diseases induced by hepatitis B (HBV) and hepatitis C (HCV), alcohol abuse, and non-alcoholic steatohepatitis. Regardless of etiology, the incidence of HCC is higher in males than in females, with a male to female ratio between 2:1 and 4:1[1]. However, the biological role of sex hormones and their receptors in HCC remains poorly understood. The androgen

receptor appears to contribute to HCC development by acting as a tumor promoter[2], whereas the estrogen receptor (ER) appears to act as a tumor suppressor[3]. Oophorectomy performed during premenopausal years has been found to be a risk factor for HCC[4]. The human liver is important in the metabolism of progesterone. Progesterone is known to inhibit autophagy and to augment epirubicin-induced apoptosis in hepatoma cells by increasing oxidative stress and upregulating Fas/FasL[5,6]. In a clinical trial, HCC patients with variant ERs had a significantly longer median survival if megestrol acetate was given[7], suggesting that progesterone is protective against HCC.

Progesterone receptor membrane component 1 (PGRMC1) and PGRMC2, which belong to the membrane-associated progesterone receptor (MAPR) family, have been suggested to be non-classical progesterone receptors[8,9]. These proteins contain a cytochrome b5-like heme/steroid-binding domain. Both PGRMC1 and PGRMC2 are derived from a single gene. The structure of PGRMC1 contains two SH2 target sequences, a SH3 target sequence, a tyrosine kinase target site, two acidophilic kinase (CK2, casein kinase 2) target sites, and binding sites for ERK1 and PDK1. PGRMC2 differs from PGRMC1 in the following aspects: First, the transmembrane domain and N-terminals are different, resulting in diverse interaction partners in the lumen of sub-cellular organelles or on the cell membrane surface. Second, the SH3 target sequence of PGRMC1 with its consensus CK2 site is absent in PGRMC2, suggesting that PGRMC2 may not interact with SH3-containing proteins. Third, PGRMC2 has a predicted PDGFR or EGFR target and an additional potential CK2 site[8]. Therefore, these two proteins may have different interacting partners in terms of connecting with the cellular membrane, organelles and cell signaling molecules.

In the case of tumorigenesis, PGRMC1 expression is associated with advanced-stage disease and poor prognoses in both breast and ovarian cancer[10,11]. However, several studies have shown that PGRMC1 mediates the anti-mitotic actions of progesterone in endometrial and ovarian cancer cells[12,13]. With regard to PGRMC2, copy number loss has been correlated with nodal metastasis in uterine cervical adenocarcinoma, suggesting that PGRMC2 can function as a metastasis suppressor[14]. PGRMC2 negatively affects SKOV-3 ovarian cell migration[15]. Therefore, PGRMC1 and PGRMC2 may have multiple biological functions related to metabolism and carcinogenesis. A proteomic study showed that PGRMC1 was expressed in HCC[16] but there is no information regarding PGRMC1 or PGRMC2 expression patterns in HCC or their clinical significance in this disease. To address this issue, we examined PGRMC1 and PGRMC2 expression in a clinical cohort of paired HCC and non-tumor tissue samples (n = 89). We analyzed an independent HCC cohort (n = 373) from The Cancer Genome Atlas (TCGA cohort) to validate our findings. We also investigated the significance of PGRMC1 in cell proliferation, differentiation, migration, and invasion *in vitro*.

MATERIALS AND METHODS

Patients and samples

Eighty-nine patients who underwent surgical resection for HCC at National Cheng Kung University Hospital (NCKUH) from January 1995 to September 2000 were included in this study. Frozen tissue, serum samples and archival paraffin blocks were retrieved from the Human Biobank at NCKUH. HCC differentiation was categorized according to the World Health Organization (WHO) system[17]. Six paraffin samples and four frozen liver samples were retrieved from six normal non-hepatitis patients who underwent surgery for cavernous hemangioma and acted as controls.

Bioinformatic TCGA dataset analysis

We analyzed the TCGA provisional dataset (TCGA dataset, https://tcga-data.nci.nih.gov/tcga/), which contained 373 HCC patients with mRNA expression data (RNA Seq V2 RSEM), clinicopathological indicators, and follow-up information. Of these patients, 50 had expression data pertaining to HCC and matched adjacent non-tumor tissue samples. Disease-free survival (DFS) and overall survival (OS) were calculated based on *PGRMC1* and *PGRMC2* expression. Expression levels greater than the median were classified as high expression; otherwise, they were classified as low expression.

Western blotting

Protein lysates were prepared from either frozen tissue samples or HCC cell lines. Equal amounts of protein (50 micrograms) were separated *via* 8% sodium dodecyl sulfate-polyacrylamide gel electrophoresis (SDS-PAGE) under reducing conditions. The proteins were then transferred to nitrocellulose membranes and stained with Ponceau S to assess transfer quality and ensure equal sample loading. The primary antibodies used were anti-PGRMC1 (Abnova Corporation, Walnut, CA, United States. PAB20135, 1:3000), anti-PGRMC2 (Abnova Corporation. H00010424-M04, 1:1000), anti-PR (Ventana Medical Systems, Inc. 790-2223, 1:100), anti-alpha-fetoprotein (Dako Cytomation, Inc., Carpinteria, CA, USA. A0008, 1:1000), anti-Glypican3 (BioMosaics, Burlington, VT, United States. 1G12, 1:1000) and anti-β-actin (GeneTex Inc. GTX109639, 1:10000). The indicated secondary antibodies (anti-rabbit and anti-mouse, IgG-HRP; Santa Cruz Biotechnology) were used to amplify the signals as appropriate.

Immunohistochemical staining and interpretation

Immunohistochemical staining was performed with primary antibodies against ER (Ventana Medical Systems, Inc., Arizona, United States), PR (Ventana

Medical Systems, Inc.), PGRMC1 (Abnova Corporation, Walnut, CA, United States. PAB20135) or PGRMC2 (Abnova Corporation. H00010424-M04). ER, PR, PGRMC1 and PGRMC2 expression was graded independently by two pathologists (Tsai HW and Ho CL) according to the percentages of stained hepatocytes or HCC cells. Because PGRMC1 is found in the cytosol and subcellular organelles[8], cytoplasmic staining was considered to be positive. High PGRMC expression was defined as more than two-thirds of the cells exhibited positive staining. In the case of ER and PR, nuclear staining was considered to be positive.

In-gel trypsin digestion and mass spectrometry

Fifty micrograms of tissue extracts were resolved using 12% SDS-PAGE and were stained using Coomassie brilliant blue r-250. The protein spot located between 20-28 kDa was excised and then in-gel digested using 20 ng/μL of trypsin (Promega, San Luis Obispo, CA, United States, sequencing grade) in 10 mmol/L NH_4HCO_3 with an enzyme-to-substrate ratio of 1:100 at 37 ℃ overnight. Peptides were extracted using 50% acetonitrile in 1% formic acid followed by sonication.

A nanoflow high-performance liquid chromatography system (LC Packings, Amsterdam, The Netherlands) equipped with a C18 nano-precolumn cartridge (*i.d.* = 300 μm × 1 mm, 5 μm C18, P/N160458; LC Packings) and a C18 column (*i.d.* = 75 μm, o.d. = 280 μm × 15 cm, 3 μm C18, LC Packings) was coupled online to a Q-TOF micro-instrument (Micromass, Manchester, United Kingdom). Mobile phase A was 0.1% formic acid in a 5% acetonitrile solution, and mobile phase B was 0.1% formic acid in 80% acetonitrile. A linear gradient from 5% to 90% B over 60 min at a flow rate of 250 nL/min was applied. A survey MS spectrum with a mass-to-charge ratio ranging from 400 to 1600 was followed by a MS/MS scan at a mass-to-charge ratio ranging from 50 to 2000. The threshold to switch from MS to MS/MS was 10 counts. Raw data were processed into peak lists, and then a Mascot search on a Swiss-Prot (human) protein database was conducted.

The mass tolerance was set at 0.2 Da for both the precursor and product ions. Dimethyl labeling of both the N-terminal and lysine residues was chosen for variable modifications; Carbamidomethyl (C) was chosen for fixed modification, and one miss cleavage on Arg-C was allowed. A cutoff value of 20 was set for the ion score to eliminate proteins with low matches. The default significance threshold for protein identification was set at $P < 0.05$.

Measurement of progesterone levels in sera and tissue

Tissue samples were minced and homogenized at a 1:10 (w:v) ratio with phosphate buffered saline at pH 7.4 using a homogenizer (PRO Scientific Inc., Oxford, CT, United States). The homogenates were centrifuged at 9000 × *g* at 4 ℃ for 30 min and the supernatants were immediately analyzed. The progesterone levels in the sera and tissue supernatants were analyzed using the Elecsys and Cobas e-immunoassay analyzer (Roche Diagnostics, Mannheim, Germany).

Cell lines

The HepG2 and Huh7 cell lines were maintained in Dulbecco's modified Eagle's medium (DMEM, Invitrogen Corp., Carlsbad, CA, United States) supplemented with 10% fetal bovine serum (FBS), penicillin (100 U/mL), and streptomycin (100 μg/mL) in a humidified incubator at 37 ℃ with 5% CO_2, whereas the PLC/PRF/5 and Hep3B cell lines were maintained in modified Eagle's medium (MEM, Invitrogen Corp.) supplemented with 10% FBS, penicillin (100 U/mL), and streptomycin (100 μg/mL) in a humidified incubator at 37 ℃ with 5% CO_2. Huh-7 cells were obtained from JCRB. Hep3B, HepG2 and PLC/PRF/5 cells were obtained from BCRC.

Knockdown and overexpression of PGRMC1

pLKO.1 plasmids expressing small hairpin RNA (shRNA) were purchased from the National RNAi Core Facility (Academia Sinica, Taipei, Taiwan). Lentivirus particles were obtained from RNAi Core of the Research Center of Clinical Medicine, NCKUH. The following shRNAs were used to knock down PGRMC1 expression in HepG2 and Hep3B cells: sh-1: TRCN0000311671, target sequence: 5'-ACTGTGTACTCAGATGAGGAA-3'; sh-2: TRCN0000363644, target sequence: 5'-CGCCGACCCAAGCGATCTGGA-3'; and sh-3: TRCN0000349346, target sequence: 5'-AGGATGAGTACGATGACCTTT -3'. A pLKO_TRC005 plasmid was used as a negative control. PGRMC1 knockdown was performed as described previously[15].

The pMSCVpuro (BD Clontech), pMSCV-PGRMC1, and pSUPERretro vectors were co-transfected into GP2-293T packaging cells along with VSV-G plasmids for 48 h using the calcium phosphate method. Either PLC/PRF/5 or Huh7 cells (1×10^6 cells/well) were seeded in a 6-cm dish and incubated overnight under 5% CO_2 at 37 ℃. The retroviral supernatant was treated with 8 ng/mL polybrene (Sigma, St. Louis, MO, United States) to infect the cells. Pooled PLC/PRF/5 or Huh7 cells expressing either pMSCVpuro or pMSCV-PGRMC1 were selected using 0.7 μg/mL puromycin (Sigma-Aldrich).

XTT proliferation assay

Stable pools were seeded in 24-well plates for 96 h. Triplicate wells were plated at each time point and examined at 24-h intervals over 4 d. The number of viable cells for each time point was determined using the XTT reagent, according to standard protocols (Roche Diagnostics GmbH, Vienna, Austria). To evaluate the impact of progesterone treatment, control cells and PGRMC1-overexpressing cells were cultured to 50% confluence and treated with progesterone (0, 10, 100, or 1000 nmol/L) for 48 h before the XTT assay.

In vitro migration and invasion assay

Transwell migration and invasion assays were performed using 24-well 8-micrometer pore Transwell plates,

Table 1 Prognostic significance of clinicopathological indicators, PGRMC1 and PGRMC2 for disease-free survival in the clinical cohort (*n* = 89)

Factor	DFS univariate				DFS multivariate		
	Group	HR	95%CI	*P* value	HR	95%CI	*P* value
Age, yr	< 60/≥ 60	0.997	0.609-1.632	0.989			
Sex	Male/female	1.014	0.599-1.715	0.960			
Viral infection				0.825			
	B/C	1.177	0.703-1.971				
	B/B + C	1.068	0.448-2.547				
Child-Pugh score	5/≥ 6	2.407	1.346-4.302	0.003[a]	2.005	(1.097-3.665)	0.024[a]
Cirrhosis	-/+	0.743	0.664-1.776	0.299			
Serum AFP	< 100/≥ 100 ng/ml	1.357	0.823-2.238	0.231			
Differentiation	W/M-P	1.682	0.943-2.999	0.078			
Multifocal tumor	-/+	0.985	0.514-1.888	0.965			
Satellite nodule	-/+	2.173	1.303-3.624	0.003[a]			NS
Tumor size	< 5/≥ 5 cm	2.446	1.486-4.028	< 0.001[a]			NS
Tumor capsular invasion	-/+	0.985	0.545-1.780	0.959			
Vascular invasion	-/+	2.551	1.553-4.190	< 0.001[a]			NS
Liver capsule penetration	-/+	2.235	1.010-4.945	0.047[a]			NS
Bile duct invasion	-/+	3.200	0.986-10.385	0.053			
Margin status, mm	≥ 1 /< 1	3.793	2.079-6.920	< 0.001[a]	4.720	(2.458-9.063)	< 0.001[a]
AJCC stage	I-II/ IIIA-C	2.907	1.738-4.861	< 0.001[a]	3.262	(1.895-5.617)	< 0.001[a]
PGRMC1	H/L	1.918	1.145-3.213	0.013[a]	2.384	(1.377-4.128)	0.002[a]
PGRMC2	H/L	1.377	0.798-2.379	0.251			
ER	-/+	0.528	0.128-2.173	0.376			
PR	-/+	0.777	0.243-2.484	0.670			

[a]*P* < 0.05. DFS: Disease-free survival; AFP: Alpha-fetoprotein; AJCC: American Joint Committee on Cancer; H: High expression; L: Low expression.

according to the manufacturer's instructions (Corning, New York, NY, United States). A total of 5 × 10^4 cells in serum-free DMEM medium were split onto the upper Transwell chamber, the membrane of which was coated with (for invasion) or without (for migration) Matrigel (BD Biosciences, San Diego, CA, United States). The lower chamber was filled with DMEM containing 10% FBS as a chemoattractant. After incubation for 24 h at 37 ℃, non-invading cells on the upper side of the chamber were removed from the surface of the membrane by scrubbing, and the membrane was fixed with 4% paraformaldehyde for 10 min. The cells on the membrane were stained using crystal violet solution and detected *via* microscopy. Mean cell numbers were calculated from five random fields.

Statistical analysis

The correlations between PGRMC1 expression, PGRMC2 expression, viral infection status, and clinicopathological indicators were assessed using the Wilcoxon rank sum test, the χ^2 test, or Fisher's exact test, as appropriate. Paired data were analyzed using paired Student's *t*-tests or the Wilcoxon signed-rank test. For the *in vitro* experiments, a Student's *t*-test was used for simple comparisons. Data are presented as the mean ± SEM. DFS and OS were calculated using the Kaplan-Meier method, and the log-rank test was used to assess the differences between groups. A Cox proportional hazards regression model was used to measure the independence of different factors. A Cox regression was performed *via* a forward stepwise analysis, and only the prognostic variables that were significant in the univariate analysis were included in the model. *P* values less than 0.05 were considered statistically significant.

RESULTS

Identification and analysis of PGRMC1 and progesterone expression in HCC

The HCC tissue extract was resolved using SDS-PAGE. The protein spot located between 20 to 28 kDa was in-gel trypsinized and subjected to mass spectrometry (MS). PGRMC1 was detected using MS (Supplementary Table 1). We subsequently examined the expression of PGRMC1 in 10 paired tumor and non-tumor liver samples (7 males and 3 females) using Western blotting. Another membrane-associated progesterone receptor family member, PGRMC2 was also examined for comparison. The age of the patients ranged from 57 to 77 years. Expression of PGRMC1 and PGRMC2 was lower in all HCC samples compared with the corresponding non-tumor liver samples (Figure 1A). Furthermore, both PGRMC1 and PGRMC2 were highly expressed in the normal liver as was the case in the non-tumor liver samples (Supplementary Figure 1A).

Progesterone expression was also evaluated in the HCC patients (*n* = 10). Serum progesterone levels (mean: 0.276 ng/mL for male patients and 0.167 ng/mL for female patients) were within the 5th-95th physical range in men (0.2-1.4 ng/mL) and postmenopausal women (0.1-0.8 ng/mL) (Figure 1D). However, progesterone levels in the HCC tissue were significantly lower than in the non-tumor liver tissue (*P* = 0.007, Figure 1B and C).

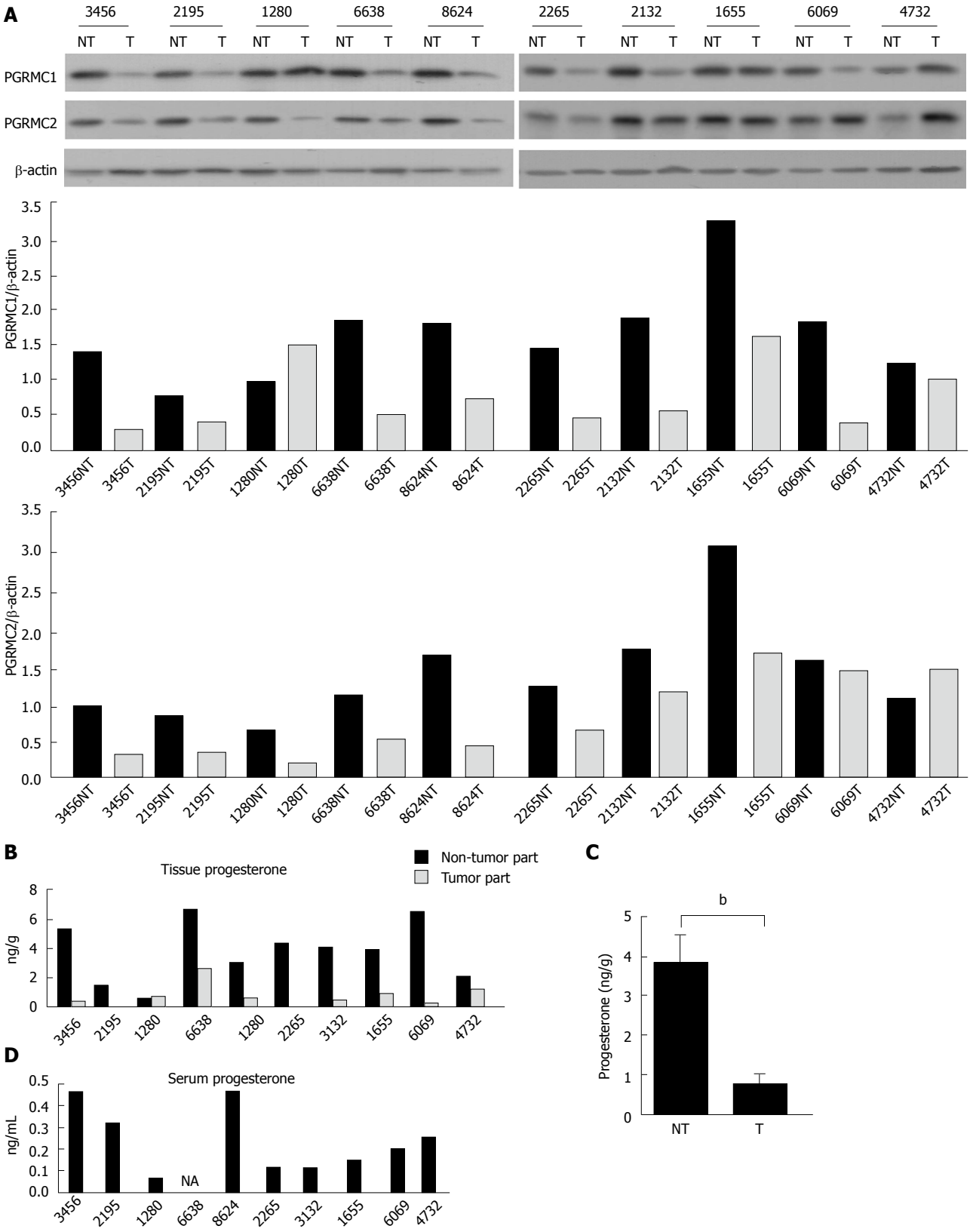

Figure 1 Western blot analysis of PGRMC1 and PGRMC2 expression in 10 paired hepatocellular carcinoma tumor (T)/non-tumor liver (NT) samples (A). B: Progesterone level in HCC tissue samples and non-tumor liver tissue; C: A comparison of progesterone levels in HCC (T) and non-tumor liver (NT) tissue samples; D: Serum progesterone level in the corresponding HCC patients. [b]$P < 0.01$.

Patient profiles

Immunohistochemical (IHC) staining for PGRMC1 and PGRMC2 was performed in the clinical cohort of 89 paired HCC and non-tumor liver samples. The profiles of the 89 patients are summarized in Supplementary Table 2. The patient population included 65 men and 24 women. The mean age was 55.2 years. The mean follow-up duration was 44.5 mo (range, 0.9-133.1

Table 2 Prognostic significance of clinicopathological indicators, *progesterone receptor membrane component 1* and *PGRMC2* for disease-free survival in The Cancer Genome Atlas cohort (*n* = 373)

Factor		DFS univariate			DFS multivariate		
	Group	HR	95%CI	*P* value	HR	95%CI	*P* value
Age, yr	< 60/≥ 60	1.019	0.756-1.373	0.903			
Sex	Male/female	1.157	0.845-1.585	0.364			
HCC risk factors				0.014[a]			< 0.001[a]
	B/NAFLD	1.433	0.601-3.414	0.417	2.903	(1.130-7.461)	0.027[a]
	B/Alcohol	1.449	0.948-2.217	0.087	1.002	(0.595-1.689)	0.993
	B/C	2.421	1.422-4.121	0.001[a]	3.368	(1.773-6.395)	< 0.001[a]
Child-Pugh score	A/B-C	1.332	0.709-2.504	0.372			
Cirrhosis	-/+	1.117	0.761-1.641	0.572			
Serum AFP, ng/ml	< 100/≥ 100	1.097	0.752-1.599	0.632			
Tumor grade	2/4/2001	1.330	0.868-2.038	0.191			
Vascular invasion	-/+	2.001	1.418-2.823	< 0.001[a]	3.040	(1.889-4.891)	< 0.001[a]
Residual tumor	-/+	1.733	0.938-3.200	0.079			
AJCC stage	Ⅰ-Ⅱ/Ⅲ-Ⅳ	2.354	1.693-3.272	< 0.001[a]	1.899	(1.107-3.255)	0.020[a]
PGRMC1	H/L	1.834	1.359-2.475	< 0.001[a]	2.857	(1.781-4.584)	< 0.001[a]
PGRMC2	H/L	1.242	0.923-1.671	0.152			

[a]*P* < 0.05. DFS: Disease-free survival; NAFLD: Non-alcoholic fatty liver disease; AFP: Alpha-fetoprotein; AJCC: American Joint Committee on Cancer; H: High expression; L: Low expression.

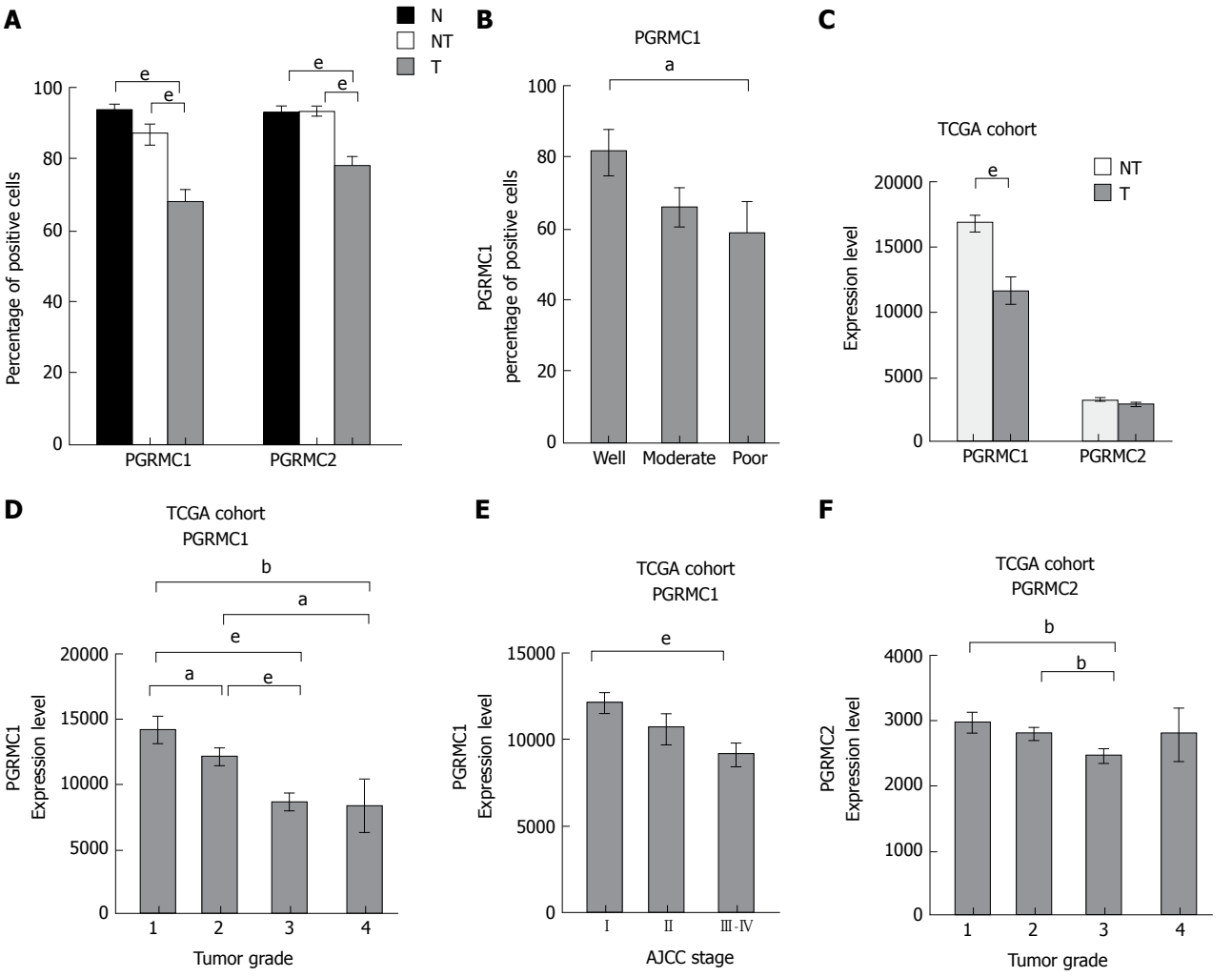

Figure 2 PGRMC1 and PGRMC2 expression levels, expressed as positive immunohistochemical staining percentages in the clinical cohort (A and B) and as normalized mRNA expression in the TCGA cohort (C-F). A: A comparison of PGRMC1 and PGRMC2 staining in HCC (T), non-tumor liver (NT) and normal liver (N) tissue samples; B: A comparison of PGRMC1 staining in HCC samples with different degrees of tumor differentiation; C: A comparison of PGRMC1 and PGRMC2 mRNA expression levels in HCC (T) and non-tumor liver (NT) samples; D: A comparison of PGRMC1 mRNA expression levels in HCC samples with different tumor grades; E: A comparison of PGRMC1 mRNA expression levels in HCC samples with different tumor stages; F: A comparison of PGRMC2 mRNA expression levels in HCC samples with different tumor grades. [a]*P* < 0.05, [b]*P* < 0.01, [e]*P* < 0.001.

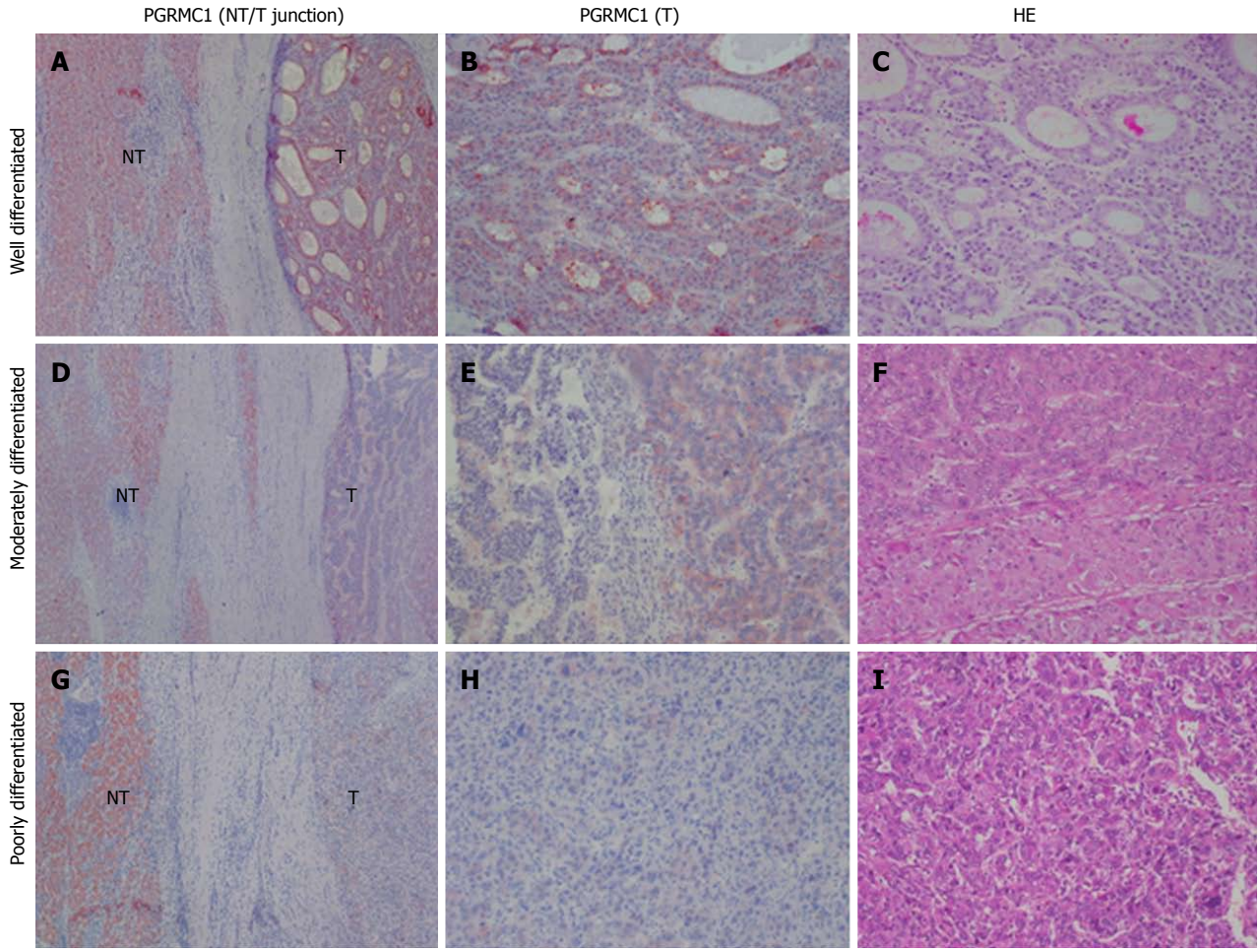

Figure 3 Representative images of PGRMC1 immunohistochemical staining in hepatocellular carcinoma. A-C: Well-differentiated HCC; D-F: Moderately differentiated HCC; G-I: Poorly differentiated HCC. Note that higher PGRMC1 expression was observed in non-tumor liver tissue samples (NT) as compared to HCC tissue samples (T) (A, D and G: 40 ×; B, C, E, F, H, and I: 100 ×).

mo). Sixty-seven patients (75.3%) developed local recurrence at a mean of 21.8 mo after surgery (range, 0.2-115.1 mo). A total of 45 patients (50.1%) died of HCC after having survived for a mean of 35.4 mo after surgery (range, 1.3-123.4 mo). The profiles of the 373 patients in the TCGA cohort are summarized in Supplementary Table 3.

The association of PGRMC1 and PGRMC2 expression with clinicopathological indicators

Few HCC cases expressed ER or PR (5.6% and 4.5%, respectively) (Supplementary Figure 2A-C). The mean cell percentage of ER expression was lower in the HCC tissue than in the non-tumor tissue (mean: 0.7% *vs* 12.4%, $P < 0.001$) (Supplementary Figure 2D). The mean cell percentage of PR expression was very low in the HCC tissue and non-tumor tissue (mean: 0.12% *vs* 0.01%, $P = 0.172$) (Supplementary Figure 2E). Positive IHC staining for PGRMC1 and PGRMC2 was observed in 80 (89.9%) and 89 (100%) cases of HCC, respectively. PGRMC1 (mean: 67.9% *vs* 86.9%, $P < 0.001$) and PGRMC2 (mean: 77.3% *vs* 92.6%, $P < 0.001$) were expressed at lower percentages in tumor cells than in non-tumor cells (Figure 2A, and 3, and Supplementary Figure 3). IHC expression of PGRMC1 and PGRMC2 in the normal liver tissue was not significantly different from that in the non-tumor liver samples, a result consistent with the Western blot experiment (Figure 2A and Supplementary Figure 1B and 1C). The PGRMC1 and PGRMC2 expression levels were compared among the normal livers of healthy persons, non-cirrhotic livers, and cirrhotic livers of HCC patients (Supplementary Figure 4A and B). There were no significant differences between the liver samples of healthy persons and those of HCC patients. In both non-cirrhotic patients and cirrhotic patients, the PGRMC1 and PGRMC2 expression levels were downregulated in the HCC tissue compared to non-tumor liver tissue (Supplementary Figure 4C-F). In the TCGA cohort, the HCC tissue samples exhibited lower *PGRMC1* mRNA expression levels than in the non-tumor tissue samples ($P < 0.001$), while *PGRMC2* levels between the HCC and non-tumor livers were not significantly different (Figure 2C).

Lower PGRMC1 expression in HCC was associated with poor HCC differentiation ($P = 0.045$) (Figure 2B

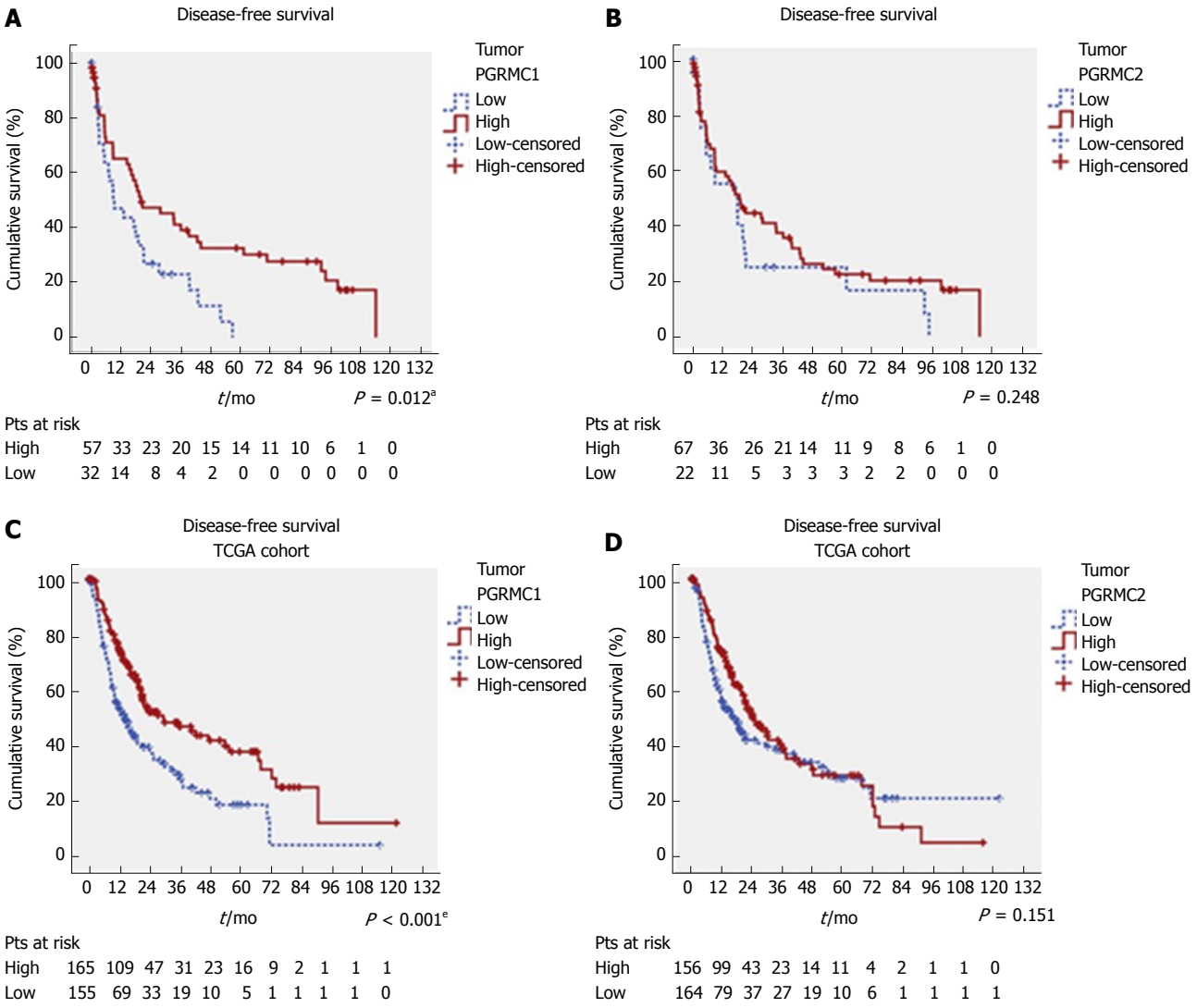

Figure 4 Kaplan-Meier analysis of the relationships of PGRMC1 and PGRMC2 expression with disease-free survival (DFS) in the clinical cohort (A-B) and TCGA cohort (C-D). [a]*P* < 0.05, [e]*P* < 0.001.

and Figure 3), younger age (*P* = 0.016), higher serum alpha-fetoprotein (AFP) levels (*P*=0.004), and liver capsule penetration (*P* = 0.038) (Supplementary Table 4). Lower PGRMC2 expression in HCC was significantly associated with tumor capsular invasion (*P* = 0.048), liver capsule penetration (*P* = 0.035), and bile duct invasion (*P* = 0.032) (Supplementary Table 4). In the TCGA cohort, lower *PGRMC1* expression in HCC was associated with higher tumor grade (*P* < 0.001) (Figure 2D), younger age (*P* = 0.014), female gender (*P* = 0.015), higher serum AFP expression (*P* < 0.001), vascular invasion (*P* = 0.007), and higher AJCC stage (Figure 2E) (*P* = 0.002) (Supplementary Table 5). Lower *PGRMC2* expression in HCC was significantly associated with higher tumor grade (*P* = 0.022) (Figure 2F) and younger age (*P* = 0.006) (Supplementary Table 5). Female patients exhibited higher baseline non-tumor liver tissue *PGRMC1* expression in the TCGA cohort (*P* < 0.001) (Supplementary Figure 5A-D). Using corresponding non-tumor liver tissue samples as a reference, it was determined that female HCC patients in the TCGA cohort exhibited greater *PGRMC1* down-regulation than male patients (Supplementary Figure 5E-H).

Prognostic significance of PGRMC1 and PGRMC2 in HCC

Low IHC PGRMC1 expression in HCC was significantly associated with worse DFS (*P* = 0.012) (Figure 4A), but was not significantly associated with OS (*P* = 0.395) (Supplementary Figure 6A). In contrast, PGRMC2 expression was not correlated with survival status (Figure 4B and Supplementary Figure 6B). The univariate analysis showed that the Child-Pugh scores (*P* = 0.003), satellite lesions (*P* = 0.003), tumor size (*P* < 0.001), vascular invasion (*P* < 0.001), liver capsule perforation (*P* = 0.047), insufficient surgical margins (*P* < 0.001), AJCC stage (*P* < 0.001), and low PGRMC1 expression (*P* = 0.013) were significant predictors of worse DFS (Table 1). The multivariate analysis showed that the Child-Pugh scores (*P* = 0.024, HR = 2.005, CI: 1.097-3.665), surgical margins (*P* < 0.001, HR =

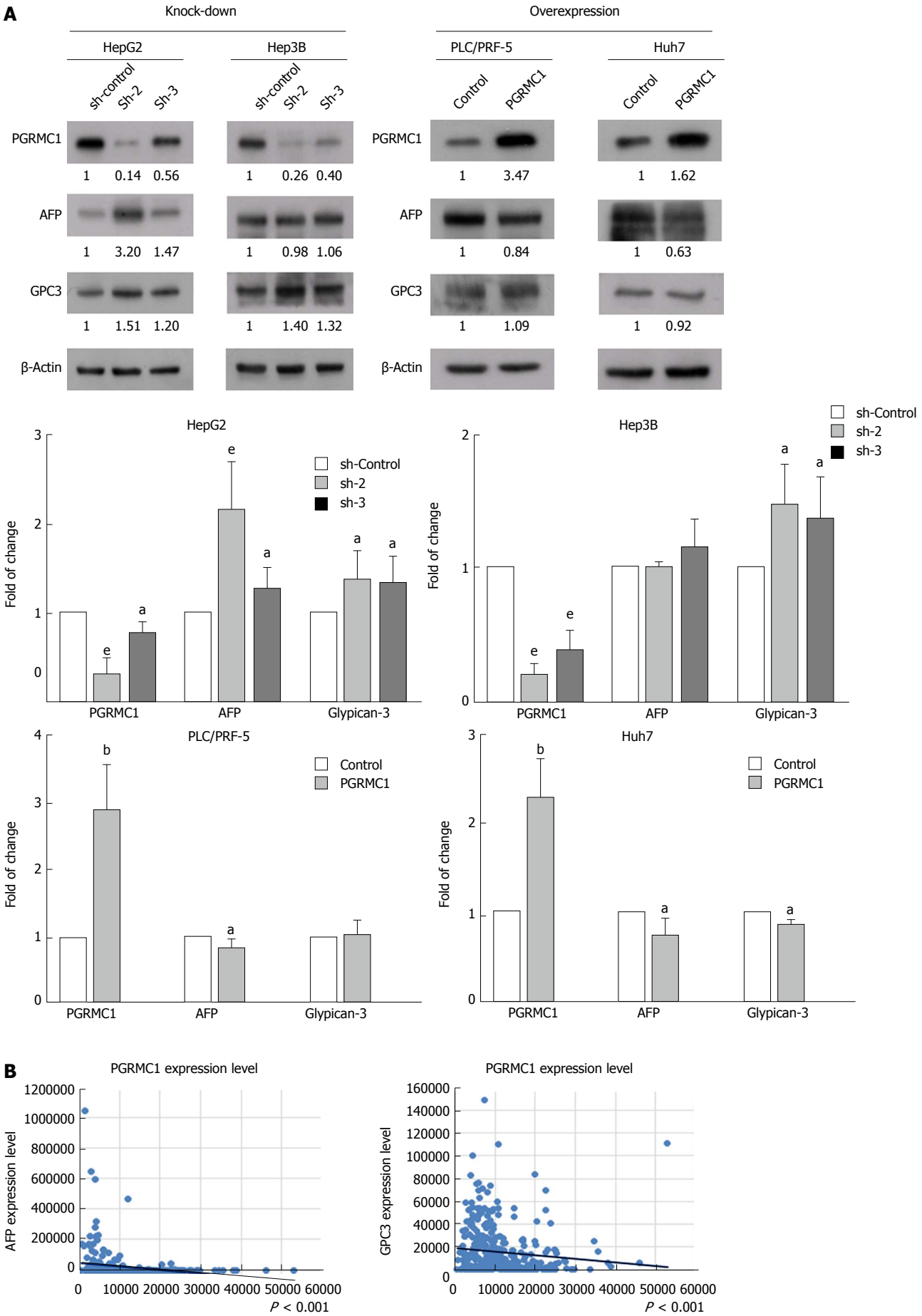
A
Knock-down
Overexpression
HepG2
Hep3B
PLC/PRF-5
Huh7
sh-control
Sh-2
Sh-3
Control
PGRMC1
PGRMC1
AFP
GPC3
β-Actin
1 0.14 0.56
1 0.26 0.40
1 3.47
1 1.62
1 3.20 1.47
1 0.98 1.06
1 0.84
1 0.63
1 1.51 1.20
1 1.40 1.32
1 1.09
1 0.92
HepG2
Hep3B
PLC/PRF-5
Huh7
sh-Control
sh-2
sh-3
Control
PGRMC1
Fold of change
PGRMC1
AFP
Glypican-3
B
PGRMC1 expression level
AFP expression level
GPC3 expression level
0 10000 20000 30000 40000 50000 60000
P < 0.001

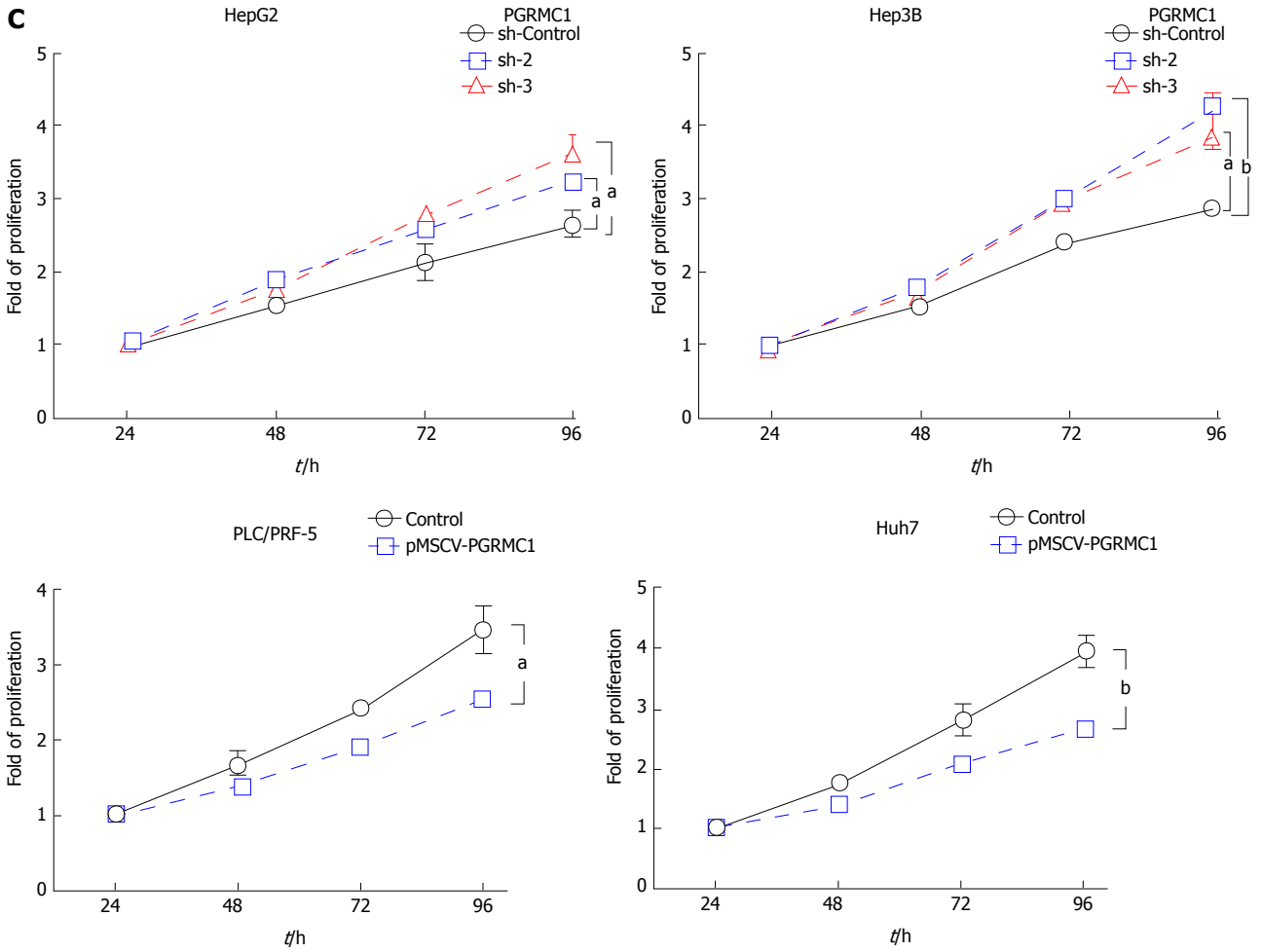

Figure 5 Alpha-fetoprotein and glypican-3 expression in PGRMC1-knockdown HepG2 and Hep3B cells and PGRMC1-overxpressing PLC/PRF/5 and Huh7 cells (A). B: The correlation of PGRMC1 with AFP and GPC3 in HCC tissue samples in the TCGA cohort; C: Cell proliferation assay (XTT) of PGRMC1-knockdown HepG2 and Hep3B cells and PGRMC1-overxpressing PLC/PRF/5 and Huh7 cells. The experiment was performed in triplicate. $^{a}P < 0.05$, $^{b}P < 0.01$, $^{e}P < 0.001$. AFP: Alpha-fetoprotein; GPC3: Glypican-3.

4.720, CI: 2.458-9.063), AJCC stage ($P < 0.001$, HR = 3.262, CI: 1.895-5.617), and low PGRMC1 expression ($P = 0.002$, HR = 2.384, CI: 1.377-4.128) were independently associated with DFS (Table 1).

To validate our findings, we analyzed the TCGA cohort data. Patients with low *PGRMC1* expression consistently exhibited worse DFS ($P < 0.001$) and OS than those with high *PGRMC1* expression ($P = 0.013$), as determined by the Kaplan-Meier and log-rank test analyses (Figure 4C and Supplementary Figure 6C). *PGRMC2* expression was not correlated with survival status (Figure 4D and Supplementary Figure 6D). The univariate analysis showed that HCC risk factors ($P = 0.014$), vascular invasion ($P < 0.001$), AJCC stage ($P < 0.001$), and low *PGRMC1* expression ($P < 0.001$) were significant predictors of worse DFS (Table 2), and that AJCC stage ($P < 0.001$) and low *PGRMC1* expression ($P = 0.014$) were significant predictors of worse OS (Supplementary Table 6). The multivariate analysis showed that low *PGRMC1* expression was an independent predictor of both worse DFS ($P < 0.001$, HR = 2.857, CI: 1.781-4.584) and worse OS ($P = 0.020$, HR = 1.556, CI: 1.072-2.260) (Table 2 and Supplementary Table 6).

Effects of PGRMC1 on proliferation, differentiation, migration and invasion of HCC cells

As PGRMC1 was significantly associated with HCC prognosis, we examined its biological significance *in vitro*. HepG2 and Hep3B cells exhibited higher PGRMC1 expression than PLC/PRF/5 and Huh7 cells. Therefore, we knocked down PGRMC1 in HepG2 and Hep3B cells and overexpressed PGRMC1 in PLC/PRF/5 and Huh7 cells (Figure 5A). Both AFP and glypican-3 (GPC3) are well-known oncofetal proteins in malignant transformation and dedifferentiation of HCC. Higher expression of these markers has been associated with poor differentiation of HCC[18,19]. Knockdown of PGRMC1 resulted in increased expression of AFP and GPC3 in HepG2 cells, while GPC3 expression was increased in Hep3B cells (Figure 5A). In contrast, overexpression of PGRMC1 suppressed expression of AFP in PLC/PRF/5 cells and suppressed expression of AFP and GPC3 in Huh7 cells (Figure 5A). In addition, PGRMC1

expression was inversely correlated with AFP and GPC3 expression in the HCC tissue samples (Figure 5B) and serum AFP levels (Supplementary Tables 4 and 5). PGRMC1 knockdown resulted in significantly increased proliferation of HepG2 and Hep3B cells (Figure 5C). In contrast, PGRMC1 overexpression resulted in decreased proliferation of PLC/PRF/5 and Huh7 cells (Figure 5C). PGRMC1 did not have significant effects on cell migration and invasion (Supplementary Figure 7).

As PGRMC1 was downregulated in HCC and it has been suggested that it mediates the anti-proliferative effects of progesterone[12,13], we assessed if overexpression of PGRMC1 in HCC cells could increase the anti-proliferative effect under progesterone treatment. PGRMC1 overexpression resulted in a significant decrease in the proliferation of PLC/PRF-5 cells and Huh7 cells in response to progesterone treatment (10^{-6} mol/L) (Supplementary Figure 8A and B). Expression of PR was not increased in these cells (Supplementary Figure 8C). On this basis, it is suggested that a more plausible explanation for the significant progesterone treatment effect on PGRMC1-overexpressing PLC/PRF-5 and Huh7 cells may be the overexpression of PGRMC1 *per se* rather than upregulated PR in these cells.

DISCUSSION

In this study, few HCC cases expressed ER and PR (5.6% and 4.5%, respectively), implying that an alternative hormone-related event may be involved in this sexually dimorphic malignancy. Both PGRMC1 and PGRMC2 were expressed in normal liver and non-tumor liver, but were down-regulated in HCC. In addition, the level of progesterone was lower in the HCC as compared to the non-tumor liver, suggesting that progesterone-related signaling is down-regulated in the pathogenesis of HCC. As down-regulated PGRMC1 and PGRMC2 were correlated with poorer differentiation and higher tumor grading, PGRMC down-regulation may play an important role in the progression of hepatocarcinogenesis. PGRMC1 differs from PGRMC2 in the transmembrane domain, N-terminals and SH3 target sequence, resulting in different interaction partners in terms of connecting with the cellular membrane, organelles and cell signaling molecules[8]. PGRMC1 has been proposed as a sigma-2 receptor with capability to inhibit tumor growth[20-22]. In our study, PGRMC1 was inversely associated with AFP and AJCC stage compared with PGRMC2. In multivariate analysis, PGRMC1 was an independent parameter in predicting better patient survival in two different cohorts. Therefore, only PGRMC1 was proved to be a prognostic biomarker in HCC. All of our patients had HBV and/or HCV infections, while more than half of the patients in the TCGA cohort had alcoholic and/or non-alcoholic fatty liver disease, suggesting that the findings of this investigation are universal. Together, PGRMCs, especially PGRMC1, may play a protective role in liver tumorigenesis.

Experiments *in vitro* demonstrated that PGRMC1 knockdown results in a poorly differentiated phenotype of HCC cells and increased proliferation. PGRMC1 contains two SH2 target sequences, an SH3 target sequence, a tyrosine kinase target site, two acidophilic kinase target sites, and ERK1 and PDK1 consensus binding sites[8]. A prior report showed that PGRMC1 can interact with beta-tubulin and inhibit mitosis by increasing mitotic spindle stability[13]. PGRMC1 protein has also been proposed as a sigma-2 receptor binding site[20], and activation of the sigma-2 receptor can inhibit tumor growth[21,22]. Thus, PGRMC1 is speculated to inhibit HCC progression through activation of hormone-independent signaling events.

PGRMC1 contains a motif common to heme-binding proteins, suggesting a role in oxidative metabolism[23]. Free heme, *i.e.,* heme not appropriately bound by hemoproteins or heme-binding proteins, is a powerful pro-oxidant agent and therefore potentially toxic[24]. Heme-binding proteins are required to maintain cellular stasis and to detoxify cells. Excessive heme iron has been reported to increase the risk of several types of cancer, such as colon cancer[25], gastric cancer[26], esophageal cancer[27], and HCC[28]. As a heme-binding protein, PGRMC1 has been reported to interact with P450 proteins and protect cells from DNA damage[29-31]. Therefore, PGRMC1 may protect hepatocytes from oxidative stress and suppress carcinogenesis by appropriate heme delivery or heme containment.

Most prior PGRMC1 studies have been focused on the female genital organs or female-related cancers. PGRMCs are involved in regulating the menstrual cycle and ovarian granulosa cell function by acting as progesterone receptors[9,32]. Endometrial expression of PGRMC1 in menstrual cycling is most abundant during the proliferative phase, while expression of PGRMC2 is highest during the secretory phase. These results highlight the differences between PGRMC1 and PGRMC2 in response to steroid hormones[32]. Previous reports showed that PGRMC1 mediates the anti-mitotic actions of progesterone in endometrial and ovarian cancer cells[12,13,33]. In immortalized granulosa cells, PGRMC1 suppresses cell cycle entry by binding to the GTPase activating protein binding protein 2[33]. PGRMC1 also suppresses the T-cell-specific transcription factor/lymphoid enhancer factor (Tcf/Lef) and its downstream c-myc activity in ovarian granulosa cells[9]. In this investigation, we provide evidence that overexpression of PGRMC1 may also activate the non-classical PR pathway in tumorigenesis. The potential of PGRMC1 being an alternative target for auxiliary anti-HCC treatment deserves further investigation.

Previous studies have shown that high levels of progesterone can be observed in patients with cirrhosis[34]. This is likely due to impairment of progesterone metabolism in the liver. It is controversial whether high levels of progesterone are associated with premalignant cirrhosis. Previous studies have shown that the occurrence of natural menopause at a younger

age or oophorectomy performed at age 50 or younger is associated with increased risk of HCC[4,35]. PR expression in HCC has been correlated with a better prognosis[36]. These findings suggest that progesterone may be protective against HCC. Furthermore, progesterone can serve as the precursor for the major steroid hormones (androgens, estrogens, and corticosteroids). The oncogenic effects of androgen and the protective effects of estrogen and progesterone in liver may also depend on the hormonal receptors expressed on hepatocytes or cancer cells[4].

Sex hormones can exert different tumorigenic properties depending on the tissue type. For example, contrary to their hypothetical protective role in liver cancer development, chronic exposure to estrogens favors carcinogenesis in the breast and uterus. Expression of PGRMC1 was shown to be upregulated in breast cancer and ovarian cancer and was found to be associated with advanced stage or poor prognosis[10,11]. Its expression was more often detected in ER-negative breast cancers[10], and it may act *via* cross-talk with nuclear or extranuclear ER receptors[37]. PGRMC1 has been localized in hypoxic areas of breast cancer[10] and demonstrated to activate the expression of vascular endothelial growth factor in glial cells[38]. A D120G mutant of PGRMC1 increased the susceptibility of breast cancer cells to doxorubicin and camptothecin treatment[39]. However, PGRMC1 has been reported to be associated with EGFR in lung cancer cells and to enhance susceptibility to the EGFR inhibitor, erlotinib[40]. Overexpression of PGRMC1 in the MCF-7 breast cancer cell line sensitizes cancer cells to hydrogen peroxide treatment with corresponding hyperphosphorylation of Akt and IkB proteins[29]. These findings suggest that PGRMC1 plays a plethora of biological roles in human cancers. In contrast to breast and ovarian cancer, PGRMC1 is downregulated in HCC. PGRMC1 is located on chromosome Xq22-q24. A prior genomic study found a frequent loss of heterozygosity of Xq (43%) in HCC[41] with a progressive increase in fractional allelic imbalance from cirrhotic nodules at progressive stages (11%-57%) to HCC, suggesting its involvement in hepatocarcinogenesis. Furthermore, let-7/miR-98 was reported to repress PGRMC1[42,43], and gradually elevated miR-98 has been associated with the progression of liver cancer[44]. Therefore, microRNA could be an alternative regulatory mechanism in suppression of PGRMC1 expression. Further study is needed to clarify the mechanisms of PGRMC downregulation in HCC.

Overall, men are two to four times more likely to develop HCC than women[1]. Estrogen has been shown to inhibit IL-6 production[45]. Foxa1/a2 may interact with either the ER or AR to activate different hepatocyte target genes[46]. HBx can increase AR N-terminal transactivation domain activation through c-Src kinase and enhance AR dimerization by inhibiting GSK-3 activity[47]. This information may explain, in part, the molecular mechanisms underlying gender differences in HCC development. Female patients in the current study exhibited higher baseline non-tumor liver tissue *PGRMC1* mRNA expression and greater HCC *PGRMC1* down-regulation than male patients, suggesting that greater PGRMC1 down-regulation is needed to induce HCC transformation in female patients, thus causing the gender disparities associated with HCC development.

In conclusion, expression of PGRMC1 and PGRMC2 was suppressed in HCC, and PGRMC1 down-regulation promoted HCC progression. PGRMC1 may play a protective role in hepatocarcinogenesis by inhibiting cell proliferation and tumor dedifferentiation. Further study is necessary to evaluate the potential of targeting PGRMC1 in HCC treatment.

ARTICLE HIGHLIGHTS

Research background

Hepatocellular carcinoma (HCC) is a sexually dimorphic disease with a significantly higher incidence in males than females. The androgen receptor appears to function as a tumor promoter, whereas the estrogen receptor appears to act as a tumor suppressor for HCC. Whether additional hormone-related events are implicated in the pathogenesis of HCC remain to be clarified.

Research motivation

The membrane-associated progesterone receptors, *i.e.* PGRMC1 and PGRMC2, have been investigated in female cancers of the breast, endometrium and ovary. PGRMC1 is thought to coordinate non-classical progesterone signaling. PGRMC1 was demonstrated to mediate the anti-mitotic actions of progesterone in endometrial and ovarian cancer cells. This study was performed to examine the significance of PGRMC1 and/or PGRMC2 in the progression of HCC.

Research objectives

The aim of this study was to clarify the potential significance of PGRMCs as prognostic biomarkers in HCC and their biological effects *in vitro*.

Research methods

Immunohistochemical staining of the estrogen receptor (ER), progesterone receptor (PR), PGRMC1 and PGRMC2 was performed in a clinical cohort consisting of 89 cases of paired HCC and non-tumor liver. The clinical implications of PGRMCs in HCC (n = 373) from The Cancer Genome Atlas (TCGA) database were *also analyzed*. The expression of PGRMC1 and PGRMC2 was correlated with clinicopathological indicators and the clinical outcome of HCC patients. The impact of PGRMC1 on the biological effects of HCC was investigated by knocking down its expression in HepG2 and Hep3B cell lines, and overexpressing in PLC/PRF-5 and Huh7 cell lines. The analyzed cellular functions included proliferation, differentiation, migration, and invasion.

Research results

Primary HCC demonstrated a high incidence of PGRMC1 (89.9%) and PGRMC2 (100%) expression, respectively. Down-regulated PGRMC1 was significantly associated with higher serum alpha-fetoprotein levels, poor tumor differentiation, liver capsule penetration, and the risk of recurrence. Low PGRMC1 expression was an independent indicator of worse disease-free survival. Knock-down of PGRMC1 promoted a poorly differentiated phenotype and proliferation of HCC *in vitro*, while over-expression of PGRMC1 suppressed cell proliferation.

Research conclusions

PGRMC1 is a prognostic marker for HCC. PGRMC1 may play a protective role in hepatocarcinogenesis by inhibiting cell proliferation and tumor

dedifferentiation.

Research perspectives

PGRMC1 could be a novel therapeutic target for human HCC, especially as a biotarget of chemoprevention.

ACKNOWLEDGEMENTS

We are grateful for the support from the Human Biobank, Research Center of Clinical Medicine and the Cancer Data Bank of National Cheng Kung University Hospital.

REFERENCES

1 **El-Serag HB**, Rudolph KL. Hepatocellular carcinoma: epidemiology and molecular carcinogenesis. *Gastroenterology* 2007; **132**: 2557-2576 [PMID: 17570226 DOI: 10.1053/j.gastro.2007.04.061]
2 **Ma WL**, Hsu CL, Yeh CC, Wu MH, Huang CK, Jeng LB, Hung YC, Lin TY, Yeh S, Chang C. Hepatic androgen receptor suppresses hepatocellular carcinoma metastasis through modulation of cell migration and anoikis. *Hepatology* 2012; **56**: 176-185 [PMID: 22318717 DOI: 10.1002/hep.25644]
3 **Keng VW**, Largaespada DA, Villanueva A. Why men are at higher risk for hepatocellular carcinoma? *J Hepatol* 2012; **57**: 453-454 [PMID: 22425699 DOI: 10.1016/j.jhep.2012.03.004]
4 **Yeh YT**, Chang CW, Wei RJ, Wang SN. Progesterone and related compounds in hepatocellular carcinoma: basic and clinical aspects. *Biomed Res Int* 2013; **2013**: 290575 [PMID: 23484104 DOI: 10.1155/2013/290575]
5 **Chang WT**, Hsieh BS, Cheng HL, Lee KT, Chang KL. Progesterone augments epirubicin-induced apoptosis in HA22T/VGH cells by increasing oxidative stress and upregulating Fas/FasL. *J Surg Res* 2014; **188**: 432-441 [PMID: 24594218 DOI: 10.1016/j.jss.2014.01.063]
6 **Chang WT**, Cheng HL, Hsieh BS, Chiu CC, Lee KT, Chang KL. Progesterone increases apoptosis and inversely decreases autophagy in human hepatoma HA22T/VGH cells treated with epirubicin. *ScientificWorldJournal* 2014; **2014**: 567148 [PMID: 24971383 DOI: 10.1155/2014/567148]
7 **Villa E**, Ferretti I, Grottola A, Buttafoco P, Buono MG, Giannini F, Manno M, Bertani H, Dugani A, Manenti F. Hormonal therapy with megestrol in inoperable hepatocellular carcinoma characterized by variant oestrogen receptors. *Br J Cancer* 2001; **84**: 881-885 [PMID: 11286465 DOI: 10.1054/bjoc.2000.1534]
8 **Cahill MA**. Progesterone receptor membrane component 1: an integrative review. *J Steroid Biochem Mol Biol* 2007; **105**: 16-36 [PMID: 17583495 DOI: 10.1016/j.jsbmb.2007.02.002]
9 **Peluso JJ**, Pru JK. Non-canonical progesterone signaling in granulosa cell function. *Reproduction* 2014; **147**: R169-R178 [PMID: 24516175 DOI: 10.1530/REP-13-0582]
10 **Neubauer H**, Clare SE, Wozny W, Schwall GP, Poznanovic S, Stegmann W, Vogel U, Sotlar K, Wallwiener D, Kurek R, Fehm T, Cahill MA. Breast cancer proteomics reveals correlation between estrogen receptor status and differential phosphorylation of PGRMC1. *Breast Cancer Res* 2008; **10**: R85 [PMID: 18922159 DOI: 10.1186/bcr2155]
11 **Peluso JJ**, Liu X, Saunders MM, Claffey KP, Phoenix K. Regulation of ovarian cancer cell viability and sensitivity to cisplatin by progesterone receptor membrane component-1. *J Clin Endocrinol Metab* 2008; **93**: 1592-1599 [PMID: 18319313 DOI: 10.1210/jc.2007-2771]
12 **Friel AM**, Zhang L, Pru CA, Clark NC, McCallum ML, Blok LJ, Shioda T, Peluso JJ, Rueda BR, Pru JK. Progesterone receptor membrane component 1 deficiency attenuates growth while promoting chemosensitivity of human endometrial xenograft tumors. *Cancer Lett* 2015; **356**: 434-442 [PMID: 25304370 DOI: 10.1016/j.canlet.2014.09.036]
13 **Lodde V**, Peluso JJ. A novel role for progesterone and progesterone receptor membrane component 1 in regulating spindle microtubule stability during rat and human ovarian cell mitosis. *Biol Reprod* 2011; **84**: 715-722 [PMID: 21148105 DOI: 10.1095/biolreprod.110.088385]
14 **Hirai Y**, Utsugi K, Takeshima N, Kawamata Y, Furuta R, Kitagawa T, Kawaguchi T, Hasumi K, Noda T. Putative gene loci associated with carcinogenesis and metastasis of endocervical adenocarcinomas of uterus determined by conventional and array-based CGH. *Am J Obstet Gynecol* 2004; **191**: 1173-1182 [PMID: 15507938 DOI: 10.1016/j.ajog.2004.04.015]
15 **Albrecht C**, Huck V, Wehling M, Wendler A. In vitro inhibition of SKOV-3 cell migration as a distinctive feature of progesterone receptor membrane component type 2 versus type 1. *Steroids* 2012; **77**: 1543-1550 [PMID: 23064006 DOI: 10.1016/j.steroids.2012.09.006]
16 **Lee NP**, Chen L, Lin MC, Tsang FH, Yeung C, Poon RT, Peng J, Leng X, Beretta L, Sun S, Day PJ, Luk JM. Proteomic expression signature distinguishes cancerous and nonmalignant tissues in hepatocellular carcinoma. *J Proteome Res* 2009; **8**: 1293-1303 [PMID: 19161326 DOI: 10.1021/pr800637z]
17 **Bosman FT**, Carneiro F, Hruban RH, Theise ND. WHO classification of Tumours of the Digestive System. Lyon: International Agency for Research on Cancer, 2010
18 **Shafizadeh N**, Ferrell LD, Kakar S. Utility and limitations of glypican-3 expression for the diagnosis of hepatocellular carcinoma at both ends of the differentiation spectrum. *Mod Pathol* 2008; **21**: 1011-1018 [PMID: 18536657 DOI: 10.1038/modpathol.2008.85]
19 **Liu C**, Xiao GQ, Yan LN, Li B, Jiang L, Wen TF, Wang WT, Xu MQ, Yang JY. Value of α-fetoprotein in association with clinicopathological features of hepatocellular carcinoma. *World J Gastroenterol* 2013; **19**: 1811-1819 [PMID: 23555170 DOI: 10.3748/wjg.v19.i11.1811]
20 **Xu J**, Zeng C, Chu W, Pan F, Rothfuss JM, Zhang F, Tu Z, Zhou D, Zeng D, Vangveravong S, Johnston F, Spitzer D, Chang KC, Hotchkiss RS, Hawkins WG, Wheeler KT, Mach RH. Identification of the PGRMC1 protein complex as the putative sigma-2 receptor binding site. *Nat Commun* 2011; **2**: 380 [PMID: 21730960 DOI: 10.1038/ncomms1386]
21 **Hornick JR**, Spitzer D, Goedegebuure P, Mach RH, Hawkins WG. Therapeutic targeting of pancreatic cancer utilizing sigma-2 ligands. *Surgery* 2012; **152**: S152-S156 [PMID: 22763259 DOI: 10.1016/j.surg.2012.05.014]
22 **Huang YS**, Lu HL, Zhang LJ, Wu Z. Sigma-2 receptor ligands and their perspectives in cancer diagnosis and therapy. *Med Res Rev* 2014; **34**: 532-566 [PMID: 23922215 DOI: 10.1002/med.21297]
23 **Mifsud W**, Bateman A. Membrane-bound progesterone receptors contain a cytochrome b5-like ligand-binding domain. *Genome Biol* 2002; **3**: RESEARCH0068 [PMID: 12537557]
24 **Correia MA**, Sinclair PR, De Matteis F. Cytochrome P450 regulation: the interplay between its heme and apoprotein moieties in synthesis, assembly, repair, and disposal. *Drug Metab Rev* 2011; **43**: 1-26 [PMID: 20860521 DOI: 10.3109/03602532.2010.515222]
25 **Bastide NM**, Pierre FH, Corpet DE. Heme iron from meat and risk of colorectal cancer: a meta-analysis and a review of the mechanisms involved. *Cancer Prev Res* (Phila) 2011; **4**: 177-184 [PMID: 21209396 DOI: 10.1158/1940-6207.CAPR-10-0113]
26 **Jakszyn P**, Agudo A, Lujan-Barroso L, Bueno-de-Mesquita HB, Jenab M, Navarro C, Palli D, Boeing H, Manjer J, Numans ME, Igali L, Boutron-Ruault MC, Clavel-Chapelon F, Morois S, Grioni S, Panico c, Tumino R, Sacerdote C, Quirós JR, Molina-Montes E, Huerta Castaño JM, Barricarte A, Amiano P, Khaw KT, Wareham N, Allen NE, Key TJ, Jeurnink SM, Peeters PH, Bamia C, Valanou E, Trichopoulou A, Kaaks R, Lukanova A, Bergmann MM, Lindkvist B, Stenling R, Johansson I, Dahm CC, Overvad K, Olsen A, Tjonneland A, Skeie G, Broderstad AR, Lund E, Michaud DS, Mouw T, Riboli E, González CA. Dietary intake of heme iron and risk of gastric cancer in the European prospective investigation into cancer and nutrition study. *Int J Cancer* 2012; **130**: 2654-2663

[PMID: 21717452 DOI: 10.1002/ijc.26263]
27 **Ward MH**, Cross AJ, Abnet CC, Sinha R, Markin RS, Weisenburger DD. Heme iron from meat and risk of adenocarcinoma of the esophagus and stomach. *Eur J Cancer Prev* 2012; **21**: 134-138 [PMID: 22044848 DOI: 10.1097/CEJ.0b013e32834c9b6c]
28 **Freedman ND**, Cross AJ, McGlynn KA, Abnet CC, Park Y, Hollenbeck AR, Schatzkin A, Everhart JE, Sinha R. Association of meat and fat intake with liver disease and hepatocellular carcinoma in the NIH-AARP cohort. *J Natl Cancer Inst* 2010; **102**: 1354-1365 [PMID: 20729477 DOI: 10.1093/jnci/djq301]
29 **Hand RA**, Craven RJ. Hpr6.6 protein mediates cell death from oxidative damage in MCF-7 human breast cancer cells. *J Cell Biochem* 2003; **90**: 534-547 [PMID: 14523988 DOI: 10.1002/jcb.10648]
30 **Hughes AL**, Powell DW, Bard M, Eckstein J, Barbuch R, Link AJ, Espenshade PJ. Dap1/PGRMC1 binds and regulates cytochrome P450 enzymes. *Cell Metab* 2007; **5**: 143-149 [PMID: 17276356 DOI: 10.1016/j.cmet.2006.12.009]
31 **Mallory JC**, Crudden G, Johnson BL, Mo C, Pierson CA, Bard M, Craven RJ. Dap1p, a heme-binding protein that regulates the cytochrome P450 protein Erg11p/Cyp51p in Saccharomyces cerevisiae. *Mol Cell Biol* 2005; **25**: 1669-1679 [PMID: 15713626 DOI: 10.1128/MCB.25.5.1669-1679.2005]
32 **Pru JK**, Clark NC. PGRMC1 and PGRMC2 in uterine physiology and disease. *Front Neurosci* 2013; **7**: 168 [PMID: 24065879 DOI: 10.3389/fnins.2013.00168]
33 **Peluso JJ**, Griffin D, Liu X, Horne M. Progesterone receptor membrane component-1 (PGRMC1) and PGRMC-2 interact to suppress entry into the cell cycle in spontaneously immortalized rat granulosa cells. *Biol Reprod* 2014; **91**: 104 [PMID: 25253729 DOI: 10.1095/biolreprod.114.122986]
34 **Farinati F**, De Maria N, Marafin C, Fagiuoli S, Della Libera G, Naccarato R. Hepatocellular carcinoma in alcoholic cirrhosis: is sex hormone imbalance a pathogenetic factor? *Eur J Gastroenterol Hepatol* 1995; **7**: 145-150 [PMID: 7712307]
35 **Yu MW**, Chang HC, Chang SC, Liaw YF, Lin SM, Liu CJ, Lee SD, Lin CL, Chen PJ, Lin SC, Chen CJ. Role of reproductive factors in hepatocellular carcinoma: Impact on hepatitis B- and C-related risk. *Hepatology* 2003; **38**: 1393-1400 [PMID: 14647050 DOI: 10.1016/j.hep.2003.09.041]
36 **Vizoso FJ**, Rodriguez M, Altadill A, González-Diéguez ML, Linares A, González LO, Junquera S, Fresno-Forcelledo F, Corte MD, Rodrigo L. Liver expression of steroid hormones and Apolipoprotein D receptors in hepatocellular carcinoma. *World J Gastroenterol* 2007; **13**: 3221-3227 [PMID: 17589901 DOI: 10.3748/wjg.v13.i23.3221]
37 **Schneck H**, Ruan X, Seeger H, Cahill MA, Fehm T, Mueck AO, Neubauer H. Membrane-receptor initiated proliferative effects of dienogest in human breast cancer cells. *Gynecol Endocrinol* 2013; **29**: 160-163 [PMID: 23116217 DOI: 10.3109/09513590.2012.730572]
38 **Swiatek-De Lange M**, Stampfl A, Hauck SM, Zischka H, Gloeckner CJ, Deeg CA, Ueffing M. Membrane-initiated effects of progesterone on calcium dependent signaling and activation of VEGF gene expression in retinal glial cells. *Glia* 2007; **55**: 1061-1073 [PMID: 17551930 DOI: 10.1002/glia.20523]
39 **Crudden G**, Chitti RE, Craven RJ. Hpr6 (heme-1 domain protein) regulates the susceptibility of cancer cells to chemotherapeutic drugs. *J Pharmacol Exp Ther* 2006; **316**: 448-455 [PMID: 16234411 DOI: 10.1124/jpet.105.094631]
40 **Ahmed IS**, Rohe HJ, Twist KE, Craven RJ. Pgrmc1 (progesterone receptor membrane component 1) associates with epidermal growth factor receptor and regulates erlotinib sensitivity. *J Biol Chem* 2010; **285**: 24775-24782 [PMID: 20538600 DOI: 10.1074/jbc.M110.134585]
41 **Yeh SH**, Chen PJ, Shau WY, Chen YW, Lee PH, Chen JT, Chen DS. Chromosomal allelic imbalance evolving from liver cirrhosis to hepatocellular carcinoma. *Gastroenterology* 2001; **121**: 699-709 [PMID: 11522754 DOI: 10.1053/gast.2001.27211]
42 **Panda H**, Chuang TD, Luo X, Chegini N. Endometrial miR-181a and miR-98 expression is altered during transition from normal into cancerous state and target PGR, PGRMC1, CYP19A1, DDX3X, and TIMP3. *J Clin Endocrinol Metab* 2012; **97**: E1316-E1326 [PMID: 22492871 DOI: 10.1210/jc.2012-1018]
43 **Wendler A**, Keller D, Albrecht C, Peluso JJ, Wehling M. Involvement of let-7/miR-98 microRNAs in the regulation of progesterone receptor membrane component 1 expression in ovarian cancer cells. *Oncol Rep* 2011; **25**: 273-279 [PMID: 21109987]
44 **Sukata T**, Sumida K, Kushida M, Ogata K, Miyata K, Yabushita S, Uwagawa S. Circulating microRNAs, possible indicators of progress of rat hepatocarcinogenesis from early stages. *Toxicol Lett* 2011; **200**: 46-52 [PMID: 21035526 DOI: 10.1016/j.toxlet.2010.10.013]
45 **Naugler WE**, Sakurai T, Kim S, Maeda S, Kim K, Elsharkawy AM, Karin M. Gender disparity in liver cancer due to sex differences in MyD88-dependent IL-6 production. *Science* 2007; **317**: 121-124 [PMID: 17615358 DOI: 10.1126/science.1140485]
46 **Li Z**, Tuteja G, Schug J, Kaestner KH. Foxa1 and Foxa2 are essential for sexual dimorphism in liver cancer. *Cell* 2012; **148**: 72-83 [PMID: 22265403 DOI: 10.1016/j.cell.2011.11.026]
47 **Yang WJ**, Chang CJ, Yeh SH, Lin WH, Wang SH, Tsai TF, Chen DS, Chen PJ. Hepatitis B virus X protein enhances the transcriptional activity of the androgen receptor through c-Src and glycogen synthase kinase-3beta kinase pathways. *Hepatology* 2009; **49**: 1515-1524 [PMID: 19205031 DOI: 10.1002/hep.22833]

P- Reviewer: Elalfy H, Guan YS, Hashimoto N **S- Editor**: Gong ZM
L- Editor: Webster JR **E- Editor**: Ma YJ

World Journal of Gastroenterology

Submit a Manuscript: http://www.f6publishing.com

World J Gastroenterol 2018 March 14; 24(10): 1167-1180

DOI: 10.3748/wjg.v24.i10.1167

ISSN 1007-9327 (print) ISSN 2219-2840 (online)

META-ANALYSIS

Colonic lesion characterization in inflammatory bowel disease: A systematic review and meta-analysis

Richard Lord, Nicholas E Burr, Noor Mohammed, Venkataraman Subramanian

Richard Lord, Nicholas E Burr, Noor Mohammed, Venkataraman Subramanian, Department of Gastroenterology, Leeds Teaching Hospitals NHS Trust, Leeds LS97TF, United Kingdom

Richard Lord, Nicholas E Burr, Venkataraman Subramanian, University of Leeds, Leeds Institute of Biomedical and Clinical Sciences, Leeds LS97TF, United Kingdom

ORCID number: Richard Lord (0000-0002-8356-7824); Nicholas E Burr (0000-0003-1988-2982); Noor Mohammed (0000-0003-0180-1080); Venkataraman Subramanian (0000-0003-3603-0861).

Author contributions: Subramanian V envisaged and designed the research; Subramanian V performed the statistical analysis; Lord R wrote the paper and did the information searching; Lord R and Burr NE performed the Selection of papers and data abstraction; Lord R and Mohammed N performed the study quality analysis; all authors have reviewed the manuscript.

Conflict-of-interest statement: The authors deny any conflict of interest.

PRISMA 2009 checklist statement: The authors have read the PRISMA 2009 Checklist, and the manuscript was prepared and revised according to the PRISMA 2009 Checklist.

Manuscript source: Invited manuscript

Correspondence to: Venkataraman Subramanian, CCST, MBBS, MD, MRCP, Assistant Professor, Department of gastroenterology, Leeds Teaching Hospitals NHS Trust, Beckett St, Leeds LS97TF, United Kingdom. v.subramanian@leeds.ac.uk

Telephone: +44-113-2068691
Fax: +44-113-2068688

Received: January 8, 2018
Peer-review started: January 9, 2018
First decision: February 5, 2018
Revised: February 18, 2018
Accepted: February 15, 2018
Article in press: February 15, 2018
Published online: March 14, 2018

Abstract

AIM

To perform a systematic review and meta-analysis for the diagnostic accuracy of *in vivo* lesion characterization in colonic inflammatory bowel disease (IBD), using optical imaging techniques, including virtual chromoendoscopy (VCE), dye-based chromoendoscopy (DBC), magnification endoscopy and confocal laser endomicroscopy (CLE).

METHODS

We searched Medline, Embase and the Cochrane library. We performed a bivariate meta-analysis to calculate the pooled estimate sensitivities, specificities, positive and negative likelihood ratios (+LHR, -LHR), diagnostic odds ratios (DOR), and area under the SROC curve (AUSROC) for each technology group. A subgroup analysis was performed to investigate differences in real-time non-magnified Kudo pit patterns (with VCE and DBC) and real-time CLE.

RESULTS

We included 22 studies [1491 patients; 4674 polyps, of which 539 (11.5%) were neoplastic]. Real-time CLE had a pooled sensitivity of 91% (95%CI: 66%-98%), specificity of 97% (95%CI: 94%-98%), and an AUSROC of 0.98 (95%CI: 0.97-0.99). Magnification endoscopy had a pooled sensitivity of 90% (95%CI: 77%-96%)

and specificity of 87% (95%CI: 81%-91%). VCE had a pooled sensitivity of 86% (95%CI: 62%-95%) and specificity of 87% (95%CI: 72%-95%). DBC had a pooled sensitivity of 67% (95%CI: 44%-84%) and specificity of 86% (95%CI: 72%-94%).

CONCLUSION
Real-time CLE is a highly accurate technology for differentiating neoplastic from non-neoplastic lesions in patients with colonic IBD. However, most CLE studies were performed by single expert users within tertiary centres, potentially confounding these results.

Key words: Inflammatory bowel disease dysplasia; Lesion characterization; Confocal laser endomicroscopy; Narrow band imaging; I-scan; Fujinon intelligence chromoendoscopy

Core tip: *In vivo* lesion characterization in colonic inflammatory bowel disease presents many challenges. Lesions tend to be morphologically different and potentially associated with surrounding/overlying inflammation, obscuring the pit pattern. The ability to accurately characterize lesions *in vivo* could reduce costs and complications by decreasing the need for polypectomies. Virtual chromoendoscopy (VCE) and dye-based chromoendoscopy currently cannot be recommended for lesion characterization. Confocal laser endomicroscopy is an accurate technology at differentiating neoplastic from non-neoplastic lesions but studies within this meta-analysis involved single expert center with single advanced endoscopic operators, reducing its generalizability. Larger studies are required specifically looking at lesion characterization, especially with rapid technological advancements in VCE (Narrow band imaging, i-scan, Fujinon intelligence chromoendoscopy).

Lord R, Burr NE, Mohammed N, Subramanian V. Colonic lesion characterization in inflammatory bowel disease: A systematic review and meta-analysis. *World J Gastroenterol* 2018; 24(10): 1167-1180 Available from: URL: http://www.wjgnet.com/1007-9327/full/v24/i10/1167.htm DOI: http://dx.doi.org/10.3748/wjg.v24.i10.1167

INTRODUCTION

The association between colonic inflammatory bowel disease (IBD) and colorectal cancer (CRC) has been acknowledged for almost 100 years[1]. Several meta-analyses have attempted to estimate this increased risk with varying results, reflecting the heterogeneity of studies included[2-4]. Nevertheless all agree that disease duration, disease activity and extent of IBD increase the risk for developing CRC. In response, surveillance colonoscopy is recommended by most gastroenterology societies worldwide. Yet, there is still disparity amongst the societies with regards timing of surveillance intervals.

Most CRC within IBD is thought to develop along the inflammation-dysplasia-cancer pathway; however in rare cases it may not always evolve in this stepwise fashion, and its rate of transition could potentially be accelerated in some lesions[5].

With advancements in endoscopic technology and recommendations for surveillance during inactive disease, most dysplasia is now believed to be visible[6]. Gastroenterological societies currently advocate targeted biopsies for detection of dysplasia, owing to the low yield from random biopsies, with evidence supporting dye-based chromoendoscopy (DBC) for enhancing lesion detection[6-8]. An international consensus group in 2015 recommended that dysplastic polypoid or non-polypoid lesions within a colitic segment should be treated as significant and that well circumscribed lesions with no endoscopic features of submucosal invasion can now be resected[6]. The risk for developing CRC following complete endoscopic resection is now thought to be lower than previous studies suggested[9].

Novel technologies, including narrow band imaging (NBI), fujinon intelligence chromoendoscopy (FICE), i-scan, magnification endoscopy and confocal laser endomicroscopy (CLE), have been studied to obtain an *in-vivo* optical diagnosis of colorectal lesions. DBC using contrast agents, such as indigo-carmine, or absorptive agents, like methylene blue, are customarily applied *via* a spray catheter to provide mucosal enhancement. Virtual chromoendoscopy (NBI, FICE, i-scan) are dye-less enhancement technologies that are built into the colonoscope or processor. NBI uses optical filter enhancement at the distal end of the endoscope, narrowing the light bandwidth, thereby improving visualization of the mucosa. FICE and i-scan use digital post-processing technology with spectral estimation to achieve mucosal enhancement. Magnification endoscopy possesses a variable lens, providing magnification up to 150-fold, permitting detailed examination of the mucosal pit patterns. Whilst CLE technology involves focusing laser light onto the mucosa and the reflected light is returned *via* a pinhole. This filters out non-focused light, giving a highly magnified, real-time histological diagnosis. CLE can either be integrated (iCLE) within the endoscope or *via* a probe (pCLE), which can be passed through the biopsy channel.

In patients without colitis, multiple studies have looked at *in-vivo* optical diagnosis of colorectal lesions using these technologies, allowing differentiation between neoplastic and non-neoplastic lesions. The hope that this would be cost-effective, reduce risk associated with polypectomy and provide instant determination of polyp surveillance intervals for the patient. A recent meta-analysis by the ASGE group looked at novel technologies to allow a "diagnose and leave" and "resect and discard" strategy[10]. To achieve

a "diagnose and leave" strategy, (a decision to leave in-situ diminutive rectosigmoid polyps), the technology had to achieve > 90% NPV for adenomatous histology. To achieve a "resect and discard" strategy, (remove diminutive adenomatous polyps without histological assessment), the technology should provide > 90% agreement in post-polypectomy surveillance intervals. The meta-analysis showed that this could only be achieved with NBI technology, in endoscopists that were experienced and that the assessment of the polyp was made with high confidence. Recently a large multicenter prospective study evaluated the use of NBI assisted optical diagnosis in non-expert endoscopists for small colonic polyps and was found to not achieve the above criteria[11].

The accuracy of these technologies during surveillance colonoscopy in colonic IBD is unclear with the majority of studies being small and assessed as secondary outcomes. With additional hurdles to overcome in patients with colitis, such as active inflammation and the fact that lesions tend to be morphologically different (flatter rather than polypoid), how precise are we at characterizing lesions in IBD with the current technologies available. Our objective was to perform the first systematic review and meta-analysis for the diagnostic accuracy of optical imaging techniques for *in-vivo* lesion characterization in colonic IBD. We aimed to calculate the pooled estimated sensitivities, specificities, positive and negative likelihood ratios (+LHR, -LHR), diagnostic odd ratios (DOR), and area under summary receiver-operator characteristic (AUSROC) curve for each technology type, with histopathology as the reference standard. We also planned to perform a subgroup analysis looking at the accuracy of studies using real-time non-magnified Kudo pit pattern (Kudo PP) and real-time CLE[12].

MATERIALS AND METHODS

Information sources and search strategy

We performed a meta-analysis in concordance with the preferred reporting items for systematic reviews and meta-analyses (PRISMA) guidelines[13]. RL searched Medline (from 1946 to May 2017) and Embase (from 1974 to May 2017), using the healthcare databases advanced search (HDAS) system. The search terms used included: ((((("high definition").ti,ab OR (HD).ti,ab OR ("white light").ti,ab OR (WL).ti,ab OR (chromoendoscop*).ti,ab OR (CE).ti,ab OR (NBI).ti,ab OR ("narrow band").ti,ab OR (FICE).ti,ab OR ("fujinon intelligent chromoendoscopy").ti,ab OR ("I-scan").ti,ab OR (AFI).ti,ab OR (autofluorescence).ti,ab OR (CLE).ti,ab OR ("confocal laser").ti,ab OR ("real time histology").ti,ab) AND ((("colon imag*").ti,ab OR ("intestinal imag*").ti,ab OR (colonoscop*).ti,ab)) AND (("inflammatory bowel disease").ti,ab OR (IBD).ti,ab OR (coliti*).ti,ab OR (uc).ti,ab OR ("ulcerative coliti*").ti,ab OR ("crohns coliti*").ti,ab OR ("crohn's coliti*").ti,ab)) AND ((lesion*).ti,ab OR (polyp*).ti,ab OR (dysplas*).ti,ab OR (neoplas*).ti,ab)". A Cochrane Library search for any systematic reviews relevant to this area was also performed. No language restrictions were used. The results for each database were combined and any duplicates removed.

Inclusion and exclusion criteria

Study inclusion and exclusion was determined by predefined criteria.

Inclusion criteria: (1) Studies using novel technologies to provide *in-vivo* optical characterization of lesions in patients with colonic IBD during colonoscopy; (2) characterized lesions into neoplastic and non-neoplastic using histology as the reference standard; (3) able to extract data to obtain a 2 × 2 contingency table to calculate the true positive (TP), false positive (FP), false negative (FN) and true negative (TN); and (4) Real-time characterization or retrospective image-review.

Exclusion criteria: (1) Case studies or case series; (2) studies not involving patients with colonic ibd; (3) inability to construct a 2 × 2 contingency table from the data given; (4) inability to differentiate detection from characterization studies; and (5) not used histology as reference standard (6) children (age < 16).

Study selection and data extraction

RL and NB identified study eligibility using the above inclusion and exclusion criteria. We searched the combined list of results for relevant studies, looking at the abstract or if supplementary information required, the full article. Reference lists of selected papers were also checked for potential missed articles. Abstract or articles for clinical trials or observational studies were eligible for inclusion if characterization of lesions by NBI, FICE, i-scan, DBC, magnification endoscopy or CLE, differentiated neoplastic from non-neoplastic lesions in colonic IBD, using histopathology as the gold standard. From this, data was extracted using a 2 × 2 contingency table. If exact figures for the true positive (TP), false positive (FP), false negative (FN) and true negative (TN) were not represented in the articles, it was calculated from the documented sensitivity, specificity, accuracy, positive predictive value (PPV) or negative predictive value (NPV). RL and VS performed data ascertainment and calculations. If TP, FP, FN and TN couldn't be calculated from the article data, attempts were made to contact relevant authors by email for clarification of figures.

Risk of study bias

As studies included were diagnostic, RL and NM used the QUADAS-2 (quality assessment of diagnostic accuracy studies) tool to independently assess the degree of study validity[14]. This looks at the risk of bias and applicability regarding four domains: patient

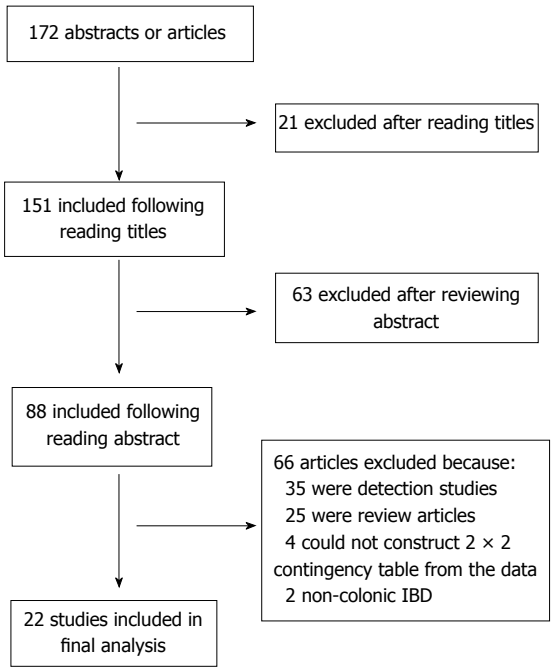

Figure 1 Study flow chart for studies eventually included into the meta-analysis. IBD: Inflammatory bowel disease.

selection, index test, reference standard, flow and timing. Risk of bias (involved all four domains) and applicability (involved three domains) is scored using low risk, high risk or unclear. Any indifference on determining risk between RL and NM was discussed and clarified with VS, who made the final decision.

Statistical analysis

In performing a systematic review for diagnostic studies, a bivariate meta-analysis using a random effects model was performed, allowing for the assumption of heterogeneity between the studies[15]. A random effects model was used in order to provide a more conservative result due to differences between study methods such as endoscopic expertise, classification model, study type and the population studied. We obtained summary estimates for sensitivity, specificity, +LHR, -LHR and DOR, with their 95% confidence intervals. A hierarchical summary receiver-operator characteristic (ROC) curve was plotted, with its summary point estimate, and a dashed line around representing its 95% confidence interval. The area under the SROC curve (AUROC) served as a marker of test accuracy. Forest plots were also calculated to demonstrate study sensitivity and specificity.

Heterogeneity between studies was assessed using the Cochrane *Q* and I^2 tests. Cochrane *Q* is established upon the chi-squared test, providing a weighted sum of the squared differences of each study estimate from the overall pooled estimate. *P* valves are given. I^2 describes the percentage of variation between studies that is due to heterogeneity rather than chance and is not dependent on the number of studies included. I^2 quantifies the impact of heterogeneity on the meta-analysis rather than just the extent of heterogeneity. Results range from 0-100%: 0% indicates there is no heterogeneity between the studies, whereas scores > 50% equate to moderate heterogeneity and > 75% high heterogeneity.

To help determine factors that may account for heterogeneity, we performed a subgroup analysis concentrating on real-time mucosal characterization, dividing into two groups: non-magnified Kudo PP (using VCE and DBC) and CLE. We also pooled results for all studies (real-time and retrospective image-capture) looking at non-magnified Kudo PP.

The Deeks *et al*[16] funnel plot assessed for publication bias. This uses regression of diagnostic log odds ratio against1/sqrt (effective sample size), weighting by sample size with a $P < 0.10$ for the slope coefficient as an indicator of substantial asymmetry.

All data analysis was done using Stata version 13 (Stata Corp, Texas, United States) using the user written command Midas (Dwamena, 2009)[17].

RESULTS

Study selection

One hundred and seventy-two abstracts and articles were obtained following the initial keyword search, following removal of duplicates (Figure 1). 21 studies were excluded following screening of the title, leaving 151 citations. A further 63 studies were excluded following review of the abstract, leaving 88 citations. 66 more studies were excluded following review of papers as a result of: 35 being detection studies, 25 were review articles, 2 involved patients without colonic IBD and 4 we were unable to construct a 2 × 2 contingency table.

Study characteristics

The characteristics of the 22 studies included are presented in Table 1[18-39]. Twenty-one studies included 1491 patients, with one study not reporting the number of patients included, and 4674 lesions, of which 539 (11.5%) were neoplastic.

The VCE group consisted of five studies, with one study looking at i-scan technology, two studies involved NBI and a further two used FICE. Three of the papers were abstracts and two being articles. All of these studies used endoscopic real-time diagnosis of lesions.

The DBC group entailed six studies, using either indigo-carmine (0.2%-0.4%) or methylene blue (0.1%) as the contrast agent. One of these studies performed endoscopic lesion diagnosis using a retrospective image-captured questionnaire, whilst the others used real-time diagnosis. Two were abstracts with the others being articles.

The CLE group comprised of nine studies; four studies used iCLE and five studies used pCLE. Three studies were retrospective image based, with the

Table 1 Study characteristics

Authors	Year	Abstract/ article	Technology	Number of endoscopists	Study design	Real time *vs* Image review	No. of Patients	No. of Polyps	Mucosal classification method
Virtual Chromoendoscopy									
Cassinotti *et al*[22]	2016	Abstract	i-scan HD	/	Single centre/prospective cohort Prospective cohort	Real time	40	287	Kudo PP + other endoscopic features
Efthymiou *et al*[21]	2013	Article	NBI HD	2	Single centre/prospective cohort	Real time	44	121	Kudo PP + low level magnification
Van den broek *et al*[23]	2011	Article	NBI HD	4	Single centre/randomized cross-over	Real time	48	153	Kudo PP
Cassinotti *et al*[24]	2015	Abstract	FICE HD	1	Single centre/randomized parallel	Real time	41	261	Kudo PP
Cassinotti *et al*[25]	2015	Abstract	FICE HD	1	Single centre/prospective cohort	Real time	59	205	Kudo PP
Dye-based Chromoendoscopy									
Carballal *et al*[26]	2016	Article	IC 0.4% SD/HD	15	Multi-centre/prospective cohort	Real time	350	595	Kudo PP + 10 other items
[1]Buchner *et al*[27]	2016	Abstract	MB 0.1% HD	/	Prospective cohort	Real time	22	21	/
[2]Wanders *et al*[20]	2016	Article	MB 0.1% SD	> 1	Multi-centre/prospective cohort	Real time	61	66	Kudo PP
Munoz *et al* [28]	2016	Abstract	IC 0.2%-0.4% HD	> 1	Multi-centre/retrospective cohort	Real time	243	953	Kudo PP
Wanders *et al*[29]	2015	Article	MB 0.1% or IC 0.3%	17	Multi-centre/retrospective questionnaire	Image review	/	30	/
[3]Hlavaty *et al* [18]	2011	Article	IC 0.4% SD	2	Single centre/prospective cohort	Real time	30	100	Kudo PP
Confocal Laser Endomicroscopy									
[2]Wanders *et al*[20]	2016	Article	iCLE	> 1	Multi-centre/prospective cohort	Real time	61	60	Mainz criteria
Dlugosz *et al*[30]	2016	Article	pCLE	1 endoscopist (2 reviewed images)	Single centre/retrospective cohort	Image review	69	644	Crypt + vessel architecture
[1]Buchner *et al*[27]	2016	Abstract	pCLE	/	Prospective cohort	Real time	22	20	Miami classification
Freire *et al*[31]	2014	Article	iCLE	1	Single centre/randomized trial	Real time	72	104	Mainz criteria
Rispo *et al*[32]	2012	Article	pCLE	1	Single centre/prospective cohort	Real time	51	15	De Palma classification
Shahid *et al*[33]	2011	Abstract	pCLE	3 reviewed images	Single centre/retrospective cohort	Image review	25	61	/
[3]Hlavaty *et al*[18]	2011	Article	iCLE	2	Single centre/prospective cohort	Real time	30	68	Mainz classification
[4]Van den broek *et al*[19]	2011	Article	pCLE	4 endoscopists (2 reviewing images)	Single centre/retrospective cohort	Image review	22	48	Crypt + vessel architecture
Keisslich *et al*[34]	2007	Article	iCLE	/	Single centre/randomized trial	Real time	80	134	Mainz classification
Magnification endoscopy									
Nishiyama *et al*[35]	2016	Article	NBI	5 reviewed images	Single centre/retrospective cohort	Image review	27	33	Surface + vessel patterns
[4]Van den broek *et al*[19]	2011	Article	NBI	4	Single centre/prospective cohort	Real time	22	48	Kudo PP + vascular patterns
Van den broek *et al*[36]	2008	Article	NBI	3	Single centre/randomized trial	Real time	50	98	Kudo PP
Matsumoto *et al*[37]	2007	Article	NBI	1	Single centre/prospective cohort	Real time	46	296	Surface structure
Keisslich *et al*[38]	2003	Article	MB 0.1%	1	Single centre/randomized trial	Real time	84	118	Kudo PP
Studies using combined technologies									
Bisschops *et al*[39]	2013	Abstract	Dye-based chromo/NBI	10 reviewed images	Multi-centre/retrospective cohort	Image review	27	50	Kudo PP

List of studies included in meta-analysis and displayed according to technology type. PP: Pit pattern; /: Data missing. [1]Two different technologies from same abstract; [2]Two different technologies from same article; [3]Two different technologies from same article; [4]Two different technologies from the same article.

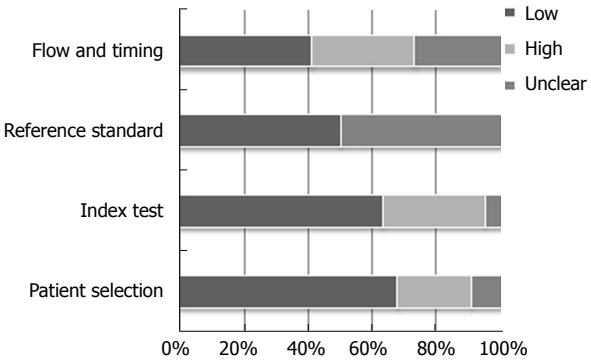

Figure 2 Stacked bar charts showing proportion of studies with low, high or unclear risks of bias. Vertical axis represents the four domains of the quality assessment of diagnostic accuracy studies 2.

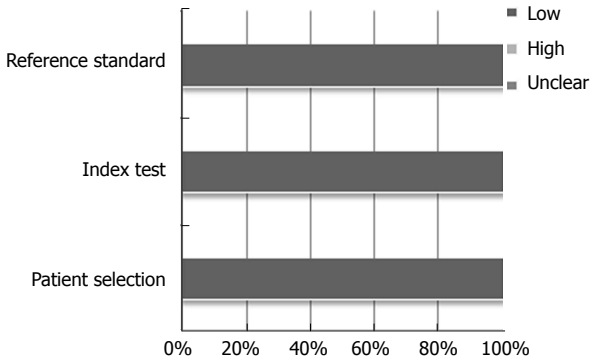

Figure 3 Stacked bar charts showing proportion of studies with low, high or unclear applicability. Vertical axis represents the three domains of the quality assessment of diagnostic accuracy studies 2.

remaining being real-time studies. Two were abstracts and the others being articles.

The magnification endoscopy group consisted of five studies, four of which being used in conjunction with NBI and one used with DBC. One study was retrospective image-based, with the others being real-time diagnosis. All were articles.

For the subgroup analysis, real-time non-magnified Kudo PP involved ten studies and real-time CLE involved six studies. The "all study" Kudo PP included twelve studies of which two were retrospective image-based abstracts.

Quality of assessment

The results for the study quality assessment using the QUADAS 2 tool are presented using stacked bar charts (Figure 2 and 3), displaying risk of bias and applicability. Individual study quality assessment can be seen in the supplementary table (Table 2). Results varied across the twenty-two studies. Abstracts predominantly scored "unclear" for domains associated with "risk of bias", due to lack of in-depth information within the abstract. However studies also scored "unclear" for "risk of bias" with regards "reference standard" if it did not clearly state if the histopathologist was blinded to the endoscopic diagnosis. Papers scoring "high" for "patient selection", "index test" and "flow and timing" for "risk of bias", were generally associated with retrospective image-captured studies which selected and reviewed only clear images of lesions, thereby introducing attrition bias. All studies scored "low" for all three domains with regards "applicability".

Pooled diagnostic accuracy results

A summary for the pooled diagnostic accuracy estimates for the different technologies and for the subgroup analysis is outlined in Table 3.

The meta-analysis for the five studies involving VCE showed it was fairly accurate at differentiating neoplastic from non-neoplastic lesions with a pooled sensitivity of 86% (95%CI: 62%-95%), specificity of 87% (95%CI: 72%-95%), and the area under the SROC curve was 0.93 (95%CI: 0.90-0.95).

Pooled results of the six studies for DBC revealed the least accurate results for lesion characterization, with a sensitivity of 67% (95%CI: 44%-84%), specificity of 86% (95%CI: 72%-94%) and an area under the SROC curve was 0.84 (95%CI: 0.81-0.87). Most of the studies within this group were multi-centre with more than one endoscopist.

Results of the five studies for magnification endoscopy showed a pooled sensitivity of 90% (95%CI: 77%-96%), specificity of 87% (95%CI: 81%-91%), and an area under the SROC curve was 0.93 (95%CI: 0.91-0.95). The results are similar to those of VCE; however these were mainly single centre, single expert endoscopist studies.

Meta-analysis of nine studies for CLE showed a sensitivity of 87% (95%CI: 71%-95%), specificity of 94% (95%CI: 87%-97%), with an area under the SROC curve of 0.96 (95%CI: 0.94-0.97). Again these mere all single centre, single expert endoscopist studies.

A subgroup analysis was performed involving studies using real-time endoscopic mucosal characterisation of lesions, divided into real-time non-magnified Kudo PP (with VCE and DBC) and real-time CLE. Both the forest plots and SROC curves for real-time non-magnified Kudo PP and real-time CLE are given in Figures 4 and 5. The subgroup for real-time Kudo PP included ten studies, with a pooled estimate sensitivity of 78% (95%CI: 57%-91%), specificity of 89% (95%CI: 80%-94%), with an area under the SROC of 0.91 (95%CI: 0.89-0.94). The subgroup analysis looking at real-time CLE included 6 studies. The pooled estimated sensitivity was 91% (95%CI: 66%-98%), specificity was 97% (95%CI: 94%-98%), and the area under the AUSROC was 0.98 (0.97-0.99).

A further subgroup analysis was performed looking at all (real-time and image review) non-magnified Kudo PP. This included twelve studies. The pooled estimate sensitivity was 78% (95%CI: 61%-88%), specificity of 86% (95%CI: 76%-92%), and an area under the

Table 2 quality assessment of diagnostic accuracy studies 2 for each study

	Cassinotti *et al*[22] 2016	Efthymiou *et al*[21] 2013	Van den broek *et al*[23] 2011	Cassinotti *et al*[24] 2015	Cassinotti *et al*[25] 2015	Carballel *et al*[26] 2016	Buchner *et al*[27] 2016	Wanders *et al*[20] 2016	Munoz *et al*[28] 2016	Wanders *et al*[29] 2015	Hlavaty *et al*[18] 2011	Dlugosz *et al*[30] 2016	Freire *et al*[31] 2014	Rispo *et al*[32] 2012	Shahid *et al*[33] 2011	Van den broek *et al*[19] 2011	Keisslich *et al*[34] 2007	Nishiyama *et al*[35] 2016	Van den Broek *et al*[36] 2008	Matsumoto *et al*[37] 2007	Keisslich *et al*[38] 2003	Bisschops *et al*[39] 2013
DOMAIN 1 Patient selection Risk of bias																						
Could selection of patients introduced bias?	L	L	L	L	L	L	U	L	L	H	U	L	L	L	H	H	L	H	L	L	L	H
Concerns regarding applicability																						
Concern included patients don't match review question?	L	L	L	L	L	L	L	L	L	L	L	L	L	L	L	L	L	L	L	L	L	L
DOMAIN 2 Index test Risk of bias																						
Conduct or interpretation of index test introduced bias?	L	L	L	L	L	L	L	L	U	H	H	H	L	L	H	H	L	H	L	L	L	H
Concerns regarding applicability																						
Concern index test, its conduct or interpretation differs from review question?	L	L	L	L	L	L	L	L	L	L	L	L	L	L	L	L	L	L	L	L	L	L

DOMAIN 3 Reference standard Risk of bias																						
Could reference standard, conduct or interpretation have introduced bias?	U	U	L	U	U	U	U	L	U	U	L	L	L	L	U	L	L	U	L	L	L	U
Concerns regarding applicability																						
Concern target condition as defined by reference standard not match review question?	L	L	L	L	L	L	L	L	L	L	L	L	L	L	L	L	L	L	L	L	L	L
DOMAIN 4 Flow and timing																						
Risk of bias																						
Could patient flow introduced bias?	U	L	H	U	U	L	U	L	U	H	H	U	L	L	H	H	L	H	L	L	L	H

L: Low risk; H: High risk; U: Unclear.

SROC of 0.89 (95%CI: 0.86-0.92).

Test for heterogeneity

I^2 and Cochrane Q were used to test for heterogeneity. Heterogeneity for VCE was moderate to high with an I^2 = 63% (95%CI: 16%-100%) and Q = 5.347 (P = 0.034). DBC showed extremely high levels of heterogeneity between studies with an I^2 = 89% (95%CI: 78%-100%) and Q = 18.573 (P = 0.00). Magnification [I^2 = 0 (95%CI: 0%-100%) and Q = 0.607 (P = 0.369)] and CLE [I^2 = 40% (95%CI: 0%-100%) and Q = 3.335 (P = 0.094)] represented low levels of heterogeneity between studies, however had very broad 95% confidence intervals.

Real-time non-magnified Kudo PP had an I^2 = 96% (95%CI: 92-99) and Q = 45.575 (P < 0.001) showing exceptionally high levels of heterogeneity. Real-time CLE studies had low levels of heterogeneity, with an I^2 = 0 (95%CI: 0-100%) and Q = 1.697 (P = 0.214).

Table 3 Accuracy of the different technologies

Analysis groups	No. of studies	Pooled estimates (95%CI)		Likelihood ratios (95%CI)		Diagnostic odds ratio (95%CI)	Area under SROC curve (95%CI)
		Sensitivity	Specificity	LHR+	LHR-	DOR	
All							
VCE	5	0.86 (0.62-0.95)	0.87 (0.72-0.95)	6.7 (2.6-17.8)	0.17 (0.05-0.53)	41 (6-297)	0.93 (0.90-0.95)
DBC	6	0.67 (0.44-0.84)	0.86 (0.72-0.94)	4.9 (2.1-11.3)	0.38 (0.20-0.73)	13 (3-48)	0.84 (0.81-0.87)
Magnification	5	0.90 (0.77-0.96)	0.87 (0.81-0.91)	7.0 (4.6-10.7)	0.11 (0.05-0.28)	62 (18-209)	0.93 (0.91-0.95)
CLE	9	0.87 (0.71-0.95)	0.94 (0.87-0.97)	14.0 (6.1-32.4)	0.14 (0.06-0.33)	101 (23-442)	0.96 (0.94-0.97)
Real-time							
Kudo PP	10	0.78 (0.57-0.91)	0.89 (0.80-0.94)	6.9 (3.5-13.5)	0.24 (0.11-0.55)	28 (7-110)	0.91 (0.89-0.94)
CLE	6	0.91 (0.66-0.98)	0.97 (0.94-0.98)	28.4 (13.6-59.1)	0.09 (0.02-0.43)	322 (41-2529)	0.98 (0.97-0.99)
All Kudo PP	12	0.78 (0.61-0.88)	0.86 (0.76-0.92)	5.5 (2.9-10.1)	0.26 (0.14-0.50)	21 (7-66)	0.89 (0.86-0.92)

All using both real-time and image based studies for the different technologies. Real-time, sub-group analysis with studies using only real time Kudo pit pattern (both VCE and DBC) and real-time CLE. All Kudo PP includes all studies using Kudo pit pattern (real-time and image-based). VCE: Virtual chromoendoscopy; DBC: Dye-based chromoendoscopy; CLE: Confocal laser endomicroscopy; Kudo PP: Kudo pit pattern; LHR+: Positive likelihood ratios; LHR-: Negative likelihood ratios; DOR: Diagnostic odd ratios.

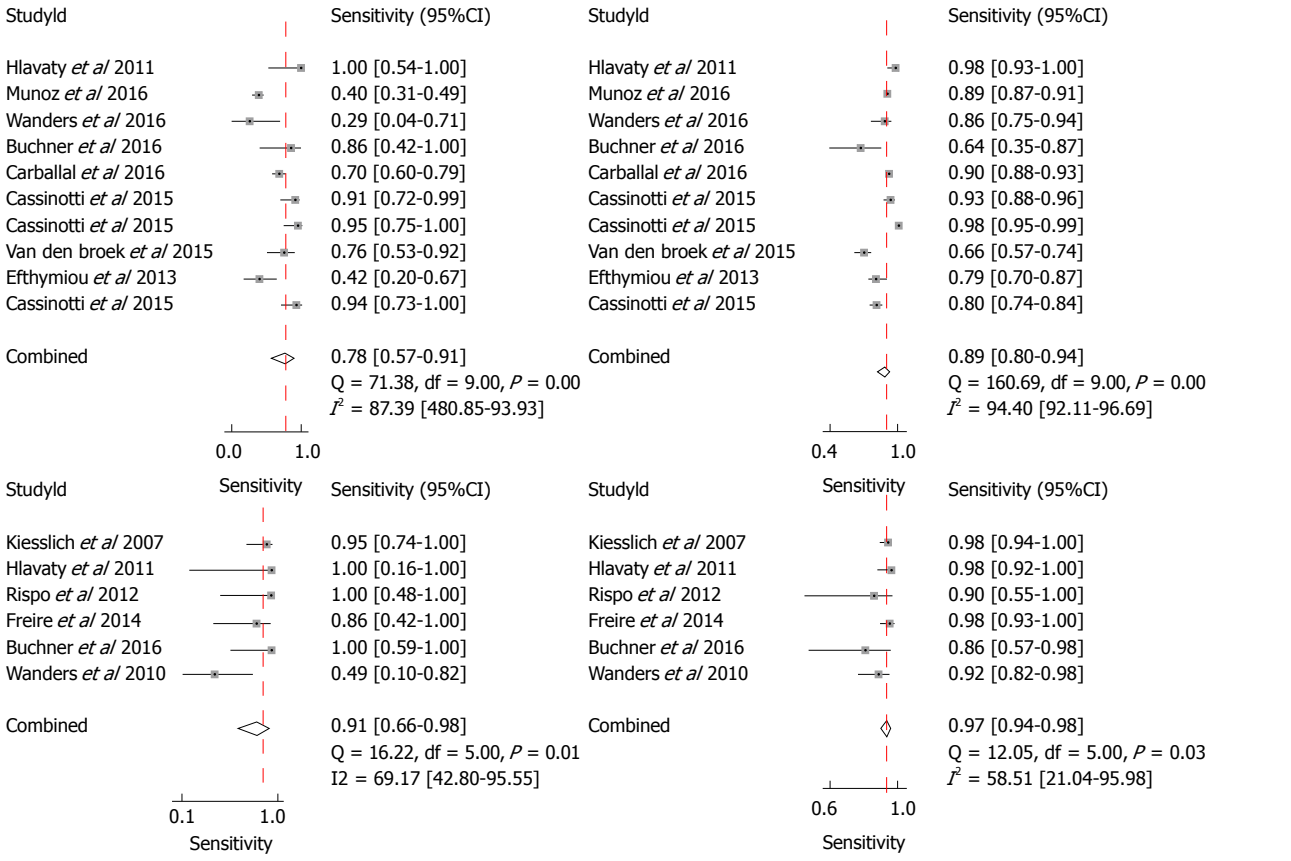

Figure 4 Forest plot for real-time Kudo pit pattern (A), and forest plot for real-time confocal laser endomicroscopy (B).

Publication bias

Deeks *et al*[15] funnel plot, seen in Figure 6, was used to assess publication bias. The funnel plot has slope coefficient of 9.84 (P = 0.194). The non-significant P valve would suggest a low likelihood of publication bias in this meta-analysis.

DISCUSSION

Our meta-analysis illustrates that real-time CLE currently appears to be the best technology in performing *in-vivo* lesion characterization in patients with colonic IBD, with an impressive AUSROC of 0.98 (95%CI: 0.97-0.99). It demonstrates an extremely high specificity, 97% (95%CI: 94%-98%), and sensitivity, 91% (95%CI: 66%-98%), in differentiating neoplastic from non-neoplastic lesions. Using all study types (real-time and image capture) CLE again out-performs the other technologies, with an area under SROC cure of 0.96 (95%CI: 0.94-0.97). Magnification and VCE technologies also show a good accuracy with a SROC of 0.93 (95%CI: 0.91-0.95) and 0.93 (95%CI: 0.90-0.95),

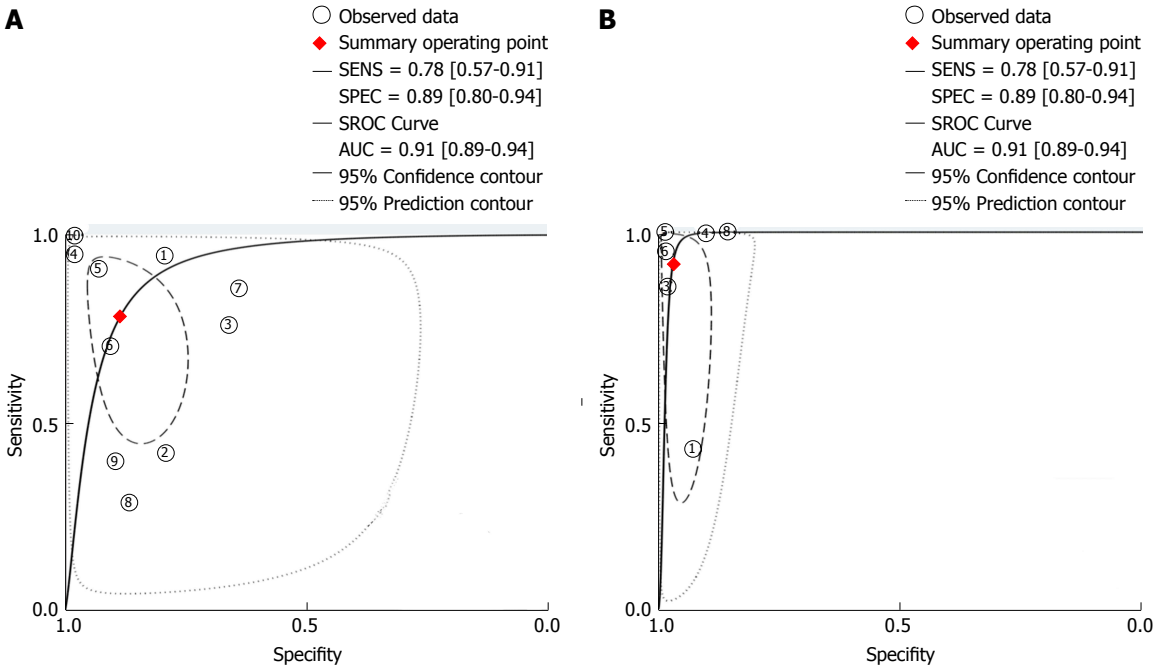

Figure 5 Area under SROC curve for real-time Kudo pit pattern (A) and area under SROC curve for real-time confocal laser endomicroscopy (B).

respectively.

Despite CLE being a highly accurate technology in lesion characterization, there are several concerns with regards applicability. Most of the studies in our meta-analysis for CLE involved a single endoscopy operator within a single-centre. They were vastly experienced in IBD surveillance endoscopy and in using CLE technology. Studies in which inexperienced operators used this technology, they themselves did not make real-time lesion diagnosis. Instead, people trained in the interpretation of the histology reviewed the images retrospectively. This is because CLE is not a routinely used modality. It requires expertise in handling, positioning of the colonoscope/probe onto the lesion and in analysing/interpreting *in-vivo* histology. Bowel preparation has to be meticulous, as any faecal material can interfere with image capture and lesion interrogation. This is unlikely to be achieved consistently during "real-life" surveillance lists. In one study, 32% of lesions were not accessible to CLE evaluation and a second study, 1.5% of lesions the histology was not visualised by CLE. These unclassified lesions aren't accounted for in the final results, contributing to attrition bias in the observed results. In addition, IV fluorescein injection is required before lesion analysis, further adding to procedure time. One study showed the mean additional time per procedure being 20 min. Adoption of this technology in throughout less experienced centres is doubtful. It would demand vast resources for training, education and require new guidance for endoscopic competence.

A further concern with CLE was equipment failure. In one multi-centre study, four of the five centres had to send the equipment back to the manufactures as the lens on the endomicroscope broke. Repair took the teams months to address, significantly affecting recruitment, resulting in the study being underpowered. With concerns over equipment failure, costs of purchasing the technology and repairs, CLE could in fact be a financial burden, negating any benefit obtained from the reduction in polypectomies and histological analysis. Therefore, questions still remain unanswered with regards practicalities and applicability for this technology.

VCE showed relatively good accuracy although fell short of reaching the 90% mark for sensitivity and specificity. One major limitation for this technology was the small number of studies for VCE technology. We therefore combined the NBI, FICE and i-scan to obtain pooled results. Although the technologies have been grouped as one, there are obvious differences in the way they achieve the modified image and the modes used with that technology. NBI endoscopes contain a rotating filter in front of the light source at the end of the endoscope, allowing a narrow wavelength of light to strike the mucosa resulting in image enhancement, whereas both FICE and i-scan use a post-processing technology built within the processer to provide a coloured-enhanced image. There were several other drawbacks with the VCE group analysis. One study in our meta-analysis used the first generation NBI technology, resulting in images being less bright, undoubtedly having an impact on lesion characterization when compared with newer generation technology. Three of the five studies for VCE were abstracts making critical analysis for the quality of these studies difficult to determine. From our results we cannot currently recommend using VCE solely as an accurate

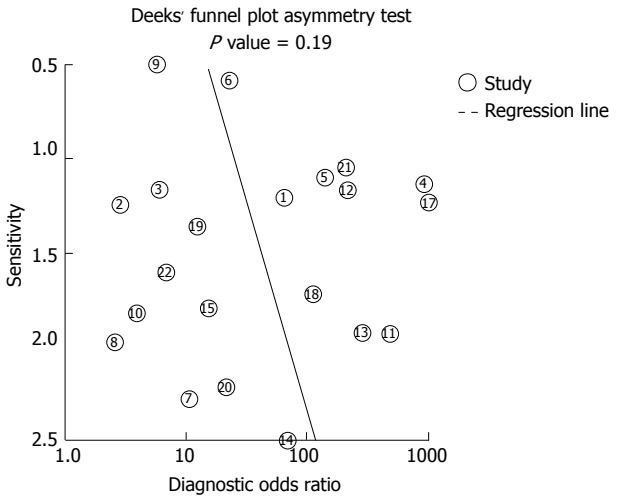

Figure 6 Funnel plot with superimposed regression line looking for publication bias.

technology for lesion characterization in IBD. However, with newer generation endoscopes, further evaluation is clearly warranted as these technologies continue to improve. In comparison with CLE, VCE is potentially less complicated to use, more robust, economical as they are almost universal in newer endoscope processors, and training is more likely to be attainable.

Magnification endoscopy achieves similar accuracy to VCE technology. However in the majority of these studies magnification was used in combination with NBI, predominantly using older NBI technology. This makes it challenging to differentiate the two technologies. With new colonoscopes delivering digital magnification, like "near focus" technology, it is questionable the additional information optical magnification will provide. A threshold may be reached at which further magnification provides no additional benefit for differentiating neoplastic from non-neoplastic pit patterns. However, this meta-analysis cannot necessarily address that question.

DBC pooled results were suboptimal for lesion characterization. However, more than half of the studies used standard-definition colonoscopies, reducing image resolution, and therefore impacting on lesion interpretation. With most centres now using high-definition colonoscopies accuracy is likely to improve. Another confounding factor was that the majority of the studies were multi-centred, with multiple operators, undoubtedly accounting for a diverse range of endoscopic experience and therefore skill at lesion classification.

A subgroup analysis was performed in order to look for potential sources of heterogeneity and to determine whether it was the type of mucosal classification used that influenced the accuracy rather than the technology. Real-time studies were used as this provided the most clinically authentic evaluation of lesions and minimises bias as a result of photographic selection and time for analysis. Most studies used Kudo PP or a variation on the Kudo PP (Kudo PP plus additional features) and therefore we pooled the results for both real-time VCE and DBC. Real-time Kudo PP had an area under the SROC curve of 0.91 (95%CI: 0.89-0.94), with a reasonable specificity of 89% (95%CI: 80%-94%) but a sensitivity of 78% (95%CI: 57%-91%). The poor sensitivity likely reflects inclusion of the DBC group with the majority involving standard-definition scopes. The use of Kudo PP and Kudo PP plus did not seem to influence the accuracy of lesion characterisation, independent of the technology. Caution however, has to be noted for combining DBC and VCE using Kudo PP as a mucosal classification system. Studies have shown a lack of pit pattern agreement between chromoendoscopy and NBI[40]. This has leading to the adoption of new classification systems, such as NICE for NBI[41]. Further mucosal classification systems may need to be studied, especially for i-scan and FICE. However, determining the ideal post-processing mode for these software systems could be challenging as these technologies have multiple combination options of modes.

Another important issue that wasn't clearly stated for studies in this meta-analysis was the degree of mucosal inflammation in which the lesions resided. Varying degrees of mucosal inflammation unquestionably contribute to difficulties in pit pattern and vasculature interpretation and therefore diagnostic accuracy. Future studies looking at *in-vivo* lesion diagnostic accuracy could stratify patients depending on the degree of inflammation surrounding the lesions.

As with any meta-analysis there are limitations. The number of studies for each technology group was fairly limited, except for the CLE group. Seven of the twenty-two studies were abstracts introducing concerns with regards data extraction and interrogation for study validity.

Despite an extensive literature review, no papers had direct head-to-head studies, comparing the different technologies against each other. However, this would require a very large cohort looking specifically at lesion characterisation and all endoscopists participating being familiar with the different technologies. Endoscopic familiarity with certain technologies in such a study could potentially confound the accuracy of lesion interpretation.

In the majority of studies, lesion characterization was a secondary outcome, therefore in some studies the number of lesions being characterised was small. Some studies didn't clearly state the TP, FP, FN and TN, therefore calculations had to be performed in order to achieve this.

There was also a large degree of heterogeneity within the VCE and DBC groups that was further increased when we performed real-time Kudo PP assessment. Further areas of subgroup classification that were not explored within this meta-analysis were the number of endoscopists performing the procedures in each study and also whether it was a single centre

or multi-centre study. This undoubtedly will have an impact on the accuracy of the technology being used. Single-centre, single endoscopist studies are more likely to achieve better results.

Suggested avenues to explore in future studies looking at *in-vivo* lesion characterization in colonic IBD include: accuracy according to varying endoscopic experience, accuracy dependent on the degree of surrounding mucosal inflammation, whether the endoscopist confidence (high or low) in lesion characterization impacts accuracy and exploring new mucosal lesion classification for different technologies.

CONCLUSION

Real-time CLE appears to be currently the best commercially available technology at differentiating neoplastic from non-neoplastic lesions in patients with colonic IBD, with an area under the SROC of 0.98 (95%CI: 97%-99%). However, most CLE studies were single centered with single expert users, which could significantly confound the results, and some studies not reporting non-interpretable images, contributing to attrition bias. Clinical applicability for this technology is likely to be a challenge. VCE technology performed well but currently cannot be recommended for *in-vivo* lesion characterization in such a high-risk group. However, with improved endoscopes and newer generation technologies further studies are required to assess their real-time performance in clinical settings with trained colonoscopists.

ARTICLE HIGHLIGHTS

Research background

Patients with inflammatory bowel disease (IBD) colitis are known to have an increased risk of colorectal cancer compared to that of non-colitic patients. This is thought to progress along the inflammation-dysplasia-carcinoma pathway. Many studies and meta-analyses have been performed for lesion detection in IBD but few studies have looked into *in-vivo* lesion characterization. This is the first meta-analysis on lesion characterization in colonic IBD.

Research motivation

Characterization of colonic lesions in IBD maybe more challenging because they tend to be flatter and their pit-pattern maybe obscured by inflammation. Some patients also have numerous pseudopolyps throughout the colon, making polypectomy impractical, time-consuming, costly and potentially associated with increased risk. If we are able to characterize these lesions with a high accuracy without needing to perform polypectomy, we could potentially circumvent these problems.

Research objectives

Our objective was to perform the first systematic review and meta-analysis for the diagnostic accuracy of optical imaging techniques for *in-vivo* lesion characterization in colonic IBD.

Research methods

We conducted a review of the current literature and included studies which characterized lesions *in-vivo* into neoplastic and non-neoplastic, using histology as the gold standard. Data was pooled for each technology using a bivariate meta-analysis with a random effects model to account for study differences. Sensitivities, specificities, positive and negative likelihood ratios, diagnostic odds ratio, and area under summary receiver-operator characteristic curve, were calculated for each technology type.

Research results

Confocal laser endomicroscopy (CLE) had the greatest accuracy for differentiating neoplastic from non-neoplastic lesions *in-vivo*. Magnification and virtual chromoendoscopy (VCE) performed well, whilst dye-based chromoendoscopy (DBC) had suboptimal accuracy.

Research conclusions

CLE is highly accurate at *in-vivo* lesion characterization but studies are within experienced centres with mainly single expert users limiting its generalizability.

Research perspectives

Future studies should look at newer generation virtual chromoendoscopic technology [narrow band imaging (NBI), i-scan, fujinon intelligence chromoendoscopy (FICE)] for lesion characterization. A standardised mucosal lesion classification system specific for lesions in IBD colitis accounting for the technology being used should be explored.

REFERENCES

1 **Crohn B,** Rosenberg H. The sigmoidoscopic picture of chronic ulcerative colitis (non- specific). *AM J MED SCI* 1925; **170**: 220-227 [DOI: 10.1097/00000441-192508010-00006]

2 **Eaden JA**, Abrams KR, Mayberry JF. The risk of colorectal cancer in ulcerative colitis: a meta-analysis. *Gut* 2001; **48**: 526-535 [PMID: 11247898 DOI: 10.1136/gut.48.4.526]

3 **Jess T**, Rungoe C, Peyrin-Biroulet L. Risk of colorectal cancer in patients with ulcerative colitis: a meta-analysis of population-based cohort studies. *Clin Gastroenterol Hepatol* 2012; **10**: 639-645 [PMID: 22289873 DOI: 10.1016/j.cgh.2012.01.010]

4 **Lutgens MW**, van Oijen MG, van der Heijden GJ, Vleggaar FP, Siersema PD, Oldenburg B. Declining risk of colorectal cancer in inflammatory bowel disease: an updated meta-analysis of population-based cohort studies. *Inflamm Bowel Dis* 2013; **19**: 789-799 [PMID: 23448792 DOI: 10.1097/MIB.0b013e31828029c0]

5 **Zisman TL**, Rubin DT. Colorectal cancer and dysplasia in inflammatory bowel disease. *World J Gastroenterol* 2008; **14**: 2662-2669 [PMID: 18461651 DOI 10.3748/wjg.14.2662]

6 **Laine L**, Kaltenbach T, Barkun A, McQuaid KR, Subramanian V, Soetikno R; SCENIC Guideline Development Panel. SCENIC international consensus statement on surveillance and management of dysplasia in inflammatory bowel disease. *Gastroenterology* 2015; **148**: 639-651.e28 [PMID: 25702852 DOI: 10.1053/j.gastro.2015.01.031]

7 **Cairns SR**, Scholefield JH, Steele RJ, Dunlop MG, Thomas HJ, Evans GD, Eaden JA, Rutter MD, Atkin WP, Saunders BP, Lucassen A, Jenkins P, Fairclough PD, Woodhouse CR; British Society of Gastroenterology; Association of Coloproctology for Great Britain and Ireland. Guidelines for colorectal cancer screening and surveillance in moderate and high risk groups (update from 2002). *Gut* 2010; **59**: 666-689 [PMID: 20427401 DOI: 10.1136/gut.2009.179804]

8 **Annese V**, Daperno M, Rutter MD, Amiot A, Bossuyt P, East J, Ferrante M, Götz M, Katsanos KH, Kießlich R, Ordás I, Repici A, Rosa B, Sebastian S, Kucharzik T, Eliakim R; European Crohn's and Colitis Organisation. European evidence based consensus for endoscopy in inflammatory bowel disease. *J Crohns Colitis* 2013; **7**: 982-1018 [PMID: 24184171 DOI: 10.1016/j.crohns.2013.09.016]

9 **Wanders LK**, Dekker E, Pullens B, Bassett P, Travis SP, East JE. Cancer risk after resection of polypoid dysplasia in patients with longstanding ulcerative colitis: a meta-analysis. *Clin Gastroenterol Hepatol* 2014; **12**: 756-764 [PMID: 23920032 DOI: 10.1016/j.cgh.2013.07.024]

10 **ASGE Technology Committee**, Abu Dayyeh BK, Thosani N, Konda V, Wallace MB, Rex DK, Chauhan SS, Hwang JH,

Komanduri S, Manfredi M, Maple JT, Murad FM, Siddiqui UD, Banerjee S. ASGE Technology Committee systematic review and meta-analysis assessing the ASGE PIVI thresholds for adopting real-time endoscopic assessment of the histology of diminutive colorectal polyps. *Gastrointest Endosc* 2015; **81**: 502.e1-502.e16 [PMID: 25597420 DOI: 10.1016/j.gie.2014.12.022]

11 **Rees CJ**, Rajasekhar PT, Wilson A, Close H, Rutter MD, Saunders BP, East JE, Maier R, Moorghen M, Muhammad U, Hancock H, Jayaprakash A, MacDonald C, Ramadas A, Dhar A, Mason JM. Narrow band imaging optical diagnosis of small colorectal polyps in routine clinical practice: the Detect Inspect Characterise Resect and Discard 2 (DISCARD 2) study. *Gut* 2017; **66**: 887-895 [PMID: 27196576 DOI: 10.1136/gutjnl-2015-310584]

12 **Kudo S**, Tamura S, Nakajima T, Yamano H, Kusaka H, Watanabe H. Diagnosis of colorectal tumorous lesions by magnifying endoscopy. *Gastrointest Endosc* 1996; **44**: 8-14 [PMID: 8836710 DOI: 10.1016/S0016-5107(96)70222-5]

13 **Liberati A**, Altman DG, Tetzlaff J, Mulrow C, Gøtzsche PC, Ioannidis JP, Clarke M, Devereaux PJ, Kleijnen J, Moher D. The PRISMA statement for reporting systematic reviews and meta-analyses of studies that evaluate healthcare interventions: explanation and elaboration. *BMJ* 2009; **339**: b2700 [PMID: 19622552 DOI: 10.1136/bmj.b2700]

14 **Whiting PF**, Rutjes AW, Westwood ME, Mallett S, Deeks JJ, Reitsma JB, Leeflang MM, Sterne JA, Bossuyt PM; QUADAS-2 Group. QUADAS-2: a revised tool for the quality assessment of diagnostic accuracy studies. *Ann Intern Med* 2011; **155**: 529-536 [PMID: 22007046 DOI: 10.7326/0003-4819-155-8-201110180-00009]

15 **Dwamena BA.** MIDAS: Stata module for meta-analytical integration of diagnostic test accuracy studies. Statistical Software Components S456880. Boston, MA: Boston College Department of Econonics. 2009

16 **Deeks JJ**, Macaskill P, Irwig L. The performance of tests of publication bias and other sample size effects in systematic reviews of diagnostic test accuracy was assessed. *J Clin Epidemiol* 2005; **58**: 882-893 [PMID: 16085191 DOI: 10.1016/j.jclinepi.2005.01.016]

17 **StataCorp.** 2013. Stata Statistical Software: Release 13. College Station, TX: StataCorp LP. 2013

18 **Hlavaty T**, Huorka M, Koller T, Zita P, Kresanova E, Rychly B, Toth J. Colorectal cancer screening in patients with ulcerative and Crohn's colitis with use of colonoscopy, chromoendoscopy and confocal endomicroscopy. *Eur J Gastroenterol Hepatol* 2011; **23**: 680-689 [PMID: 21602687 DOI: 10.1097/MEG.0b013e32834791b4]

19 **van den Broek FJ**, van Es JA, van Eeden S, Stokkers PC, Ponsioen CY, Reitsma JB, Fockens P, Dekker E. Pilot study of probe-based confocal laser endomicroscopy during colonoscopic surveillance of patients with longstanding ulcerative colitis. *Endoscopy* 2011; **43**: 116-122 [PMID: 21165821 DOI: 10.1055/s-0030-1255954]

20 **Wanders LK**, Kuiper T, Kiesslich R, Karstensen JG, Leong RW, Dekker E, Bisschops R. Limited applicability of chromoendoscopy-guided confocal laser endomicroscopy as daily-practice surveillance strategy in Crohn's disease. *Gastrointest Endosc* 2016; **83**: 966-971 [PMID: 26358329 DOI: 10.1016/j.gie.2015.09.001]

21 **Efthymiou M**, Allen PB, Taylor AC, Desmond PV, Jayasakera C, De Cruz P, Kamm MA. Chromoendoscopy versus narrow band imaging for colonic surveillance in inflammatory bowel disease. *Inflamm Bowel Dis* 2013; **19**: 2132-2138 [PMID: 23899540 DOI: 10.1097/MIB.0b013e31829637b9]

22 **Gordon H**, Langholz E. The EpiCom Survey-Registries Across Europe, Epidemiological Research and Beyond. *J Crohns Colitis* 2017; **11**: 1019-1021 [PMID: 28158624 DOI: 10.1093/ecco-jcc/jjx013]

23 **van den Broek FJ**, Fockens P, van Eeden S, Stokkers PC, Ponsioen CY, Reitsma JB, Dekker E. Narrow-band imaging versus high-definition endoscopy for the diagnosis of neoplasia in ulcerative colitis. *Endoscopy* 2011; **43**: 108-115 [PMID: 21165822 DOI: 10.1055/s-0030-1255956]

24 **Cassinotti A,** Ardizzone S, Buffoli F, Fociani P, Villanacci V, Nebuloni M, Fichera M, Salemme M, Lombardini M, Molteni P, Sampietro G, Furfaro F, Dell'Era A, Gambitta P, Foschi D, Duca P, De Franchis R, Maconi G. Virtual chromoendoscopy with FICE is superior to standard colonoscopic surveillaillance for flat visibile dysplasic lesions and raised lesions (polyps and pseudopolyps) evaluation in long-standing ulcerative colitis: a prospective, randomized, trial. *J CROHNS COLITIS* 2015; **9** Suppl 1: S1-S479

25 **Gordon H**, Langholz E. The EpiCom Survey-Registries Across Europe, Epidemiological Research and Beyond. *J Crohns Colitis* 2017; **11**: 1019-1021 [PMID: 28158624 DOI: 10.1093/ecco-jcc/jjx013]

26 **Carballal S**, Maisterra S, López-Serrano A, Gimeno-García AZ, Vera MI, Marín-Garbriel JC, Díaz-Tasende J, Márquez L, Álvarez MA, Hernández L, De Castro L, Gordillo J, Puig I, Vega P, Bustamante-Balén M, Acevedo J, Peñas B, López-Cerón M, Ricart E, Cuatrecasas M, Jimeno M, Pellisé M; EndoCAR group of the Spanish Gastroenterological Association and Spanish Digestive Endoscopy Society. Real-life chromoendoscopy for neoplasia detection and characterisation in long-standing IBD. *Gut* 2018; **67**: 70-78 [PMID: 27612488 DOI: 10.1136/gutjnl-2016-312332]

27 **Buchner AM,** Ma GK, Ginsberg GG, Lichtenstein GR, Kerner C. Chromoendoscopy-Guided Probe Based Confocal Laser Endomicroscopy: A Novel Approach for Dysplasia Evaluation in IBD Surveillance. *Gastroenterology* 2016; **150**: S627 [DOI: 10.1016/S0016-5085(16)32152-7]

28 **Muñoz J,** García M, Sicilia B, Sierra M, Fernandez N, Arias L, Barrio J, Velayos B, Hernandez-Villalba L. Results of dysplasia surveillance programme with chromoendoscopy for inflammatory bowel disease. *Journal of Crohn's and Colitis* 2016; **10** Suppl: 158

29 **Wanders LK**, Mooiweer E, Wang J, Bisschops R, Offerhaus GJ, Siersema PD, D'Haens GR, Oldenburg B, Dekker E. Low interobserver agreement among endoscopists in differentiating dysplastic from non-dysplastic lesions during inflammatory bowel disease colitis surveillance. *Scand J Gastroenterol* 2015; **50**: 1011-1017 [PMID: 25794268 DOI: 10.3109/00365521.2015.1016449]

30 **Dlugosz A**, Barakat AM, Björkström NK, Öst Å, Bergquist A. Diagnostic yield of endomicroscopy for dysplasia in primary sclerosing cholangitis associated inflammatory bowel disease: a feasibility study. *Endosc Int Open* 2016; **4**: E901-E911 [PMID: 27540581 DOI: 10.1055/s-0042-111203]

31 **Freire P**, Figueiredo P, Cardoso R, Donato MM, Ferreira M, Mendes S, Silva MR, Cipriano A, Ferreira AM, Vasconcelos H, Portela F, Sofia C. Surveillance in ulcerative colitis: is chromoendoscopy-guided endomicroscopy always better than conventional colonoscopy? A randomized trial. *Inflamm Bowel Dis* 2014; **20**: 2038-2045 [PMID: 25185683 DOI: 10.1097/MIB.0000000000000176]

32 **Rispo A**, Castiglione F, Staibano S, Esposito D, Maione F, Siano M, Salvatori F, Masone S, Persico M, De Palma GD. Diagnostic accuracy of confocal laser endomicroscopy in diagnosing dysplasia in patients affected by long-standing ulcerative colitis. *World J Gastrointest Endosc* 2012; **4**: 414-420 [PMID: 23125900 DOI: 10.4253/wjge.v4.i9.414]

33 **Shahid MW,** Wang YR, Cangemi JR, Wallace MB, Picco MF. The Role of Probe-Based Confocal Laser Endomicroscopy in Detection of Neoplasia in Polypoid Lesions in Ulcerative Colitis: An Exploratory Pilot Study. *Gastrointest Endosc* 2011; **73**: AB302-AB3 [DOI: 10.1016/j.gie.2011.03.608]

34 **Kiesslich R**, Goetz M, Lammersdorf K, Schneider C, Burg J, Stolte M, Vieth M, Nafe B, Galle PR, Neurath MF. Chromoscopy-guided endomicroscopy increases the diagnostic yield of intraepithelial neoplasia in ulcerative colitis. *Gastroenterology* 2007; **132**: 874-882 [PMID: 17383417 DOI: 10.1053/j.gastro.2007.01.048]

35 **Nishiyama S**, Oka S, Tanaka S, Sagami S, Hayashi R, Ueno Y, Arihiro K, Chayama K. Clinical usefulness of narrow band imaging magnifying colonoscopy for assessing ulcerative colitis-associated cancer/dysplasia. *Endosc Int Open* 2016; **4**: E1183-E1187 [PMID: 27853744 DOI: 10.1055/s-0042-116488]

36 **van den Broek FJ**, Fockens P, van Eeden S, Reitsma JB, Hardwick JC, Stokkers PC, Dekker E. Endoscopic tri-modal imaging for surveillance in ulcerative colitis: randomised comparison of high-resolution endoscopy and autofluorescence imaging for neoplasia detection; and evaluation of narrow-band imaging for classification of lesions. *Gut* 2008; **57**: 1083-1089 [PMID: 18367559 DOI: 10.1136/gut.2007.144097]
37 **Matsumoto T**, Kudo T, Jo Y, Esaki M, Yao T, Iida M. Magnifying colonoscopy with narrow band imaging system for the diagnosis of dysplasia in ulcerative colitis: a pilot study. *Gastrointest Endosc* 2007; **66**: 957-965 [PMID: 17826773 DOI: 10.1016/j.gie.2007.04.014]
38 **Kiesslich R**, Fritsch J, Holtmann M, Koehler HH, Stolte M, Kanzler S, Nafe B, Jung M, Galle PR, Neurath MF. Methylene blue-aided chromoendoscopy for the detection of intraepithelial neoplasia and colon cancer in ulcerative colitis. *Gastroenterology* 2003; **124**: 880-888 [PMID: 12671882 DOI: 10.1053/gast.2003.50146]
39 **Bisschops R,** Bessissow T, Bhandari P, Dekker E, East JE, Ignjatovic A, Parra-Blanco A, Ragunath K, Rutter MD, Schoon EJ, Baert FJ, Rutgeerts PJ, Ferrante M. Chromo-Endoscopy and NBI for Ruling out Neoplasia in Ulcerative Colitis: an International Multicenter Interobserver Study. *Gastrointest Endosc* 2013; **77**: AB444-AB455 [DOI: 10.1016/j.gie.2013.03.356]
40 **East JE**, Suzuki N, Saunders BP. Comparison of magnified pit pattern interpretation with narrow band imaging versus chromoendoscopy for diminutive colonic polyps: a pilot study. *Gastrointest Endosc* 2007; **66**: 310-316 [PMID: 17643705 DOI: 10.1016/j.gie.2007.02.026]
41 **Hewett DG**, Kaltenbach T, Sano Y, Tanaka S, Saunders BP, Ponchon T, Soetikno R, Rex DK. Validation of a simple classification system for endoscopic diagnosis of small colorectal polyps using narrow-band imaging. *Gastroenterology* 2012; **143**: 599-607.e1 [PMID: 22609383 DOI: 10.1053/j.gastro.2012.05.006]

P- Reviewer: Espinel J, Guerra IG, Tang ST **S- Editor**: Wang XJ
L- Editor: A **E- Editor**: Ma YJ

Published by **Baishideng Publishing Group Inc**
7901 Stoneridge Drive, Suite 501, Pleasanton, CA 94588, USA
Telephone: +1-925-223-8242
Fax: +1-925-223-8243
E-mail: bpgoffice@wjgnet.com
Help Desk: http://www.f6publishing.com/helpdesk
http://www.wjgnet.com

ISSN 1007-9327